

University of Nottingham
UK | CHINA | MALAYSIA

Maximising the Nutritional Value of Microalgae (*Chlamydomonas reinhardtii*) Through Cultivation and Downstream Bioprocessing

Patchaniya Eakpetch

This thesis is submitted in fulfilment of the requirements for a degree of Doctor of Philosophy

Division of Food, Nutrition and Dietetics

School of Bioscience, University of Nottingham

July 2019

ABSTRACT

Chlamydomonas reinhardtii (*C. reinhardtii*) has the potential to be a novel food and feed given the range of nutrients and bioactive compounds it contains, but its multilayer cell wall (hydroxyproline-rich glycoprotein [HRPGs]) could restrict the bioaccessibility of its nutrients. Although *C. reinhardtii* is well characterised, its potential as a functional food/feed ingredient has not been explored. The objectives of the thesis were as follows: (1) investigate the influence of growth media manipulation on the nutritional value of *C. reinhardtii*; (2) test the impact of mechanical forces on the integrity of *C. reinhardtii* cells; and (3) measure the impact of a selected cell disruption technique on the bioaccessibility of target nutrients (chlorophyll and carotenoids) *in vitro* and *in vivo* digestion.

C. reinhardtii was cultivated in a range of media and the nutrients measured. Protein (41.4–43.8%) contains the following amino acids: glutamine, leucine and alanine with trace levels of cysteine, aspartic acid and methionine. Lipid (13.2–20.9%) is comprised of fatty acids (FAs), mostly C16 and C18 in length: α-linolenic acid (C18:3ω3) 5.53 – 27.7% total FAs; palmitic acid (C16:0) 24.5–47.6% total FAs; and oleic acid (C18:1ω9) 8.28–15.7% total FAs. Carbohydrate represents 21.5–27.8% of the dry weight, and the ash comprises 10.1–12.9%. Minerals include calcium (Ca), magnesium (Mg), phosphorus (P), potassium (K) and trace elements (Fe, Cu, Zn, Mn, Mo, Se); this varies depending on the composition of the cultivation medium.

C. reinhardtii cells were exposed to two types of mechanical disruption methods. Ultrasonication caused significant cell breakage, with most of the nutrients analysed

released from the cells into the external aqueous environment. On the other hand, cells exposed to hydrodynamic cavitation (HDC) retained their overall cellular structure. HDC-treated cells were also more permeable to Nile Red dye, but only a limited portion of nutrients were found in the external aqueous environment. HDC under the condition tested caused some disruption or cell wall breaching, but most of the cells remained intact and retained nutritional content. Any perforations created, as suggested by the dye infiltration, must be small enough to limit the release of nutrients, many of which are associated with subcellular organelles that are, presumably, larger than the pores that appear to have been generated by HDC. This method therefore appears to modify the surface nature of *C. reinhardtii*.

An *in vitro* model of human digestion was used to measure the bioaccessibility of chlorophylls (*a* and *b*) and carotenoids (*β*-carotene and lutein) from intact and HDC-disrupted *C. reinhardtii* freeze-dried biomass. The loss of wall integrity by the disruption process led to the more digestible structure but lowered the persistence of nutrients chlorophyll (*a* and *b*) and *β*-carotene. Both intact and HDC-disrupted *C. reinhardtii* biomass provided a favourable level of lutein bioaccessibility, 34.7 and 34.1%, respectively. Consequently, this finding could pave the way forward to an *in vivo* assimilation study of lipophilic pigment from *C. reinhardtii* biomass.

In vivo studies showed that growth and other significant parameters for freeze-dried intact *C. reinhardtii* fed zebrafish were significantly improved compared with fish consuming a standard fish diet. A visible yellow pigmentation of zebrafish (egg in the female and skin in the male) fed with *C. reinhardtii* only was distinct from the control, which resulted from lutein assimilable. The retinol level in the body of zebrafish increased from 0.5 in the

control to 1.85 and 3.5 μg/g at a *C. reinhardtii* inclusion-level in feed of 10% and 20%, respectively. Thus, it is deduced that zebrafish were able to assimilate *β*-carotene from *C. reinhardtii* and convert it to vitamin A.

ACKNOWLEDGEMENT

I would like to express my sincere gratitude to my advisor, Associate Professor Dr David Gray for his continuous support of my PhD studies and related research, and for his patience and immense knowledge. His guidance helped me throughout the research and writing of this thesis, which I know will benefit me for the rest of my life. I would also like to thank Professor Andrew Taylor for many insightful discussions and his guidance on my dissertation and manuscripts.

Besides my advisor, I would like to thank the rest of my thesis committee, Professor Keith Waldron, Dr Neil Doherty, and Associate Professor Andrew Rosenthal, for their insightful comments and encouragement, but also for the difficult questions that gave me the incentive to widen my research.

My special thanks go to the Algae Parc Team at Wageningen University for providing me with inside knowledge of large-scale algae cultivation and the algae biorefinery regime. Also, the Algae Europe team who inspired me as a young researcher to move forward into algae research field. Thanks to the University of Liverpool Aquarium Facility Team, Dr Iain Young and Dr Kieran Magee, for their kind cooperation and training on fish feeding trails. Thanks to the School of Life Sciences Imaging Team, Dr Robert Markus at the Centre for Biomolecular Sciences and Denise Mclean in the Advanced Microscopy Unit, for their assistance and advice on microscopy techniques.

I greatly appreciate the microalgae and chloroplast team for the hard work of developing the group protocols during the years. Thanks to all staff and researchers, in both the Bioenergy & Brewery Science and Food Science buildings. Thanks to the James

Cameron Clifford library team who always helped me while I was writing up, and for the sleepless nights we were working together before deadlines.

Here I also want to thank the Suratthani Rajabhat University for funding my research. Thanks for all the support and inspiration from colleagues in the Department of Food Science, Suratthani Rajabhat University, Thailand

Last but not least, I would like to thank my family, especially my parents, brothers and to my partner for supporting me spiritually throughout the writing of this thesis, and my life in general.

CONTENTS

ABSTRACT ..... **I**

ACKNOWLEDGEMENT ..... **IV**

CONTENTS ..... **VI**

LIST OF TABLES ..... **XII**

LIST OF FIGURES ..... **XIV**

CHAPTER 1 ..... **XXI**

INTRODUCTION ..... **XXI**

CHAPTER 2 ..... **1**

BACKGROUND AND RELATED WORKS **1**

2.1 BIOLOGY OF ALGAE 1

2.1.1 Anatomy of *C. reinhardtii* 4

2.1.2 *C. reinhardtii* Cell Wall Characteristics 7

2.1.3 Reproduction 16

2.2 BIOPROCESSING AND BIO-PRODUCTS 20

2.2.1 Cultivation 20

2.2.2 Bio-products 24

2.3 CELL DISRUPTION 37

2.3.1 Definition, Classification and Mechanism 37

2.4 BIOACCESSIBILITY OF DIETARY NUTRIENTS 44

2.4.1 *In vitro* Human Digestion 44

2.4.2 In vivo Zebra Fish as a Model 48

2.4.3 Impact of Microalgae Cell Wall on Bioaccessibility of Dietary Nutrients ... 52

RESEARCH STRATEGY 57

CHAPTER 3 58

MATERIALS AND METHODS 58

3.1 MATERIAL AND METHODS FOR THE BIOCHEMICAL RESPONSE OF *C. REINHARDTII* AS INFLUENCED BY GROWTH MEDIA MANIPULATION 58

3.1.1 Biochemical response of *C. reinhardtii* under mixothrophic culturing. 58

3.1.2 Nitrogen Stress Media on the Proximate Analysis of *C. reinhardtii* 69

3.2 MATERIALS AND METHODS FOR IMPACT OF HYDRODYNAMIC DISRUPTION ON C. REINHARDTII CELLS AND NUTRITIVE COMPOSITIONS 75

3.2.1 Microalgae Culture Preparations 75

3.2.2 Determination of Cavitation Device Power 75

3.2.3 Microalgae Cell Disruption 78

3.2.4 Ultra-Structural Analysis by Light Microscope 79

3.2.5 Freeze-Dried *C. reinhardtii* Biomass 79

3.2.6 Pigment Release Analysis 80

3.2.7 Protein Release Analysis 80

3.2.8 Structure Illumination Microscope (SIM) and Confocal Microscopy 81

3.2.9 Lipid Extraction 81

3.2.10 Chlorophyll and Carotenoids Analysis 81

3.3 IN VITRO BIOACCESSIBILITY OF CHLOROPHYLL (*A* AND *B*) AND CAROTENOIDS (*B*-CAROTENE AND LUTEIN) FROM INTACT AND HDC-DISRUPTED *C. REINHARDTII* 82

3.3.1 The Changes on Cell Wall Morphology and Phase Behaviour of Intact *C. reinhardtii* during the i*n vitro* Human Digestion 82

3.3.2 *In vitro* Bioaccessibility of Chlorophyll (a and b) and Carotenoids (*β*-Carotene and Lutein) from Intact and HDC-Disrupted *C. reinhardtii* 86

3.4 MATERIAL AND METHODS FOR IMPACT OF *C. REINHARDTII* INCLUSION IN ZEBRAFISH DIET ON THEIR GROWTH PERFORMANCE AND KEY METABOLITES 91

3.4.1 Microalgae Preparation 91

3.4.2 Diet Formulation 91

3.4.3 Subjects and Husbandry 94

3.4.4 Growing Procedure 95

3.4.5 Ethical Issues 96

3.4.6 Experimental Procedures 96

3.5 STATISTICAL ANALYSIS 99

CHAPTER 4 100

THE BIOCHEMICAL RESPONSE OF *C. REINHARDTII* AS INFLUENCED BY GROWTH MEDIA MANIPULATION 100

4.1 INTRODUCTION 100

4.2 RESULTS AND DISCUSSION 101

4.2.1 Growth Kinetic and Biomass Productivity of *C. reinhardtii* Response to Mixothrophic Culturing 101

4.2.2 Biochemical Compound Response to Mixothrophic Culturing of *C. reinhardtii* 103

4.2.3 Morphological Structure of *C. reinhardtii* 107

4.2.4 Effect of Nitrogen Stress Media on the Proximate Analysis of Freeze-Dried *C. reinhardtii* Biomass 111

4.2.5 Amino Acid Profile and Protein Quality 116

4.2.6 Protein separation 121

4.2.7 Fatty Acids 123

4.2.8 Minerals 130

CONCLUSION 132

CHAPTER 5 133

IMPACT OF CAVITATION DISRUPTION ON C. REINHARDTII CELL AND NUTRITIVE COMPOSITIONS 133

5.1 INTRODUCTION 133

5.2 RESULTS AND DISCUSSION 134

5.2.1 Effect of Hydrodynamic Cavitation and Ultrasonication on Metabolite Release and Cell Structure of *C. reinhardtii* 134

5.2.2 Effect of Hydrodynamic Cavitation Disruption on the Retention of Selected Nutrients 139

5.2.3 Effect of Hydrodynamic Cavitation Disruption on Membrane Permeability of Lipophilic Dye 141

CONCLUSION 143

CHAPTER 6 144

***IN VITRO* BIOACCESSIBILITY OF CHLOROPHYLL (*A* AND *B*) AND CAROTENOIDS (*B*-CAROTENE AND LUTEIN) FROM INTACT AND HYDRODYNAMIC DISRUPTED *C. REINHARDTII* 144**

6.1 INTRODUCTION 144

6.2 RESULTS AND DISCUSSION 146

6.2.1 The Changes on Cell Wall Morphology and Phase Behaviour of Intact *C. reinhardtii* during the *in vitro* Human Digestion 146

6.2.2 Nutritive value of intact and disrupted freeze-dried *C. reinhardtii* during in vitro human digestion 150

6.2.3 In vitro Bioaccessibility of Chlorophylls (*a* and *b*) and Carotenoids (*β*-Carotene and Lutein) from Intact and HDC-Disrupted *C. reinhardtii.* 151

6.2.4 Structural Change of Intact and Disrupted Freeze-Dried *C. reinhardtii* Biomass During *in vitro* Static Human Digestion 160

CHAPTER 7 164

IMPACT OF C. REINHARDTII INCLUSION IN ZEBRAFISH DIET ON THEIR GROWTH AND KEY METABOLITES 164

7.1 INTRODUCTION 164

7.2 Results and Discussion 167

7.2.1 Growing and Palatability Criteria 167

7.2.2 Impact of Consuming *C. reinhardtii* on Fish Body and Egg Carotenoid Levels 169

7.2.3. Quantitative Analysis of Carotenoids in Fish Body and Eggs 172

CHAPTER 8 177

SUMMARY 177

CHAPTER 9 180

SUGGESTED FUTURE RESEARCH 180

I. Cultivation Conditions 180

II. Cell wall disruption 180

III. Bioaccessibility Studies 181

IV. Potential of Commercial Development and Impact 181

REFERENCES 183

APPENDIX A 221

APPENDIX B 224

LIST OF TABLES

TABLE 2.1: CLASSIFICATION SCHEME OF DIFFERENCE ALGAE SPECIES. 3

TABLE 2.2 : THE CHEMICAL COMPOSITIONS OF THE *CHLAMYDOMONAS* 'S CELL WALL 8

TABLE 2. 3: COMPARABLE OF DIFFERENCE CULTURING MEDIA.....22

TABLE 2. 4: FATTY ACID COMPOSITION OF DIFFERENCE SPECIES OF ALGAE.. 32

TABLE 3.1: THE MOLAR COMPOSITION OF STANDARD CULTURE MEDIA. 59

TABLE 3.2: LIST OF CONCENTRATION OF ELECTROLYTE STOCK SOLUTION FOR SIMULATED DIGEST FLUID. 83

TABLE 3.3: COMPOUND FORMULATION OF EXPERIMENTAL DIET.....92

TABLE 3.4: THE NUTRITIONAL COMPOSITION OF EXPERIMENTAL DIET. 93

TABLE 4.1: NUTRITIONAL COMPOSITION (MG/G DWB) OF FREEZE-DRIED *C. REINHARDTII* BIOMASS. 113

TABLE 4.2: AMINO ACID PROfiLE OF DIFFERENT *C. REINHARDTII* COMPARED WITH CONVENTIONAL PROTEIN SOURCES AND THE FAO/WHO/UNU REFERENCE PATTERN (MG/G PROTEIN) 120

TABLE 4.3: FA COMPOSITION OF *C. REINHARDTII* (MG/G FREEZE-DRIED BIOMASS) DETERMINATION BY FAME ANALYSIS THROUGH GC-MS.. 125

TABLE 4.4: MINERAL PROFILE OF MAJOR AND TRACE MINERALS IN FREEZE-DRIED *C. REINHARDTII* BIOMASS AND DRI. 131

TABLE 5.1: EFFECT OF CELL DISRUPTION METHOD ON THE RELEASE OF SELECTED METABOLITES FROM *C. REINHARDTII* INTO THE AQUEOUS PHASE (µG/ML). 137

TABLE 5.2: EFFECT OF EXPOSING *C. REINHARDTII* CELL TO HDC ON THE RETENTION OF SELECTED NUTRIENTS.....139

LIST OF FIGURES

FIGURE 2.1: EVOLUTIONARY RELATIONSHIPS OF 20 SPECIES WITH SEQUENCED GENOMES 2

FIGURE 2.2: MEDIAN SECTION OF A WILD-TYPE *C. REINHARDTII* CELL.. 4

FIGURE 2.3: THE STRUCTURE OF THE HYDROXYPROLINE-RICH OF EXTS AND THEIR INTERMOLECULAR BONDS. 9

FIGURE 2.4: CHEMICAL STRUCTURES AND POSSIBLE IN *VIVO* REACTION FOR THE FORMATION OF IDT (ISODITYROSINE) AND DI-IDT (DI-ISOTYROSINE) FROM TYR (TYROSINE) 11

FIGURE 2.5: THE PROPOSED STRUCTURE OF PULCHEROSINE AND DI-IDT. PULCHEROSINE FORMED BY LINKING OF A TYR THROUGH ITS PHENOL GROUP TO AN IDT UNIT. 12

FIGURE 2.6: SCHEMATICS FOR THE LATERAL ALIGNMENT OF EXT CHAINS AND TYR INTERCHAIN CROSS-LINK TYPES. 13

FIGURE 2.7: THE DIAGRAMS OF THE *C. REINHARDTII* CELL WALL BASED ON THE THIN SECTION STUDIES OF GOODENOUGH AND HEUSER, (1985)..... 15

FIGURE 2.8: STAGE OF THE MICROALGAE REPRODUCTION PROCESS 17

FIGURE 2.9: GROWTH PHASES IN MICROALGAE BATCH CULTURE (SOLID LINE) AND NUTRIENT CONCENTRATION (DASHED LINE): (1) LAG PHASE, (2) EXPONENTIAL PHASE, (3) LINEAR PHASE, (4) DECLINING GROWTH PHASE, (5) STATIONARY PHASE, AND (6) DEATH PHASE 18

FIGURE 2.10: OVERVIEW SCHEME OF ALGAE BIO REFINERY PROCESS. 21

FIGURE 2.11: GENERAL COMPOSITION OF DIFFERENCE ALGAE AND CYANOBACTERIA COMPARE TO CONVENTIONAL FOOD SOURCES (%DWB) 26

FIGURE 2.12: AMINO ACIDS OF SELECTED PLANTS 28

FIGURE 2.13: AMINO ACIDS OF *C. REINHARDTII* COMPARE TO OTHER SPECIES OF FRESH WATER MICROALGAE, SELECTED MARINE MICROALGAE, CYANOBACTERIAL AND INSECTS 29

FIGURE 2.14: COMMON LIPID SPECIES REPORTED FOR *C. REINHARDTII* CELLS. LABELS R1, R2 AND R3 REPRESENT DIFFERENT FATTY ACID ACYL RESIDUES. 31

FIGURE 2.15: CHEMICAL STRUCTURE OF CHLOROPHYLL *A* AND CHLOROPHYLL *B* 34

FIGURE 2.16: THE STRUCTURE OF CAROTENOIDS OBTAIN FROM ALGAE 36

FIGURE 2.17: TECHNIQUES APPLICABLE FOR THE DOWNSTREAM PROCESSING OF CELL DISRUPTION. 39

FIGURE 2.18: A SCHEMATIC REPRESENTATION OF HYDRODYNAMIC CAVITATION. 41

FIGURE 2.19: A SCHEMATIC REPRESENTATION OF ULTRASONICATION.....42

FIGURE 2.20: DOWNSTREAM PROCESSING STEPS FOR THE RECOVERY OF PROTEINS, CARBOHYDRATES, LIPIDS, AND PIGMENTS 43

FIGURE 2.21: DEFINITION OF BIOAVAILABILITY AS A SUM OF BIOACCESSIBILITY AND BIOACTIVITY WITH DESCRIPTION OF THE PHYSIOCHEMICAL EVENTS INVOLVED AT EACH STAGE 45

FIGURE 2.22: A SIMPLIFIED DIGESTIVE TRACT: MAJOR COMPARTMENTS AND ORGAN OF DIGESTIVE TRACT REPRESENT DIGESTION OF PROTEINS, LIPIDS, AND CAROTENOIDS. 47

FIGURE 2.23: ZEBRAFISH AS A MODEL ORGANISM AND ITS ANALOGY WITH HUMAN. CNS; CIRCULATORY SYSTEM 49

FIGURE 2.24: AN ILLUSTRATION OF DIFFERENCE DIGESTIVE SYSTEM IN ZEBRAFISH 51

FIGURE 2.25: ANATOMICAL FEATURES OF ADULT ZEBRAFISH INTESTINE. 52

FIGURE 2.26: SCHEMATIC DEPICTION OF THE CELL WALL OF *C. VULGARIS*. 55

FIGURE 2.27: SCHEMATIC DEPICTION OF THE CELL WALL OF CYANOBACTERIA (*SPIRULINA*). 56

FIGURE 3.1: ILLUSTRATION OF THE DOWNSTREAM BIOPROCESSING OF *C. REINHARDTII*. 60

FIGURE 3.2: THE EXPERIMENTAL SETUP OF *C. REINHARDTII* UNDER MIXOTHROPHIC CULTIVATION IN THE LAB SCALE SYSTEM.....61

FIGURE 3.3: THE SCHEMATIC DIAGRAM OF *C. REINHARDTII* STRAIN MAINTAINING. 62

FIGURE 3.4: DIAGRAM (A), DEVICE (B) AND FLOW OF THE FLUID INTO THE HYDRODYNAMIC CAVITATION DEVICE (C). 76

FIGURE 3.5: DIAGRAM (A), DEVICE (B) AND SONOTRODE GENERATION OF THE ULTRASONICATION DEVICE (C). 77

FIGURE 3.6: OVERVIEW AND FLOW DIAGRAM OF A SIMULATED *IN VITRO* DIGESTION METHOD. 84

FIGURE 3.7: THE DIAGRAM OF THE CELL WALL MORPHOLOGY AND PHASE BEHAVIOR DURING *IN VITRO* DIGESTION OF INTACT FREEZE-DRIED *C REINHARDTII*. 85

FIGURE 3.8: THE DIAGRAM FOR *IN VITRO* BIOACCESSIBILITY OF THE INTACT AND DISRUPTED EXPERIMENTS.....87

FIGURE 3.9: THE AQUATIC HABITAT ZEBRAFISH TANKS FOR GROWING FISH FEEDING TRAIL.....94

FIGURE 3.10: REPRESENTS THE CHROMATOGRAM OF INORGANIC CONTENT IN STANDARD *C. REINHARDTII* FREEZE-DRIED BIOMASS. 111

FIGURE 3.11: CHROMATOGRAM OF STANDARD AMINO ACIDS DETECTED USING ION EXCHANGE CHROMATOGRAPHY WITH PHOTOMETRIC DETECTION AT 570 NM. 118

FIGURE 3.12: CHROMATOGRAM OF STANDARD AMINO ACIDS DETECTED USING ION EXCHANGE CHROMATOGRAPHY WITH PHOTOMETRIC DETECTION AT 440 119

FIGURE 3.13: FATTY ACID PROFILE CHROMATOGRAM OF *C. REINHARDTII* FREEZE-DRIED BIOMASS. 125

FIGURE 4.1: THE GROWTH KINETICS OF *C. REINHARDTII*. THE CELLS WERE CULTIVATED UNDER THE TAP GROWTH MEDIA UNDER THE STANDARD CONDITION ..102

FIGURE 4.2: THE RELATIONSHIP OF THE BIOMASS PRODUCTION (G/ML), CELL NUMBER AND AGE OF CULTURE OF *C. REINHARDTII*. 103

FIGURE 4.3: THE PROTEIN CONTENT OF *C. REINHARDTII* BIOMASS. THE CELLS WERE CULTIVATED IN THE TAP GROWTH MEDIA UNDER THE STANDARD CONDITION. 104

FIGURE 4.4: THE TOTAL LIPID CONTENT OF *C. REINHARDTII* BIOMASS. THE CELLS WERE CULTIVATED IN THE TAP GROWTH MEDIA UNDER THE STANDARD CONDITION 105

FIGURE 4.5: THE PIGMENT CONTENT (CHLOROPHYLL *A*, CHLOROPHYLL *B* AND CAROTENOIDS) OF *C. REINHARDTII* BIOMASS. THE CELLS WERE CULTIVATED IN THE TAP GROWTH MEDIA UNDER THE STANDARD CONDITION 106

FIGURE 4.6: TEM IMAGES OF *C. REINHARDTII* AT DIFFERENT STAGE OF CULTURING. THE CELLS WERE CULTIVATED IN TAP MEDIA UNDER CONTROL CONDITIONS 108

FIGURE 4.7: MORPHOLOGICAL STRUCTURES OF *C. REINHARDTII*. THE CELLS WERE CULTIVATED IN TAP MEDIA UNDER CONTROL CONDITIONS 110

FIGURE 4.8: SIMPLIFIED CENTRAL CARBON METABOLIC NETWORK OF A UNICELLULAR PHOTOAUTROTOPHIC MICROALGAE 114

FIGURE 4.9: PROTEIN ELECTROPHORESIS PATTERN SHOWING THE MOLECULAR WEIGHT OF INTACT *C. REINHARDTII* FREEZE-DRIED BIOMASS. 122

FIGURE 4.10: THE SEPARATION OF LIPID EXTRACT FROM FREEZE-DRIED *C. REINHARDTII* BIOMASS USING IN-HOUSE METHODS 124

FIGURE 4.11: FAS COMPOSITION OF *C. REINHARDTII* (MG/G FREEZE-DRIED BIOMASS) DETERMINATION BY FAME ANALYSIS THROUGH GC-MS. 127

FIGURE 5.1: EFFECT OF CELL DISRUPTION METHOD ON *C. REINHARDTII* INTEGRITY. 135

FIGURE 5.2: VISUALISING OF (A) INTACT, (B) HYDRODYNAMIC CAVITATION-DISRUPTED AND (C) ULTRASONICATION-DISRUPTED *C. REINHARDTII* SUSPENSION. .135

FIGURE 5.3: THE PROPOSED SCHEMATIC EFFECT OF ULTRASONICATION OR HYDRODYNAMIC CAVITATION ON THE INTEGRITY OF *C. REINHARDTII* CELLS. 138

FIGURE 5.4: VISUALIZATION OF INTACT (A) AND HDC-DISRUPTED (B) *C. REINHARDTII* SUSPENSIONS. SINGLE OPTICAL SLICES ARE SHOWN. 142

FIGURE 6.1: TEM IMAGES OF *C. REINHARDTII* THROUGHOUT THE DIGESTION STEPS (ORAL, GASTRIC, INTESTINE) REPRESENTING THE INTACT *C. REINHARDTII* FREEZE-DRIED BIOMASS TO THE CONTROL SAMPLE (LEFT)HAS BEEN SUBJECT IN THE ABSENCE OF ENZYMES. THE REAL SAMPLE (RIGHT) HAS BEEN SUBJECTED IN THE PRESENCE OF ENZYME WITH THE SAME PH CHANGE, TEMPERATURE AND SHAKING. 147

FIGURE 6.2: THE DIFFERENCES BETWEEN THE CONTROL (ABSENCE OF DIGESTIVE ENZYME) AND THE REAL (PRESENCE OF DIGESTIVE ENZYMES) OF INTACT *C. REINHARDTII* FREEZE-DRIED BIOMASS THROUGHOUT THE DIGESTION STAGES. 149

FIGURE 6.3: ILLUSTRATION THE CHANGING OF *C. REINHARDTII* DIGESTA COLOUR DURING *IN VITRO* DIGESTION PROCESS. 149

FIGURE 6.4: THE CHANGING OF THE CHLOROPHYLL STRUCTURAL AND PHEOPHYTIN FORMATION IN THE ACIDIC CONDITIONS 150

FIGURE 6.5: THE CHLOROPHYLL (*A* AND *B*) AND CAROTENOIDS (*Β*-CAROTENE AND LUTEIN) CONTENT OF TOTAL DIGESTA OF INTACT *C. REINHARDTII* IN THE PRESENCE AND ABSENCE OF DIGESTIVE ENZYME. 151

FIGURE 6.6: SEPARATION OF AQUEOUS MICELLAR FRACTION AND EXTRACTION FROM INTACT AND DISRUPTED *C. REINHARDTII*. 153

FIGURE 6.7: PARTICULATE MATERIAL FROM DIGESTED INTACT AND DISRUPTED FREEZE-DRIED *C. REINHARDTII* AT DIFFERENT STAGES DURING SIMULATION OF DIGESTION.. 162

FIGURE 6. 8: THE PROPOSED SCHEMATIC EFFECT OF INTACT AND HDC DISRUPTED ON THE INTEGRITY OF *C. REINHARDTII* CELLS DURING *IN VITRO* HUMAN DIGESTION. 156

FIGURE 7.2: ZEBRAFISH (*DANIO RERIO*) EGG PIGMENTATION AND COLOUR VARIATION DUE TO CAROTENOID ACCUMULATION IN RESPONSE TO CAROTENOID- RICH DIETS.....170

FIGURE 7.3: EGG COLOUR VARIATIONS DEPENDING OF ZEBRAFISH FED WITH THREE DIFFERENT LEVELS OF PARTIAL REPLACEMENT OF FISH MEAL BY

C. REINHARDTII (10%, 20% AND 50%) AS COMPARED TO THE ZEBRAFISH FED WITH THE ORIGINAL DIET SET (CONTROL). 171

FIGURE 7.4: THE LIPID SOLUBLE PIGMENT EXTRACT OF THE WHOLE BODY FISH OF ZEBRAFISH FED WITH THREE DIFFERENT LEVELS OF PARTIAL REPLACEMENT OF FISH MEAL BY *C. REINHARDTII* (10%, 20% AND 50%) AS COMPARED TO THE ZEBRAFISH FED WITH THE ORIGINAL DIET SET (CONTROL).....172

FIGURE 7.5: LUTEIN CONTENT OF THE LIPID EXTRACTED FROM WHOLE BODY FISH (A) AND EGG (B) OF ZEBRAFISH FED WITH THREE DIFFERENT LEVELS OF PARTIAL REPLACEMENT OF FISH MEAL BY *C. REINHARDTII* (10%, 20% AND 50%) AS COMPARED TO THE ZEBRAFISH FED WITH THE ORIGINAL 173

CHAPTER 1

INTRODUCTION

Algae have been proposed as a future, sustainable food source that is non-competing with traditional agriculture and can be salt-water or fresh-water based. Algae are classified into two broad types, namely the macroalgae (such as seaweeds) and microalgae which are simpler organisms (e.g. single cell organisms). Recent reviews on the nutritional properties of algae and their use in human foods (Bleakley and Hayes, 2017 have highlighted both the current state of knowledge and the ongoing research challenges, which are listed below.

- Most studies have focused on the amount and nutritional quality of algal proteins
- There is much less information on algal micronutrients like vitamins
- Literature reports of nutritional composition are variable as a consequence of different growing conditions for the algae, which can significantly change the amounts of the macro- and micro-nutrients
- To make the nutrients in algae bioaccessible, some form of processing is needed to weaken the tough outer layers of algae
- Processing can release nutrients but, if decomparmentalisation occurs, then enzymes can become activated and may transform the nutrients into inactive forms

The aim of this research is to examine some of the micronutrients in microalgae to assess whether they could be developed as a source of vitamins. To address the issues in the bulleted points above, the following approach was adopted. A well-characterised model microalga, *C. reinhardtii* was chosen as there is much published information on its growth conditions and general composition is needed. For all investigations, *C. reinhardtii* was grown under standardised conditions to minimise compositional difference between batches of algae. The focus of the investigation was on the oil-soluble micronutrients (like *β*-carotene and lutein), which could comprise a useful algal vitamin supplement. The effect of two cavitation-based, tissue-disruption techniques on the release of nutrients from cells was studied. The paragraphs below explain in more detail the key principles of the experimental approach and try to define what the optimum disruption status should be to increase bioaccessibility of micronutrients without subjecting them to degradation.

Microalgae cell wall structure and disruption

Chlamydomonas are covered with a multilayer cell wall, making the availability and extraction of intracellular products challenging (Mayfield *et al.*, 2007). The primary cell wall components of *C. reinhardtii* are the hydroxyproline-rich glycoproteins, which are glycosidically linked to oligosaccharides and a monosaccharide with arabinose and galactose as the predominant sugars (Harris, 2009; Marzol *et al.*, 2018). The glycoproteins of this species are comparable with the hydroxyproline-rich glycoproteins of higher plants, but the sugar composition and molecular organization are distinct (Harris, 2009). Briefly, the cell walls have seven layers: the inner-triplet layer is a fibrous network; the intermediate triplet layer is a loose assembly; the outer layer is thin, which

depolymerizes into two glycoprotein species, one fibrous and one globular (Gould *et al.*, 2008).

Because of the cell wall complexity, a variety of mechanical techniques have been applied to disrupt *Chlamydomonas* species to investigate their nutrient bioacessibility (Gille *et al.*, 2016). For the extraction of potential micronutrients, mechanical disruption is preferred to chemical disruption, so as to avoid chemical contamination of the extract. Cavitation is the key mechanism in several mechanical disruption methods, such as ultrasonication (Lee *et al.*, 2012), optical cavitation (Feliu *et al*, 1998) or hydrodynamic cavitation (Vogel and Lauterborn, 1988). Cavitation is defined as the phenomenon of the formation, growth and subsequent collapse of microbubbles, or cavities in liquids, that occur at small-scale intervals and release large amounts of energy into very small volumes (energy release per unit volume) (Gogate and Pandit, 2008). The release of energy breaks down physical structures like cell walls but can also create structures like emulsions under certain conditions (Canselier and Delmas, 2002). The energy can also inactivate some enzymes; this has been attributed to the formation of free radicals during cavitation (Feng *et al.*, 2011). Therefore, the overall effect of cavitation on cells is difficult to predict and measurements are required to assess the full range of physical and chemical changes, some of which can be positive, others negative depending on the aim of the disruption applied.

Balance between disruption, nutrient release, degradation and delivering nutrients in the *vivo*

It is clear that the release of micronutrients from *C. reinhardtii* during digestion needs some disruption of the cell wall but it is also clear that disruption may cause undesirable

changes due to decompartmentalization of endogenous enzymes. It is also important to consider the ultimate method of delivery of the micronutrients in the diet. Will they be fully extracted from the cells and delivered as an oil-soluble preparation or will they be delivered as a cell-based preparation?

The former format will require optimised extraction of micronutrients from the cells and deliver a concentrated micronutrient preparation but will require more processing and therefore increase cost. The latter format requires the micronutrients to be available during the digestive process and therefore some subtle modification of the cells could make the micronutrients bioavailable while decreasing the chances of excessive degradation (see Wells *et al*. 2017 for discussion on bioavailability factors). Therefore, choosing the appropriate process depends on the type of product required as well as optimisation of process parameters, namely to minimise nutrient losses through endogenous enzyme activation, to avoid overheating of the material during cavitation processes, or to control cell wall disruption to decrease loss of nutrients to the aqueous phase.

Measurement of disruption

Several quantitative measures of disruption efficiency are available such as direct microscopic methods (that allow the number of cells lysed or disintegrated to be enumerated), or indirect methods (that analyse the release of target molecules from the biomass). Additionally, physical properties of disrupted cells (size of cell debris, particle size distribution, viscosity) can be examined (Bzducha-Wróbel *et al*., 2014). To assessed the efficiency of *C. reinhardtii* cell disruption using hydrodynamic cavitation (HDC) compared to that of ultrasonication. The degree of cell wall damage was established by

measuring the release of metabolites (chlorophyll and protein) from *C. reinhardtii*, and by observing the physical structure of the cells after disruption. The impact of these cell disruption methods on the stability of some target nutrients (chlorophyll and carotenoids) was also studied.

Finally, understanding nutrient digestibility and bioactive substance delivery in the body is critical before new ingredients can be accepted as human food. The physical nature of food and its microstructure will affect the release of its nutrients during digestion (Johnson and Williamson, 2003). For example, plant cell walls can restrict access of digestive enzyme to their substrates and so limit the bioaccessibility of nutrients (Johnson and Williamson, 2003). Therefore, understanding factors that constrain the release of nutrients from biomass in which they are contained during *in vitro* and *in vivo* digestion is crucial.

Correspondingly, we examine our main research question based on the literature and present research: "Does *C. reinhardtii* have the potential to deliver a range of nutrients during digestion and does the disruption of its cell wall improve bioaccessiblity of target nutrients; such as lipophilic pigments

CHAPTER 2

Background and Related Works

2.1 Biology of Algae

Algae are photosynthetic organisms without roots, stems or leaves that are commonly divided into two forms (Richmond and Hu, 2013). The macroalgae (also termed seaweeds) are multicellular organisms inhabiting coastal zones. They can be classified by colour, based on their various pigments, which separate them into green, brown and red algae (Metting, 1996). Microalgae, as the name suggests, are microscopic algae typically found in freshwater and marine systems, with their size ranges depending on the species (Suganya *et al.*, 2016). In contrast, the cyanobacteria, which were formerly known as blue-green algae, are prokaryotic organisms and are also able to carry out photosynthesis.

An evolutionary relationships of 20 species with sequenced genomes shown in **Figure 2.1.** The *Chlorophyta* (green algae), including *Chlamydomonas* and *Ostreococcus* diverged from *Streptophytes* (land plants) (Leliaert *et al.*, 2012). They comprise part of the green plant lineage (*Viridiplantae*), which previously diverged from opisthokonts (animals and fungi) (Yoon *et al.*, 2004; Gutman, 2004). **Table 2.1** reveals a classification of different algal groups, our research focuses on the *C. reinhardtii* strain, a motile unicellular green algae classified in the phylum *Chlorophyta*, class *Chlorophyceae* and family *Chlamydomonaceae* (Adl *et al.*, 2005).

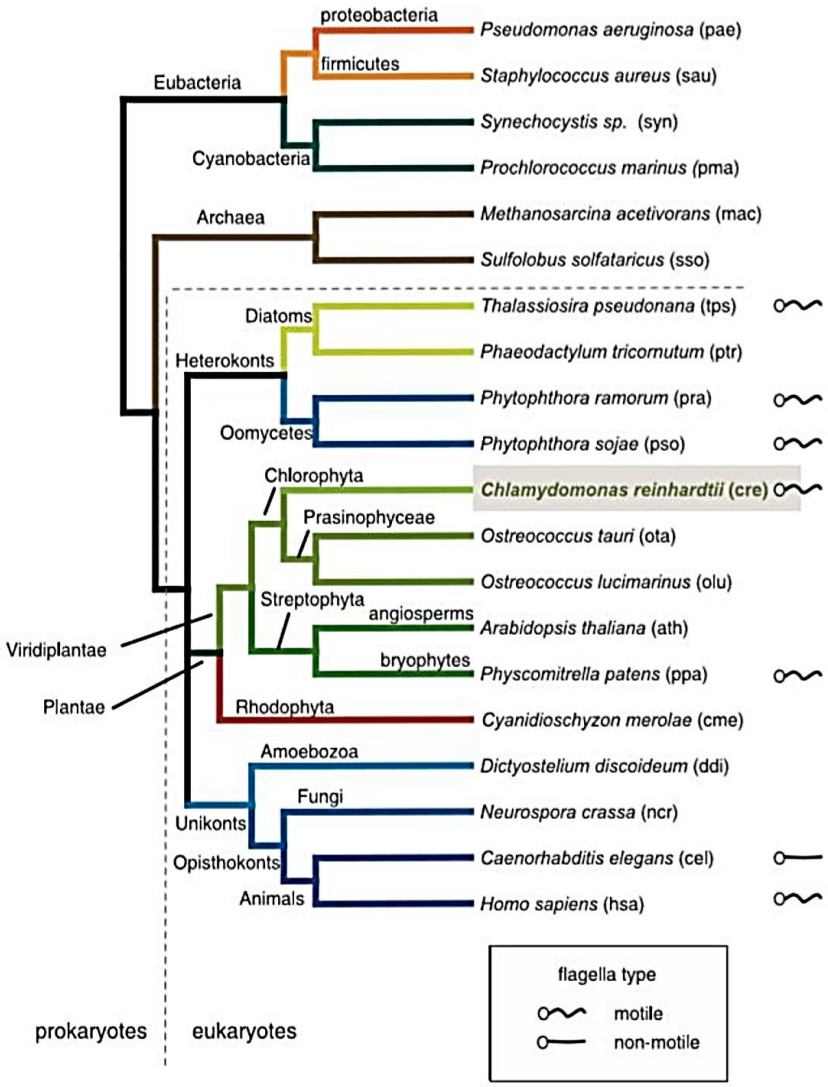


Figure 2.1: Evolutionary relationships of 20 species with sequenced genomes (Keeling *et al.*, 2005; Ciccarelli *et al.*, 2006). Endosymbiosis of a cyanobacterium by a eukaryotic protist gave rise to the green (green branches) and red (red branches) plant lineages, respectively. The presence of motile or nonmotile flagella is indicated at the right of the cladogram (Merchant *et al.*, 2010).

Table 2.1: Classification scheme of difference algae species.

Kingdom	Phylum	Subphylum	Class
Prokaryota eubacteria	*Cyanophyta*		*Cynophyceae*
Eukaryoata	*Glaucophyta*		*Glaucophyceae*
	Phodophyta	*Cyanidiophytina*	*Cyanidiophyceae*
		Euthodophytina	*Compsopogonophyceae*
			Porphyridophyceae
			Thodellophyceae
			Stylonomatophyceae
			Bangiophyceae
			Florideophyceae
	Crytophyta		*Cryptophyceae*
	Dinophyta		
	Haptophyta		*Haptophyceae*
	Ochrophyta	*Khakista*	*Bacillariophyceae*
			Bolidophyceae
		Phaeista	*Chrysophyceae*
			Synurophyceae
			Eustigmatophyceae
			Raphidophyceae
			Dicyochophyceae
			Oelagophyceae
			Pinguiophyceae
			Phaeothamniophyceae
			Crysomerophyceae
			Xanthophyceae
			Phaeophyceae
	Euglenophyta		*Euglenophyceae*
	Chlorarachniophyta		*Chlorarachiniphyceae*
	Chlorophyta	*Prasinophytina*	*Prasinophyceae*
		Tetraphytina	*Chlorophyceae*
			Chlorodendrophyceae
			Trebouxyophyceae
			Ulvophyceae
			Dasycladophyceae
	Charophyta		*Coleochaephyceae*
	(Streptophyta p.p.)		
			Conjugatophyceae
			Mesotigmatophyceae
			Klebsormidiophyceae
			Chrophyceae

Chlamydomonas is of worldwide distribution; it is found in a diversity of habitats and is often isolated from soil and freshwater samples (Hoham *et al*., 2002; Harris, 2009). *C. reinhardtii* was originally isolated from soil at a site near Amherst, Massachusetts in 1954 (Harris, 2001). *C. reinhardtii* is the most characterized algal species with the largest set of a available genetic tools (Harris, 2001; Breton and Kay, 2006; Leliaert *et al*., 2012). Therefore, they are an excellent model organism for development of food and feed applications.

2.1.1 Anatomy of *C. reinhardtii*

C. reinhardtii is often referred to as 'green yeast' (Adl *et al*., 2005). They have long been intensively used as a model system for studying for plant research such as photosynthesis, chloroplast biogenesis, flagellar assembly and function, cell-cell recognition, circadian rhythm and cell cycle control because of its well-defined genetics, and the development of efficient methods for nuclear and chloroplast transformation (Harris, 2001; Breton and Kay, 2006; Leliaert *et al*., 2012).

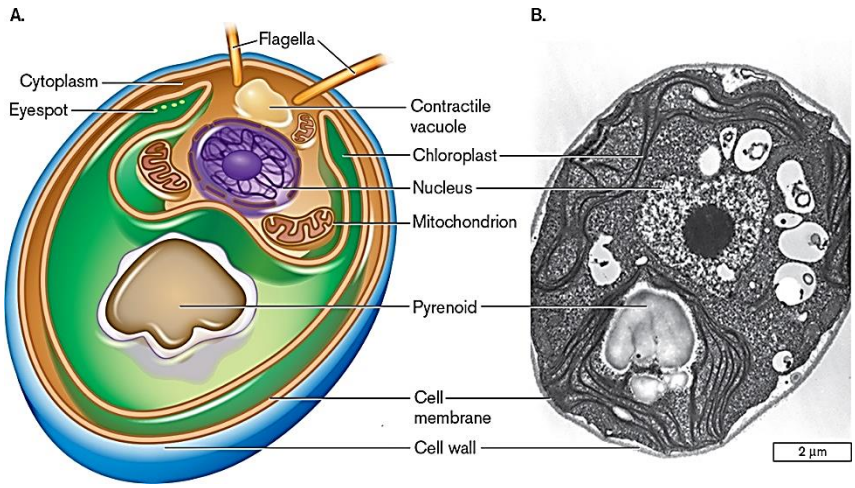


Figure 2.2: Median section of a wild-type *C. reinhardtii* cell. The arrows indicating the main organelles of this species (modified from Harris, 2009). Scale bar 2 µm.

There are numerous reviews about the cell structure and function of *C. reinhardtii*, the first study was carried out in the 1950s (Sager and Palade, 1957). **Figure 2.2** illustrates the median section of a wild-type *C. reinhardtii* cell, with arrows indicating the main organelles of this species: flagella, mitochondria, nucleus, nucleolus, chloroplast, pyrenoid, starch granules, cell membrane and cell wall (Harris, 2009). In addition to these main organelles, the cytoplasm contains other organelles, which include the endoplasmic reticulum, the small granule components of cytoplasm, and several large vacuoles (Sager and Palade, 1957). A more detailed description of selected main structures and their functions follows.

Most *C. reinhardtii* are oval-shaped with a cell size ranging from 5 to 10 µm. This species consists of two **flagellae** with a diameter of approximately 250 nm. The flagella consist of fibres or filaments, the primary function of which is to provide movement (Sager and Palade, 1957; Harris, 2009). Both circular and elongated mitochondria are found, with a size ranging between 200 and 300 nm in diameter. Some are located between the chloroplast and cell membrane, while others are scattered throughout the chloroplast cavity around the nucleus (Sager and Palade, 1957). The **nucleus** is usually centrally located with a prominent nucleolus (Harris, 2009). The **nucleolus** appears as a spherical or ovoid body approximately 2 µm in diameter (Sager and Palade, 1957).

The **chloroplast** is a single cup-shaped organelle that may partially surround the nucleus organelle, and occupies approximately half of microalgal cell volume (Sager and Palade, 1957). The primary role of the chloroplast is to conduct photosynthesis, while the photosynthetic pigment chlorophyll within captures energy from sunlight and stores it in the energy storage molecules – namely adenosine triphosphate (ATP) and nicotinamide

adenine dinucleotide phosphate (NADPH) (Engel *et al.*, 2015). Different regions of the microalgae chloroplast are associated with specific functions: carbon fixation is performed in the pyrenoid at the base of the chloroplast cup, while the sides of the cup (known as lobes) are thought to contain mature thylakoids that perform the light reactions of photosynthesis (Bohn, 2008).

The **pyrenoid** has a spherical body with a diameter of 1.2 to 2 µm (Sager and Palade, 1957). This organelle performs starch synthesis. The synthesised starch grains are large, elongated bodies (100 x 400 nm) which are stored in the plates surrounding the pyrenoid. However, under stress or other certain conditions, they can also appear elsewhere in the cell (Sager and Palade, 1957; Harris, 2009).

Lipid bodies or oil bodies are cytoplasmic lipid globules that exhibit a round shape, with a size ranging between 0.1 and 8 µm. Lipid body structure consists of hydrophobic core -neutral lipids surrounded by a hydrophilic phospholipid monolayer membrane interspersed with amphiphilic oleosin protein (Gray *et al.*, 2010 ; Chamila and Gray, 2014). The size and composition of lipid bodies can change during the periods of normal growth, and they can disappear or only exist in small organelles. However, lipid bodies can be abundant under stress conditions in culturing media (Chamila and Gray, 2014). Furthermore, *C. reinhardtii'* s **cell wall** does not contain cellulose to make it hard and inflexible like other plants cells. The detail of *C. reinhardtii* explain in the following section.

2.1.2 *C. reinhardtii* Cell Wall Characteristics

Cell walls are highly complex structures which perform a great diversity of functions during the life cycle of the plant (Brett and Waldron., 1996). In plant food tissues, the physicochemical structure and properties of cell walls influencing bioaccessibility (Noah *et al*., 1980; Tovar *et al*., 1991; Waldron *et al*., 1997; MacDougall and Selvedran, 2001; Sarah *et al*., 2008). Therefore, to study factors that affect bioaccessibility it is necessary to have a basic understanding of the physical and chemical of cell wall.

Microalgae cell walls range from cellulose–pectin complexes to ones made of glycoproteins (Domozych *et al*., 2012). It is remarkable that glycoproteins are comparable to HRGPs of higher plants, but the sugar composition and molecular organization are distinct (Miller *et al*., 1974). Sugar comprises approximately 57.1% of the cell wall. Amino acids account for another 10.2%, with hydroxyproline being the predominant one. In combination with lipid (6.9%), ash (10.2) and moisture content (8%), these various constituents make up about 92.4% of the *C. reinhardtii* cell wall**).** The chemical composition of the *Chlamydomonas* 's cell wall show in **Table 2.2** (Miller *et al*., 1974).

Table 2.2 : The chemical compositions of the *Chlamydomonas* 's cell wall (Miller *et al*., 1974).

Compositions	% Dry weight
Arabinose	24.8
Galactose	19.6
Mannose	1.4
Xylose	2.2
Glucose	1.8
Uronic acid (calculated as galacturonic acid)	5.3
Unknown sugars	2.0
Hydroxyproline	3.0
Other amino acids	7.2
Lipid	6.9
Ash	10.2
Moisture content	8.0
Total accounted	**92.4**

The HRGPs are the major proteinaceous components of the cell wall of *C. reinhardtii* (Roberts *et al*, 1985; Ferris *et al*., 2001). Generally, HRGPs are widespread, existing in a variety of plant species (Showalter, 1993; Kieliszewski and Lamport, 1994). The HRGPs family contains three major subgroups: repetitive Pro-Rich Proteins (PRPs), extensins (EXT) and ArabinoGalactan Proteins (AGPs) (Kieliszewski and Shpak, 2001; Kieliszewski *et al*., 2010).

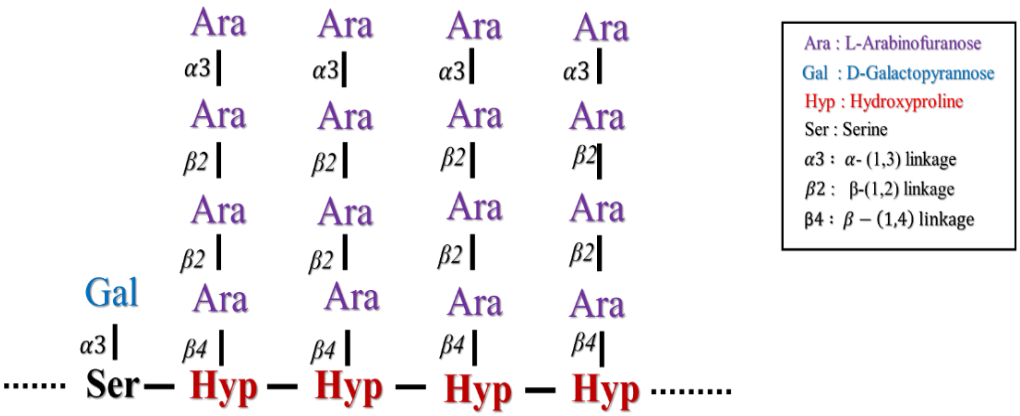


Figure 2.3: The structure of the hydroxyproline-rich region of EXTs and their intermolecular bonds. This scheme was modified from the original figure published in Marzol *et al.*, (2018).

The *C. reinhardtii* cell wall is almost entirely built up from extensin-like HRGPs (Green and Lowther, 1959). EXT **(Figure 2.3)** characterized by the motif Ser(Hyp)$_{3\text{-}5}$ – repeats throughout the protein, with most of the amino acids being glycosylated (Roberts *et al*., 1985; Marzol *et al*., 2018). The Ser is glycosylated with a single *D*-galactose unit while the Hyp residues are usually glycosylated through an *O*-glycosidic linkage with chains up to five units of *L*-arabinofuranose (Roberts *et al*, 1985; Marzol *et al*., 2018) When EXT are secreted into the cell wall, they quickly become ionically bound to acidic polysaccharides; later, they become covalently cross-linked within the wall, as evidenced by their inextractability in salts and Sodium Dodecyl Sulphate (SDS) (Fry, 1982).

The EXT molecule also contains tyrosine residues which enable them to behave as self-assembling units and form a three-dimensional network organized by inter- and intra-Tyr linkage intermolecules (Kieliszewski *et al*., 2010;. Marzol *et al*., 2018). Chemistry of an EXT cross-linking is still unclear. Hypothetically, there are three types of covalent bridge occurring: isodityrosine (Idt), di-isodityrosine (di-Idt) (Brady and Fry, 1997) or

pulcherosine (Brady *et al*, 1998). Their derivatives and roles in EXT cross-linking are described below.

Isodityrosine (Idt) serves as a short intramolecular linkage in EXT sequences containing Tyr-Tyr-Tyr or Tyr-Lys-Tyr motifs (Epstein and Lamport, 1984). Idt initially thought to occur by an oxidatively coupled dimer of Tyr (Fry, 1986). Two tyrosine units joined by a diphenyl-ether bridge was named isodityrosine, an isomer of dityrosine (Fry, 1986) **(Figure 2.4). Di-isodityrosine (di-Idt)** There are two possible routes for the conversion of isodityrosine to di-isodityrosine, either by oxidatively coupling of two molecules of isodityrosine (Idt) or via pulcherosine by the addition of single tyrosine residues (Brady, Sadler and Fry, 1998). These compounds are only involved in intermolecular cross-linking (Brady *et al*., 1996; Velasquez *et al*., 2015) **(Figure 2.4 and Figure 2.5). Pulcherosine** is formed by linking of a Tyr through its phenol group to an Idt unit (Brady *et al*., 1998). They can cross-link Idt motifs and 'free' Tyr residues between peptide chains, thereby providing another candidate for intermolecular cross-linking for EXT (Brady *et al*., 1998) **(Figure 2.5).** The schematics for the EXT chains and Tyr interaction cross-link type are also illustrated in **Figure 2.6.**

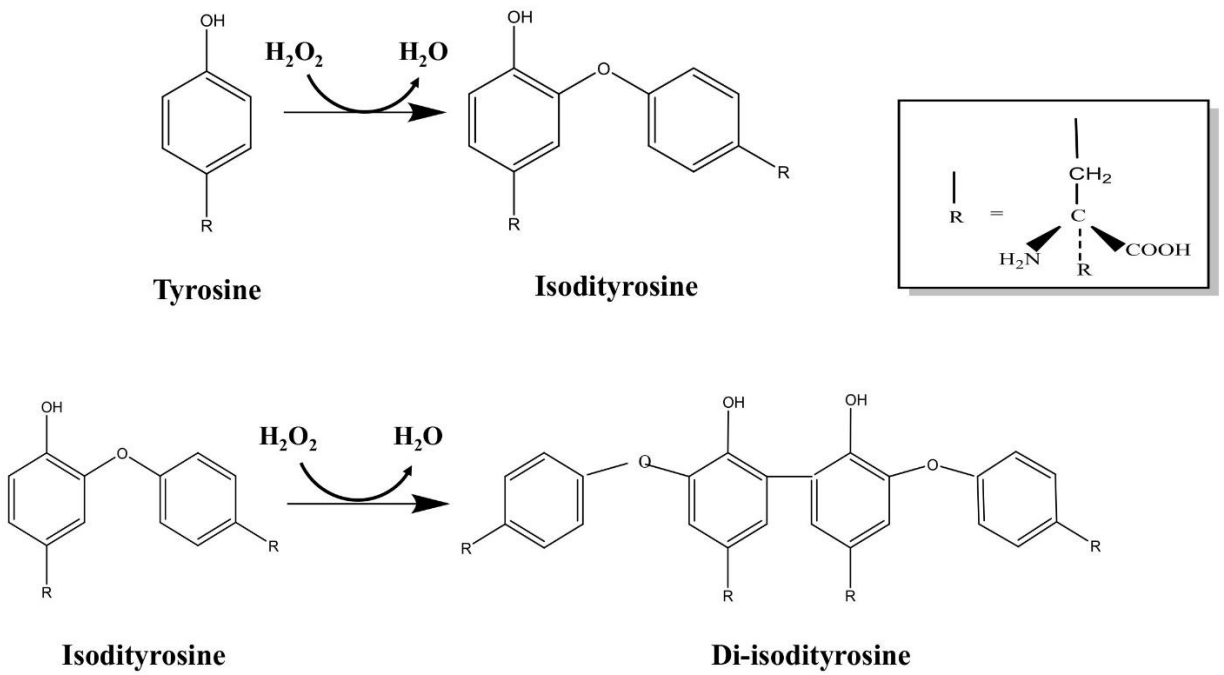


Figure 2.4: Chemical structures and possible in *vivo* reaction for the formation of Idt (isodityrosine) and Di-Idt (di-isotyrosine) from Tyr (tyrosine) (Brady and Fry, 1997). They is initially thought to occur by an oxidatively coupled dimer of Tyr and isodityrosine (isodityrosine (Idt)) that can be generated quickly and leads to both inter - and intra- polypeptide cross-link (Fry, 1986).

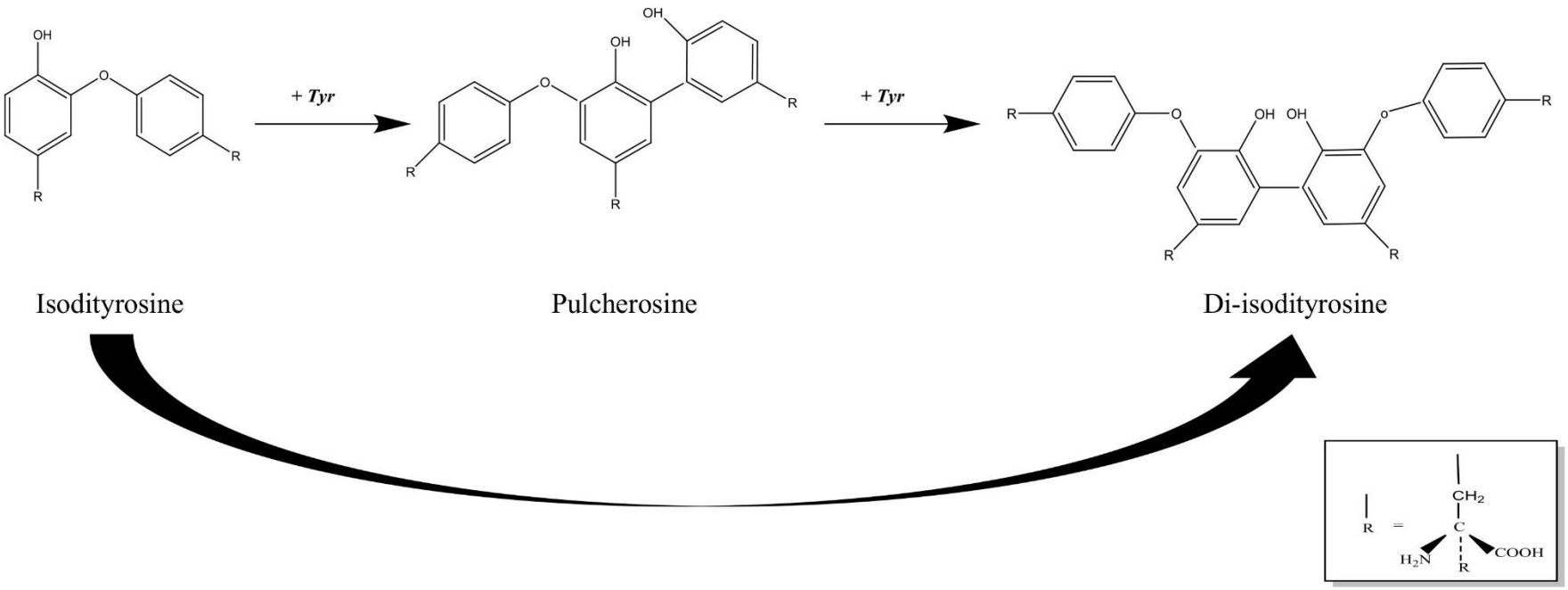


Figure 2.5: The proposed structure of pulcherosine and Di-Idt. Pulcherosine formed by linking of a Tyr through its phenol group to an Idt unit. There are two possible routes for the conversion of isodityrosine to di-isodityrosine, either by direct coupling of two molecules of isodityrosine (Idt) or via pulcherosine by the addition of single tyrosine residues (Brady *et al*., 1998)

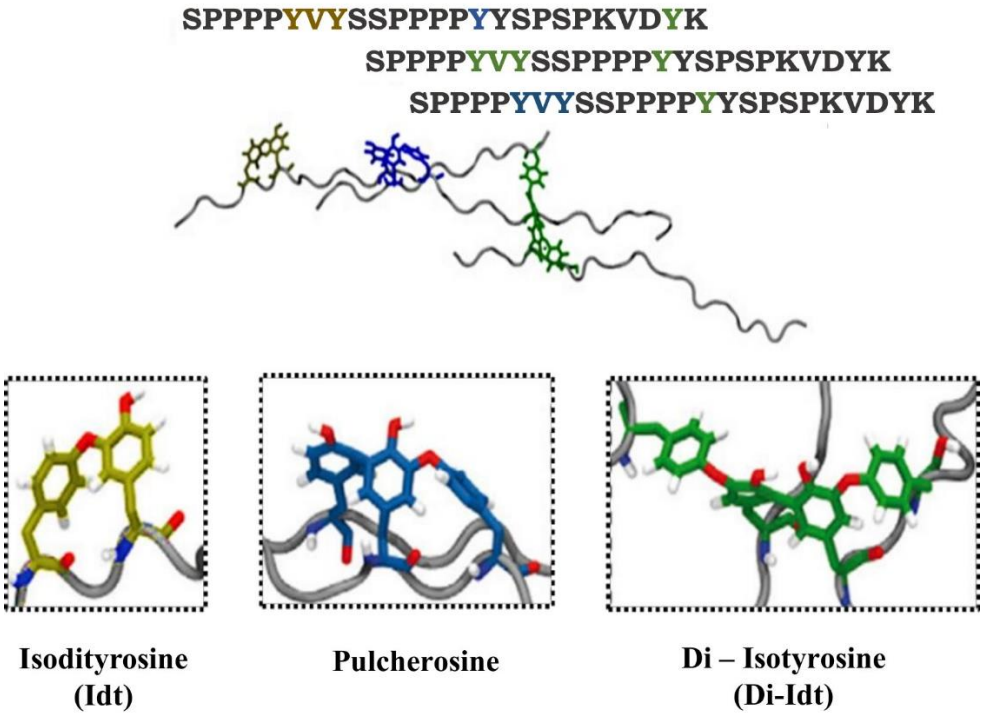


Figure 2.6: Schematics for the lateral alignment of EXT chains and Tyr interchain cross-link types. This scheme was modified from the original figure published in Velasquez *et al.*, (2015). The EXT possibility is facilitating the formation of isodityrosine from alternating Tyr residues on YVY motifs. (Velasquez et al., 2015). The bonds are represented in colours: yellow represent isodityrosine (Idt), blue represents pulcherosine and green represent Di-Isotyrosine (di-Idt).

The inter and intra bond mentioned above arrange EXT together and form the cell wall layer. The *C. reinhardtii* cell wall comprises seven layers **(Figure 2.7).** The innermost layer (W1) contains 16.4% hydroxyproline and 60% carbohydrate, of which the major sugars are galactose and arabinose. This layer is 20–200 nm in thickness (Roberts *et al.*, 1985) and insoluble in chaotropic agents such as sodium perchlorate, lithium chloride or urea (Harris, 2009). The middle layer, attached firmly to the outer face of the W1 layer, is termed the central triplets. The W2 and W6 contain two main glycoprotein species 2BI (glycine rich glycoprotein) and 2BII (hydroxyproline rich glycoprotein) are common, being a back-to-back sandwich forming a central triplet layer. Layer W3 and W5 are electron-transparent regions that are probably spaces rather than true wall components (Goodenough and Heuser, 1985). W4 is the beaded structure which contain an extensive grid-shaped framework of polygonal plates consists mainly of the mentioned glycoproteins (Adair *et al.*, 1987). The outer layers (W7) display fibre-like structures. The thickness of the outer layer varies, since it includes components that the cell takes up from its surroundings (Roberts *et al.*, 1985; Adair *et al.*, 1987).

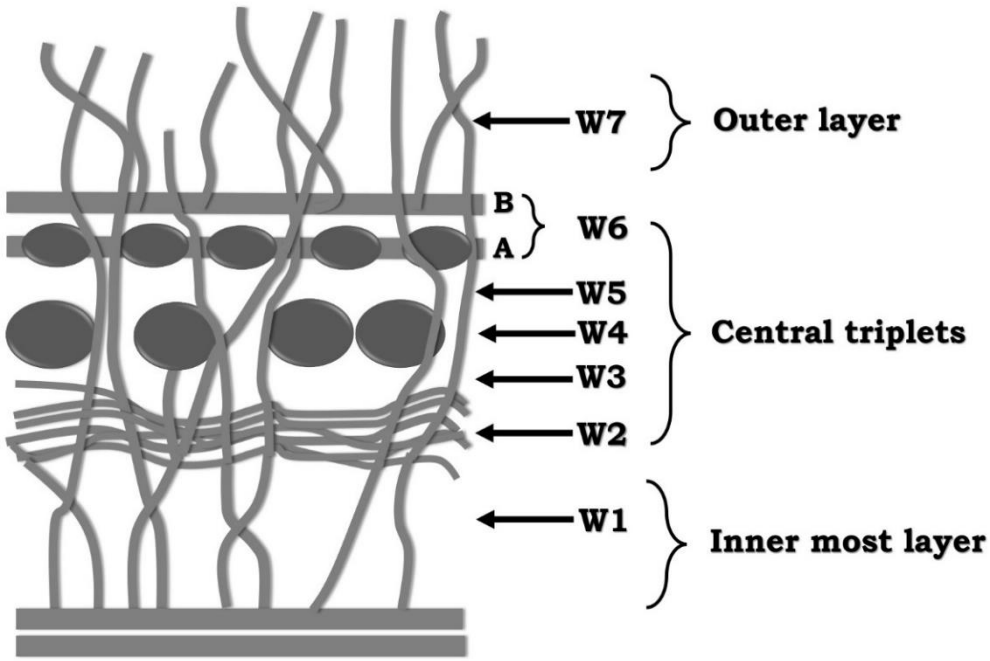


Figure 2.7: The diagrams of the *C. reinhardtii* cell wall based on the thin section studies of Goodenough and Heuser, (1985). The EXT were then linked by both the inter- and intra- linkage forming multilayer seven layers of the walls with distinctive structures. The innermost layer is W1 which contain hydroxyproline and sugar. The W2 to W6 encompass two main glycoprotein species 2BI (glycine-rich glycoprotein), and 2BII (hydroxyproline-rich glycoprotein) are common, being a back-to-back sandwich forming a central triplet layer, though, W3 and W5 are spaces. The outer layers (W7) show fibre-like structures. Their thickness could be varied as influenced by constituents that the cell takes up from its environments.

2.1.3 Reproduction

The photosynthesis mechanism occurs by light energy from sunlight, which is absorbed by pigments and converted into chemical energy using carbon dioxide and water, as per the following equation:

$$6CO_2+12H_2O+\text{Nutrients}+\text{Energy from light sources} \rightarrow C_6H_{12}O_6+6O_2+6H_2O$$

The biomass production potential of *C. reinhardtii* over a given time is much higher than other plants due to its short generation time and ability to reach high cell densities (Harris, 2001). Under favourable growth conditions, *Chlamydomonas* reproduces asexually, and only reproduces sexually when conditions are unfavourable (Hallmann, 2010). The stages of microalgae reproduction are illustrated in **Figure 2.8.** Briefly, during asexual reproduction, cells grow and undergo two or more rounds of mitosis and cytokinesis before daughter cells hatch from the old cell wall. Mating types include the plus mating type (mt+) **(Figure 2.8a)** and the minus mating type (mt-) **(Figure 2.8b),** which exhibit identical asexual life cycles. Sexual reproduction **(Figure 2.8c)** is induced by unfavourable conditions (nitrogen limitation), and asexual cells of both mating types develop into gametes. Gametes of opposite mating types can form aggregates via flagellar agglutination. After the release of cell walls, mating structures are built, and the gametes fuse (plasmogamy and karyogamy) to create a zygote. The zygote further matures into a dormant and diploid zygospore. During spore germination, meiosis occurs to form four haploid progeny cells (two of each mating type), each of which grows into an asexual cell of the respective mating type (Hallmann, 2010).

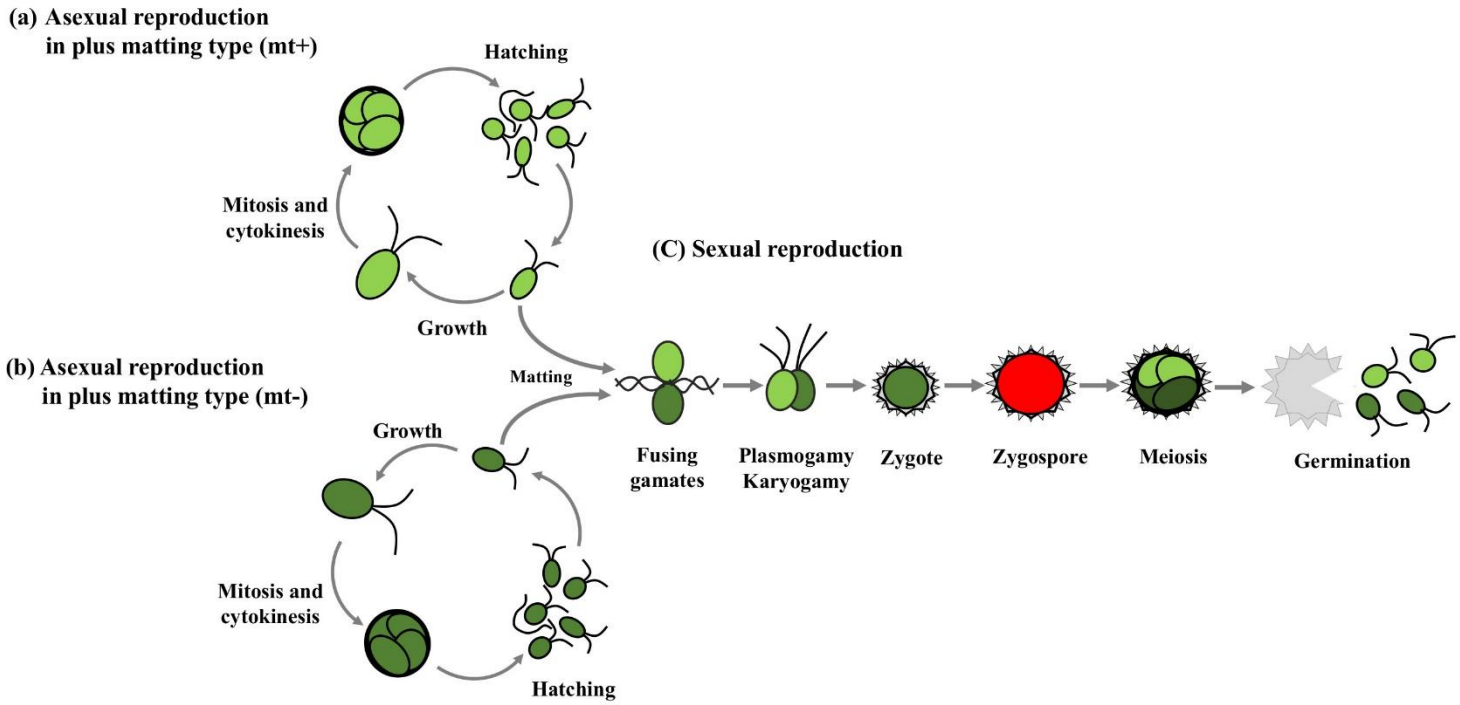


Figure 2.8: Stage of the microalgae reproduction process (Hallmann, 2010).

The microalgae growth pattern can be divided into six stages depending on cell reproduction rate: (1) lag phase, (2) exponential phase, (3) linear phase, (4) declining growth phase, (5) stationary phase, and (6) death phase, where the exponential phase represents the maximum growth rate under the specific conditions **(Figure 2.9)** (Lee *et al.*, 2015).

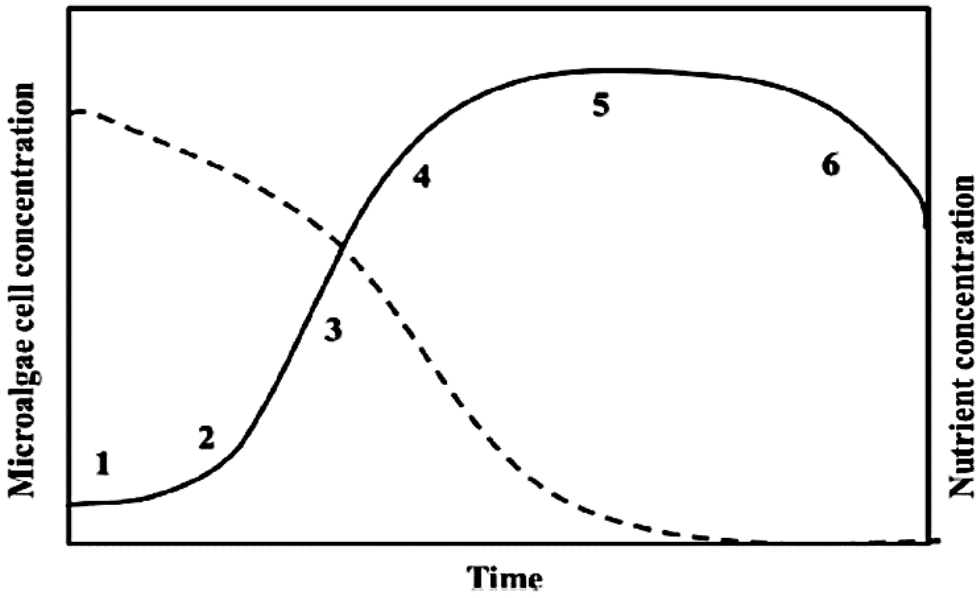


Figure 2.9: Growth phases in microalgae batch culture (solid line) and Nutrient concentration (dashed line): (1) lag phase, (2) exponential phase, (3) Linear phase, (4) declining growth phase, (5) stationary phase, and (6) death phase (Lee *et al.*, 2015).

Once suitable climatic conditions and sufficient nutrients are present, microalgae can grow abundantly. Commonly, microalgae doubles in biomass within 3.5 h or 24 h during the exponential growth phase (Chisti, 2007). Furthermore, microalgae grown in batch culture undergo predictable changes in growth rate as nutrient levels decline over time,

exhibiting high cell density during the logarithmic phase where nutrients in the culturing media sufficiently support high rates of growth (Fredriksson and Nystrom, 2006).

Thereafter, cells division terminates, and cell numbers do not change during the stationary phase, which lead to senescence phase in which cells endure metabolic and structural changes that can result in death and a subsequent reduction in cell numbers. The mechanisms of microalgae senescence may play an essential role in nutrient recycling and survival. Senescence refers to the term of transition from the log-phase to the stationary phase, where division ceases and cell numbers are maintained. During this phase, cells undergo metabolic and structural changes that can lead to death and a reduction in cell numbers (Fredriksson and Nystrom, 2006; Humby *et al*., 2013). The significant biochemical composition established throughout all microalgae growth stages permits harvesting at any stage, depending on the intended use. Annamalai and Nallamuthu (2014) determined that the growth curve of microalgae *C. vulgaris* and *C. reinhardtii* exhibited a steady increase in slope up to the 25th day of outdoor culturing. Among pigments of both the cultures, *C. vulgaris* cells revealed richer pigmentation than *C. reinhardtii*. Primary and secondary metabolites were also assessed at periodic intervals of 5 days in both species. Both cultures were a rich source of primary proteins and lipids as well as secondary metabolites. Humby *et al*., (2013) identified that photosynthetic proteins LHCII, D1, PsaA, Cyt f, RuBisCO, and a LHC-like protein (LHCSR) began to decrease as cells entered the stationary phase and reached their lowest levels in the mid-death phase in *Chlamydomonas* cultured using mixotrophic batch culturing.

2.2 Bioprocessing and Bio-products

Microalgae cultivation is the sum of procedures and techniques to produce the feedstock biomass that is subsequently refined to obtain valuable products. Therefore, prospecting, selecting, or developing a strain (by genetic or metabolic engineering) together with microalgae cultivation, and growth medium preparation belong to the "upstream" part of the entire process of biomass harvesting, while de-watering, extraction of valuable compounds, transformation and purification belong to the "downstream" part of the bioprocess (Octavio and Yoav, 2015). **Figure 2.10** presents an overview of the complete biorefinery process and highlights where the microalgae cultivation step fits (Perez-Garcia and Bashan, 2015).

2.2.1 Cultivation

Most of the *Chlamydomonas* species are obligate phototrophs with the exception of *C. reinhardtii* which is a facultative heterotroph. This means *C. reinhardtii* can produce and accumulate compounds in the presence of both light and dark. In the dark it can use acetate as a carbon source, when present, whereas in the presence of light it can do photosynthesis (Harris, 2001). Three significant modes have been adopted for this species: photoautotrophic (photosynthesis with CO_2 as a carbon source), heterotrophic (organic compounds as the energy and carbon source), and mixotrophic (light as the energy source and inorganic compounds as the carbon source) (Harris, 2009; Prokop *et al.*, 2015). The growth of microalgae under mixotrophic conditions is the most flexible method of gathering both carbon and energy demand simultaneously using organic and inorganic carbon sources and light (Prokop *et al.*, 2015). *C. reinhardtii* can be cultured in the laboratory in either liquid culture or on agar, and many culture recipes have been

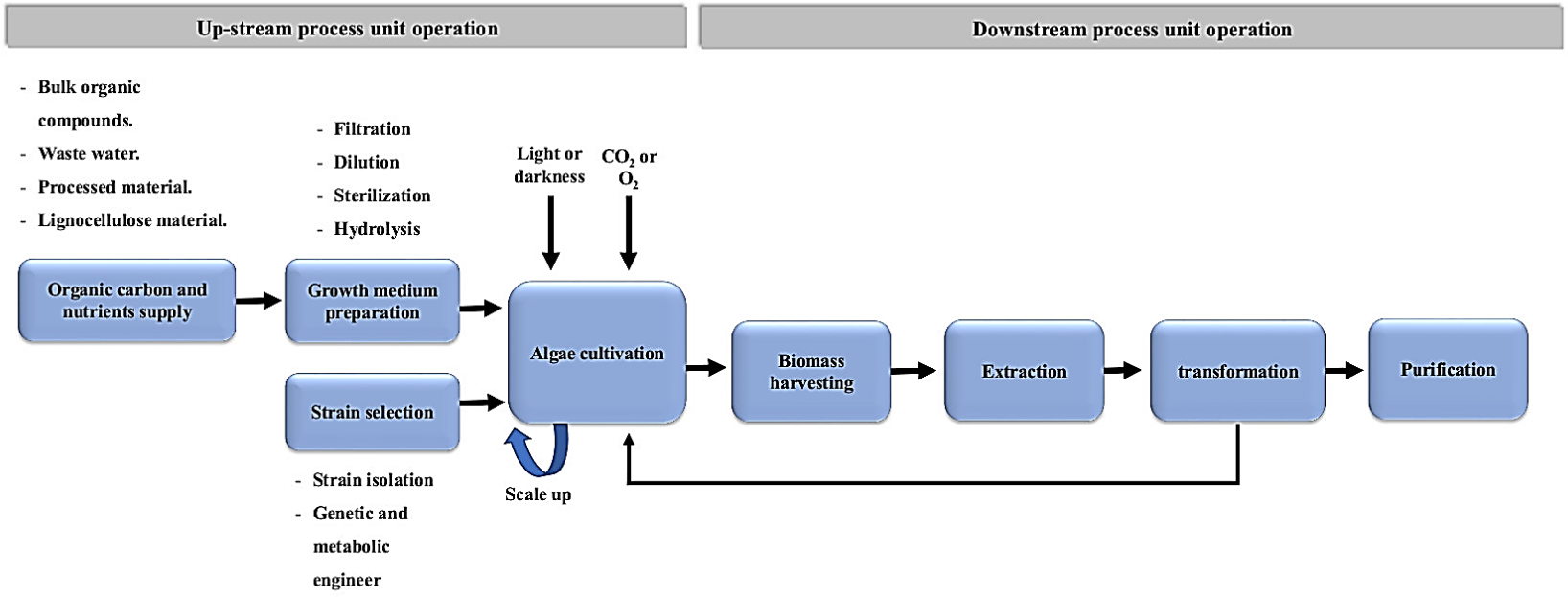


Figure 2.10: Overview scheme of algae bio refinery process. Each box represents a specific unit operation (a part of the overall multi-step process with a specific functional) achieved by a specific sub-process, arrow represent flow of mater or energy and bullet points above and below boxes specify sub-processes varieties or methods (Perez-Garcia and Bashan, 2015).

Table 2. 3: Comparable of difference culturing media.

Component	Sager-Granick	Eversole	Sueoka	Kuhl	Bold	TAP
Major component (mM)						
NH_4^+	3.7	93.5	9.35	6 x 10^{-5}	-	7.48
K^+	1.88	0.52	22.12	10.0	2.70	1.94
Na^+	5.1	0.027	0.27	5.5	3.37	0.27
Ca^+	0.36	0.09	0.068	0.10	0.17	0.34
Mg^{2+}	1.2	2.03	0.081	1.0	0.30	0.41
Fe^{3+}	0.37	-	-	-	-	-
NO_3^-	3.7	-	-	10.0	2.94	-
Cl^-	1.83	112.9	9.55	0.20	0.78	8.22
SO_4^{2-}	1.2	2.03	0.182	1.03	0.38	0.51
PO_4^{3-}	1.31	0.115	13.6	5.0	1.72	1.0
Tris	-	50.0	-	-	-	20.0
Citrate	1.7	-	-	-	-	-
Acetate	-	-	-	-	-	17.4
Trace composition						
Fe^{2+}	-	1.79	17.9	25	17.9	17.9
Zn^{2+}	3.5	7.65	76.5	1.0	30.7	76.5
Cu^{2+}	.25	0.63	6.3	0.01	6.3	6.3
$Co2^+$	.84	0.68	6.8	-	1.7	6.8
Mn^{2+}	2.0	2.56	25.6	1.0	7.3	25.6
Mo^+	0.82	0.62	6.2	0.07	4.9	6.2
Bo_3^{3-}	16	18.4	184	1.0	184	184
EDTA	-	13.4	134	25	171.1	134

proposed for this species **(Table 2.3)**. Primary growth medium composition for mixotrophic culturing is similar to phototrophic and heterotrophic systems, with the sole exception of adding an inorganic carbon source (Prokop *et al*., 2015). Namely, Tris-Acetate Phosphate (TAP) media has been utilised for the culturing process, as it is well-buffered and relatively low in phosphate, making it the optimal medium for *C. reinhardtii* cultivation (Harris, 2009).

Chlamydomonas can perform photosynthesis using both the active carbon dioxide (CO_2) and hydrogen carbonate ion (HCO^-_3) uptake system, where CO_2 diffusion is much slower than in terrestrial environments and HCO^-_3 frequently becomes the dominant inorganic carbon (Ci) species. Both uptake systems enable switching between different modes of Ci acquisition. Therefore, they can more rapidly adapt to environments that are continually changing in both level and Ci type (Baroukh *et al*., 2013).

In mixotrophic cultivation, microalgae generate chemical energy from Ci through photosynthesis, and utilise organic carbon sources such as glucose, acetate, glycerol, fructose, maltose, and sucrose (Zhang *et al*., 2011). Desired product is not only a nutrient-dependent process, but also relies on the suitability of other environmental factors – particularly temperature and light intensity. For example, *Chlamydomonas* grows well at temperatures between 20 and 25 ºC. Moreover, they can tolerate temperatures as low as 15 ºC, and as high as 35 ºC. Furthermore, a light intensity of 200-400 µmol $m^{-2}s^{-1}$ is optimal. Notably, it is possible to control light energy in photo-bioreactors by varying the number of fluorescent lamps, irradiance, and the distance between lamps and the

bioreactor's surface (Prokop *et al.*, 2015). Mixotrophic culturing will also benefit from bubbling with sterile air without CO_2 addition.

Large-scale microalgae cultivation can occur in either open or closed photobioreactor systems (FAO., 2012; Singh *et al.*, 2011). *C. reinhardtii* have been introduced into outdoor cultivation systems to test the viability of the strain as a producer of biomass (Schoepp *et al.*, 2014), biohydrogen (Scoma *et al.*, 2012) and even high-value bio-products (Manuell *et al.*, 2007). Continuing studies are still vital for understanding and addressing the challenges of bringing *C. reinhardtii* laboratory strains into commercial production.

2.2.2 Bio-products

Notably, microalgae have been used in a variety of food and nutraceutical products in response to the current demand for consumer health products. The health benefits of microalgae, which include antioxidant activity and prevention of cataracts, age-related macular degeneration, inflammation, and cancer, put them on the superfood list (Lunn, 2006; Chacón-Lee and González-Mariño, 2010). Thousands of microalgae species are described in the literature, but only a handful of genera and species are currently produced commercially. Some species, such as *Chlorella sp., Dunaliella sp., Spirulina sp., Haematococcus pluvialis, Phaeodactylum tricornutum, Skeletonema costatum, Isochysis galabana, Oscillatoria sp., Thalassiosira sp., Nostoc sp.*, have been accepted by consumers (Pereira and Neto, 2015). *C. reinhardtii*, a freshwater green microalga, is also safe for human consumption and categorised as generally recognised as safe (GRAS) by

the Food and Drug Administration of United States of America (US FDA); it does not contain toxins and human pathogens such as viruses or prions (Griesbeck *et al.*, 2006 ; Murbach *et al*., 2018).

As with any higher plant, the chemical composition of algae is not an intrinsic constant factor but varies over a wide range of environmental factors (Gouveia *et al.*, 2008). The indicative values of chemical compositions of *C. reinhardtii* compared to other species of algae and conventional food sources are shown in **Figure 2.11.** It is shown that protein is the key composition in *C. reinhardtii*. Their protein level is comparable to other commercial algae and cyanobacteria species and some conventional food stuffs. However, to the best of our knowledge, *C. reinhardtii* has not been previously used as a food ingredient or nutritional supplement. Therefore, continue research to establish the credentials for using *C. reinhardtii* as a food source is vital.

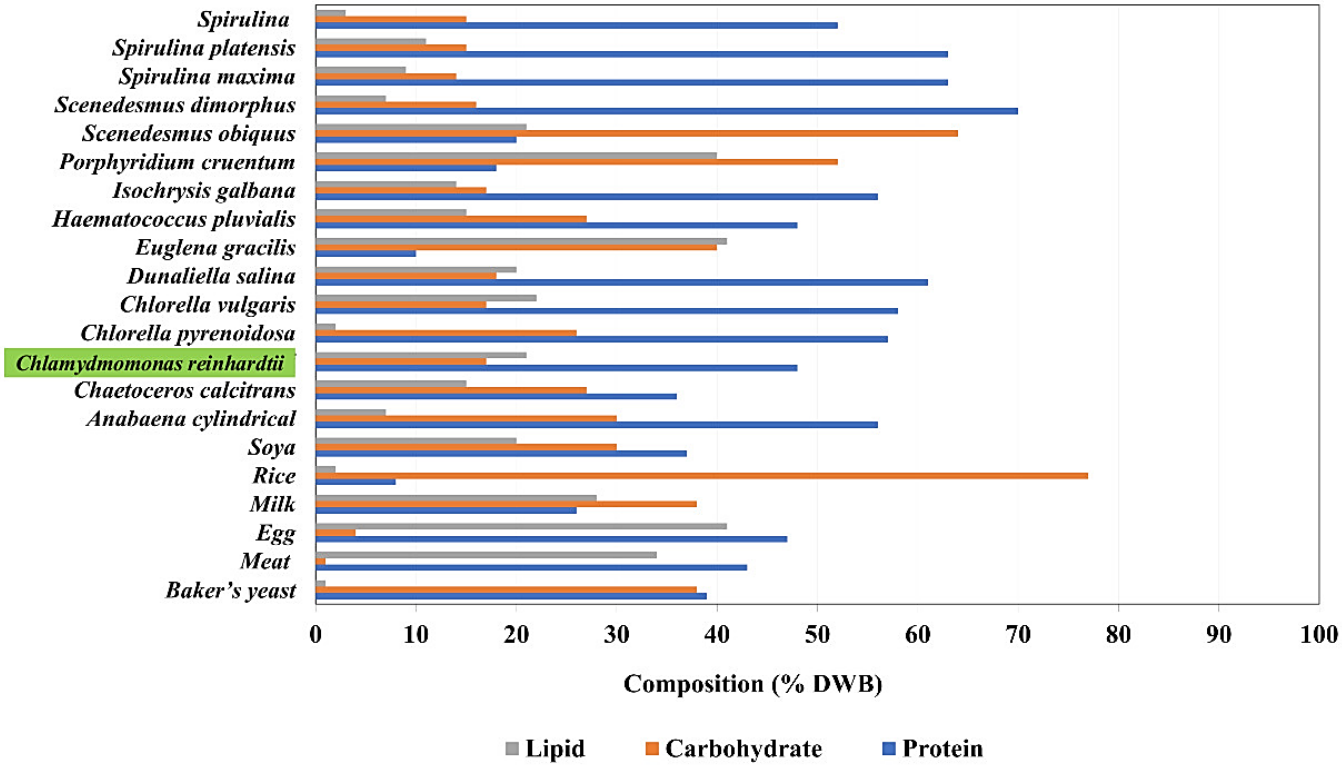


Figure 2.11: General compositions of difference algae species and cyanobacteria compare to conventional food sources (%DWB) (Spolaore *et al.*, 2006; Natrah *et al.*, 2007; Gouveia *et al.*, 2008).

2.2.2.1 Protein

The thylakoid membranes are the sites of photosynthetic light reactions and functional proteins unique to microalgae (Vaughn, 2013). According to (Schwenzfeier *et al*., (2011) microalgae do not accumulate distinct storage proteins, but instead, contain many different types of protein. Since microalgae are photosynthetic organism most proteins present be expected to be enzymes involved in photosynthesis or other essential activities for survival and growth. Ribulose-1,5 bisphosphate carboxylase/ oxygenase (RuBisCO) is an enzyme complex that catalyses the first significant step in carbon fixation. It is densely-packed inside the chloroplast stroma at a concentration of approximately 300 mg/mL (van de Velde *et al*., 2011; Suarez Ruiz *et al*., 2018). These enzymes (e.g. RuBisCO) can consist of multiple polypeptide chains (Schwenzfeier *et al*., 2011). Microalgae protein is likely to be dominated by globular and membrane-associated protein (Cavonius, 2016). For a protein to be considered high- quality, it must contain the essential amino acids at or above concentrations as determined by the World Health Organization (FAO/WHO/UN, 2007). The concentration of amino acids may range and depend on the source of origin. The amino acid compositions of *Chlamydomonas* compared to selected plant and algae are illustrated in **Figure 2.12** and **Figure 2.13** Amino acid composition determines the protein quality of algae. The reviewed data of McCusker *et al.* (2014) reveal that the levels of the essential amino acids in *Chlamydomonas* was either similar to, or greater than, the levels of the same amino acids in the reference foods, thus indicating a high protein quality. These might be maintained by the control of growth condition.

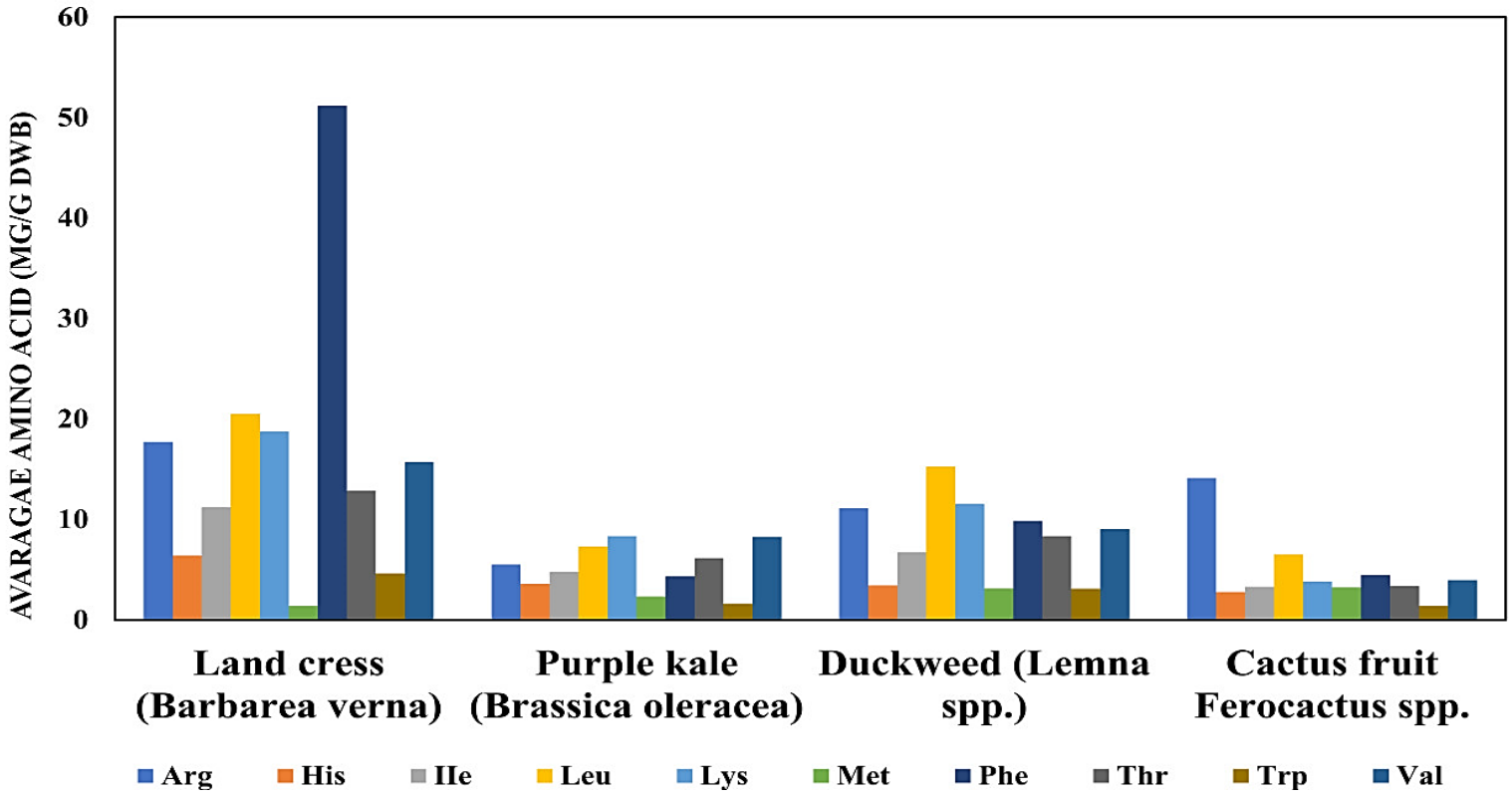


Figure 2.12: Essential amino acids of selected plants (McCusker *et al.*, 2014).

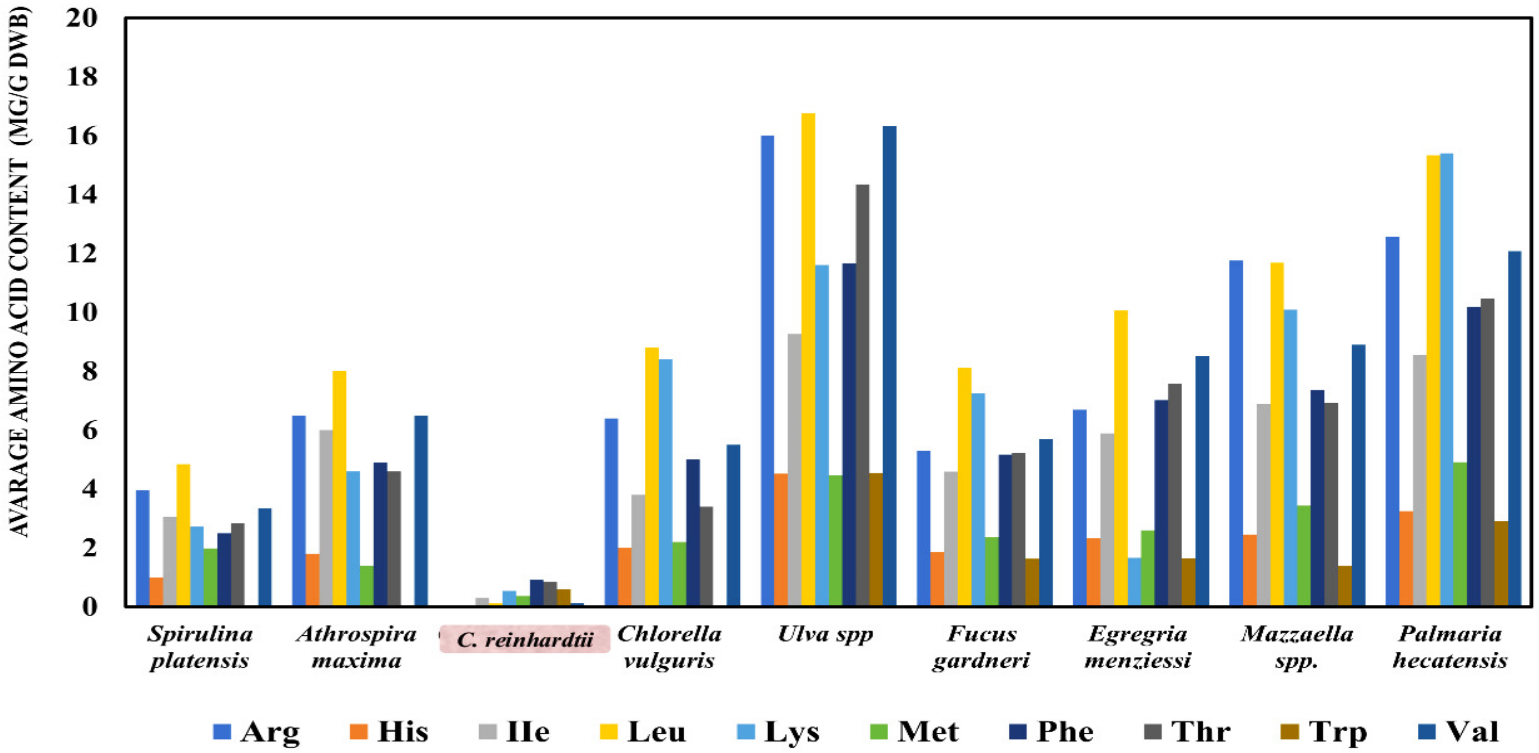


Figure 2.13: Essential amino acids of *C. reinhardtii* compare to other species of fresh water microalgae, selected marine microalgae and cyanobacterial (McCusker *et al.*, 2014).

2.2.2.2 Lipid

Lipids present in microalgae can be classified into two groups. Storage lipids (non-polar lipids) or triacylglycerols (TAGs) primarily consist of saturated FAs, and some unsaturated FAs. Structural lipids naturally possess heightened amounts of polyunsaturated fatty acids (PUFAs) (Sharma *et al*., 2012). The most abundant lipid class in microalgae is glycolipid In thylakoid membranes, the majority (80–90%) of lipids are glycolipids including monogalactosyldiaclyglycerol (MGDG; 40–50% of thylakoid membrane lipids), digalactosyldiacylglycerol (DGDG; 20–30%), and sulfoquinovosyldiacylglycerol (SQDG; 20–30%) (Harwood and Jones, 1989). The structure of membranes and storage lipids are presented in **Figure 2.14.**

Microalgae are the primary natural producers of omega-3 long chain polyunsaturated fatty acid (LC-PUFA), the biosynthesis of which begins with α-linolenic acid (ALA). When humans consume microalgae, omega-3 short chain poly unsaturated fatty acid (SC-PUFA) is converted to omega-3 LC-PUFA, though this process varies by individuals (Abedi and Sahari, 2014). The health benefits associated with LC-PUFA particularly stem from eicosapentaenoic acid (EPA, 20:5 n-3), docosapentaenoic acid (DPA, 22:5 n-3), and docosahexaenoic acid (DHA, 22:6 n-3). Omega-3 LCPUFA exhibits physical health benefits for neuropsychiatric disorders including depression and dementia, reduces the risk of heart disease, and has a positive impact on the incidence of stroke and rheumatoid arthritis (Ruxton *et al*., 2004; Abedi and Sahari, 2014).

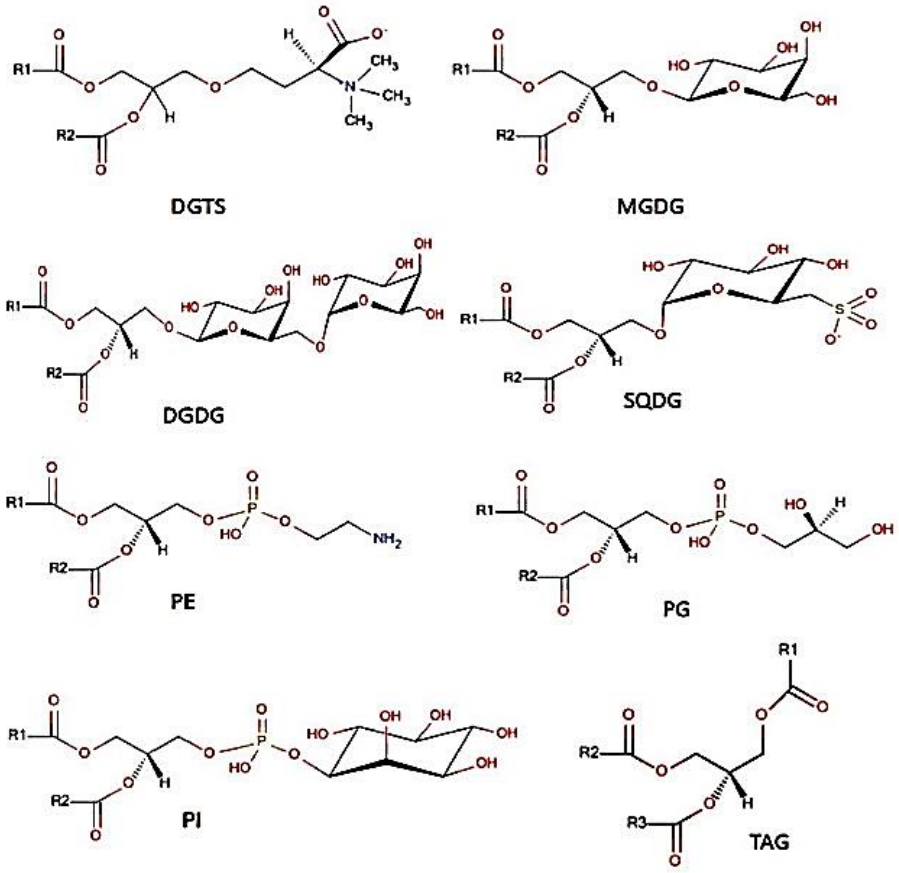


Figure 2.14: Common lipid species reported for *C. reinhardtii* cells. Labels R1, R2 and R3 represent different fatty acid acyl residues. Abbreviations: DGTS:Diacylglyceryltrimethylhomo-Ser, MGDG: monogalactosyldiacylglycerol, DGDG: digalactosyldiacylglycerol, SQDG sulfoquinovosyldiacylglycerol, PE: phosphatidylethanolamine, PC: phosphatidylcholine, PG: phosphatidylglycerol, PI: Phosphatidylinositol, TAG : triacylglycerol (Yang *et al*., 2015).

Table 2.4: Fatty acid composition of difference species of algae. ND = not detect of present in very low amount (Nakamura and Beisson, 2016).

	Fatty acid composition (% of total)												
	14:0	16:0	16:1	16:2	16:3	16:4	18:1	18:2	18:3	18:4	20:4	20:5	22:6
Freshwater species													
Scenedesmus obliquus	1	35	2	ND.	ND.	15	9	6	30	20	-	-	-
Chlorella vulgaris	2	26	8	7	2	-	2	33	20	-	-	-	-
Chlamydomonas reinhardtii	1	21	4	1	4	23	7	6	31	2	-	-	-
Salt-tolerant species													
Ankistrodesmus sp.	ND.	13	3	1	1	14	25	2	29	2	-	1	-
Isochrysis sp.	16	15	4	1	1	-	21	5	4	17	nd	nd	9
Nannochlorsis atomus	1	20	10	4	15	-	5	10	22	3	2	3	Nd
Marine phytoplankton													
Monoshrysis lutheruu (Chrysophyceae)	10	13	22	5	7	1	3	1	nd	2	1	18	7
Olisthodiscus spp (Xanthophyceae)	8	14	10	2	2	1	4	4	6	18	2	19	2
Amphidinium carteale	3	24	1	1	nd	-	5	1	2	15	-	14	25
Dunaliella salina	Nd	41	15	nd.	-	-	11	8	19	-	-	-	-

Glycolipids have received increased attention due to their applications in various industries, including cosmetics, pharmaceuticals and food. Due to their amphiphilic characteristics, glycolipids are currently being used as a type of biosurfactant, which has received extensive attention (Kitamoto *et al* ., 2009). Notably, *C. reinhardtii* has received much attention in biofuel production. Various stress factors induce changes in the metabolic activities of a cell, such as activation of starch and accumulation of TAGs, which results in the gathering of lipid bodies in algae. Additionally, *C. reinhardtii* contains higher proportions of C16 and less C18 fatty acid than most plants. Furthermore, PUFA are typically absent or present in low levels for freshwater algae (Nakamura and Beisson, 2016) data shown in **Table 2.4.**

2.2.2.3 Pigments

2.2.3.3.1 Chlorophyll

There are two main types of chlorophyll, chlorophyll *a* and chlorophyll *b*. However, exposure of chlorophyll molecules to weak acids, oxygen or light accelerate their oxidation and result in the formation of numerous degradation products (Cubas *et al*., 2008; Humby *et al*., 2013). The skeleton of chlorophyll molecule is the porphyrin macrocycle, which comprises of four pyrrole rings (Humphrey, 1980). An attachment of a single isocyclic ring to one of the pyrrole rings gives rise to the phorbin structure (Humphrey, 1980). Each pyrrole ring contains four carbon atoms and one nitrogen atom. All of the nitrogen atoms face inward creating a central hole where a magnesium (Mg^{2+}) ion easily binds (Lennarz and Lane, 2004). In chlorophyll *b*, the methyl group in ring II of chlorophyll *a* is replaced by a formyl group (Cubas *et al*., 2008). This structural difference results in chlorophyll *a* being a blue/green pigment with maximum absorbance from 660 to 665 nm and chlorophyll *b* being a green/yellow with maximum absorbance from 642 to 652 nm (Humphrey, 1980) **(Figure 2.15).**

Most microalgae have chlorophyll *a*, but some may have chlorophyll *b* and *c*, such as *Dinophyta* (Barsanti and Gualtieri, 2014). Microalgae contain chlorophyll from 0.5 to 1.0% DWB (Spolaore *et al*., 2006). Amin *et al*., (2018) evaluated the chlorophyll concentration of the two microalgae species, *Chlorella* and *Nannochloropsis*. The microalgae was cultured with Conway medium under laboratory condition to get biomass for the further experiments. The concentration of chlorophyll *a* and *b* extract was evaluated by spectrophotometric. According to the results, *Chlorella* has chlorophyll *a* (8.45 µg/ml) and Chlorophyll *b* (4.33 µg/ml),

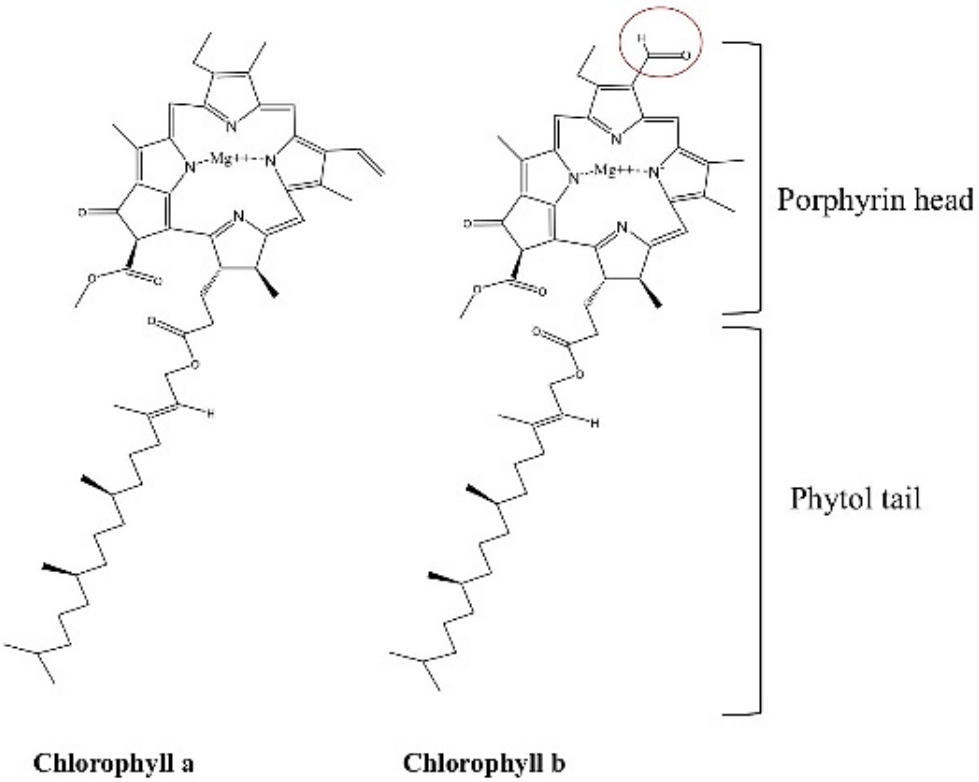


Figure 2.15: Chemical structure of chlorophyll *a* and chlorophyll *b* (Khanra *et al.*, 2018).

Nannochloropsis has chlorophyll *a* (21.24 µg/ml) and chlorophyll *b* (9.66 µg/ml) respectively. Annamalai and Nallamuthu (2014) monitor growth of the algal cultures at the regular intervals of 5 days. Measurement of growth and synthesis of metabolites found that the methanol extract of *C. reinhardtii* biomass shown highest chlorophyll *a* (4.02 mg/mL) and chlorophyll *b* content (4.02 mg/mL) at 15th and 10th day of cultivation. Chlorophyll have beneficial biological activities, such as antioxidant, anticancer, anti-inflammatory, anti-obesity, anti-angiogenic, and neuroprotective (Guedes *et al.*, 2011; Ciccone *et al.*, 2013).

2.2.3.3.2 Carotenoids

Carotenoids are a group of organic pigments produced in higher plants and other photosynthetic organisms (Sun *et al.*, 2016). Most carotenoids are bound to integral membrane proteins, which are associated with light-harvesting complexes (LHCs), where they absorb light across a broader range of the spectral region and transfer energy to chlorophyll, which initiates the photochemical events of photosynthesis (Polívka and Frank, 2010).

Different carotenoids are derived primarily via modification in base structure by cyclisation of the end groups and introduction of oxygen, which of provide them with their characteristic colours and antioxidant properties (Sun, *et al*., 2016). Three of these carotenoids, namely *α*-carotene, *β*- carotene, and *β*-cryptoxanthin, can be converted into retinol, and are thus referred to as provitamin A carotenoids. Lycopene, lutein, and zeaxanthin have no vitamin A activity, and are therefore referred to as non-provitamin A carotenoids (Dufossé *et al.*, 2005) **(Figure 2.16).** Di Lena *et al*., (2018) evaluated the carotenoid profiles of biomass from five eukaryotic microalgae, *Porphyridium cruentum*, *Isochrysis galbana*, *Phaeodactylum tricornutum*, *Tetraselmis suecica* and *Nannochloropsis gaditana,* produced at an industrial plant in outdoor photobioreactors. Results reveal that *β*-carotene was the only carotenoid common to all species. The Rhodophyta *P. cruentum* exhibited the lowest total carotenoid content (16.7 mg/100g DW). The *Haptophyta Isochrysis galbana* and the *Bacillariophyta Phaeodactylum tricornutum* were the species with the highest total carotenoid content (1760 mg and 1022 mg/100 g DW, respectively).

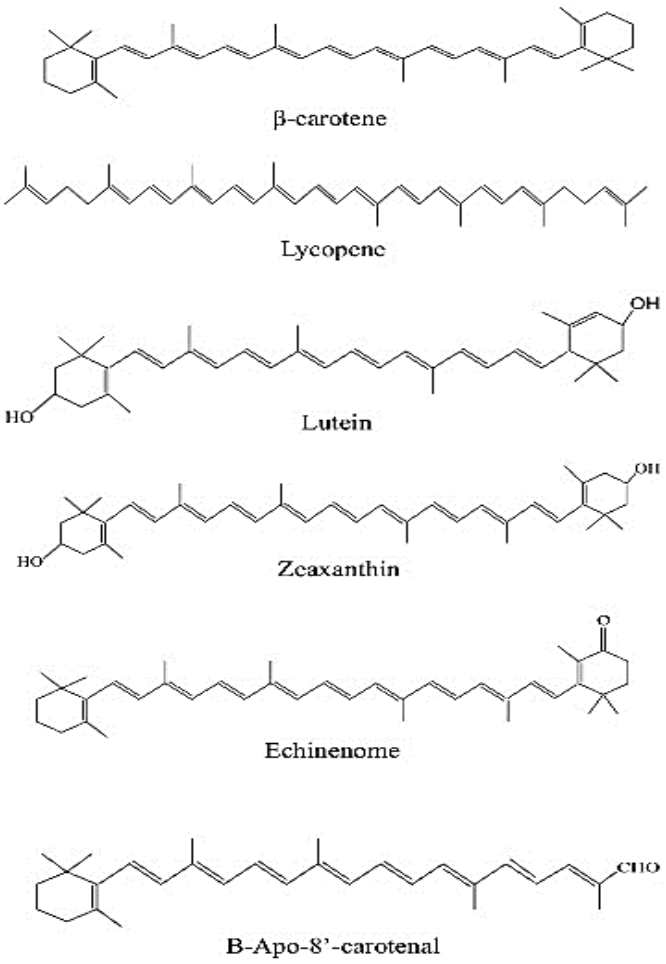


Figure 2.16: The structure of carotenoids obtain from algae (Dufossé *et al*., 2005).

The Chlorophyta *Tetraselmis suecica* was the species showing the greatest variety of carotenoids, with both α- carotene and β-carotene and their derivatives present. (All-E)-lutein (85.4 mg/100 g DW) and (all-E)-violaxanthin (81.8 mg/100 g DW) were the major pigments in this species. In the Ochrophyta *Nannochloropsis gaditana*, (all-E)-violaxanthin was the prevalent carotenoid (336.7 mg/100 g DW), followed by (all-E)-*β*-carotene (100.1 mg/100 g DW). Annamalai and Nallamuthu (2014) found that the highest carotenoid level in methanol extract of *C. reinhardtii* at the 4.03 mg/mL at 25th day of cultivation.

Currently, these natural pigments are preferred over synthesised substances, and are finding commercial applications – primarily in the food and feed industries. Carotenoid-rich extracts from *Scenedesmus almeriensis* at levels of 0.1 mg of extract per mL of olive oil, enhance the colour of olive oil, turning it orange-reddish. Additionally, the quality, shelf life, and nutritional value of olive oils were improved since peroxidation was inhibited, and *β*-carotene and lutein contents increased considerably alongside oxidative stability (Limón *et al*., 2015). Furthermore, biomass extracts from microalgae are also applied in biodegradable films using cassava starch combined with biomass or biomass extract of the microalgae *Heterochlorella luteoviridis* and *Dunaliella tertiolecta*. Such film contains 2.0% *H. luteoviridis* extract, which presents the lowest water vapour permeability and excellent mechanical characteristics – ideal for applications in salmon packaging (Carissimi *et al*., 2018). Additionally, these species were used as feed additives for many aquatic organisms in order to enhance the reddish colour of salmon, trout, and shrimp flesh, and to supplement feed for certain types of zooplankton (e.g., rotifers and copepods (Christaki *et al*., 2015). Also, microalgae pigments could be used to enrich the yellowish colour of chicken egg yolk (Conradie *et al*., 2017).

2.3 Cell Disruption

2.3.1 Definition, Classification and Mechanism

Cell disruption is an essential aspect of biotechnology and the downstream processes related to the manufacturing of biological products **(mentioned in Figure 2.10 of section 2.2.).** Cell ruption can be broadly divided into two main categories: mechanical and non-mechanical disruption, each with its own unique benefits **(Figure 2.17).** Consequently, it is logical that these categories are often combined to provide better release than that of

any single method. A vast number of cell disruption techniques have been applied to microalgae, though mechanical disruption is preferred to chemical disruption as it avoids chemical contamination and preserves cell functionality (Lopez-Sanchez *et al.*, 2011). Cavitation is defined as the formation, growth, and subsequent collapse of microbubbles or cavities occurring at small-scale intervals and releases large amounts of energy into tiny volumes (energy release per unit volume) (Gogate and Pandit, 2008).

Acoustic cavitation is caused by ultrasound waves (20 kHz to 1 MHz) in aqueous media. The oscillating sonothrode pushes fluid away, and then retracts immediately afterward, creating a low-pressure field at the front end of the monochrome (Flickinger, 2013). **Hydrodynamic cavitation** is produced by pressure variations obtained by using the geometry of the system to create velocity variations (Gogate, 2002). This type of cavitation can be generated by the passage of liquid through a constriction such as an orifice plate or throttling valve (Gogate, 2002). When the fluid passes through the compression, the kinetic energy/velocity of the liquid increases, with a corresponding decrease in pressure (Gogate and Pandit, 2005). Millions of cavities are generated if the

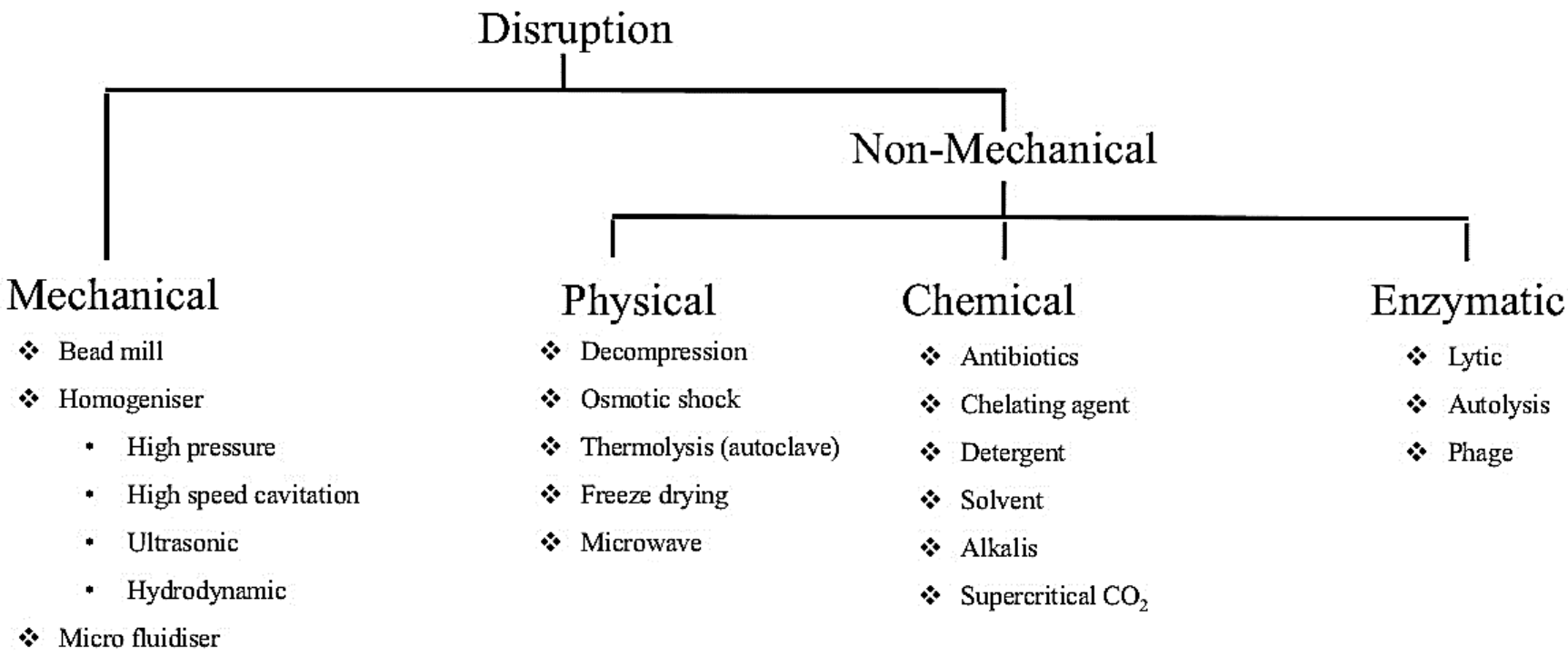


Figure 2.17: Techniques applicable for the downstream processing of cell disruption (adapted from Middelburg, 1995).

control sufficiently causes the stress around the orifice point to fall below the threshold pressure for cavitation. Subsequently, as the liquid jet expands, pressure recovery and the cavities collapse (Gogate and Pandit, 2005). The hydrodynamic cavitation method used by our research group is the pump device, which uses pressure created via a motor. In this system, the liquid flows into the inlet system through the orifices, leading to a rapid change of pressure as the static pressure becomes lower than the liquid vapour pressure. As a result, bubbles condense back to the liquid on return to static pressure. This fluid flow with low pressure but high speed is created while passing the cavitator. Regarding cavitation bubbles in the fluid, numerous bubbles grow and then violently collapse, which emits secondary spherical shock waves. The schematic model of the bubble collapse mechanism generated by hydrodynamic cavitation and ultrasound is illustrated in **Figure 2.18** and **2.19.**

For **hydrodynamic cavitation (Figure 2.18),** liquid flows from the tank to the downstream tubing containing the pump and pressure gauge. Rapid formation and collapse of vapour bubbles occurs within liquids. The emerging bubbles expand at the end of cavitator. At the orifice, where the cross-sectional area is very small, local pressure is low, and cavities are generated if the fluid pressure falls below a threshold level. Subsequently, pressure recovers after the fluid passes through the orifice plate, and the cavities collapse.

Unlike **ultrasound (Figure 2.19),** the oscillating sound wave is generated by the probe. This generates compression and refraction, which causes the formation of bubbles in the fluid. The rebound of compression and refraction causes bubbles grown over many cycles to reach an unstable size and subsequently collapse. At the instant of this collapse,

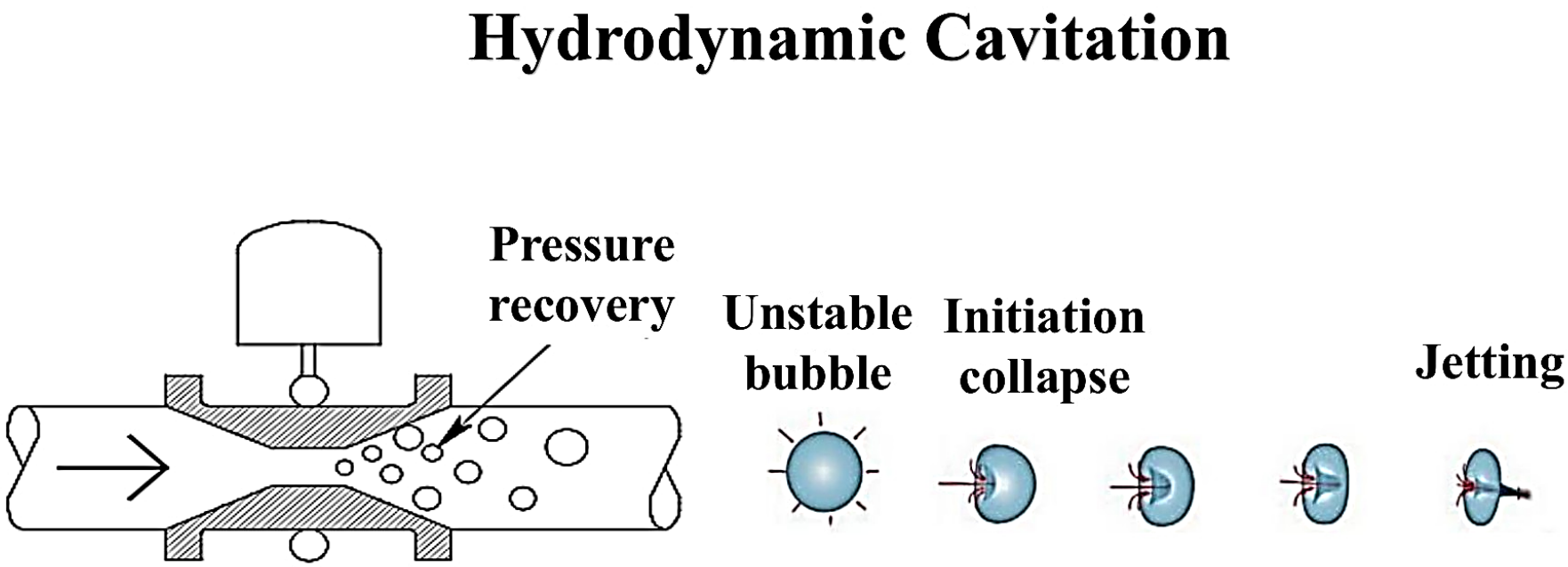


Figure 2.18: A schematic representation of hydrodynamic cavitation.

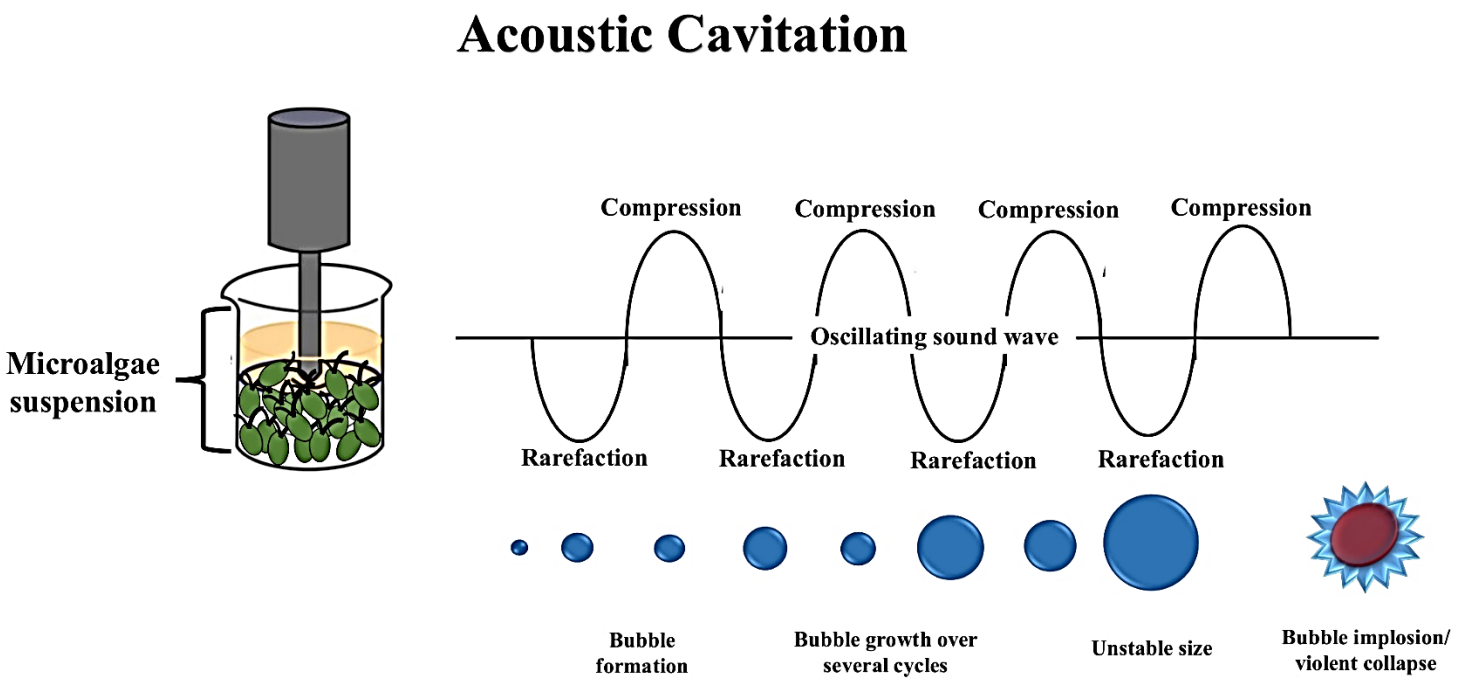


Figure 2.19: A schematic representation of ultrasonication.

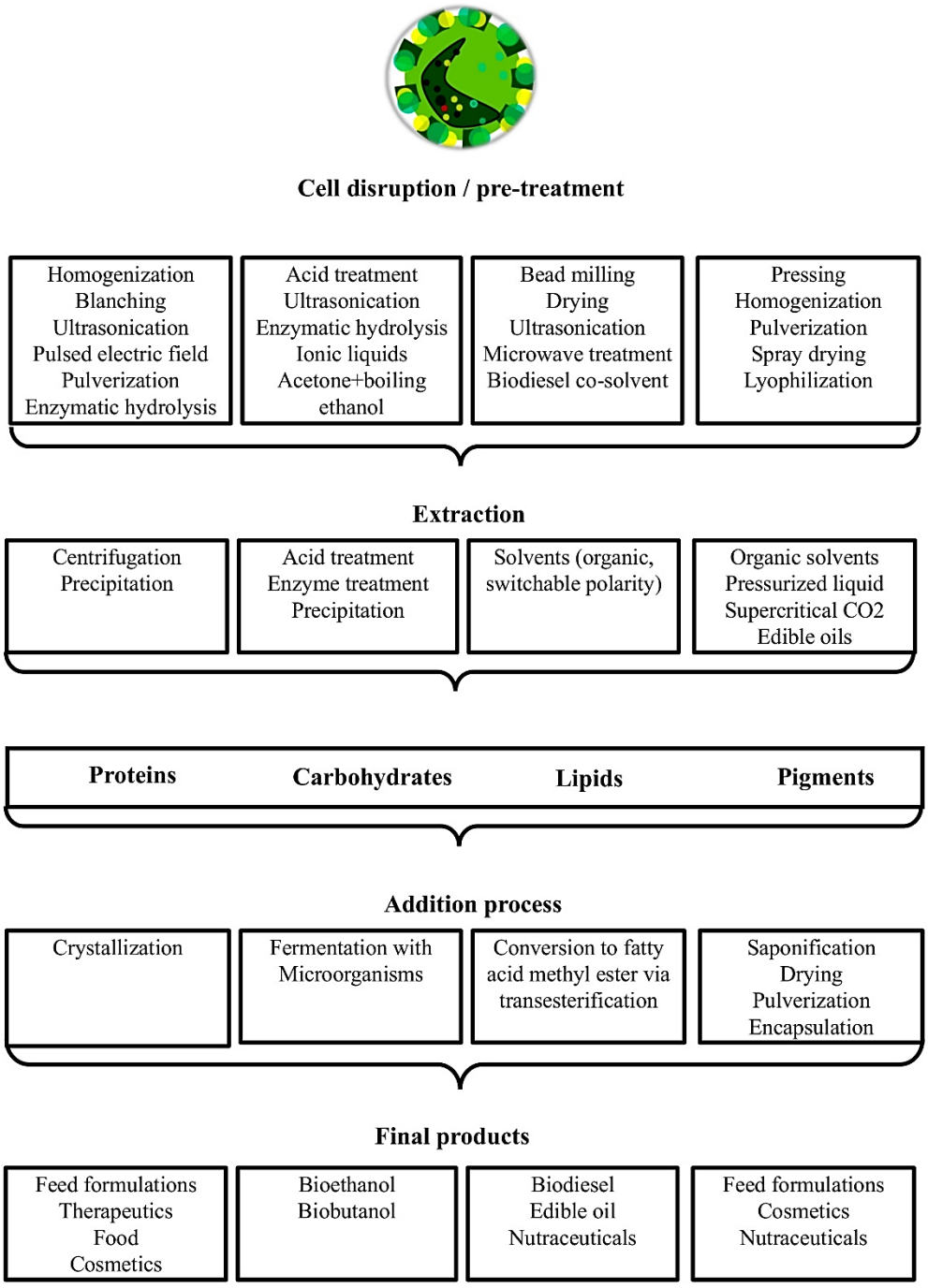


Figure 2.20: Downstream processing steps for the recovery of proteins, carbohydrates, lipids, and pigments (Dixon and Wilken, 2018).

high temperature and pressure is generated – which is known as jetting. This jetting attacks the microalgae cells, disrupting the cell wall layer or breaking a portion of the cell wall or cell membrane. After cell walls and membranes have been thoroughly disrupted, extraction and recovery of target products or molecules is the next downstream processing step. Existing downstream processing operations are primarily designed for the extraction and recovery of one target molecule (proteins, lipids, carbohydrates, pigments, etc.) **(Figure 2.20)** (Dixon and Wilken, 2018).

2.4 Bioaccessibility of Dietary Nutrients

Bioaccessibility refers to the amount of an ingested nutrient that is potentially available for absorption. This depends on the digestion and release from the food matrix. Specifically, bioavailability is defined as the amount of an ingested nutrient that is absorbed and available for physiological functions, and depends on digestion, release from food matrix, absorption by intestinal cells, and transport to body cells **(Figure 2.21).** Therefore, digestion is a crucial step in releasing the food component of microalgae.

2.4.1 *In vitro* Human Digestion

The primary physiological function of the gastrointestinal tract (GIT) is to digest food constituents that can subsequently be absorbed as nutrients, while simultaneously providing an efficient barrier to toxic materials including peptides, viruses, and bacteria (Lundquist and Artursson, 2016). The GIT includes organs from the mouth to the anus, and can be divided into the upper and the lower tracts. The upper tract consists of the oral cavity, oesophagus, stomach, duodenum, jejunum, and ileum. Together, the latter three

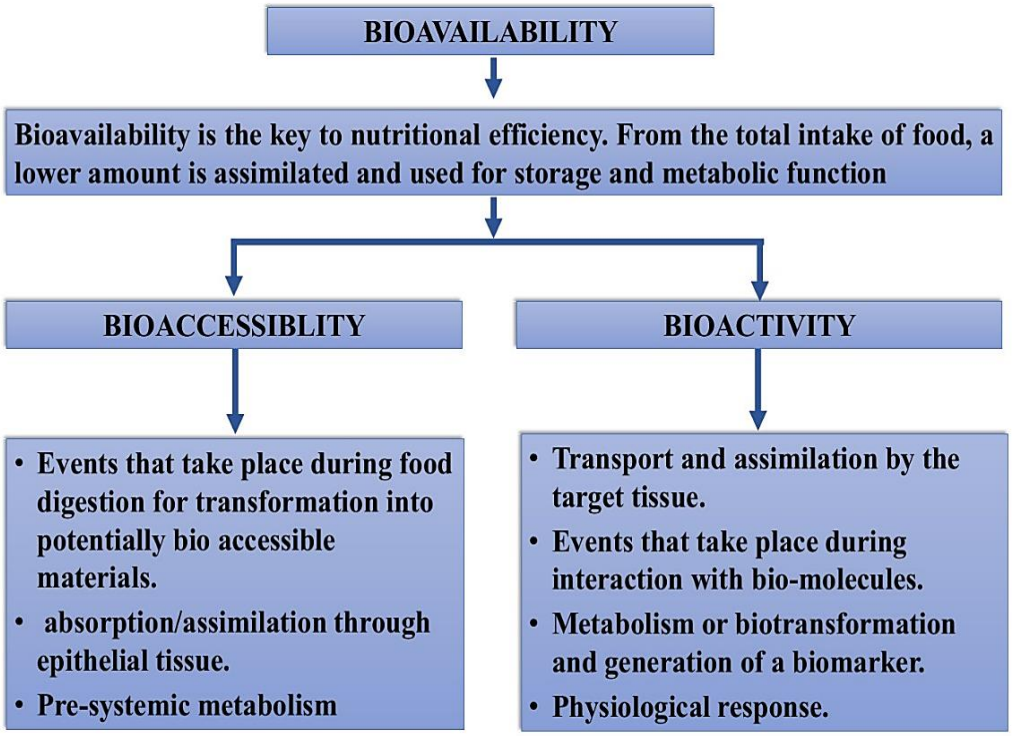


Figure 2.21: Definition of bioavailability as a sum of bioaccessibility and bioactivity with description of the physiochemical events involved at each stage (Fernández-García *et al.*„ 2009).

represent the small intestine (Ball, 1995). Food begins disintegration upon exposure to the GIT, as chemical and physical modifications render ingested food constituents absorbable by the small intestine (Verhoeckx *et al.*, 2015). As soon as food begins to interact with the GIT, it is modified in size, shape, and structure by digestive enzymes, mechanical grinding/shearing, and changes in pH and or ionic conditions. Food disintegration is broken down into three phases: oral, gastric, and intestinal (Guo *et al.*, 2017).

The oral stage represents the first stage of the GIT: salivary glands introduce salivary amylase into the mouth, which hydrolyse starch molecules into dextrin and maltose. The optimal pH for oral amylase activity is approximately 6.8 (Ball, 1995). Saliva moistens

the food and binds masticated food into a bolus that can be easily swallowed while liquid food briefly remains in the mouth before being swallowed directly (McClements and Decker, 2009; Guo *et al.*, 2017).

Next, hydrochloric acid in the stomach is secreted to convert the proenzymes into active enzymes, such as pepsinogen (Ball, 2013). Food particles are further broken down into smaller particles by grinding alongside gastric juices (Guo *et al.*, 2017). During this stage, proteins are significantly hydrolysed by pepsin, while lipids are only partially digested, and very little breakdown of carbohydrates occurs (Guo *et al.*, 2017).

Finally, at the small intestine, pancreatic juice is produced by the inducing of the secretin hormone produced by the small intestinal mucosa. This juice displays a high bicarbonate concentration, which effectively neutralises the gastric acid is presented by the stomach, and is mixed into the chyme, resulting in optimised pancreatic enzyme activity at the small intestine stage (Ball, 1995). The chyme produced in the stomach then enters the duodenum, where it mixes with pancreatic, intestinal, and hepatic secretions. Food macronutrients are then physically and chemically broken down with the aid of the enzymes produced. Pre-existing emulsified oils and fats, or emulsions formed *in-situ* in the duodenum or stomach, are then exposed to the environment for hydrolysis and uptake (Guo *et al.*, 2017). A simplified digestive tract: major compartments and digestion of proteins, lipids, and carotenoids shown in **Figure 2.22.**

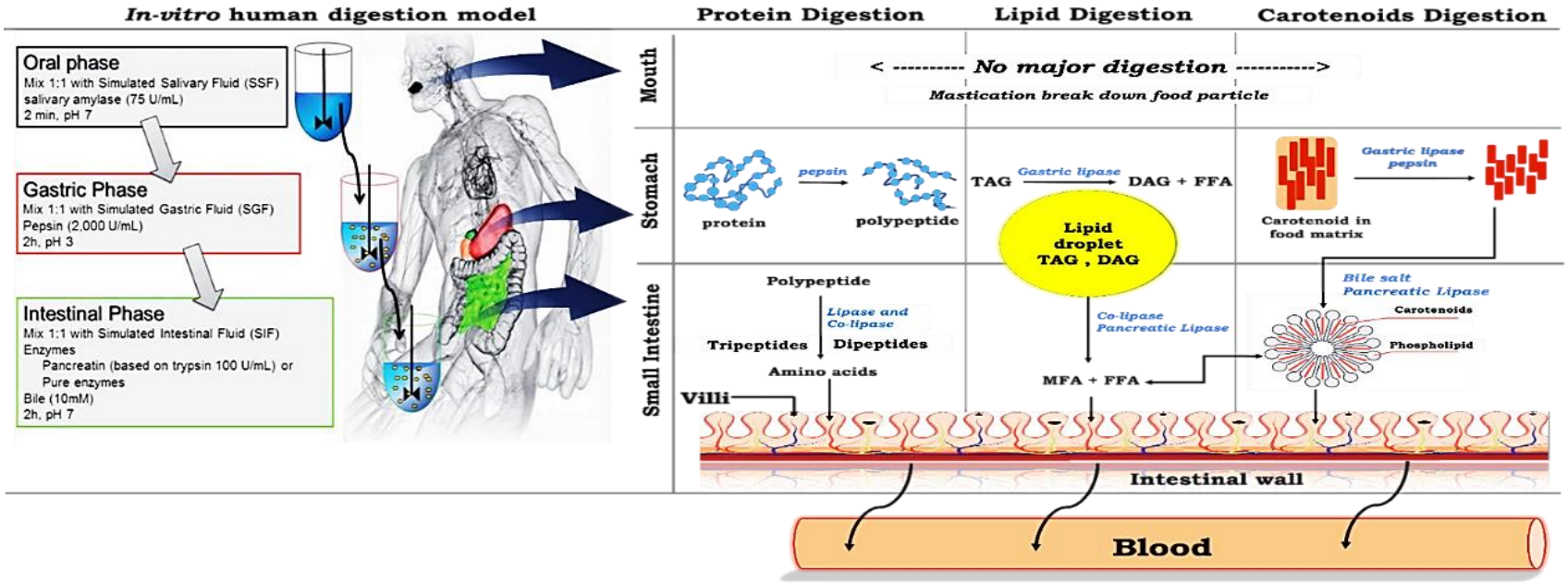


Figure 2.22: A simplified digestive tract: major compartments and organ of digestive tract represent digestion of proteins, lipids, and carotenoids. (Cavonius, 2016; Minekus *et al.*, 2014). Protein digestion begins in the stomach by the action of pepsin, which hydrolyses the long chains of proteins into polypeptides at acidic pH. Hydrolysis continues in the small intestine, where polypeptides are cleaved into tripeptides, dipeptides, and amino acids, which are then absorbed by enterocytes. Lipid digestion begins in the stomach when triacylglycerol (TAG), present in lipid droplets, is converted by gastric lipase to diacylglycerol (DAG) and free fatty acids (FFA). The small intestine hydrolyses TAG and DAG to monoacylglycerol (MAG), and FFAs and is catalysed (e.g., by pancreatic lipase anchored to the surface of lipid droplets by co-lipase). Then, a pool of MAGs and FFAs diffuses in and out of mixed micelles (stabilised by bile acids from the liver) before being absorbed by enterocytes (Cavonius, 2016). Carotenoid digestion begins by release of carotenoids from the food matrix or plant cells by mastication in the mouth. They are further hydrolysed into small molecules by pepsin and gastric lipase in the stomach. The released carotenoids then pass through small intestine, where they are hydrolysed by pancreatic enzymes. Micelles are formed by mixing of bile extract.

2.4.2 *In vivo* Zebra Fish as a Model

Zebra fish (*Danio rerio*), belongs to the family of *Cyprinidae*, they are a warm water omnivore which naturally consumes aquatic insects as well as phytoplankton (Spence *et al.*, 2008). Zebrafish have been used for years as a vertebrate model for monitoring many biological processes due to their unique characteristics. These include their small size, the lower cost compared with mice and rats, the relative of handling as a whole body, rapid external development, visual clarity and use of high resolution imaging (Ho *et al.*, 2004, Schwendinger-Schreck, 2013, Gemberling *et al.*, 2013).

Zebrafish display also a high degree of similarity to humans in terms of their genetics (80% of zebrafish genes are similar to human genes), cell development, molecular mechanisms and organ physiology (Kent *et al.*, 2012, Howe *et al.*, 2013). A simple diagram showing these similarities is depicted in **Figure 2.23.** Accordingly, Zebrafish has been used extensively as an assay to understand many aspects of lipid biology and in the studies of lipid absorption inhabitation drugs (Harper and Lawrence, 2016). It has also been effectively employed in investigating many physiological and pathophysiological processes including embryogenesis, organogenesis, genomics and cancerogenesis as well as examinations in toxicology and drug research (Gemberling *et al.*, 2013).

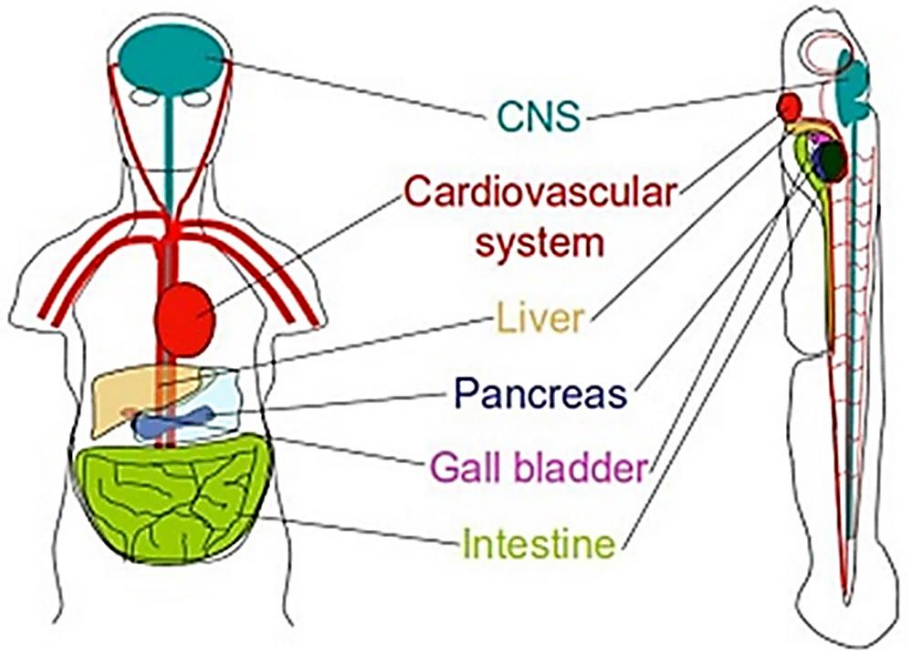


Figure 2.23: Zebrafish as a model organism and its analogy with human. CNS; circulatory system (Williams and Hong, 2011).

2.4.2.1 Digestion in Zebra Fish

Bony fish (*Teleosts*) constitute the largest group of vertebrate life, exhibiting huge diversity in more than 20,000 species of ray-finned fishes across 40 orders (Woo *et al.*, 2011). Although, it have been believed that its digestive system is very similar to most vertebrates, the unique feature which needs to be addressed is the presence/absence and functionality of the stomach (Hidalgo *et al.*, 1999, Kwek *et al.*, 2009). While some species, such as Nile Tilapia and Atlantic cod, contain a stomach, others, such as common Carp, pufferfish and zebrafish, lack a stomach (Brugman, 2016). Alternatively, Zebrafish has an intestinal bulb which is an interior intestine with a bigger lumen than the posterior one, and thus it functions as a reservoir and anterior intestine called the intestinal bulb. This intestinal bulb, however, does not have a low pH value (the lowest is 7.5 under homeostatic conditions) as it lacks gastric glands (Nalbant *et al.*, 1999). Nonetheless, there

is a functional homology; Zebrafish intestine does not contain five distinct segments as in mammals namely; jejunum, duodenum, ileum, cecum and colon. Instead, Zebrafish intestine contains three distinct parts differentiated based on their morphology and gene expression. These are the anterior, the intestinal bulb that substitutes the stomach as mentioned earlier, the midgut and the posterior gut segment (Wallace *et al*., 2005). The digestive system in fish is shown in **Figure 2.24** the details in **Figure 2.25** below, and a brief illustration of the main and common parts is demonstrated.Wang *et al* (2010)divided the adult Zebrafish gut into 7 equal segments (S1 to S7) with three distinct regions (Wang *et al*., 2010). S1 to S5, the same authors concluded, hold the same molecular feature of the mammalian small intestine. Genes analysis of segments 1-5, which represent the anterior and mid intestinal region, shows a high expression of human small intestinal marker enzymes, such as the intestinal fatty acids binding protein 2 (fabp2) and other enzymes involved in fatty acid metabolism (Mudumana *et al*., 2004, Wang *et al*., 2010). S6 and S7 represent the large intestine; they are involved in dynamic water absorption. S5 is believed to have a role in zebrafish immunity (Wang *et al*., 2010).

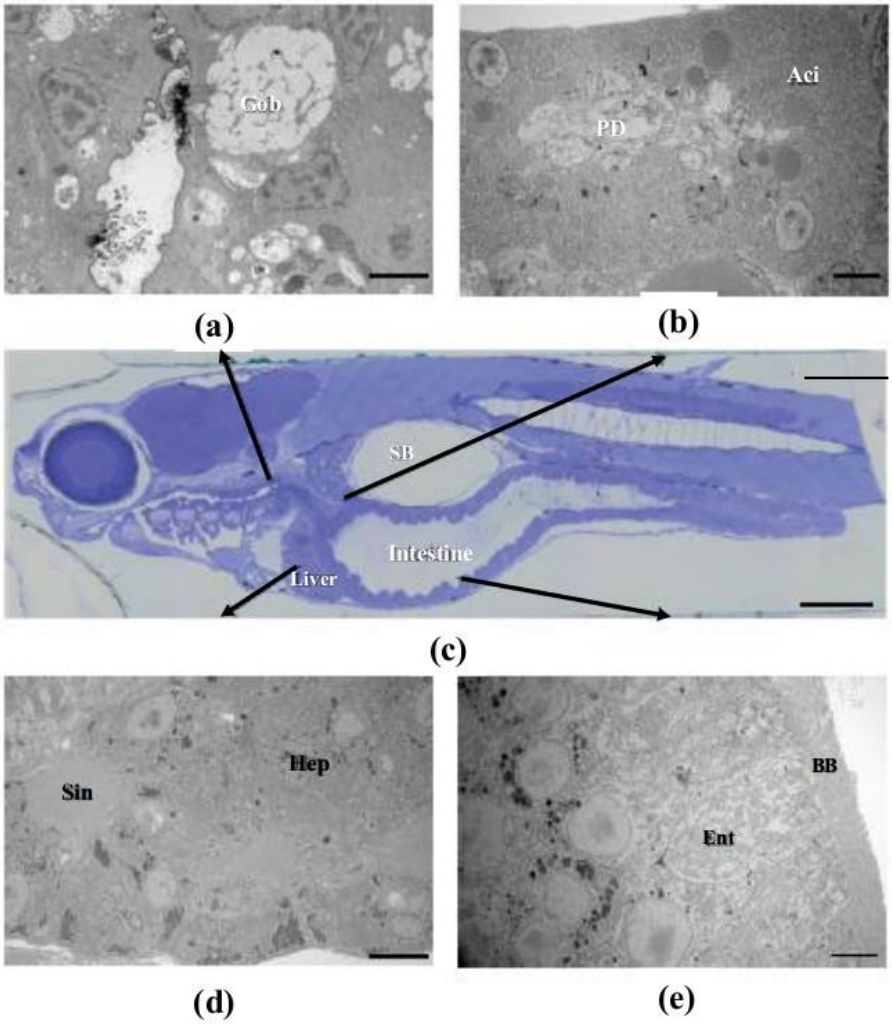


Figure 2.24: An illustration of difference digestive system in zebrafish (Cheng *et al.*, 2016). The zebrafish stained with toluidine blue and imaged with light microscopy, showing the different components of the digestive system (c). Corresponding EM images of the different regions include the oesophageal area, rich in goblet cells (Gob) (a), the pancreas, with a pancreatic duct (PD) in the middle and surrounded by acinar cells (Aci) rich in zymogen granules (b). The liver and its hepatocytes (Hep) surrounded by sinusoids (Sin) and its network of bile ducts are shown in (d), as well as the intestine lined with enterocytes (Ent) rich in villi forming the intestinal brush border (BB) in (e). (SB) is the swim bladder. Scale bar = 20 µm (LM) and 5 µm (EM).

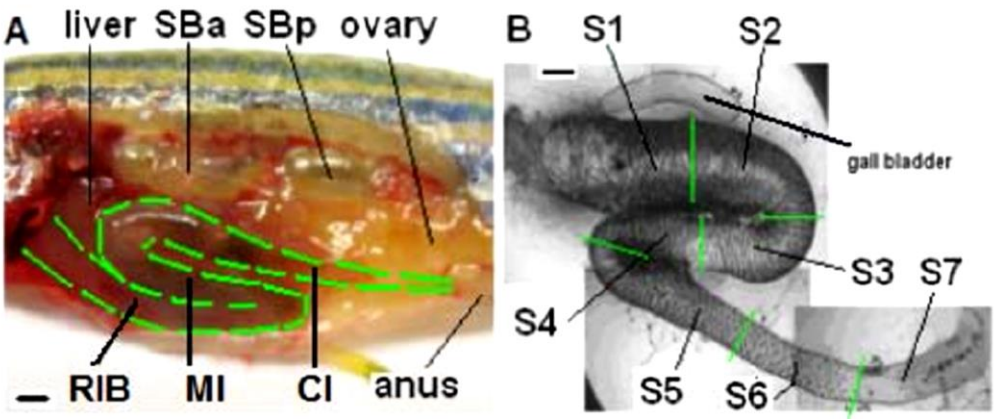


Figure 2.25: Anatomical features of adult zebrafish intestine. A partially dissected 6-month-old zebrafish to show the folding of the three portions of intestine in *vivo*: rostral intestinal bulb (RIB), mid-intestine (MI) and caudal intestine (CI). Liver, ovary, anus, swim bladder anterior (Sba) and posterior (SBp) chambers are indicated. (B) An isolated zebrafish intestine *in vitro* after removal of the surrounding mesentery. The isolated intestine was divided into seven roughly equal-length segments as indicated by green lines: S1-S2 from RIB, S3-S4 from MI and S5-S7 from CI. The associated gall bladder is indicated. Scale bars 500 µm (Wang *et al.*, 2010).

2.4.3 Impact of Microalgae Cell Wall on Bioaccessibility of Dietary Nutrients

Cell walls and chromoplasts are the two major physical barriers to nutrient release from the digested food matrix (structure) during digestion (Jeffery *et al*., 2012). To the best our knowledge very little research has been done on the effect of cell disruption on nutrient bioaccessibility for human consumption of *C. reinhardtii.* The most recent research is of Gille *et al.* (2016) who assessed the effect of sonication on the bioaccessibility of carotenoids from photoautotrophic-cultivated *C. vulgaris* and *C. reinhardtii* in an *in vitro* digestion . Results suggested that *C. reinhardtii* represents a good carotenoid source for potential use in foods without processing, while the application of processing methods,

like sonication, is necessary for *C. vulgaris*. Different species of microalgae were considered as an alternative in aquafeeds (Soletto *et al.*, 2005). A diet of 20% *Scenedesmus* meal incorporated into juvenile sea bream (*Sparus aurata*) diets increased the growth rate and protein utilisation (Vizcaíno *et al.*, 2014). Nutrient digestibility is also different between species. This is possibly due to differences in the intrinsic properties of the proteins, differences in protein accessibility caused by different cell wall matrices, or differences among fish species. It is hypothesised that the cell walls of unicellular sources thus hinder nutrient accessibility, leading to a decreased nutrient digestibility (Sarker *et al.*, 2016; Gong *et al.*, 2018).

Vast diversity exists in the cell wall structures of microalgae and cyanobacteria: from peptidoglycan cell walls to cellulosic cell walls (Palinska and Krumbein, 2000). Furthermore, it is assumed that peptidoglycan cell walls are softer than cellulose-based cell walls. Additionally, most fish lack the enzymes necessary for cellulose degradation. Thus, algae containing cellulosic cell walls are expected to be digested to a lesser extent than cyanobacteria, for example, which possesses a peptidoglycan cell wall (Teuling *et al.*, 2017). In contrast, Teuling *et al.*, (2017) assessed the effect of cell wall hardness and fish species (*Nile tilapia* and *African catfish*) on digestibility of unicellular sources (*Chlorella vulgaris*, *Scenedesmus dimorphus*, and *Nannochloropsis gaditana*) and a cyanobacterium (*Arthrospira maxima*). Differences were measured in Apparent digestibility coefficients (ADCs) of their nutrients between the sources in both fish species, at a 30% diet inclusion level. The cell wall hardness was quantified as the cells' resistance to mechanical force over the disruption time. The cells were disrupted using bead mill, as the protein release was quantified by measuring the soluble protein content release in the supernatant. The initial slope of the cell over bead mill time (% release/min)

indicates the cell hardness. The cell disruption was also quantified using flow cytometer. The total number of count of particles was plotted as a function of bead mill time, as a percent of the initial total count in an intact cell size range. To derive the time (min) needed for 50% cell breakdown. This value (min) was used to estimate cell hardness. The digestibility data suggest that the differences in nutrient accessibility of unicellular sources are dominant over the differences in digestive systems between herbivorous and omnivorous fish. Nevertheless, nutrient digestibility of the unicellular sources did not relate to the mechanical cell wall hardness.

Microalgae cell wall could range in component from cellulose–pectin complexes to ones made of HRGPs (Domozych *et al*., 2012). Even though *C. reinhardtii* have been used as the model of the study of higher plant, their walls are substantially different from those of higher plants because they seem to lack cellulose (Roberts, 1974). Instead the major wall components are layers of crystalline arabinose-rich hydroxyproline-rich glycoproteins (Bollig *et al*., 2007).

Chlorella is the commercial microalgae species that have been commercially used in food and feed applications. *Chlorella* have rigid walls composed of mainly glucosamine in a chitin-like polysaccharide. The main neutral sugars encountered beside glucosamine in the rigid wall are galactose and rhamnose (Takeda and Hirokawa, 1978). **Figure 2.26** illustrated that the cell wall of *C. vulgaris* consists of an electron-dense outer wall and a less dense inner wall (Gerken *et al*., 2012). *C. vulgaris* consists of a microfibril (poly-*β*-1.4–D-N-acetylglucosamine) crosslinked by hydrogen bonds and another matrix consisting of proteins and complex polysaccharides (hemicelluloses, pectin-like substances) (Dvoretsky and Akulinin, 2016). Their cell wall is considered to be restate to

digestion, and without breaking it, there are concerns about the bioavailability of nutrients when humans consume it (Loos and Meindl, 1982). Therefore, a number of pre-process methods has been applied to their tough cell wall to enable *Chlorella* to be digested and therefore release its abundant nutrients (Monks *et al*., 2013).

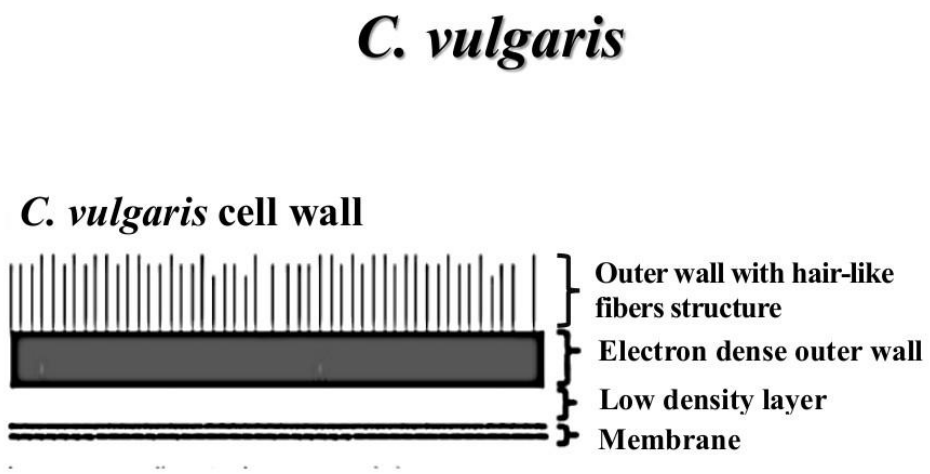


Figure 2.26: Schematic depiction of the cell wall of *C. vulgaris*. Their walls consist of an electron-dense outer wall and a less dense inner wall. On digestion with lysozyme, there is a thinning and delaminating of the outer wall and loss of hair-like fibers from the surface of the cell extraction (Gerken *et al*., 2012).

In contrast, the cell wall of *Spirulina* are similar to those of a gram-positive bacteria, contain lipolysaccharides (LPS) lining the outer membrane. The lipid composition is relatively simple, containing principally mono- and di-galactosyl diacylglycerides, phosphatidyl diacylglycerol and sulfoquinovosyl diacylglycerol (Tornabene *et al*., 1985; Kalina, 2010) **(Figure 2.27).** Although not digestible, these walls are fragile and make the cell contents readily accessible to digestive enzymes; this is a major advantage in comparison to organism with cellulosic cell wall (Gupta *et al*., 2013). Therefore, humans

can consumes it raw and unprocessed because the wall is easily broken down by human digestive enzyme (Kose *et al*., 2017).

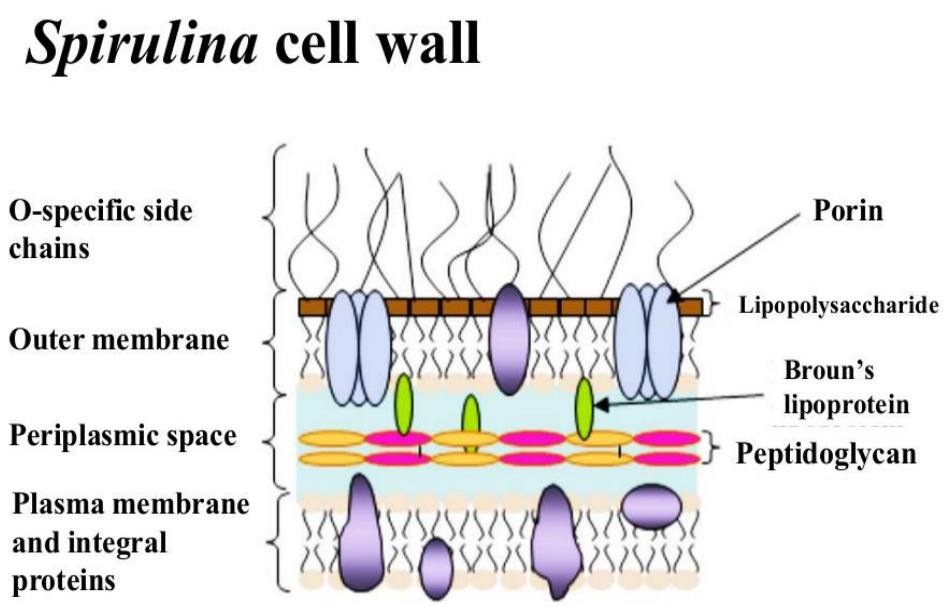


Figure 2.27: Schematic depiction of the cell wall of cyanobacteria (*Spirulina*). Their cell wall consist of peptidoglycan. An inner and an outer cell membrane and only a thin layer of peptidoglycan in the periplasmic space between the inner and outer membrane (Kalina, 2010).

C. reinhardtii cell wall must be opened, which could accomplish this through ranges of cell disruption method. This fracture or fragments the outer layer, so the essential nutrients are more bioavailable. Therefore, this research is based on the hypothesis that *C. reinhardtii* has potential to be a novel source for food and feed. They have a great ability of adapting into the manipulated culturing environments and could accumulated key biomolecules. Nevertheless, their cell wall layers (hydroxyproline-rich glycoprotein) could act as a barrier for digestive enzyme during ingestion. Applying mechanical disruption methods, such as hydrodynamic cavitation could, therefore, be an alternative

approach for improve nutrients bioaccessibility from *C. reinhardtii*. To prove our hypothesis, the research strategies were set as followed:

Research Strategy

1. Measure the biochemical composition and structural response of *C. reinhardtii* to mixothrophic culturing in our lab scale system and establish the nutritional profile of *C. reinhardtii* growth in a range of growth media; mainly focus an impact of changing the concentration of nitrogen.

2. Explore the impact of cell disruption on *C. reinhardtii* cells and their nutritive compounds.

3. Measure *in-vitro* bioaccessiblity of chlorophyll (*a* and *b*) and carotenoid (*β*-carotene and lutein) from intact and disrupted *C. reinhardtii* during simulated *in vitro* human digestion and *in vivo* zebra fish model.

CHAPTER 3

Materials and Methods

3.1 Material and Methods for The Biochemical Response of *C. reinhardtii* as Influenced by Growth Media Manipulation

3.1.1 Biochemical response of *C. reinhardtii* under mixothrophic culturing.

3.1.1.1 *C. reinhardtii* Standard Culturing under the Laboratory Conditions

The Tris-Acetate-Phosphate (TAP) growth medium was prepared by combining stock solutions containing nitrogen, phosphate and a mix of trace elements **(Table 3.1).** All stock solutions were stored unsterilized at 4 °C (no more than one month) and made up to 1 L (all stock solution were kept no more than a month). The pH of the medium was adjusted to 7.0 with acetic acid, and it was then autoclaved at 121 °C for 20 min.

The microalgae strain (*C. reinhardtii* Wild Type CC-125 mt (+), supplied from the Department of Plant Science, University of Cambridge, Cambridge, UK), was pre-grown in TAP medium by inoculating a pea-sized (6–8 mm diameter) pellet of cells from agar into 300 mL of TAP medium. These cultures were kept in the growth room. The conditions provided 23.0±2 °C under continuous illumination (cool white fluorescent bulbs, providing an intensity around 70 µmole / m^2s) light–dark cycle (16:16 h) until it reached the mid-log phase (cell density 1-5 x 10^6 cell/mL). An aliquot (50 mL) of the mid-log phase microalgae was then inoculated into the experimental cultures (2 L of TAP

medium). Cultures were kept in stable conditions until reaching the exponential phase ($8x10^6$ cell/mL). During the whole procedure, sterile conditions were maintained in a laminar flow cabinet to avoid any external contamination (Harris, 2009) Error! Reference source not found. and **Figure 3.2.**

Table 3.1: The molar composition of standard culture media.

Stock solution (SL)	Volume	Component	Conc. in final medium
Tris-Base	2.4 g	$H_2NC(CH_2OH)_3$	$2.0x10^{-2}$ M
TAP Salt	25 mL	NH_4Cl	$7.0x10^{-3}$M
		$MgSO_4 \circ 7H_2O$	$8.3x10^{-4}$M
		$CaCl_2 \circ 2H_2O$	$4.5x10^{-4}$M
Phosphate solution	1 mL	K_2HPO_4	$1.7x10^{-3}$M
		KH_2PO_4	$1.0x10^{-3}$M
Trace Element	1 mL	$Na_2EDTA \circ 2H_2O$	$25x10^{-6}$ M
		$(NH_4)_6Mo_7O_{24}$	$28.3x10^{-9}$ M
		Na_2SeO_3	$0.1x10^{-6}$ M
		$ZnSO_4 \circ 7H_2O$	$0.1x10^{-6}$ M
		$MnCl_2 \circ 4H_2O$	$6.0x10^{-6}$ M
		$FeCL_3.6H_2O$	$20.0 x10^{-6}$ M
		$CuCl_2 \circ 2H_2O$	$2.0x10^{-6}$ M
Acetic acid, conc	1 mL	CH_3COOH	

** For solid medium, add 15 g agar per liter**

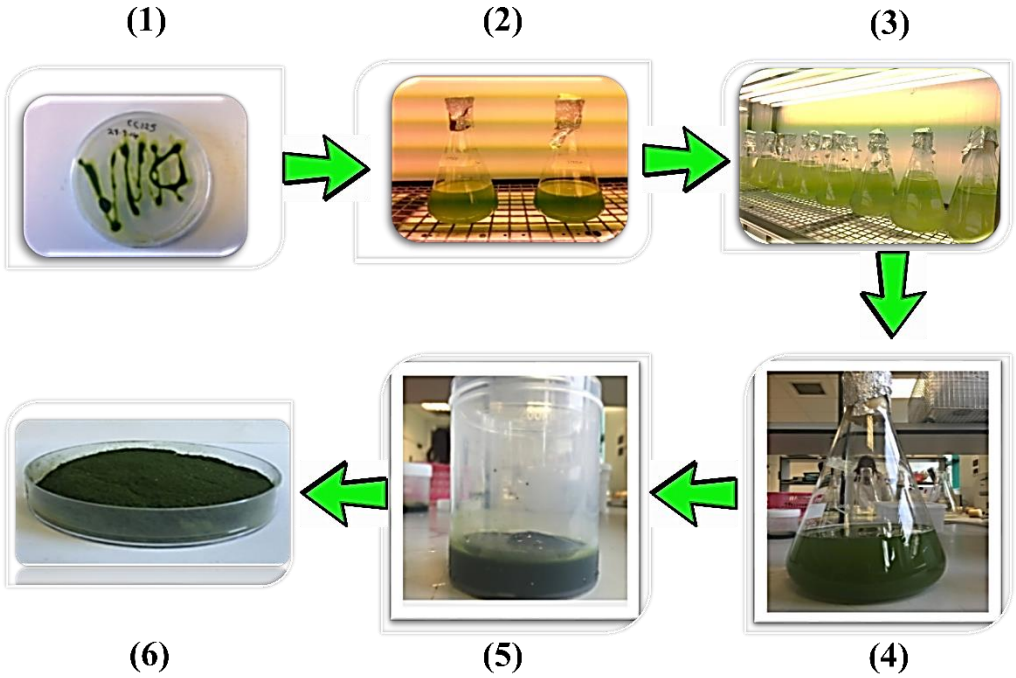


Figure 3.1: Illustration of the downstream bioprocessing of *C. reinhardtii* was pre-grown in TAP medium. These cultures were kept in the growth room ((1) – (2)). The conditions provided 23.0±2 ºC under continuous illumination (cool white fluorescent bulbs, providing an intensity around 70 µmole/m^2s) light–dark cycle (16:16 h) until it reached the mid-log phase (cell density 1-5 x 10^6 cell/mL). An aliquot (50 mL) of the mid-log phase microalgae was then inoculated into the experimental cultures (2 L of TAP medium). Cultures were kept in stable conditions until reaching the exponential phase (8 x 10^6 cell/mL) (3). The stationary phase biomass were harvested and freeze-dried (4) – (6).

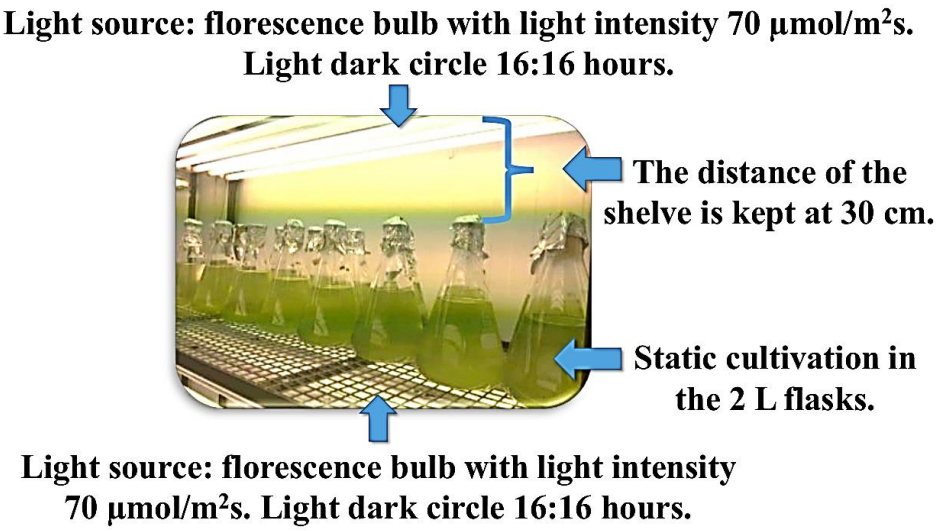


Figure 3.2: The experimental setup of *C. reinhardtii* under mixothrophic cultivation in the lab scale system. The experimental provided 23.0±2 ºC under cool white fluorescent bulbs proving the light intensity approximately 70 µmol/m^{2}s. The distance of the culturing shelves is kept constant at 30 cm. An experimental *C. reinhardtii* culture was maintained in 2 L of TAP medium in a static condition.

3.1.1.2 *C. reinhardtii* Strain Maintaining

The *C. reinhardtii* strain (*C. reinhardtii* Wild Type CC-125 mt (+) was pre-grown in into 300 mL of TAP medium under control condition until it reached the mid-log phase (cell density 1-5 x 10^6 cell/mL) . TAP media agar is prepared then pour into the petri dish plate. The *C. reinhardtii* from culture suspension are streak on the petri dish plates. All processes were performed under the sterile condition. The streaked *C. reinhardtii* petri dish plates are incubated under the control illumination. After 1-3 days of *C. reinhardtii* colonies free of bacteria can often be seen. The *C. reinhardtii* strain which should be keeping at 4^{o}C. The transferring into the new fresh TAP media agar every 6 month would be recommended to maintaining the strain **(**Error! Reference source not found.**).**

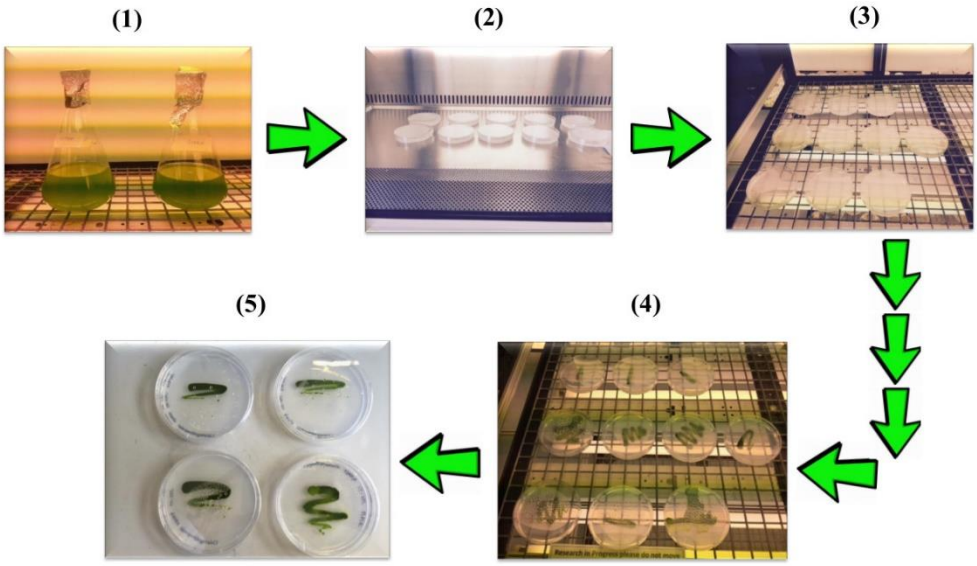


Figure 3.3: The schematic diagram of *C. reinhardtii* strain maintaining. The *C. reinhardtii* strain were pre-growth under mixothrophic cultivation in the lab scale system. The experimental provided 23.0±2 ºC under cool white fluorescent bulbs proving the light intensity approximately 70 µmol/m^{2}s (1). TAP media agar were prepared then pour into the petri dish plate under the sterile condition. The *C. reinhardtii* from culture suspension were streak onto petri dish agar (2). The streaked *C. reinhardtii* petri dish plate were incubated under the control illumination (3). After 1-3 days of *C. reinhardtii* colonies free of bacteria can often be seen (4). The *C. reinhardtii* strain which should be keeping at 4ºC. The transferring into the new fresh TAP media agar every 6 month would be recommended to maintaining the strain (5).

3.1.1.3 Growth Kinetic Monitoring

To identify the optimum absorbance of photosynthetic pigment, mainly chlorophyll, in *C. reinhardtii* culture. They were scan the spectrum during 600 - 800 nm using spectrophotometer (LKB Biochro Model 4050 Ultraspect II Spectrophotometer, Dickenson, TX, USA) (see data in **Appendix A Table 1** and **Appendix B Figure 1**). Then, the growth kinetics was monitored at regular five-day intervals by optical density

at 680 nM (LKB Biochro Model 4050 Ultraspect II Spectrophotometer, Dickenson, TX, USA); the average value of triplicate determination was used. The relation between the OD_{680} and age of culturing (days) was the plot.

3.1.1.4 Total Cell Number Analysis

Total cell number analysis, *C. reinhardtii* culturing during exponential phase were collected daily in triplicate. The total cell number was monitored using the Count star cell count (Amber Trust Technology). Briefly, the *C. reinhardtii* were mixed 1:1 with the Lugol solution in the centrifuge tube and then with the vertex mix for 1 min to ensure the *C. reinhardtii* was homogeneous. Then a 20 µL of homogenous dyed *C. reinhardtii* sample was dispensed to a count star slide. The total cell number of *C. reinhardtii* was evaluated by count star software.

3.1.1.5 Biomass Analysis

Biomass of *C. reinhardtii* was analysed during the exponential phase and collected daily in triplicate using the method modified from (Ratha *et al.*, 2016). Firstly, Whatman GF/C (47 mm diameter, 1.2 µm pore size) filter papers were dried at 60°C overnight in a hot air oven. Filter papers were placed in a vacuum desiccator for 30 min, and the empty weights were measured using an analytical balance. The drying and weighing procedure was repeated until constant weights were obtained. Samples of homogenised cultures were taken and filtered through the pre-dried and pre-weighed filter papers. Filtration was carried out in a Parsons membrane filtration assembly by vacuum suction, followed by washing the biomass thrice with 10 mL of distilled water. Filter papers containing the *C. reinhardtii* biomass were dried in the hot air oven at 60°C followed by cooling in the

vacuum desiccator. The dry biomass weights were measured in the analytical balance. Drying, desiccation and weighing were repeated until constant weights were obtained. Biomass dry weight was calculated by subtracting the empty filter paperweight from the dry weight of the filter paper with *C. reinhardtii* biomass.

3.1.1.6 Biomass production

The *C. reinhardtii* were cultivated under standard condition until reach station phase according to **section 3.1.1.1** The stationary culture were then evaluated the cell number (**method section 3.1.1.4**) and biomass (**method section 3.1.1.5**). The data were used to calculate the constancy value (biomass at the day seven (g/mL) / cell number at day seven (cell/mL)). This biomass production equation was produced and was then used to create the graph providing the relation of biomass production and age of cultivation.

$$B = aC \qquad \text{……..} \quad \textbf{(2.1)}$$

Where symbol refer to

B = Biomass production (g/mL)

C = Cell number (cell / mL)

a = Constance value depend on the culturing condition calculated from biomass at the day seven (g/mL) / cell number at the day seven (cell/mL). Under the

3.1.1.7 Volumetric Biomass Productivity

The volumetric biomass productivity (Q_x, $gL^{-1}d^{-1}$) was calculated using **Equation (3.1)** (Araya *et al*., 2014):

$$Q_x = \frac{X_f - X_o}{t_f - t_o} \qquad \text{……} \quad \textbf{(3.1)}$$

Where symbol refer to

X_f : The biomass concentration at cultivation time t_f.

X_0 : The biomass concentration at the beginning of the experiment t_0.

t_f : Time at the end of the experiment.

t_o : Time at the beginning of the experiment.

3.1.1.8 Moisture Content

The moisture content and total solid content were evaluated using the methods modified from (Sluiter *et al.*, 2008) which involved thoroughly mixing the sample and then weighing out an appropriate amount to the nearest 0.1 mg into the pre-dried weighted dish. The weight of the sample plus weighing dish were recorded, and the analysis was performed in duplicate. The sample is dried in a convection oven at 105±3ºC for a minimum of four hours. The sample was dried to constant weight, which is defined as ± 0.1% change in the weight per cent solids upon one hour of re-heating the sample. The total solid and moisture content were calculate as follows **Equation (3.2) and (3.3).**

$$\% \text{ Total solid} = \frac{(\text{Weight}_{\text{dry pan plus dry sample}} - \text{Weight}_{\text{dry pan}}) \times 10}{\text{Weight}_{\text{sample}}} \quad \ldots\ldots \quad \textbf{(3.2)}$$

If desired, the present moisture can also be calculated:

$$\% \text{ Moisture} = 100 - \frac{(\text{Weight}_{\text{dry pan plus dry sample}} - \text{Weight}_{\text{dry pan}})}{\text{Weight}_{\text{sample}}} \quad \ldots\ldots \quad \textbf{(3.3)}$$

3.1.1.9 Freeze-Dried Microalgae Biomass

Fresh *C. reinhardtii* suspensions harvested by centrifugation (J2-21 Centrifuge, Beckman Coulter) at 5000 *g* for 30 min. The wet biomass immediately froze at -80 ºC for 24 h

before freeze-drying for seven days (Edward Freeze Dryer, Super Modulyo). The dry biomass was then weighed and kept at -80 ^{o}C until required for analysis.

3.1.1.10 Protein Analysis

The protein content of freeze-dried *C. reinhardtii* was determined using a BCA protein assay (Pierce). A 2% sodium dodecyl sulphate (SDS) solution was prepared and 1 mL was added to 0.1 g of freeze-dried *C. reinhardtii*. This was heated in a water bath at 60 °C for 30 min and vortexed for 1 min prior to centrifuge at 4,000 rpm for 10 min. The sample was further diluted 1/100 using the SDS solution before 100 µl was added to 2 mL of the BCA standard working reagent and incubated for 30 min at 37°C. The absorbance was read at 562 nm using a spectrophotometer blanked with RO water; the concentration determined using the polynomial equation produced by a range of bovine serum albumin (BSA) standards (2000 µg/mL, 1500 µg/mL, 1000 µg/mL, 750 µg/mL, 500 µg/mL, 250 µg/mL, 125 µg/mL and 25 µg/mL) incubated for 30 min at 37°C with 2 mL BCA standard working reagent.

3.1.1.11 Extraction of Lipid

A chloroform: methanol (2:1) solvent was prepared, and 1.2 mL was added to 0.1 g of freeze-dried *C. reinhardtii* and vortexed for 1 min. Then, 1 mL for of a 0.9% sodium chloride solution was added and the mixture was vortexed again (1 min) before being centrifuged, using a Thermo Jouan CR3i multifunction centrifuge, at 3,000 rpm for 10 min at 4°C to separate into 3 phases. The lower stage containing the lipids was transferred to a clean vessel. A further 1.2 mL (5 mL for liquid samples) of chloroform:methanol (2:1) solvent was added to the remaining two phases, which then were vortexed (1 min)

and centrifuged again. The lipid phase was removed and pooled with the original lipid layer before a third and final sequence was completed. The pooled lipid phases were centrifuged again to separate the lipids from any residual compounds; the lipid layer was removed and dried under a flow of nitrogen. The lipid extracts were weighed to calculate the total lipid content (Folch *et al*, 1957). Samples were further analysed as described in **section 3.1.2.4.**

3.1.1.12 Ultra-Structural Analysis by Transmission Electron Microscope (TEM)

An aliquot (1 mL) of fresh cells culture, pre-digested, gastric and duodenal phases of the *C. reinhardtii* was derived and fixed with 3% glutaradehyde in 0.1 M cacodylate buffer. Samples were then transferred into an Eppendorf tube and centrifuged at 1000 g. Supernatant was removed, resuspended in a 1% aqueous osmium tetroxide and left for one hour. Samples were twice (each 5 min) washed with distilled water followed by centrifugation and removal of the supernatant each time. They were then dehydrated with a series of different ethanol concentrations (50%, 70% and 90%; 2 times each for 15 min); and further washed with pure ethanol (100%, 3 times each for 20 min) before propylene oxide (100%, 2 times each 15 min) was added to further wash. An agar Araldite resin (in the ratio of 1:3 and 1:1, resin: propylene oxide) was prepared. Initially 1 mL of resin (1:3) was added to the samples and left for 3 hrs. Samples were then centrifuged at 13,000 g, supernatant resins removed and a new resin (1:1) was added. Tubes were then left overnight under the fume hood with the lids off. Pure resin was this time suspended into the samples (3 times each for 2.5 hrs) and left in the oven (60°C) for 48 hrs. Thin sections of the samples were cut with ultra-microtome (Leica EM) using diamond knife. Thin section of each samples in the Nano scale was then visualized under the TEM.

3.1.1.13 Structured Illumination Microscopy (SIM) and Confocal Microscopy

Fresh *C. reinhardtii* cells were stained with Nile Red (5 µg/µL) and FM4-64FX (1 µg/µL) at room temperature for 10 min to visualize lipids and cell membranes, respectively (Greenspan, 1985). The fixed cells were resuspended in 20 µL poly-vinylpyrrolidone (PVP1A, Citifluor) and 10 µL of cell suspension was mounted on a slide using a high precision cover slip (Zeiss, Cat 1,5H, Cat. No. 474030-9010-000). Visualization was performed 15 min after mounting the sample. We compromised on the refractive index matching for SIM because in the water-based solution the *C. reinhardtii* cells were mobile. The higher refractive index hardening media affected the staining. Therefore, we selected PVP1A (Citifluor), a hardening mounting. The media had a lower refractive index (1,500) than optimal, but it immobilized the *C. reinhardtii* and did not affect the staining.

SIM imaging: Zeiss Elyra PS1 was used to visualize the stained *C. reinhardtii* cells using the following hardware and settings: objective Plan-Apochromat 63x/1.4 Oil DIC M27; for Nile red and FM4-64FX band pass filter: BP 570-620 + LP 750, Laser 561 nm: 4.0%. Chloroplast: long-pass filter LP 655, Laser 642 nm: 5.0%, SIM grating period 34.0 µm. Because chloroplasts were very bright, we had to compromise the imaging of the FM4-64FX in the red channel. Processing was done using Zen2 Black Edition, with SIM parameters set to auto noise, sectioning at 100/83/83 and original recorded intensity values maintained (Raw Scale set on). Images of different experimental groups were displayed with the same histogram settings.

Confocal microscopy: Zeiss LSM 780 was used to image the lipid droplets and chloroplasts, and it served as a comparison for SIM imaging. Using the 32-channel

detector, we visualized the lipid droplets and the chloroplasts separately. At acquisition, the complete separation of the lipid signal from the chlorophyll channel was not possible because Nile red emission is visible in the far-red channel with low intensity. Therefore, post-acquisition we applied linear un-mixing of the signals. Plan-Apochromat 63x/1.4 Oil DIC M27 was used. The following settings were used: lasers 405 nm: 4.0%, 488 nm: 1.0%, 561 nm: 0.15%, 633 nm: 0.2%; beam splitters MBS 488/561/633 and MBS InVis-405; detector ChS1: 428–473 nm; ChS2: 508–553 nm; ChS3: 579–624 nm; ChS4: 641–695 nm. Nile red was visible in ChS2, ChS3 and CgS4 channels, and the chloroplast was visible only in the ChS4 channel.3.1.2 Materials and Methods for Impact of Nutritional Manipulation on the Nutrition Profile of *C. reinhardtii*.

3.1.2 Nitrogen Stress Media on the Proximate Analysis of *C. reinhardtii*

3.1.2.1 *C. reinhardtii* Culturing under Nitrogen Stress Condition

Experiment culture media consisted of the TAP salt stock solution (difference in concentration of nitrogen in the TAP salt: non-added nitrogen, 0.2 M and 0.6 M; later labelled as NAN, STD and N^+ respectively) together with other components (Tris base, phosphate solution, trace elements) of standard TAP media. An appropriate exponential phase *C. reinhardtii* aliquoted (cell density 8 x 10^6 cell/mL) from standard culturing **(according to section 3.1.1.1)** was then taken to inoculate the experimental cultures media. Cultures were kept in stable conditions for 3 days before harvesting. During the whole procedure, sterile conditions were carried out in a laminar flow cabinet to avoid any external contamination.

3.1.2.2 Freeze-Dried Microalgae Biomass

The standard and optimized *C. reinhardtii* suspensions were harvested and freeze-dried according to the methods described in **section 3.1.1.9.**

3.1.2.3 Extraction of Lipid

The freeze-dried *C. reinhardtii* biomass were extracted the total lipid content using Folch *et al*. (1957) according to the method mentioned in **section 3.1.1.11.** The lipid extracted were flush with N_2 then keep at -80 ºC for analysis.

3.1.2.4 Fatty Acid Composition Analysis

The fatty acid composition of the samples was determined using a gas chromatograph (Trace GC Ultra; Thermo Scientific) equipped with an auto injection system (AS3000) and coupled to quadropole mass spectrometer (DSQ II Quadrupole GC/MS, amu 50-380; Thermo Scientific). A dried total lipid extract as described was redissolved in 2 mL of chloroform; 100 µL of a 10 mg/mL methyl pentadecanoate and heptadecanoate was then added as the internal standard to 1 mL of the lipid extract in chloroform. Esterification was achieved through the addition of 200 µL of trimethylsulfonium hydroxide. The solution was then left for a minimum of 10 min to ensure complete conversion before injection onto the GC-MS (Dron *et al.*, 2004). The lipid extracts were then filtered through 0.45 µm syringe filter into amber GC-MS vials. 10 µL of each sample, from the GC-MS vials, was injected into the capillary column (Phenonenex Zebron, ZB-FFAP, 30 m x 0.22 mm internal diameter) using a vaporising injector (split flow of 50 mL/min). The oven temperature was maintained at 120°C for 1 min and then increased to 250 °C (5°C/min) for 2 min. The retention time of each peak for the

individual fatty acids was compared with FAME standard. A standard library was also used through the "Thermo Scientific Xcalibur V 1.4" software programme. The percentage content of each fatty acid was calculated and the concentrations (mg/g) were determined using the response factor of the internal standard **(Equation 3.4).**

$$\% \text{ Individual fatty acid} = \frac{\text{Individual fatty acid peak area} * 100}{\text{Total fatty acids peak area}} \quad \textbf{…...(3.4)}$$

3.1.2.5 Protein Analysis

Freeze-dried *C. reinhardtii* was placed in a tarred tin capsule and precisely weighed using a 5-decimal place balance. The sample ranged in weight from 4 to 5 mg. The standard (sulphanilamide) also ranged in weight from 2 to 3 mg. All samples along with standards were determined using Organic Elemental Analysis Experience (Flash, Fisher Scientific) software. The Eager Experience software automatically generates the nitrogen values and then converts to protein content using 6.25 as a conversion ratio.

3.1.2.6 Amino Acid Profile Analysis

The *C. reinhardtii* freeze-dried biomass (0.5 g) were oxidized with 5 mL of mixed solution (hydrogen peroxide/formic acid/phenol). Sodium methosulphate (0.84 g) added to prevent excess oxidation. The oxidised samples were then hydrolysed with 6 M HCl for 18 h at 110ºC under nitrogen. Most of concerning of acid hydrolysis arose from the presence of oxygen in the hydrolysing solution and the presence of the free halogen in the 6 M HCl here might be some loss of tryptophan, whereas threonine, serine and tyrosine are partly destroyed. In this method methionine and cystine were either partially destroyed or oxidised to methionine sulphone and cysteic acid (Khan and Faiz, 2008).

The pH of the hydrolysate was then adjusted to 2.2 with 7.5 N NaOH. Aliquots of samples (20 mL) centrifuged (Biofuge Stratos) at 3,000 rpm for 2 min; then syringe filtered through 0.22 µm filters in glass vials. The amino acids were separated by ion exchange chromatography (Pharmacia Biochrom, Cambridge, UK) using sodium citrate buffer (150 mM, pH 2.20) and determined by reaction with ninhydrin using photometric detection at 570 nm (440 nm for proline).

3.1.2.7 Multi-Elemental Analysis by ICP-MS

The freeze-dried *C. reinhardtii* was prepared by microwave-assisted (1500 W) acid digestion method. Briefly, weigh 0.2 g of *C. reinhardtii* freeze-dried biomass was added 6 ml of conc. HNO_3 then digested at 1500 W for 1 h. Once the digestion is complete, the digested sample were made to final volume of 20 ml by Milli-Q H_2O into each digestion vessel.

The diluted solutions were transfer to a clean universal sample bottle and analysed multi-mineral content undertaken by ICP-MS (Thermo Fisher Scientific iCAP-Q; Thermo Fisher Scientific, Bremen, Germany). The instrument was run employing three operational modes, including (i) a collision-cell (Q cell) using Helium cell gas with kinetic energy discrimination (He-cell) to remove polyatomic interferences, (ii) standard mode (STD) in which the collision cell is evacuated and (iii) hydrogen mode (H_2-cell) in which H_2 gas is used as the cell gas.

External multi-element calibration standards (Claritas-PPT grade CLMS-2 from SPEX CertiPrep Inc., Metuchen, NJ, USA) included Ag, Al, As, Ba, Be, Cd, Ca, Co, Cr, Cs, Cu, Fe, K, Li, Mg, Mn, Mo, Na, Ni, P, Pb, Rb, S, Se, Sr, Tl, U, V and Zn, in the range 0–

100 µg L^{-1} (0, 20, 40, 100 µg L^{-1}). A bespoke external multi-element calibration solution (PlasmaCAL, SCP Science, France) was used to create Ca, Mg, Na and K standards in the range 0–30 mg L^{-1}. Phosphorus, boron and sulphur calibration utilized in-house standard solutions (KH_2PO_4, K_2SO_4 and H_3BO_3).

In-sample switching was used to measure B and P in STD mode, Se in H_2-cell mode and all other elements in He-cell mode. Peak dwell times were 10 mS for most elements with 150 scans per sample. Sample processing was undertaken using Qtegra™ software (Thermo Fisher Scientific) utilizing external cross-calibration between pulse-counting and analogue detector modes when required.

3.1.2.8 Protein Separation

Proteins from *C. reinhardtii* were separated using SDS-PAGE according to the method applied from Laemmli (1970), with 12% gel (Mini-protein TGX Precase Gels, Bio-Rad Laboratories, Inc, USA). To prepare the protein sample, 10 mg of the sample was placed in 1 mL of 2% SDS solution. The mixture was then vortexed and incubated at 60ºC for 30 min to dissolve protein. The homogenate was centrifuged at 14,800 rpm for 10 min at 4ºC to remove undissolved debris. The clear supernatant was collected; protein concentration was determined by BCA protein assay (Pierce) using bovine serum albumin as a standard. Protein samples (20 µg) were denatured under reducing condition, using a Laemmli buffer and 2-mercaptoethanol mixture concentration 5 µg/mL, at 95ºC for 5 min; Sample (10 µL); initial protein concentration at 20 µg/mL, were then loaded onto the gel. Electrophoresis was conducted at 500A. After separation, proteins were fixed and stained for 5 h in 0.125% Coomassie Brilliant Blue R-250 in 40% methanol and 10% glacial acetic acid. Gels were destained with destaining solution I (50%

methanol and 7.5% glacial acetic acid) for 15 min and with destaining solution II (5% methanol and 7.5% glacial acetic acid) for 3 h.

3.1.2.9 Ash Content

Ash content was determined according to (Sluiter *et al.*, 2008). Freeze-dried *C. reinhardtii* (0.5 g) were placed into pre-weight silica crucible in triplicate. The crucibles were then placed in a muffle furnace (Carbolite, AAF1100) and ignited for 8 h at 550ºC. The samples were left overnight in the muffle furnace and then removed and the crucible reweighted. The ash content was calculated as follows in **Equations (3.4)–(3.6).**

$$W_{FDS} = W_{(C+FDS)} - W_c \quad \text{.....} \quad \textbf{(3.4)}$$

$$W_{IS} = W_{(C+IS)} - W_c \quad \text{.....} \quad \textbf{(3.5)}$$

$$\%\ \text{Ash} = (W_{IS} \times 100)/W_{FDS} \quad \text{.....} \quad \textbf{(3.6)}$$

Where symbols refer to the weight of the freeze-dried sample **(W_{FDS})**, the crucible with the freeze-dried sample **($W_{(C+FDS)}$)**, the weight of the crucible **(W_c)** and the weight of the ignited sample **(W_{IS})**.

3.1.2.10 Estimation of Carbohydrate Content

The carbohydrate percentage of freeze-dried *C. reinhardtii* was estimated by difference (100 – percentage of the other macronutrients; protein, lipid and ash content).

3.2 Materials and Methods for Impact of Hydrodynamic Disruption on *C. reinhardtii* Cells and Nutritive Compositions

3.2.1 Microalgae Culture Preparations

The *C. reinhardtii* was cultured under the standard condition according to **the section 3.1.1.1** until reach the stationary phase.

3.2.2 Determination of Cavitation Device Power

The device power (W) was measured via calorimetry by recording the change in temperature over time of the 500 cm^3 water subjected to disruption **(Figure 3.4C and Figure 3.5C).** The charting experiment data **(Appendix A, Table 2 and 3)** were used to produce the graph **(Appendix B Figure 2A and B)** providing the rate of change value (change in temperature over time) that was used to calculate the power of the device in Watts (W) using the **Equation 3.7** (Briars, 2013).

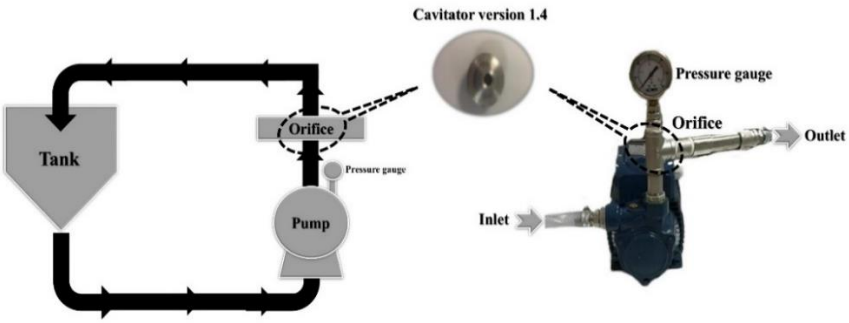
$$\text{Power (W)} = (\Delta T/\Delta t)\, C_p M \qquad \text{…….} \quad \textbf{(3.7)}$$

Where symbol refer to

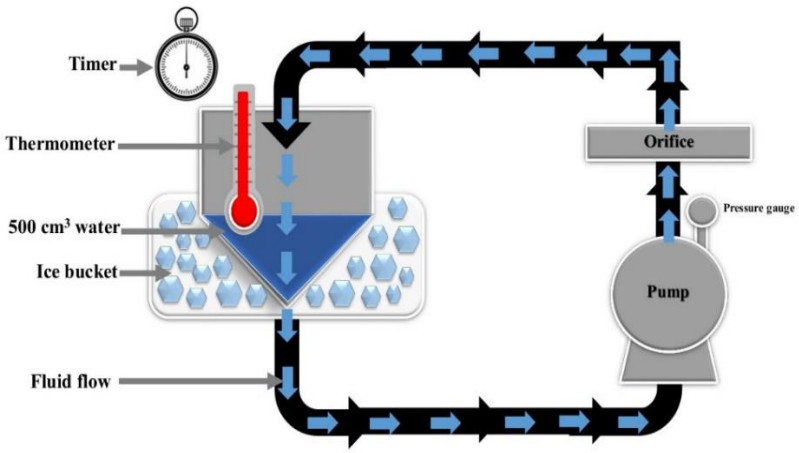
$(\Delta T / \Delta t)$ = Change in temperature over the time.

C_p = Heat capacity of the solvent (in this instance : water at 25 ^oC : 4.18.13 J kg^{-1} k^{-1})

M = Volume of solvent used (for this experiment is 500 cm^3)

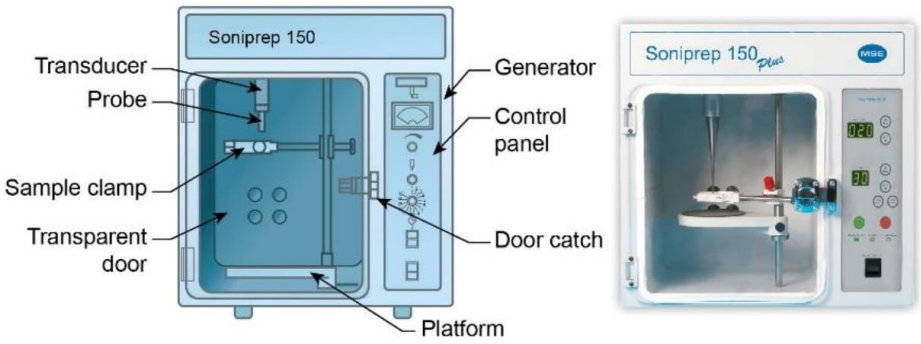


(A) Hydrodynamic cavitation diagram **(B) Hydrodynamic cavitation device**

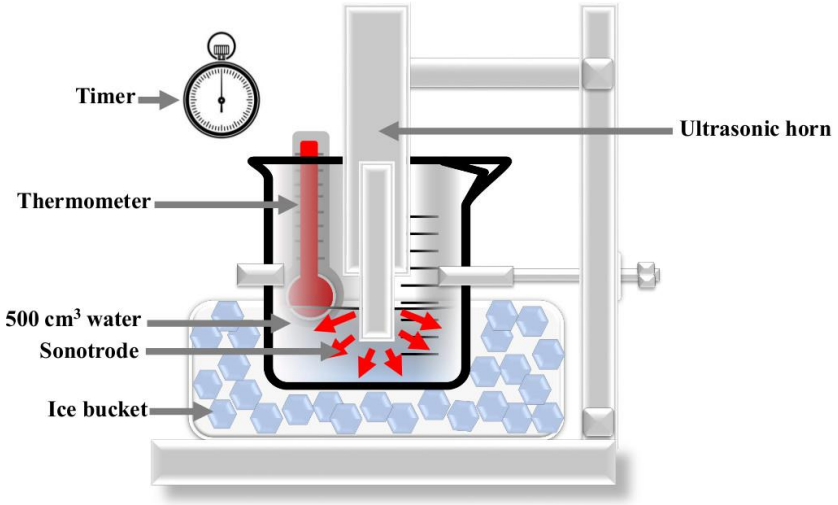


(C) The flow of the fluid for cavitation power determination.

Figure 3.4: Diagram (A), device (B) and flow of the fluid into the hydrodynamic cavitation device (C). During the whole process, the *C. reinhardtii* suspension were maintained at 4 ºC in the ice bucket to avoid overheat. The pump device create pressure via motor (1.5 kW pump, Pedro, Italy) with flow rate 30 ~ 140 L/min. The condition and power are cavitator version 1.4, cavitation power 586.43 W and power density 1.17 (W/cm^3).



(A) Ultrasonication diagram **(B) Ultrasonication device**



(C) The flow of the fluid for cavitation power determination

Figure 3.5: Diagram (A), device (B) and sonotrode generation of the ultrasonication device (C). During the whole process, the *C. reinhardtii* suspension were maintained at 4 ºC within the ice bucket to avoid overheat. The condition and power of are 20 kHz (probe 13 mm), cavitation power 12.33 W and power density 0.02 W/cm^3.

This calculation power then used to calculated the density from each particular equipment type by using **Equation 3.5**

$$\text{Power Density (W/cm}^3\text{)} = \text{Power (W)} / \text{Volume} \quad \ldots\ldots\ldots\ldots\ldots\ldots \quad \textbf{(3.5)}$$

Power density is define by the unit W/cm^3

Volume refers to the amount of water used in the calorimeter equipment (500 cm^3)

3.2.3 Microalgae Cell Disruption

3.2.3.1 Hydrodynamic Cavitation

The hydrodynamic cavitation device **(Figure 3.4A and B)** (Efficiency Technologies Limited, UK) used in this research has pump device that creates pressure via a motor (1.5 kW pump, Pedrollo, Italy) cavitator version 1.4, cavitation power 586.43 W and power density 1.17 (W/cm^3). The liquid flow into the inlet system through the orifices leads to a rapid change in pressure. Numerous cavities grow and then violently collapse, which emit secondary spherical shock waves, so called hydrodynamic cavitation. All the disruption tests were performed in triplicate. In all, 8 L of suspended *C. reinhardtii* cells were treated in under 2 mins. During the whole process, the *C. reinhardtii* suspension were maintained at 4 ºC within the ice bucket to avoid over heat. Separation was conducted by centrifugation (Thermal Jouan CR3i multifunction centrifuge, Scientific Laboratory, UK) at 10,000 *g* for 10 min at 20 °C, and the supernatant was analysed for proteins and pigments released.

3.2.3.2 Ultrasonication

The ultrasonication device **(Figure 3.5A and B)** used in this research was a probe device (Soniprep 150 Plus, Fisher, UK) :20 kHz (probe 13 mm), cavitation power 12.33 W and power density 0.02 W/cm^3,that generated acoustic cavitation in aqueous media. Briefly, the 100 mL of *C. reinhardtii* suspension was sonicated 30 min with 5 s of ultrasonication and 15 s of resting time, to prevent overheating of the device. Separation was conducted by centrifugation (Thermo Jouan CR3i multifunction centrifuge, Scientific Laboratory, UK) at 10,000 *g* for 10 min at 20 °C. The supernatant was analysed for proteins and pigments released.

3.2.4 Ultra-Structural Analysis by Light Microscope

An optical microscopy with differential interference contrast microscopy (DIC) was used (Leitz Diaplan Microscope). A drop of intact, ultra sonication and HDC-disrupted *C. reinhardtii* slurry was placed on a glass slide, topped with a cover slip and allowed to dry before being placed under the microscope. All images were taken using light microscope (Nikon Microscope Eclipse E400, Nikon Corporation) using 100X objective lens and 10X eye lens. A digital camera was attached to the microscope to capture images of the samples.

3.2.5 Freeze-Dried *C. reinhardtii* Biomass

Fresh intact *C. reinhardtii* suspensions was harvested by centrifugation (J2-21 Centrifuge, Beckman Coulter) at 5000 *g* for 30 min and frozen at -20 °C for 24 h before freeze-drying for seven days (Freeze Dryer, Super Modulyo, Edwards, UK). For hydrodynamic cavitation-disrupted *C. reinhardtii*, the suspension, without being subjected to

centrifugation, was immediately frozen at -20 ºC for 24 h before freeze-drying (Edward Freeze Dryer, Super Modulyo). The dry biomass, intact and hydrodynamic cavitation-disrupted, was then weighed and kept at -80 ºC until required for analysis.

3.2.6 Pigment Release Analysis

To measure pigment release in the supernatant fraction after centrifugation, 200 µL of aqueous extract was mixed with 1300 µL of pure methanol and incubated in the dark for 1 h at 45°C. Samples were then centrifuged (Thermo Jouan CR3i multifunction centrifuge, Scientific Laboratory, UK) at 10,000 *g* for 10 min at 20 °C. The organic phase containing the pigments and chlorophyll was recovered and analysed with spectrophotometer (Genesis 108 Vis spectrophotometer, Thermo Scientific, UK) modified from Ritchie, (2006) and Safi *et al.*, (2015). Results were determined using **Equation (3.8)**

$$\text{Total chlorophyll } (\mu g/mL) = (19.3443 \times A_{652}) + (4.381 \times A_{665}) \quad \ldots\ldots \quad (3.8)$$

Where symbol refer to

A_{652} = Absorbance of sample at optical density 652 nm.

A_{665} = Absorbance of sample at optical density 665 nm.

3.2.7 Protein Release Analysis

To measure the protein content in the supernatant fraction after centrifugation, samples containing the crude protein extract (0.2 mL) were measured by the method described in (Lowry *et al.*, 1951). A calibration curve was prepared using a concentration range of standard bovine albumin from 0 to 1500 µg/mL. The protein content was then measured

at 750 nm with spectrophotometer (Genesis 108 Vis spectrophotometer, Thermo Scientific, UK) after a baseline was set with a blank sample containing all the chemicals without the extract and expressed as mM BSA/g sample.

3.2.8 Structure Illumination Microscope (SIM) and Confocal Microscopy

Fresh intact and hydrodynamic cavitation-disrupted *C. reinhardtii* were stained by the staining solution mentioned in the **section 3.1.1.13,** to maximize the visualization of cell membrane and cell wall layer of digested sample the FM4-64 FX (1 µg/mL) were mixed into the staining solution. Their ultrastructure were visualized using SIM and Confocal microscopy.

3.2.9 Lipid Extraction

The freeze-dried intact and disrupted *C. reinhardtii* biomass analysed the total lipid content using Folch *et al*. (1989) according to the method mentioned in **section 3.1.1.11.** The lipid extracted were flush with N_2 then keep at -80 ºC for carotenoids analysis.

3.2.10 Chlorophyll and Carotenoids Analysis

The chlorophyll and carotenoids content, of freeze-dried intact and hydrodynamic cavitation-disrupted *C. reinhardtii* biomass were analysed by high-performance liquid chromatography (HPLC) with PDA detection using an Agilent 1100 system. The flow rate of the mobile phase (Acetonitrile: Methanol: Ethyl Acetate with 0.05% Triethylamine (TEA) was set at 0.5 mL/min. The use of TEA was recommended to increase carotenoid recovery (Hart and Scott, 1995). Two gradient mobile phases were

applied from 95:5:0 to 60:20:20 in 20 min, maintaining this proportion until the end of the run and re-equilibration took 15 min. Samples (10 µL) were injected through a guard-column (Waters, Nova-Pak C18, 4 µm, 3.9×20 mm) and separated on Nova-Pak C18 (4 µm, 3.9×20 mm, 22.5 °C). The extracted residues were dissolved in 0.7 mL of acetone (plus 0.1% BHT) and then filtered through a 0.45 µm Glass Micromembrane Filter (GMF). The filtrates contained the chlorophyll and carotenoids were quantified by HPLC. The chlorophyll and carotenoids were detected at 454 nm, and its concentration determined using a calibration curve of external standards (chlorophyll *a*, chlorophyll *b*, *β*-carotene and lutein) dissolved in acetone.

3.3 *In Vitro* Bioaccessibility of Chlorophyll (*a* and *b*) and Carotenoids (*β*-Carotene and Lutein) from Intact and HDC-Disrupted *C. reinhardtii.*

3.3.1 The Changes on Cell Wall Morphology and Phase Behaviour of Intact *C. reinhardtii* during the in vitro Human Digestion

3.3.1.1 *C. reinhardtii* Culture Preparations

The *C. reinhardtii* was cultured under the standard condition according to the **section 3.1.1.1** until reach the stationary phase. The cell were then harvested and freeze-dried according to the method described in **section 3.1.1.9.**

3.3.1.2 Sample Preparation for Digestion

The liquid matrix was prepared by mixing the 0.5 g freeze-dried intact *C. reinhardtii* freeze-dried biomass with 4.5 g pure thoroughly mixed using agitator.

3.3.1.3 Chemical Preparation for Digestion

All materials are standard analytical grade. The enzyme products are mostly provided by Sigma-Aldrich. The list of electrolytes stock solution of Simulated Salivary Fluid (SSF), Simulated Gastric Fluid (SGF) and Simulated Intestinal Fluid (SIF) are shown in **Table 3.2.**

Table 3.2: List of concentration of electrolyte stock solution for simulated digest fluid. The stock solution was prepared fresh. $CaCl_2(H_2O)_2$ is not added to the electrolyte stock solutions as precipitation may occur. Instead, it is added to the final mixture of simulated digestion fluid and food.

Salt solution (mol/mL)	Stock solution (mmol/L)	SSF (pH 7) (mmol/L)	SGF (pH 3) (mmol/mL)	SIF (pH 7) (mmol/L)
KCl	0.5	15.09	6.9	6.8
KH_2PO_4	0.5	1.35	0.9	0.8
$NaHCO_3$	1	13.68	25	85
NaCl	2	-	47.2	38.4
$MgCl_2(H_2O)_6$	0.15	0.15	0.12	0.33
$NH_4(CO_3)_2$	0.5	0.06	0.5	-
$CaCl_2(H_2O)_2$	0.3	1.5	0.15	0.6
HCl	6	1.1	15.6	8.4

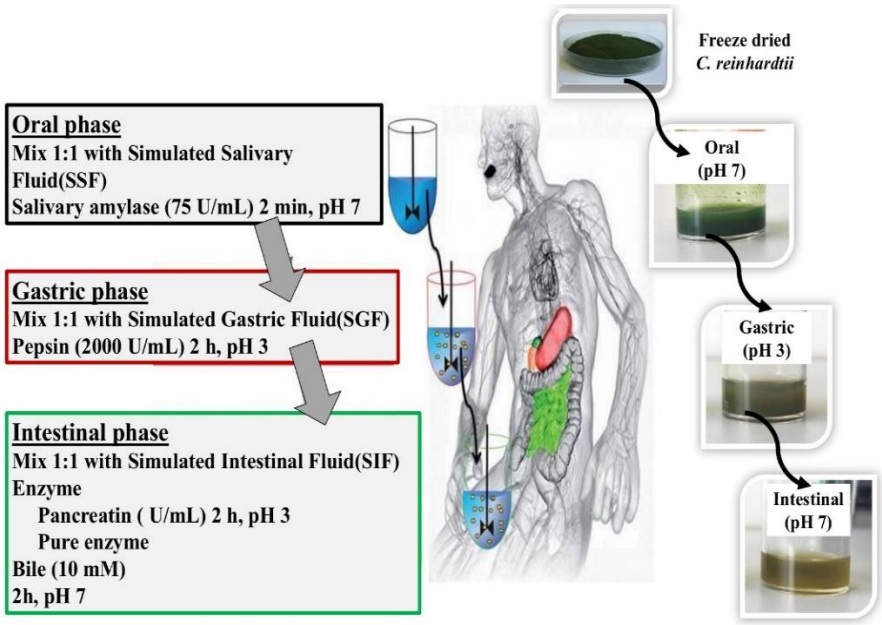


Figure 3.6: Overview and flow diagram of a simulated *in vitro* digestion method. Enzyme activities are in units per mL of final digestion mixture at each corresponding digestion phase (Minekus *et al.*, 2014).

3.3.1.4 *In vitro* Human Digestibility

The *in vitro* static human digestion was performed according to **Minekus *et al.*, (2014) (Figure 3.6).** To begin with the simulated oral digestion, the 5 g of the matrix was add to 4.0 mL of SSF electrolyte stock solution and mix together using agitator.0.5 mL salivary α-amylase solution of 1500 U/mL made up in SSF (α-amylase from human saliva Type IX-A, 1000–3000 U/mg protein, Sigma) is added, followed by 25 µL of 0.3 M $CaCl_2$ and 0.475 mL of water and thoroughly mixed and shaken (Stuart Orbital Incubator SI500, Bibby Scientific Ltd, UK) (100 rpm) for 2 min at 37°C, followed by adding 8.0 mL of SGF to the oral bolus. 1.0 mL of Porcine pepsin (EC 3.4.23.1) and 5.0 µL of $CaCl_2$ were then added to achieve 2000 U/mL and 0.075, respectively, in the final digestion mixture.

The pH was then reduced to 3 using 1 M HCl and samples were shaken (100 rpm) for 2 h at 37°C. The digest from gastric chyme (20 mL) was mixed with 11 mL of SIF, 5.0 mL of a pancreatin solution, 800 U/mL made up in SIF based on trypsin activity (pancreatin from porcine pancreas, Sigma), 2.5 mL fresh bile (160 mM in fresh bile), 40 µL of 0.3 M $CaCL_2$, 0.15 mL of 1 M NaOH to reach pH 7.0 and 1.31 mL of water. Samples were again incubated in the shaker incubator for 2 h (100 rpm, at 37 °C) (SI500 Shaking Incubator, Keison Products, UK). All treatments were run parallel with control (without enzyme and bile).

3.3.1.5 Ultra-Structural Analysis by TEM

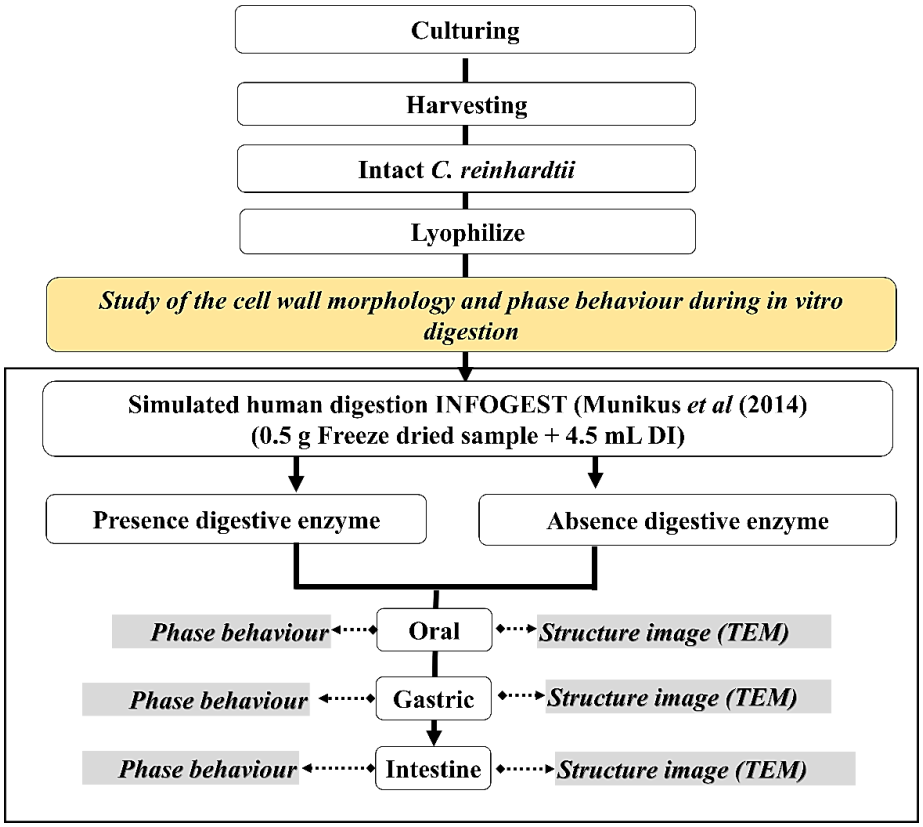


Figure 3.7: The diagram of the cell wall morphology and phase behavior during *in vitro* digestion of intact freeze-dried *C. reinhardtii*.

The cell morphology study of intact and disrupted *C. reinhardtii* freeze-dried biomass was performed according to **Figure 3.7** Briefly, an aliquot (1 mL) of pre-digested, gastric and duodenal phases of the *C. reinhardtii* in the presence and absence of digestive enzyme were visualized their cell integrity using TEM follow to the method described in **section 3.1.1.12.**

3.3.1.6 Phase behaviour

The phase behaviour study of intact and disrupted *C. reinhardtii* freeze-dried biomass. was performed according to **Figure 3.7** Briefly, an aliquot (1 mL) of pre-digested, gastric and duodenal phases of the *C. reinhardtii* in the presence and absence of digestive enzyme were taken into the eppendorf. All treatment were leave at room temperature for observing the phase behaviour.

3.3.2 *In vitro* Bioaccessibility of Chlorophyll (*a* and *b*) and Carotenoids (*β*-Carotene and Lutein) from Intact and HDC-Disrupted *C. reinhardtii*

The experimental diagram for an estimation of bioaccessibility of chlorophyll (*a* and *b*) and carotenoids (*β*-carotene and lutein) from intact and HDC-disrupted *C. reinhardtii* freeze-dried biomass illustrated in **Figure 3.8.**.

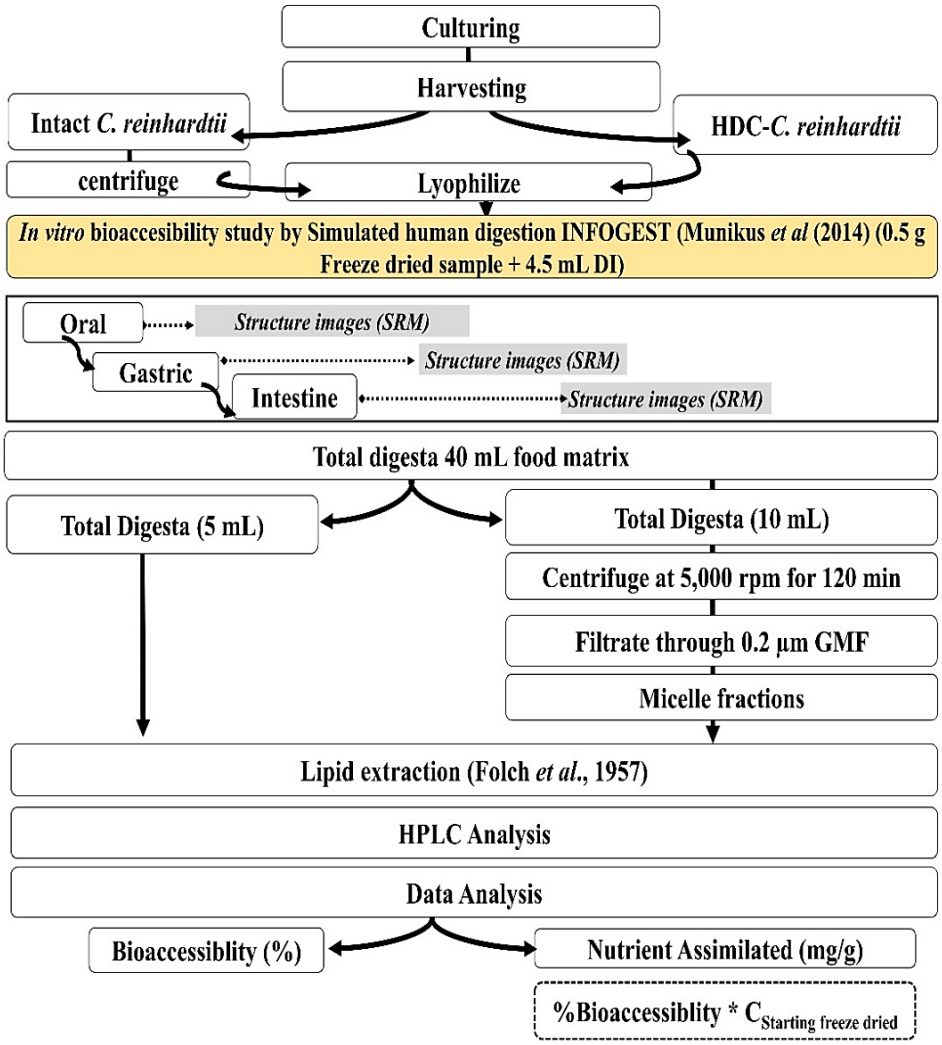


Figure 3.8: The diagram for *in vitro* bioaccessibility of the intact and disrupted experiments.

3.3.2.1 *C. reinhardtii* Culture Preparations

The *C. reinhardtii* was cultured under the standard condition according to the **section 3.1.1.1** until reach the stationary phase. The cell were then harvested and freeze dried according to the method describe in **section 3.1.1.9**

3.3.2.2 Hydrodynamic Cavitation Disrupted *C. reinhardtii* Biomass

The stationary of *C. reinhardtii* suspension was disrupted using the HDC device according to the method described in **section 3.2.3.**

3.3.2.3 Freeze-Dried *C. reinhardtii* Biomass

Fresh intact *C. reinhardtii* suspensions were harvested by centrifugation (J2-21 Centrifuges, Beckman Coulter) at 5000 *g* for 30 min and frozen at -20 °C for 24 h before freeze-drying for seven days (Freeze Dryer, Super Modulyo, Edwards, UK).

For hydrodynamic cavitation (HDC)-disrupted *C. reinhardtii*, the whole suspension, without being subjected to centrifugation, was immediately frozen at -20 ºC for 24 h before freeze-drying (Edward Freeze Dryer, Super Modulyo). The intact and HDC-disrupted freeze-dried biomass, was then weighed and kept at -80 ºC until use for *in vitro* bioaccessiblity analysis.

3.3.2.4 Sample Preparation for digestion

The liquid matrix was prepared by mixing the 0.5 g freeze-dried intact and HDC-disrupted *C. reinhardtii* freeze-dried biomass with 4.5 g pure water and thoroughly mixed using agitator.

3.3.2.5 *In vitro* Human Digestibility

To determine the *in vitro* bioaccessibility of intact and HDC-disrupted *C. reinhardtii* freeze-dried biomass. The *in vitro* static human digestion was performed according to method describe in **section 3.3.1.4**

3.3.2.6 Obtaining Micelle Fractions

The final mixture obtained after all simulated human digestion was termed total digesta, an aqueous phase containing residual solids in suspension and mixed micelles. The mixed micelles were separated from total digesta at the end of the simulated digestion by centrifugation at 5,000 rpm for 120 min using a Rotina 380R centrifuge. A clear supernatant containing mixed micelles (micelle fractions) was separated from the total digesta. The micelle fraction was then filtrated through 0.2 µm Glass Microfiber Filter (GMF) to remove unmicellised chlorophyll and carotenoids (modified from Kimura and Rodriguez-Amaya, (2002)). The filtrates containing the micellised chlorophyll and carotenoids were quantified by HPLC.

3.3.2.7 Extraction of Chlorophyll (*a* and *b*) and Carotenoid (*β*-Carotene and Lutein) from the Total Digesta and Micelle Fractions

A 5 mL aliquot of total digesta and micelle fractions was added to 5 mL of chloroform:methanol (1:1, v:v), vortexed for 1 min, added 1 mL of RO water and agitated for 1 min. The sample were then centrifuged for 10 min at 3,000 rpm (4°C). The extracts were repeated until the three-layer fractions appeared. The combined chloroform fraction (lowest phase) was dried under the nitrogen gas. The extracted residues were redissolved in 0.7 mL of acetone (plus 0.1% butylated hydroxytoluene (BHT) then filtered through a 0.45 µm GMF filter. The HPLC analysis of chlorophyll and carotenoids content was performed.

3.3.2.8 Bioaccessibility of Chlorophyll (*a* and *b*) and Carotenoids (*B*-Carotene and Lutein) Calculation

The bioaccessiblity index was calculated as micrograms of chlorophylls and carotenoids in the micellar fraction * 100 / milligram of chlorophyll (*a* and *b*) and carotenoids (*β*-carotene and lutein) in the total digesta **(Equation 3.9 – 3.10).** This index gives information of which proportion of those compounds will present in the material are ready for the enterocyte absorption.

$$\text{Bioaccessiblity (\%)} = (C_{\text{micelle fractions}} / C_{\text{total digesta}}) * 100 \quad \ldots \textbf{(3.9)}$$

$$\text{Nutrient Assimilated (mg/g DWB)} = \%\ \text{Bioaccessibility} * C_{\text{Initial freeze-dried microalgae}} \quad \ldots \textbf{(3.10)}$$

Where symbols refer to

$C_{\text{micelle fraction}}$ = Concentration of the compound present in the micelle fraction (µg/g of an initial freeze-dried microalgae).

$C_{\text{total digesta}}$ = Concentration of the compound present in the total digesta (µg/g of an initial freeze- dried microalgae).

$C_{\text{initial freeze-dried microalgae}}$ = Concentration of the compound present in an initial freeze-dried microalgae (µg/g DWB).

3.3.2.9 Structured Illumination Microscopy (SIM) and Confocal Microscopy

The intact and HDC-disrupted *C. reinhardtii* freeze-dried biomass were carried out through *in vitro* human digestibility procedure **(as descripted above section 3.3.1.4).** The 1 mL of total digesta during each stage of digestion (initial, oral, gastric and small intestinal) were taken to prepare and visualize the ultrastructure using SIM and confocal according to the methods described in **section 3.1.1.13** -

3.4 Material and Methods for Impact of *C. reinhardtii* Inclusion in Zebrafish Diet on their Growth Performance and Key Metabolites

3.4.1 Microalgae Preparation

The *C. reinhardtii* was cultured under the standard condition according to the method mentioned in **section 3.1.1.1** until reach the stationary phase. The cells were then harvested using centrifuge and freeze-dried according to the method mentioned in **section 3.1.1.9**. The biomass was then weight and kept at 80°C until use as ingredient for the fish diet formulation.

3.4.2 Diet Formulation

A control diet was formulated to meet the nutritional requirements of zebrafish using standard aquaculture ingredients. Experimental diets were designed based on a control diet with 10%, 20% and 50% reduction in the fishmeal content **(Table 3.3).** An intact *C. reinhardtii* freeze-dried biomass was incorporated into each experimental diet at maximum levels determined by their nutritional profiles, while maintaining isonitrogenous and isocalorific characteristics.

Complete diets were formulated in house at the University of Liverpool, Briefly, the desired amounts of all ingredients required were mixed using a Hobart food mixer until thoroughly mixed. Water was added until the mixture achieved dough-like consistency. The dough mixture was then spread out on trays and dried for 24 hours at 50°C using a nine shelf Parallexx Excalibur food dehydrator. Once dry, the diet was crushed and processed through a series of sieves with apertures of 425 µm and 850 µm. The desired

pellet size fell between the two. All diets were refrigerated at 4 ℃ for the duration of the study. The nutritional profiles of each diet were carried out in our laboratory and is depicted in **Table 3.4.**

Table 3. 3: Compound formulation of experimental diet.

Ingredients (%wt)	**Control**	**% Reduction in fishmeal**		
		10%	**20%**	**50%**
Fish Meal	38.74	34.12	30.98	19.62
Rapeseed Oil	4.37	-	-	-
Vitamin premix	0.31	0.32	0.32	0.33
Mineral premix	0.42	0.43	0.43	0.44
Wheat Gluten	22.91	21.64	24.29	32.98
Corn Starch	31.82	22.62	21.89	19.41
Binder (CMC powder)	0.52	0.53	0.53	0.54
C. reinhardtii	-	19.43	20.50	25.12
Arginine	-	-	0.05	0.24
Leucine	-	-	-	-
Lysine	0.90	0.90	0.99	1.31

Table 3.4 of experimental diet; no data for tryptophan was available during formulation. Essential amino acids were shading.

Nutrients		Control	% Reduction in fishmeal		
			10%	20%	50%
Gross composition	**% DM**				
Crude Protein		46.56	46.10	46.32	46.53
Crude Lipid		11.30	11.73	11.81	12.25
Carbohydrate		35.06	33.90	33.69	33.33
Crude Ash		7.94	7.74	7.19	5.22
Crude Fibre		0.13	0.01	0.01	0.01
Fatty acids	**% Lipid**				
Linoleic Acid		17.87	10.82	11.80	14.82
Linolenic Acid		11.17	25.49	25.82	27.33
Arachidonic Acid		0	0	0	0
EPA		0	0	0	0
DHA		8.49	7.22	6.51	3.97
Amino acid	**% Protein**				
Histidine		1.98	2.02	2.02	2.03
Isoleucine		3.30	3.31	3.31	3.32
Leucine		6.17	6.20	6.23	6.33
Lysine		6.09	6.17	6.13	6.07
Methionine		1.25	1.26	1.25	1.25
Phenylalanine		2.62	2.65	2.63	2.62
Threonine		2.92	2.95	2.94	2.92
Valine		3.44	3.47	3.47	3.44
Arginine		4.51	4.56	4.57	4.63
Cysteine		1.25	1.69	1.77	2.07
Tyrosine		2.62	2.65	2.63	2.62
Gross Energy	**MJ/kg DM**	21.28	19.46	19.39	19.08

3.4.3 Subjects and Husbandry

All fish were bred in-house at The Institute of Integrative Biology aquarium facility, the University of Liverpool. The first trial involved 750 juvenile *D. rerio* (AB wild type strain). The fish were approximately 2 months old at trial start. Fish were housed in groups of 15 individuals in 50 identical 1.5 L Zebrafish tanks, made by Aquatic Habitats, each measuring 25cm x 7cm x 15.5cm **(Figure 3.9)** The tanks were connected to a central system which is maintained by a sump filtration

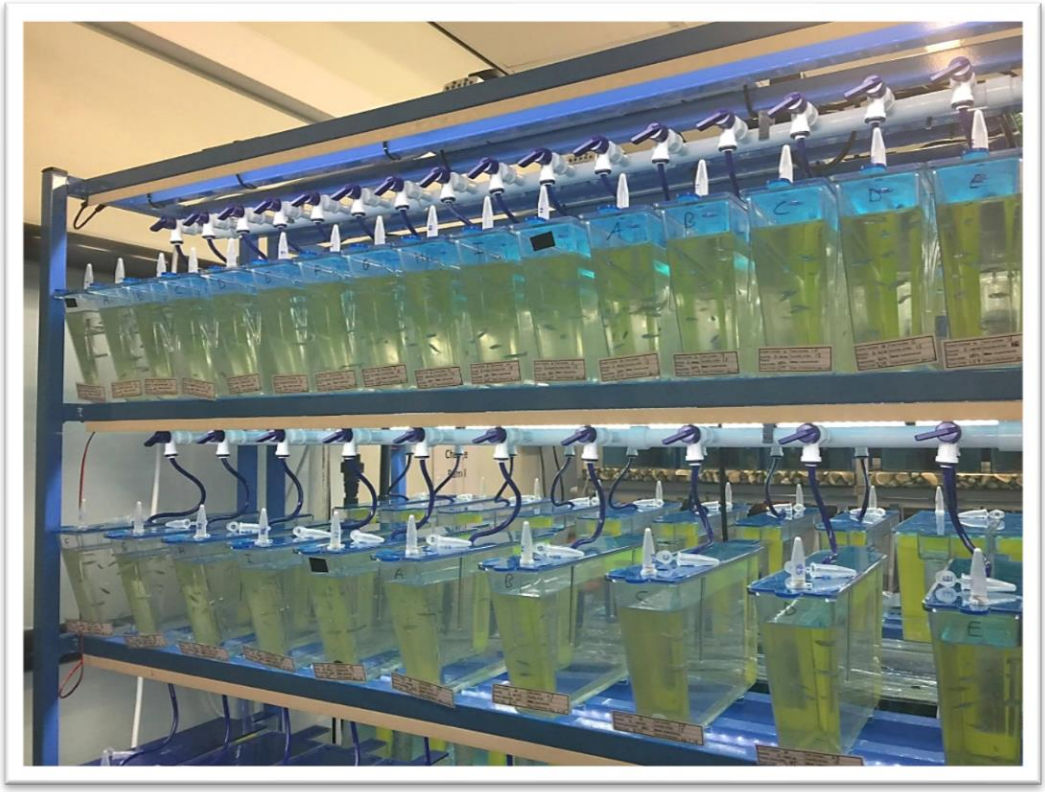


Figure 3.9: The aquatic habitat zebrafish tanks for growing fish feeding trail.

system and 20% weekly water changes. Due to the small size of the fish, tanks were fitted with a 400 µm fry mesh baffle; cleaning was conducted weekly during the weighing of the fish to prevent further disturbances. Water quality was subsequently kept stable with the following parameters: Ammonia (NH_4); 0mg/l, Nitrite (NO_2); 0mg/l, Nitrate (NO_3); <50mg/l and pH; 7.0. Fish were maintained at 28 ± 1 ^{o}C and exposed to a 12/12-hour light cycle. For the second trial, 84 juvenile *D. rerio* (*Casper strain*) were used. The fish were approximately 7 months old at the start of the trial. Fish were housed in groups of 6 individuals, either all male or all female, in 14 identical tanks, the same 1.5 L tanks as above using the same baffles. The tanks were maintained on the same system as above with the same water quality parameters and environmental conditions. Cleaning of tanks was done while fish were housed in breeding tanks.

3.4.4 Growing Procedure

Each of the four diets was fed to two tanks, one male and one female tank. Feed was given daily *ad libitum* until satiation. After 3 weeks of feeding, the fish were bred by mixing males and females together one evening in medium (3 L) aquatic habitat zebrafish tanks, measuring 11.5 cm x 25 cm x 15 cm**.** The tanks contained a mesh net, with a 2 mm aperture, used to create a false raised base with a gradient; this prevents cannibalism of the eggs by adults. The next morning, as soon as the lights came on, the flow was switched off and the net was raised slightly to stimulate breeding. After a two-hour period, fish were removed, sexed and returned to all male and all female housings. Eggs were collected from the spawning tanks by hand, transferred to sample jars then snap frozen with liquid nitrogen; samples were stored at -80°C until further analyses. Spawning was repeated every 3 days until sufficient embryos had been collected for the required sample

size. Fish were then humanely euthanized by fully trained personnel via a home office approved schedule one method; concussion followed by pithing of the brain to confirm death.

3.4.5 Ethical Issues

It is anticipated that the welfare standards of the subject fish will not be affected; they are being housed using standard methods and fed on balanced diets formulated to meet nutritional requirements. The subject fish are also bred at the University of Liverpool zebrafish facility and so endured minimal transport or housing stress prior to this experiment starting. However, welfare is monitored independently; if the welfare condition of any individual fish reached an unacceptable level, it would be removed from the trial.

3.4.6 Experimental Procedures

3.4.6.1 Weighing Fish

Fish were weighed weekly to record growth throughout. Fish were weighed by tank; 15 fish as a whole due to time constraints. A separate 1.5 L tank was used, filled with one cm of system water, placed on a fisher scientific SG-602 balance and tarred. All 15 fish were caught in a small net, lifted from the housing tank, excess water was removed gently by dabbing the net on a blue roll paper towel, the net preventing any physical harm to the fish, and then the fish were placed in the tank on the balance. The weight was recorded for each tank. While the fish were situated in the weighing tank, the housing tank and mesh baffle was cleaned before returning the fish.

3.4.6.2 Feeding and Sampling

After each tank of the fish had been weighed, one week's worth of daily feeds was premeasured using a kern 770 five-point balance at 4% body weight per day. This was repeated weekly to maintain a 4% body weight feed regime throughout the 8-week trial, which encouraged maximum growth and health. On the days when the fish were weighed, feed was given afterwards in order to gain accurate fish weights; on all other days, feed was given in the morning. Five replicate tanks were given the same experimental diet, 75 fish in total per diet. At the end of the trial period, the fish were humanely euthanized by fully trained personnel via a home office approved schedule one method; concussion followed by pithing of the brain to confirm death. Samples were then collected for analysis.

3.4.6.3 Growing Parameters Calculations and Assessments

There are number of indicators widely accepted and used for comparison of resource use within fish feeds, useful indicators for assessment of new diet formulations and incorporation of novel or alternative ingredients. The most widely used indicator of feed efficiency is Feed Conversion Ratio (FCR), FCR indicates the efficiency at which feed is converted into animal biomass, calculated as follows:

$$\text{FCR} = \frac{\text{Total feed intake (kg)}}{\text{Net aquacultural production (kg)}} \quad \textbf{……(3.11)}$$

- Total Feed Intake (TFI) = total feed given – waste output.
- Net production = Mass at end of study period – mass at start of study period. (Boyd *et al.*, 2007)

The SGR demonstrates the growth achieved per day during a time period for which subjects are fed the test diet, calculated as follows:

$$SGR\ (\%) = 100 \times (\ln W_2 - \ln W_1) \times (t_2 - t_1)^{-1}$$

Where symbol refer to

ln	=	natural log
W1	=	initial weight
W2	=	final weight;
t1	=	starting time point (day one)
t2	=	end time point (final day number).

3.4.6.4 Preparation and Analysis of the Fish for Culling

When the trail period ended, the fish were killed (ethically) and the weight of each zebrafish recorded. Each fish group of the same feeding trial was then put together in a bag and initially frozen in -20 °C. The fish were later stored at a -80°C. The fish were then freeze dried for one week (Edwards Freeze Dryer, Super Modulyo). During the freeze-drying process, samples were protected from light exposure. Samples were then ground to homogeneous powder using mortar and pestle under dim light and with a liquid nitrogen.

3.4.6.5 Lipid Extraction

The freeze-dried fish body and egg were extract the total lipid content using Folch *et al.* (1989) according to the method mentioned in **section 3.2.9.** The lipid extracted were flush with N_2 then keep at -80 °C for carotenoids analysis.

3.4.6.6 Carotenoids Analysis

Nitrogen dried lipids obtained from **section 3.3.3.11** were redissolved with 1 mL acetone and vortexed. Extracts were then vigorously mixed with an equivalent volume of methyl-tetra-butyl ether (MtBE) and 0.5 mL distilled water. The aqueous phase was extracted with additional three times using the MtBE. The combined MtBE Phases were evaporated to dryness under a gentle stream of nitrogen, suspended with 0.5 mL MtBE vortexed and passed to PTFE membrane filter (0.45 µm), sealed under nitrogen in brown glass vials and stored in the dark at -80 °C until further analysis.

The analysis was carried out using an Agilent 1100 HPLC equipped with Diode array with UV-Vis detector and using Gemini-NX C18 column (250 mm length, 4.6 mm, 5 µm particle size, Phenominix UK) and Phenomenex C18 guard column (4 µm, 3.9×20 mm). UV-vis absorption spectra were recorded 325 nm for retinol. Mobile phases consisted of two components: (A) methanol and (B) MtBE. The solvents pump was programmed to inject initially 90% A from 0-12 min, followed by linear gradients of 90-60% A from 12-13 min, maintained until 22 min followed by linear gradient back to 90% A initial conditions until the end of run at 30 min. The flow rate was 0.8 mL/min.

3.5 Statistical Analysis

Experiments were performed in triplicate. i.e. three separate samples for each experiment and the statistical analysis was carried out using the Minitab V.17 statistical package (Minitab Inc., PA, USA) using post-hoc analysis of variance (ANOVA) and according to Fishers test with statistical significance at $p \leq 0.05$.

CHAPTER 4

The Biochemical Response of *C. reinhardtii* as Influenced by Growth Media Manipulation

4.1 Introduction

The demand for natural ingredients is increasing within the modern food industry, and this is driven by consumer perceptions seeking more nutritional products (Gouveia, 2008). Microalgae have the potential to enhance the nutritional content of conventional food preparation and function as a probiotic agent with a positive impact on human health (Richmond, 2004). Processed microalgae are used in food supplements and act as food ingredients in a variety of food products, such as candy bars, cookies, pasta, beverages, etc. (Gouveia *et al*., 2008). They are also exploited in pharmaceutical and cosmetics because of their containing bioactive molecules (Wang *et al*., 2015).

The quality of microalgae biomass, expressed by chemical composition and bioactive compound content, is highly dependent on the culturing step. Nutritional composition is later considered for the commercial use of microalgae. The physical properties of microalgae cells: such as structure, shape, cell wall rigidity, are an essential feather in maintaining the architecture of the microalgae. The cell wall is the living part of the cell and is subject to composition and structure changes as the tissue growth, matures and become senescent (Johnson and Williamson, 2003). The essential biochemical composition established throughout all microalgae growth stages allows for harvesting at any stage, depending on the intended use.

The synthesis of target molecules can be optimised during the cultivation of microalgae. There are two approaches to culturing microalgae to enhance biomass and/or increase the concentration of target molecules. Firstly, nutrient stress involves changing media composition by limiting nitrogen and phosphorous limitation, and changes in carbon source. Secondly, the physical stress is described as the manipulation of operational conditions and external factors such as the application of high-light intensities, medium salinity and electromagnetic fields (Benavente-Valdés *et al*., 2016).

In this chapter we firstly evaluated the biochemical compounds and structural response in *C. reinhardtii* to mixotrophic culturing, in our lab scale system. Secondly, we focused the impact of changing the composition of nitrogen concentration on the nutrition profile of *C. reinhardtii* biomass under mixothrophic conditions, and to establish the potential of employing *C. reinhardtii* as a novel functional food ingredient.

4.2 Results and Discussion

4.2.1 Growth Kinetic and Biomass Productivity of *C. reinhardtii* Response to Mixothrophic Culturing

To characterize the growth kinetics of *C. reinhardtii*, the cells were grown in Tris-acetate phosphate media under mixotrophic conditions. Growth kinetics were determined from data obtained by sampling cultures each day for 30 days **(Figure 4.1).**

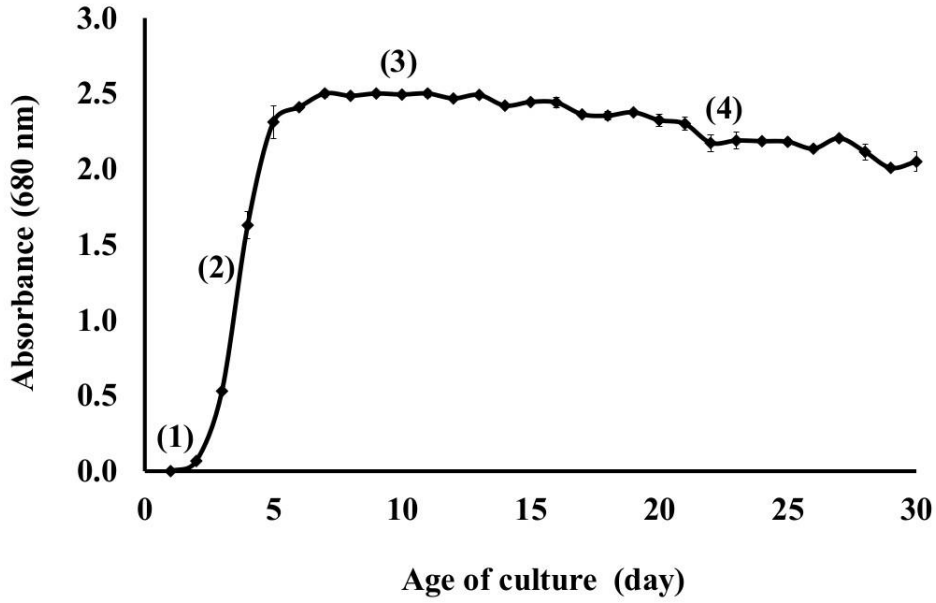


Figure 4.1: The growth kinetics of *C. reinhardtii*. Data were plotted between the optical density (OD680) versus age of culture (day). Values shown are from triplicate determination. The different numbers refer to: (1) Lag phase; (2) Exponential phase; (3) Stationary phase; (4) Decline phase.

Four phases can be identified as the typical patterns for *C. reinhardtii* : lag phase (1), exponential phase (2), stationary phase (3), and death phase (4). The lag phase finished at two days of cultivation, revealing that cells can adapt themselves to the growth media. Then, *C. reinhardtii* cells divided quickly, increasing cell population and optical density; this exponential phase took place over four days. The most growth was seen during the late exponential phase at seven days of cultivation. Thereafter followed the stationary phase, during which no further increasing cell density occurred, and nutrients were depleted. Cultures maintained excellent cell density for at least a month without any significant cell decline.

To estimate specific growth rates, the batch culture growth at the logarithmic growth phase (seventh day of cultivation) was harvested for determination of cell number and

biomass production**.** The biomass production equation was produced and was then used to create the graph providing the relation of cell number, biomass production and age of cultivation **(Figure 4.2)**. The volumetric biomass productivity is 0.01 g/L/day, respectively. This implies that at the end of the exponential phase *C. reinhardtii* produce only 0.07 g/L or 70 mg/L under lab scale system.

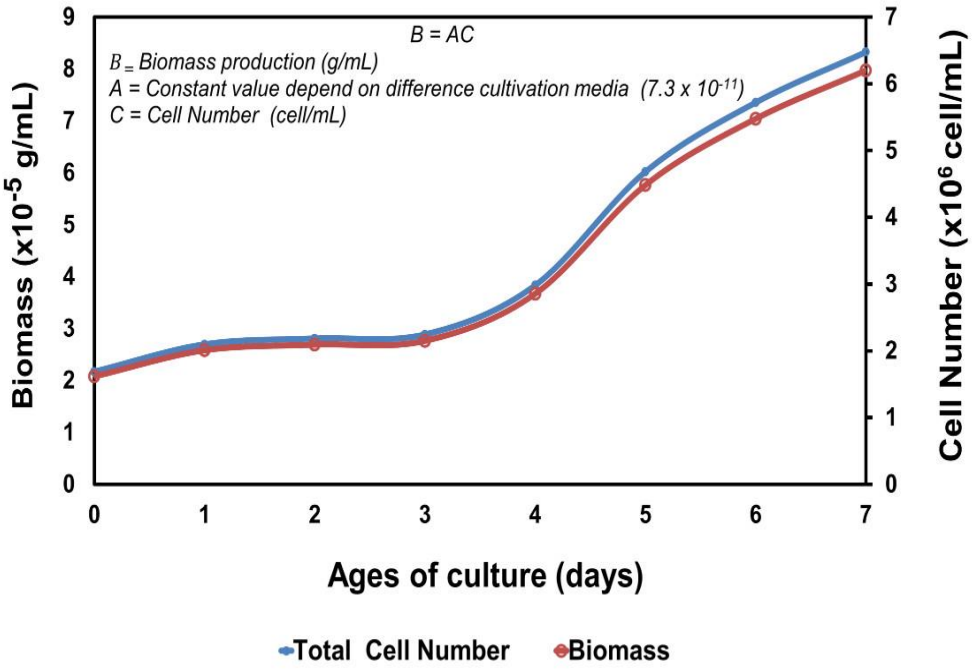
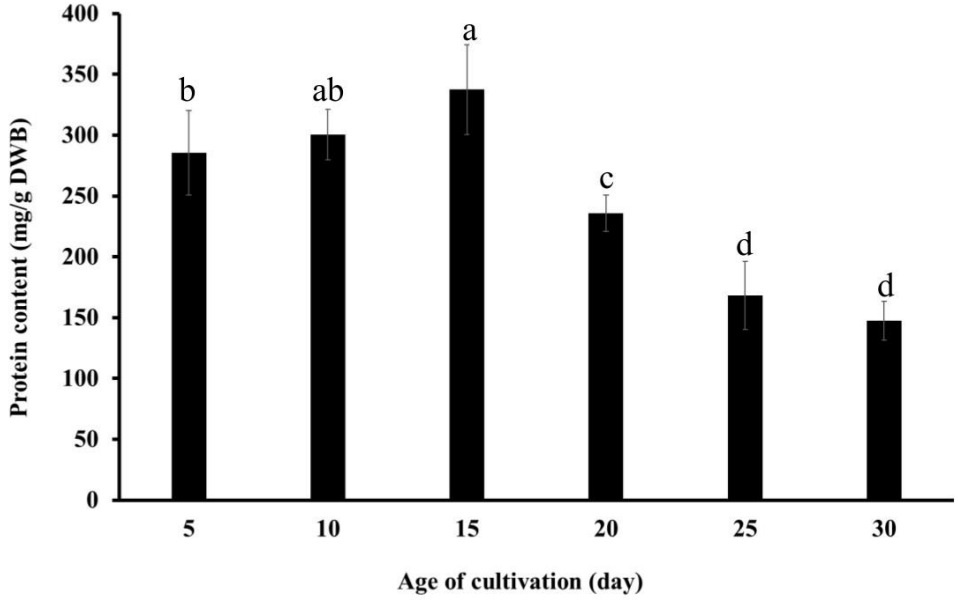


Figure 4.2: The relationship of the biomass production (g/mL), cell number and age of culture of *C. reinhardtii*. Values shown are from triplicate determination.

4.2.2 Biochemical Compound Response to Mixothrophic Culturing of *C. reinhardtii*

There was a significant difference detected over time in biochemical compositions measured versus age of cultivation. The maximum value of protein and pigments was retained during the exponential phase, decreased continuously during the stationary phase **(Figure 4.1).** These level of protein and pigments reached their lowest point during the

declining phase **(Figure 4.3 to 4.5).** In contrast, total lipid content rose and then remained high during the stationary phase. These observations imply that *C. reinhardtii* accumulates more lipid bodies as a function of nutrient deprivation. Overall, the protein content ranged from 150 to 350 mg/g **(Figure 4.3).** The total lipid content 150 – 200 mg/g **(Figure 4.4).** The pigment content ranged from 0.06 – 0.11mg/g, 0.03 – 0.03 mg/g and 0.13 to 0.18 mg/g for chlorophyll *a*, chlorophyll *b* and carotenoids, respectively **(Figure 4.5).**



:

Figure 4.3: The protein content of *C. reinhardtii* biomass. The biomass was harvested at regular five-day intervals for protein content analysis. Data were plotted between the protein content (mg/g DWB) versus age of culture (day). Values shown are from triplicate determinations. Letters on the bars not sharing the common letter indicate significant differences ($p<0.05$).

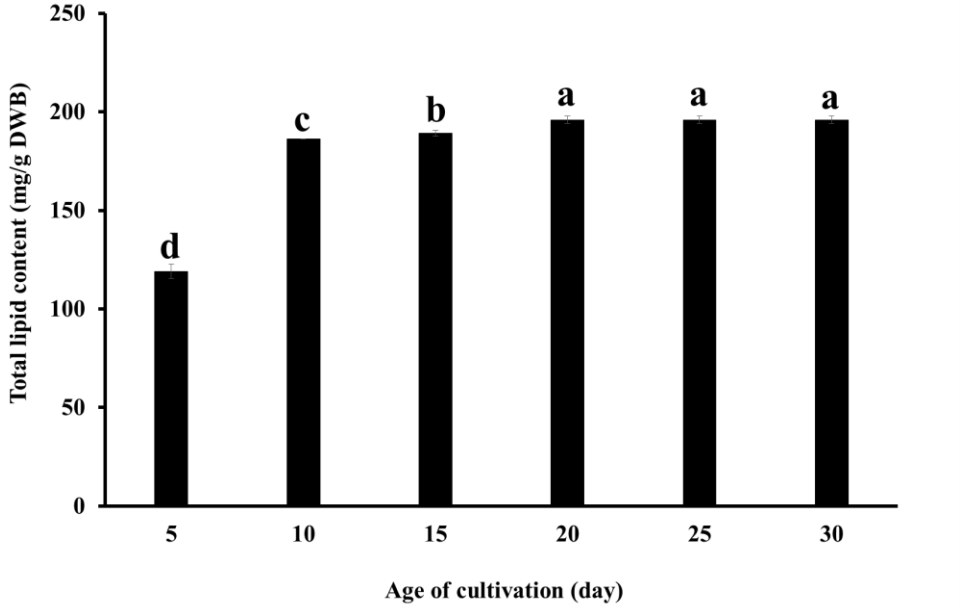


Figure 4.4: The total lipid content of *C. reinhardtii* biomass. The biomass was harvested at regular five-day intervals for lipid content analysis. Data were plotted between the lipid content (mg/g DWB) versus age of culture (day). Values shown are from triplicate determinations. Letters on the bars not sharing the common letter indicate significant differences ($p<0.05$).

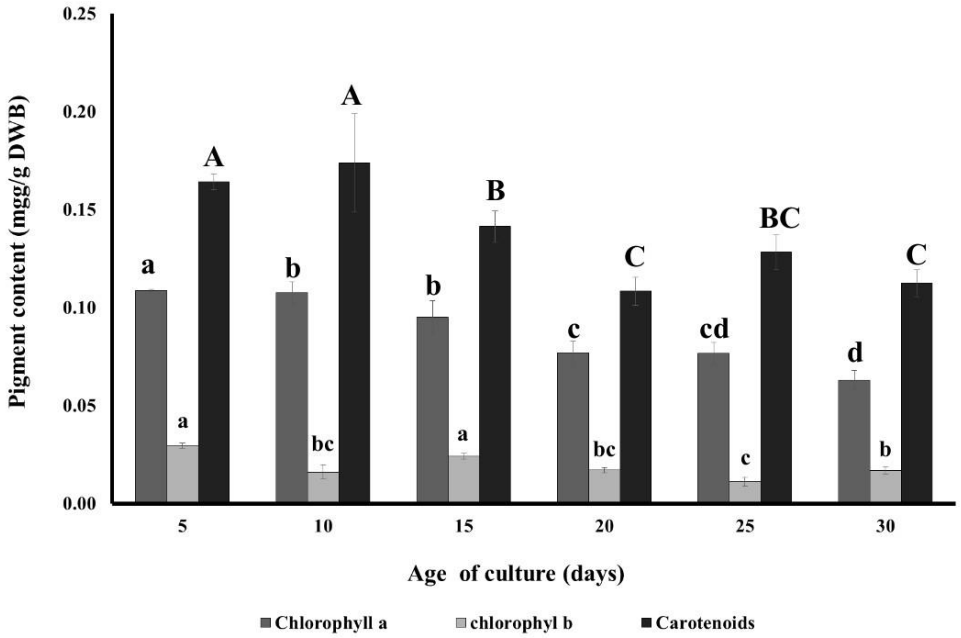


Figure 4.5: The pigment content (chlorophyll *a*, chlorophyll *b* and carotenoids) of *C. reinhardtii* biomass. The biomass was harvested at regular five-day intervals for pigment content analysis. Data were plotted between the pigment content (mg/g DWB) versus age of culture (day). Values shown are from triplicate determinations. Letters on the bars not sharing the common letter indicate significant differences ($p<0.05$).

4.2.3 Morphological Structure of *C. reinhardtii*

Selected TEM images are presented in **Figure 4.6.** The images revealed different cell sections with a detailed morphology and location of each intracellular organelle. A number of images were used to represent one status as no single section can show all the cell components clearly depending on the region and depth of each section. The round shaped images resulted from a section across the width, while the oval like images represent a section across the length (Rochaix, 2001). *C. reinhardtii* presents different structure through the cells' life cycle. Vegetative and gametic cells are highly ordered structures which carry a chaotrope-soluble crystalline layer and the zygotes elaborate new walls that are denser, thicker, lack the crystalline layer, and are insoluble in chaotropic solvents and SDS (Grief and Shaw, 1987).

The sheet-like thylakoid membranes (TM) are the main component of the chloroplast, the organelle that occupies two thirds of the cells grown under standard conditions, which is clear in **Figure 4.6 (A_2),** where chloroplasts occupy a significant part of the cell volume. TM appears in two arrangements depending on the images' section. It appears as a continuous compact arrangement in **Figure 4.6(A_2)** and a discreet peripheral collection of membrane stacks, which, although not clear in **Figure 4.6,** should be organised as a stack of three as most *Chlamydomonas* species (Simionato *et al*., 2013). The eyespot, as it appears in Figure 4.6**(A_3)**, is attached to the inner plastid membrane. In cells grown in nutrient replete media to stationary phase **Figure 4.6(A_1), (A_2) and (A_3),** all the cell organelles are observable in different sections. Also, few starch granules were detected at stationary phase and lipid bodies were identified. Both storage entities (starch granules and lipid bodies) are abundant at 30-days.

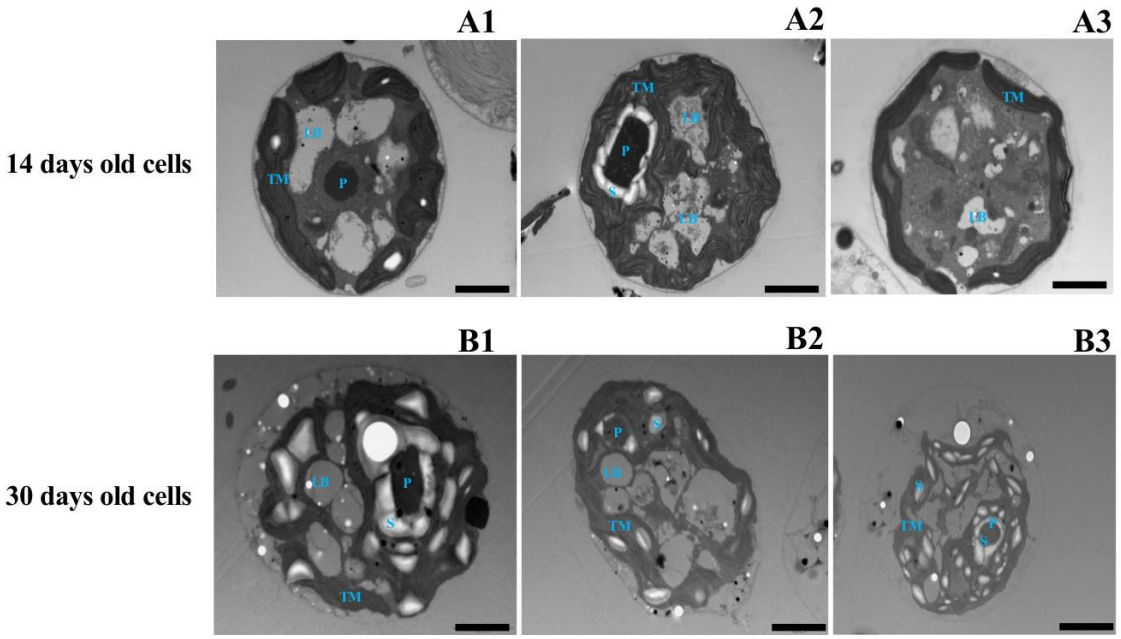


Figure 4.6: TEM images of *C. reinhardtii* at different stage of culturing. The cells harvested at 14 days and 30 days were visualized by TEM. (A1 to A3) images for 14 days old cells. (B1 to B3) images for 30 days old cells.TM: Thylakoid membrane, LB: Lipid body, P: Pyranoids; S: Starch. Scale bar = 2 µm.

This data can help specifying the best phase of *C. reinhardtii* at which cells are more digestible by human. Although, no previous studies have been conducted on the digestibility of *C. reinhardtii* using mammalian enzymes, however, when *C. reinhardtii* was used as a substrate in anaerobic fermentation there was better digestibility as determined by the amount of gas produced, than some other seaweeds like *Ulva* (Mussgnug *et al*., 2010).

The chloroplasts of green microalgae are the site of photosynthesis and carbon fixation and thus, the chloroplast has a great capacity for accumulation of endogenous proteins, starch, lipids, and pigment/ carotenoids (Engel *et al*., 2015). Understanding morphology and internal structure allows for appropriate selection of disruption techniques for recovery of products from the chloroplast (Dixon and Wilken, 2018). Therefore, the *C. reinhardtii* cells at the end of the exponential phase were visualized by Structured Illumination Microscopy (SIM). An illustration of a typical cell with autofluorescence of the chloroplast in intact microalgae revealed similar features were described previously which contained one green chloroplast of this species **(Figure 4.7).** The signal of each component represents the cell membrane (red), chloroplast (green) and lipid body (yellow) in *Chlamydomonas* cells**.**

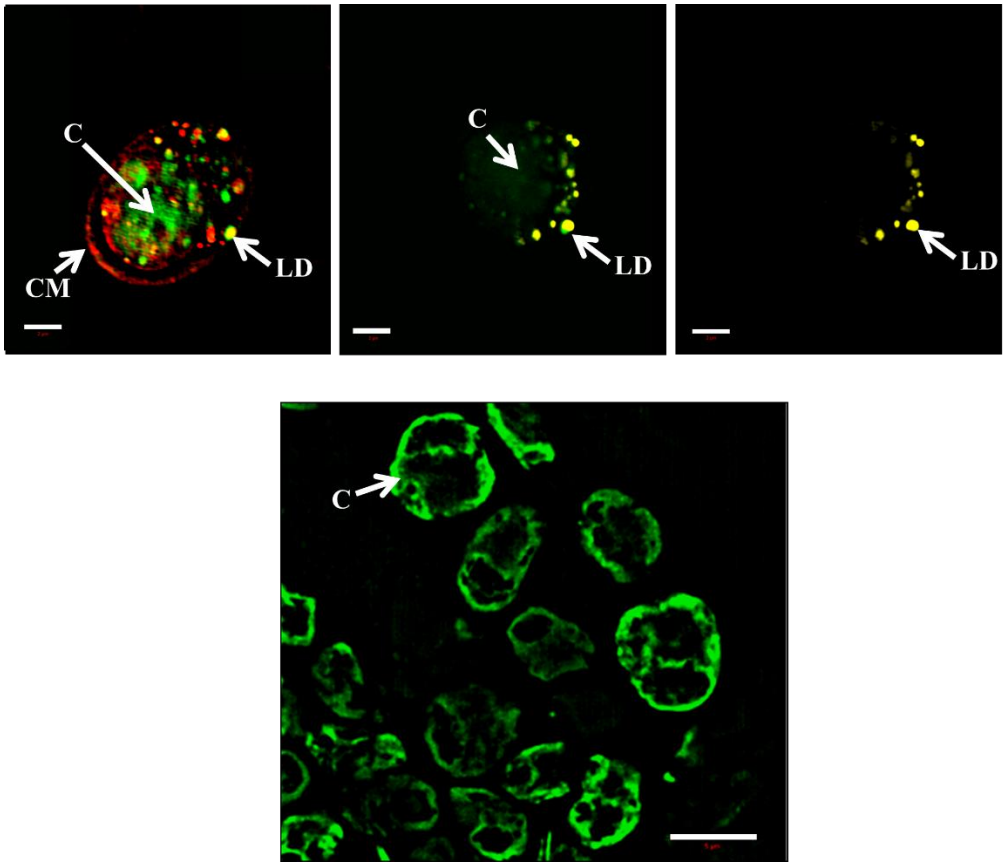


Figure 4.7: Morphological structures of *C. reinhardtii*. The cells harvested at the end of the exponential phase were visualized by structured illumination microscopy (SIM); scale bar = 2 µm. The cell membrane was stained with FM-143Fx as shown in red. Lipid droplets were stained with Nile red and shown in yellow while the autofluorescence of the chloroplast was recorded in the green channel. LD: Lipid droplets, C: Chloroplast. CM: Cell membrane.

4.2.4 Effect of Nitrogen Stress Media on the Proximate Analysis of Freeze-Dried *C. reinhardtii* Biomass

The proximate analysis (total protein, total lipid, ash, and carbohydrate content) were measured in freeze-dried *C. reinhardtii* biomass grown exponentially under standard (STD) and nitrogen stress media conditions (non-added nitrogen, 0.2 M (NAN) and 0.6 M (N^+)) shown in **Table 4.1.** Overall, the proximate analysis revealed that the protein is the dominant component in *C. reinhardtii*, and N^+-cultured biomass gave the highest protein content (437.6±3.2 mg/g DWB). The chromatogram of inorganic content (nitrogen, carbon and hydrogen) in standard *C. reinhardtii* freeze-dried biomass is shown in **Figure 4.8**. Even though there is no significant difference in total protein content was found among NAN and STD cultured biomass ($p \leq 0.05$).

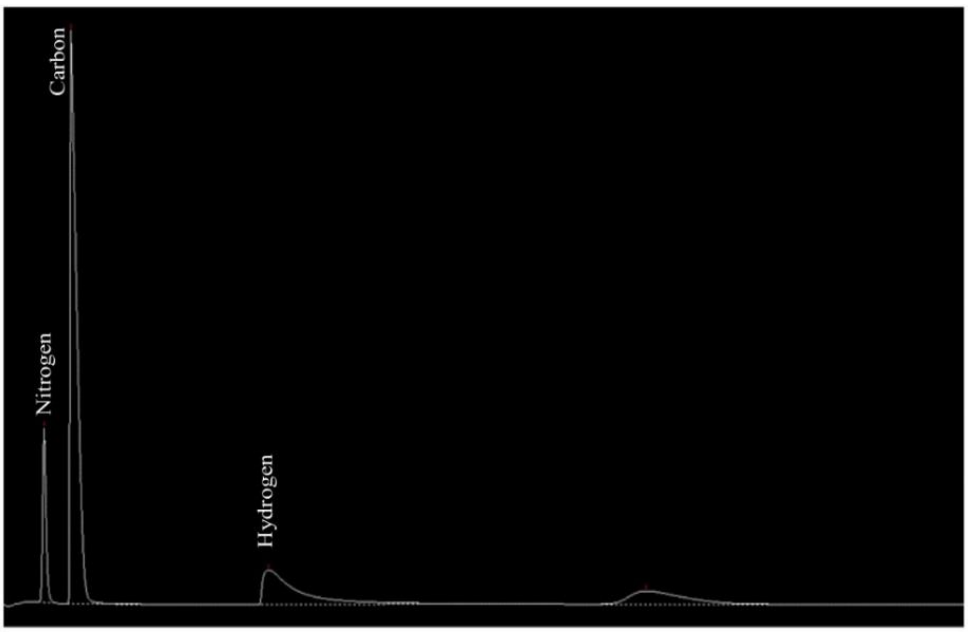


Figure 4.8: Represents the chromatogram of inorganic content in standard *C. reinhardtii* freeze-dried biomass.

Significantly higher lipid accumulations were found in NAN cultured biomass (209±0.05 mg/g DWB) compared to STD (137±0.01 mg/g DWB) and N^+ culturing biomass (161±0.01 mg/g DWB) ($p \geq 0.05$). Considering the photosynthesis process consists of two universal phases **(Figure 4.9). Light-dependent reactions** occur in the thylakoid during the first stage, which requires direct energy from sunlight, water splitting for a source of electrons and protons, generation of energy carrier molecules (NADPH and ATP), and oxygen release as a by-product. The high-energy chemical intermediates, ATP and NADPH, are utilised as an energy source for the sequence stage of light-independent reactions (Baroukh *et al*., 2014). The second stage includes **light-independent reactions** (also known as dark reactions or the Calvin cycle). This stage incorporates CO_2 through the Calvin cycle, which produces one three-carbon sugar (3-phosphoglycerate, written as G3P). Then, G3P is transformed in glyceraldehyde 3-phosphate (GAP) and transported to the cytosol of the cell (Baroukh *et al*., 2014).

Table 4.1: Nutritional composition (mg/g DWB) of freeze-dried *C. reinhardtii* biomass. The STD biomass was cultivated in STD growth media until reach an exponential phase (seven days). The NAN and N^+ biomass were grown in standard growth media until they reach exponential phase before transfer into the nitrogen stress growth media, stress cultured were maintained for three days they were harvested. All STD, NAN and N^+ biomass were cultivated and collected for nutrition analysis.

	mg/g DWB			Average Proximate content % (DWB)		
	NAN	**STD**	**N^+**	**NAN**	**STD**	**N^+**
Total protein	$425^{b} \pm 14.5$	$413^{bc} \pm 14.5$	$438^{a} \pm 3.20$	42.5	41.4	43.8
Total lipid	$209^{a} \pm 0.05$	$137^{c} \pm 0.01$	$161^{b} \pm 0.01$	20.9	13.2	16.1
Total ash	$101^{b} \pm 2.75$	$129^{a} \pm 5.63$	$109^{b} \pm 0.62$	10.1	12.9	10.9
Carbohydrate	-	-	-	21.5	26.5	27.7

Lipophilic micronutrients are considered part of the lipid, thus not included in the total sum (100) used to calculate carbohydrates by difference (100 – (protein + lipid + ash)). Mean ±SD from triplicate determinations. Letters on same row not sharing the common letter indicate significant differences ($p<0.05$). NAN - *C. reinhardtii* cultured with non-added nitrogen; STD - *C. reinhardtii* cultured with nitrogen concentration at 0.2 M and N^+ - *C. reinhardtii* cultured with nitrogen concentration at 0.6 M.

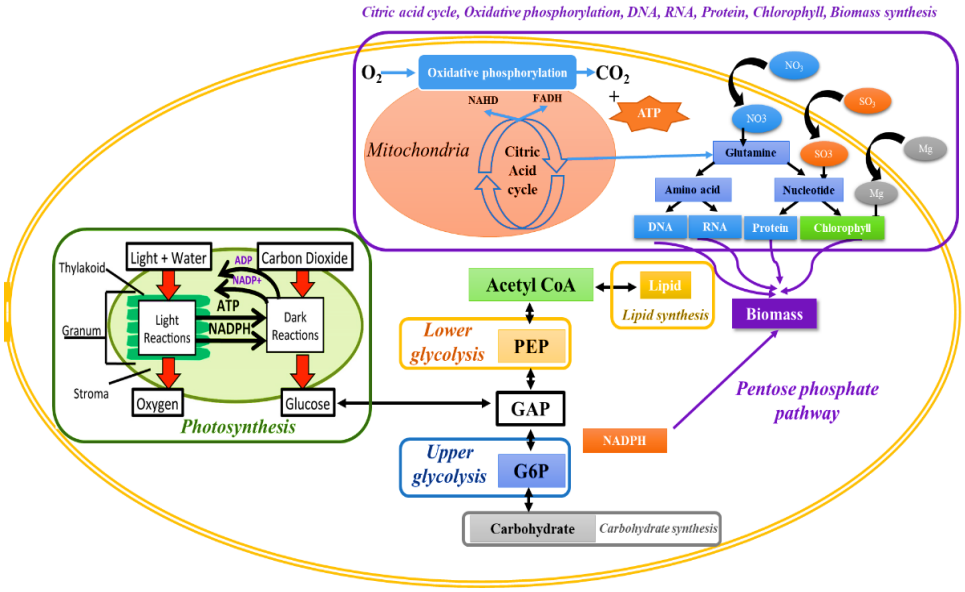


Figure 4.9: **Simplified central carbon metabolic network of a unicellular photoautrotophic microalgae (Baroukh *et al.*, 2014). glyceraldehyde 3-phosphate (GAP), 2-phosphenolpyruvate (PEP),glucose 6-phosphate (G6P), 3-phosphoglycerate (G3P).**

GAP is the end-product of photosynthesis, and is situated at the centre of glycolysis and split according to GAP into two sub-networks: lower glycolysis and upper glycolysis. **Upper glycolysis** generates glucose 6-phosphate (G6P), which is then either invested in carbohydrates synthesis or the pentose phosphate pathway to generate NADPH. **Lower glycolysis** generates 2-phosphenolpyruvate (PEP), which is subsequently invested either in lipids synthesis or the citric acid cycle, which produces the necessary intermediate metabolites for protein, DNA, RNA, chlorophyll, and biomass synthesis. Cofactors (FADH, NADH) generated by the citric acid cycle are transformed into energy (ATP) due to oxidative phosphorylation (Baroukh *et al.*, 2014). Simplified central carbon metabolic network of a unicellular photoautrotophic microalgae. The FA biosynthesis pathway can be induced by stress conditions, primarily by limiting nitrogen concentration,

which leads to the arrested biosynthesis of amino acids. The primary product of carbon fixation reactions in photosynthesis is used for lipid and starch biosynthesis.

The total ash content found in STD, N+, and NAN culturing biomass are 129.56±5.63 mg/g DWB (10%), 108±0.62 mg/g DWB (13%) and 101±2.75 mg/g DWB (11%), respectively. Other microalgae and cyanobacteria exhibit varying levels of ash, with reports of the total ash content of *Porphyridum cruentum* equivalent to 16.8 to 23.6% (Rebolloso Fuentes, 2000), *Spirulina* 7.43 to 10.4%, *Chlorella* 6.30%, and *Isochrisis* 16.08% (Tokuşoglu and uunal, 2003). In terms of total composition, *C. reinhardtii* has an extent carbohydrate content at 21.5%, 27.7%, and 26.5% for freeze-dried STD, N^+, and NAN cultured biomass, respectively. The extended carbohydrate content of *C. reinhardtii* biomass was greater than that of the other microalgae, specifically *Spirulina, Chlorella,* and *Isochrisis* (Tokuşoglu and Uunal, 2003).

The overall proximate composition of freeze-dried *C. reinhardtii* biomass consisted of proteins > carbohydrates > lipids. Regarding the average values, protein: lipid: carbohydrate of STD biomass was 41.4%, 26.5% and 13.2%. This ratio changes in nitrogen-stressed cultured biomass by increasing the lipid content **(Table 4.1).** Our results reveal the proportion of protein: lipid: carbohydrate are 42.8%: 20.9%: 21.5% under nitrogen stress condition. This value agree with previous studies reported for *Chlamydomonas* Park *et al.*, (2015) reported that *C. reinhardtii* cell consisted of protein (45%), lipid (25%) and carbohydrate (9%), on dried cell weight. These levels were changing during the N deprivation, by increased of the lipids and of total carbohydrate by ~3% of cell dry weight with a decrease in protein by 21%. Wase *et al.*, (2014) also reported increasing of total fatty acid levels of *C. reinhardtii* by about 50% after 24 hour

of nitrogen starvation from 106±6 µg/mg DWB to 165±12 µg/mg DWB and increased further to 2-fold (230 ± 16 µg/mg DCW) and 3.8-fold (404 ± 16 µg/mg DWB), respectively, of control values after 48 and 144 h.

4.2.5 Amino Acid Profile and Protein Quality

Freeze-dried *C. reinhardtii* biomass is an excellent source of amino acids **(Table 4.2).** The chromatogram of standard amino acid detected using ion exchange chromatography with photometric detection at 570 nm (A) and 440 nm for proline (B) is shown in **Figure and Figure 4.10 and 4.11.**

Glutamine, leucine and alanine with trace levels of cysteine, aspartic acid, and methionine. The NAN-cultured biomass exhibited a significant decrease in certain AAs (serine, cysteine, threonine, glutamine, lysine, and histidine) ($p \leq 0.05$). Comparing *C. reinhardtii* to a "well-balanced protein" as defined by the World Health Organization (WHO) as well as Food and Agriculture Organization (FAO), reveals that *C. reinhardtii* is a very promising protein source (FAO/WHO/UNU, 1985).

An essential amino acid (EAA) is one that humans cannot synthesize, such as phenylalanine, valine, threonine, tryptophan, methionine, leucine, isoleucine, lysine, and histidine. The amino acid score of *C. reinhardtii*, a comparison of the EAAs to the amino acid reference pattern established by the FAO/WHO offers a rough estimation of beneficial protein quality in this species. All EAAs are present in freeze-dried *C. reinhardtii* biomass, its protein content is low in sulphur-containing amino acids; notably deficient in methionine. This seems to be a standard feature in these green algae (*Chlorophyta*) (Chronakis and Madsen, 2011). Limiting capacity in methionine levels are

also found regularly in other proteins from vegetable food, particularly in soya bean (Kuiken *et al*., 1948). There are limiting factors when using large quantities of microalgae for human consumption; for example, the abundant content of nucleic acids that are metabolized to uric acid might result in adverse health effects, such as gout or kidney stones (Smith, 2004; Gantar and Svircev, 2008). An adverse effect of the microalgae consumption for consumer will be considered when microalgae have more than 10% of RNA and DNA (International Life Science Institute (ILSI) Europe Novel Food Task Force, 2000). *C. reinhardtii* biomass under standard culturing conditions at stationary phase contain DNA at 0.02±0.00 mg/100g and RNA at 0.28±0.02 mg/100 mg, respectively (Darwich, 2018). This is notably less than the minimal adverse level and so supports the potential of *C. reinhardtii* as a novel protein source for human consumption.

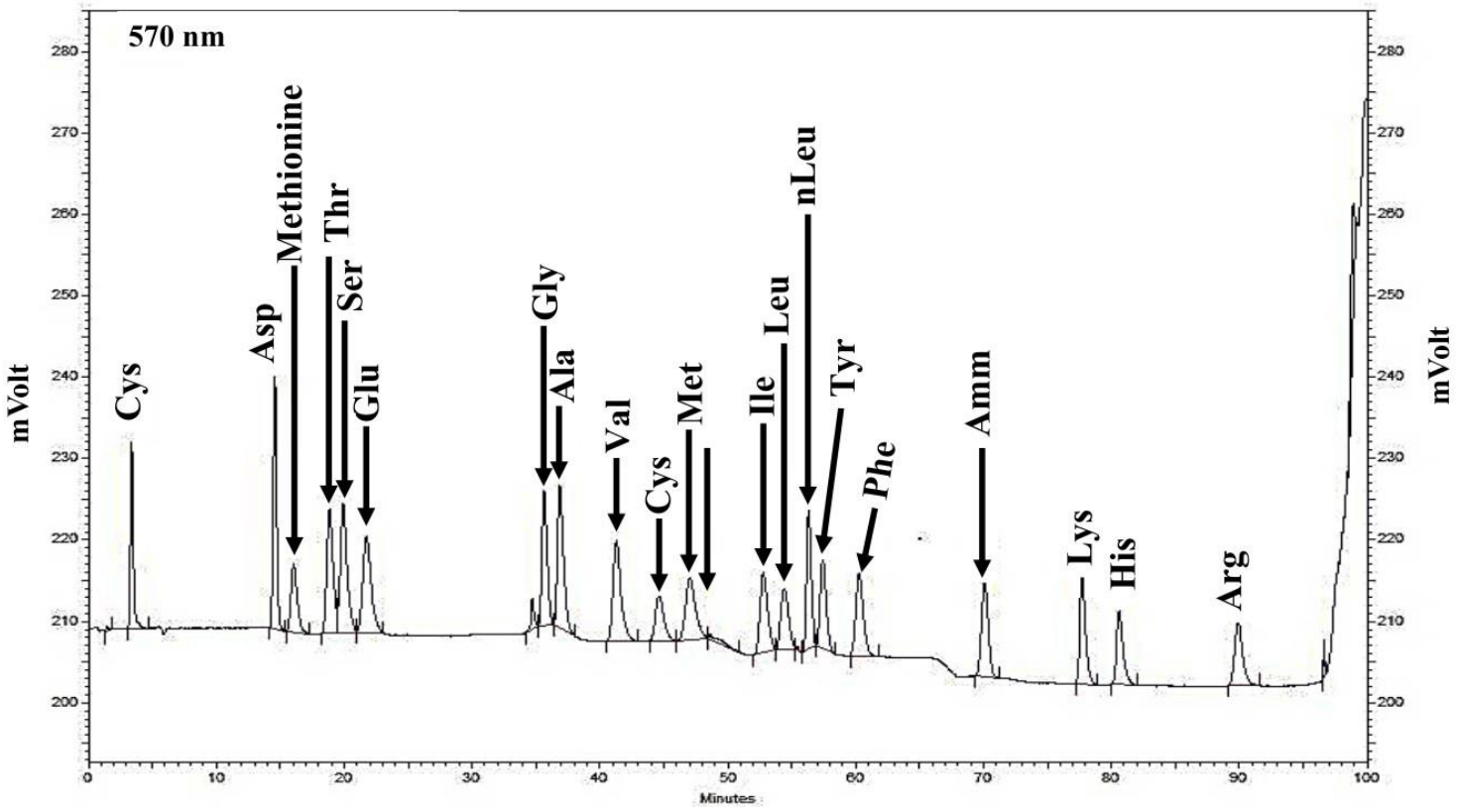


Figure 4.10: Chromatogram of standard amino acids detected using ion exchange chromatography with photometric detection at 570 nm.

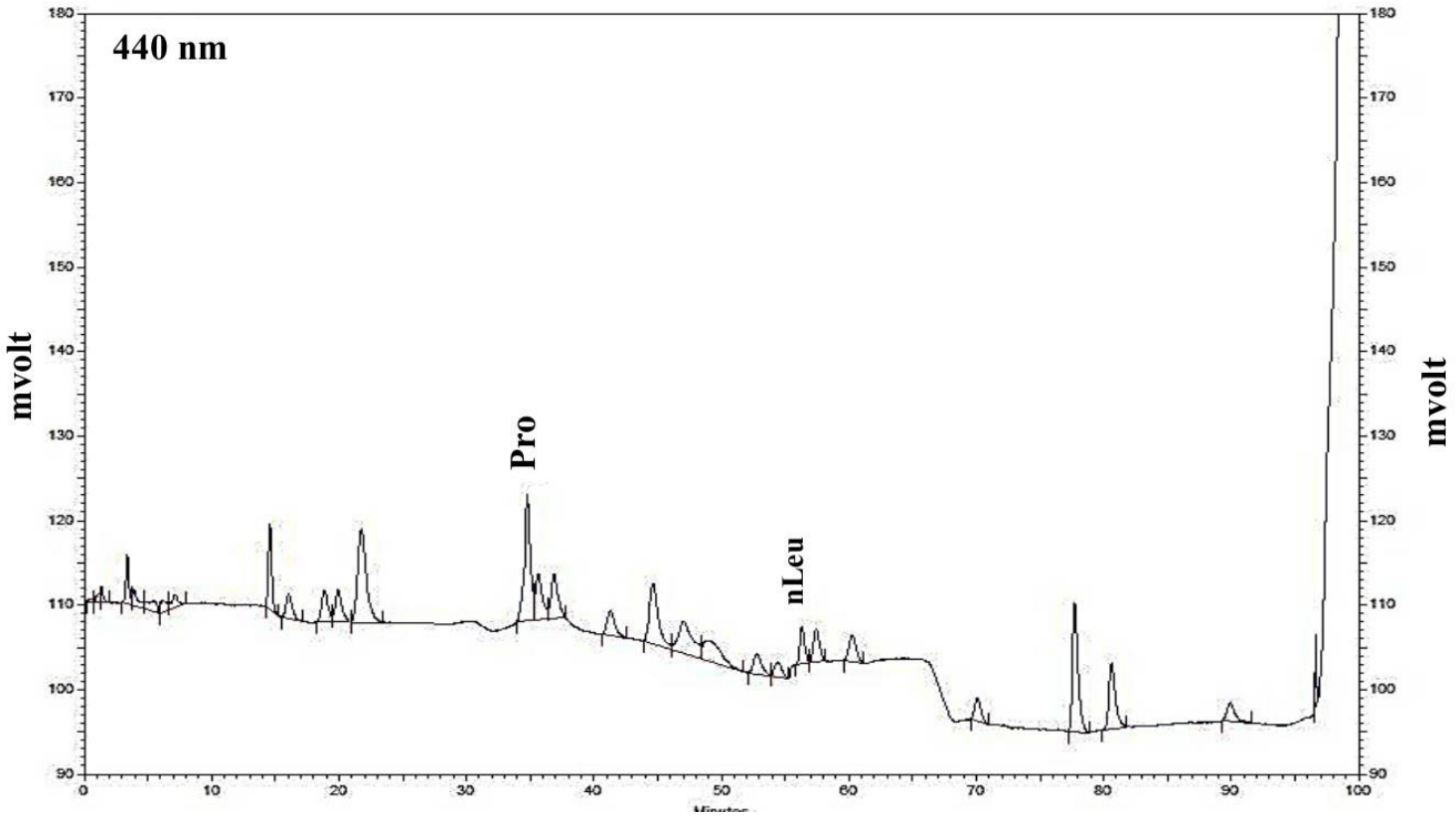


Figure 4.11: Chromatogram of standard amino acids detected using ion exchange chromatography with photometric detection at 440 nm.

Table 4.2: Amino acid profile of different *C. reinhardtii* compared with conventional protein sources and the FAO/WHO/UNU reference pattern (mg/g protein) (FAO/WHO/UNU., 1985). The STD biomass was cultivated in STD growth media until reach an exponential phase (seven days). The NAN and N+ biomass were grown in standard growth media until they reach exponential phase before transfer into the nitrogen stress growth media, stress cultured were maintained for three days they were harvested. All STD, NAN and N^+ biomass were then collected for nutrition analysis.

Amino acids (AAs)	C.reinhardtii (mg/g protein)			Soy protein (mg/g protein)	Egg white (mg/g protein)	WHO/FAO/UNU (mg/g protein)
	NAN	STD	N^+			
His	14.2 ^{b} ± 0.51	15.9 ^{a} ± 0.57	15.3 ^{a} ± 0.25	45	34.0	15
Ile	29.5 ^{a} ± 0.74	31.5 ^{a} ± 1.78	29.1 ^{a} ± 0.71	14	27.9	15
Leu	61.6 ^{b} ± 0.72	64.6 ^{a} ± 1.83	62.7 ^{b} ± 0.83	53	66.7	21
Lys	36.3 ^{b} ± 1.01	44.4 ^{a} ± 1.25	43.0 ^{a} ± 0.43	190	135.1	18
Meth	13.3 ^{a} ± 0.18	13.6 ^{a} ± 0.47	13.2 ^{a} ± 0.21	-	57.7	13
Phe	32.9 ^{a} ± 0.93	31.9 ^{a} ± 1.18	31.9 ^{a} ± 0.34	58	64.7	14
Thr	29.4 ^{b} ± 1.12	32.4 ^{a} ± 0.77	31.2 ^{a} ± 0.01	-	115.8	7
Val	43.8 ^{a} ± 0.63	45.7 ^{a} ± 2.09	43.5 ^{a} ± 0.50	40	43.8	10
Ala	49.9 ^{b} ± 0.63	55.0 ^{a} ± 1.89	53.1 ^{a} ± 0.66	50	62.8	-
Asp	14.7 ^{a} ± 2.06	15.0 ^{a} ± 1.68	16.0 ^{a} ± 1.80	26	23.2	-
Arg	38.2 ^{c} ± 0.99	47.2 ^{a} ± 1.30	44.4 ^{b} ± 0.44	50	53.9	-
Cys	6.67 ^{b} ± 0.21	8.17 ^{a} ± 0.24	7.89 ^{a} ± 0.71	-	57.0	-
Glu	78.7 ^{c} ± 1.21	95.7 ^{a} ± 3.35	91.4 ^{b} ± 0.75	13	41.8	-
Gly	37.9 ^{a} ± 0.81	40.7 ^{a} ± 2.80	39.2 ^{a} ± 0.61	19	51	-
Pro	23.5 ^{a} ± 3.60	26.0 ^{a} ± 15.15	30.6 ^{a} ± 2.23	53	31.6	-
Ser	25.3 ^{b} ± 1.11	28.7 ^{a} ± 0.81	28.5 ^{a} ± 0.49	64	70.2	
Tyr	18.9 ^{a} ± 0.59	19.1 ^{a} ± 0.71	18.6 ^{a} ± 0.15	13	175.9	-
Σ EAAs	261	279	270	342	546	
Σ non - EAA	294	336	59.8	288	567	
Total AAs	555	616	330	630	1,113	

Mean ±SD from triplicate determinations. Letters on same row not sharing the common letter indicate significant differences (p<0.05). NAN - *C. reinhardtii* cultured with non-added nitrogen; STD - *C. reinhardtii* cultured with nitrogen concentration at 0.2 M and N^+ - *C. reinhardtii* cultured with nitrogen concentration at 0.6 M. Essential amino acids are shaded.

4.2.6 Protein separation

Freeze-dried *C. reinhardtii* biomass underwent extraction for proteins and their molecular weights were estimated via the sodium dodecyl sulphate polyacrylamide gel electrophoresis (SDS-PAGE) technique. Sodium dodecyl sulphate (SDS) dissociates proteins into their constituent polypeptide chains while polyacrylamide gel electrophoresis in the presence of SDS separates polypeptide chains according to their molecular weights. Thus, the size of the polypeptide chains of a given protein can be discerned by comparing their electrophoretic mobilities on SDS gels to the movements of marker proteins (Weber *et al*., 1972). Qualitative estimation of the protein molecular weight by SDS-PAGE showed different polypeptide profiles **(Figure 4.12)** with variations in number of bands.

Certain protein were typical across all culture conditions, like 100, 50 KDa, 45 KDa, 30 KDa, 25 KDa, and 15 KDa. Results imply *C. reinhardtii* protein contained a high diversity of polypeptide compositions. The majority of these peptide chains are less than 50 kDa. According to previous report Schwenzfeier *et al*., (2011) also carried out an SDS-PAGE analysis from difference fraction of *Tetraselmis sp.* extract: algae paste, pellet, dialysed algae juice, crude algae soluble protein isolate and soluble algae protein isolate and identified a distinct band at the molecular at 50 kDa and 15 kDa which identified as large and small subunits of Rubisco. The Rubisco concentration could vary depending on the culturing condition. Losh *et al*., (2013) reported the concentration of Rubisco to represent ≤ 6% of total protein. In nutrient-replete, the concentration could range from 2 to 6% while nutrient – limited concentration the concentration was ≤ 2.5%.

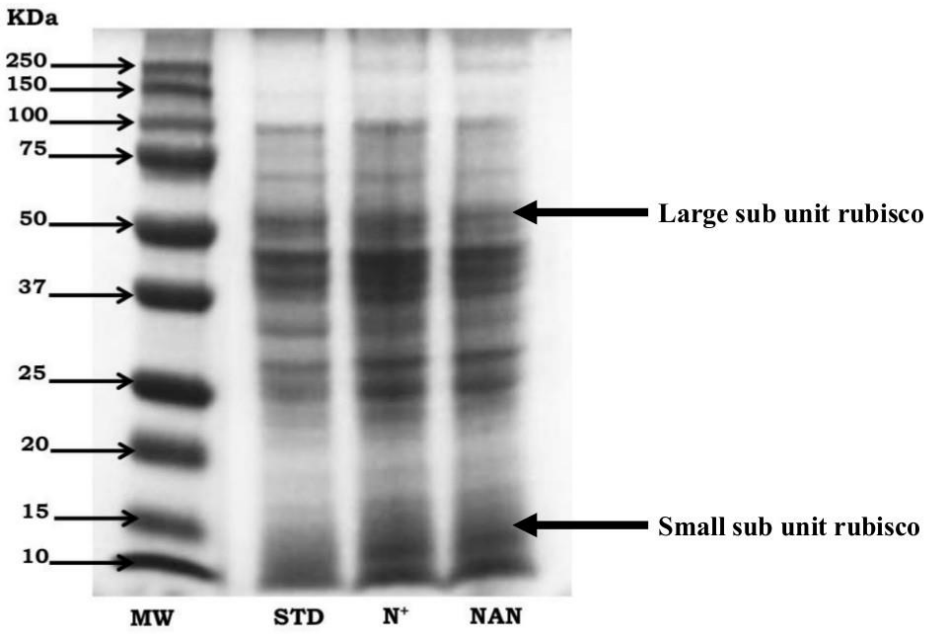


Figure 4.12: Protein electrophoresis pattern showing the molecular weight of intact *C. reinhardtii* freeze-dried biomass. MW - molecular weight marker; NAN - *C. reinhardtii* cultured with non-added nitrogen; STD - *C. reinhardtii* cultured with nitrogen concentration at 0.2 M and N^+ - *C. reinhardtii* cultured with nitrogen concentration at 0.6 M.

4.2.7 Fatty Acids

The fatty acid analysis of *C. reinhardtii* freeze-dried biomass cultured under standard and nitrogen stress media conditions was carried out using solvent-based lipid extraction (Folch *et al*, 1957) **(Figure 4. 13),** transesterification of fatty acid methyl ester (FAMEs) and quantification and identification of FAMEs using gas chromatography. An internal standard, pentadecanoate and heptadecanoate, was added before the analytical procedure. Therefore, possible losses during extraction and incomplete transesterification can then be corrected for. The fatty acid profile chromatogram of *C. reinhardtii* freeze dried biomass illustrated in **Figure 4.14.** The total fatty acid composition is given in **Table 4.3.**

The dominant fatty acid chain lengths were C16 and C18 and most of the fatty acids found in STD freeze-dried *C. reinhardtii* biomass were polyunsaturated fatty acids (PUFA) 32.8%. They comprised 27.7% of total fatty acid with α-linolenic acid (C18:3 (9, 12, 15) being the major compound with a mean value of 25.7±4.09 mg/g DWB). Saturated fatty acids (SFA) were the next biggest class of fatty acids comprising 26.6% overall with C16:0 the major fatty acid with a mean value of 22.7±3.99 mg/g DWB. Next were monounsaturated fatty acids (MUFA) at 24.5% overall and C18:1 the major compound with a mean value of 12.4±1.04 mg/g DWB.

The fatty acid contents of NAN freeze-dried biomass were compared to the STD fatty acid profile and only palmitoleic acid C16:1 showed a change with an increase from 3.02±0.64 mg/g DWB to 6.46±0.03 mg/g DWB. The ratios of SFA: MUFA: PUFA differed between the treatments; NAN (9.39 : 5.46 : 11.6) and N^+ (4.71 : 2.69 : 1.05) compared to STD (26.7 : 24.9 : 38.2) **(Table 4.3 and Figure 4.15).**

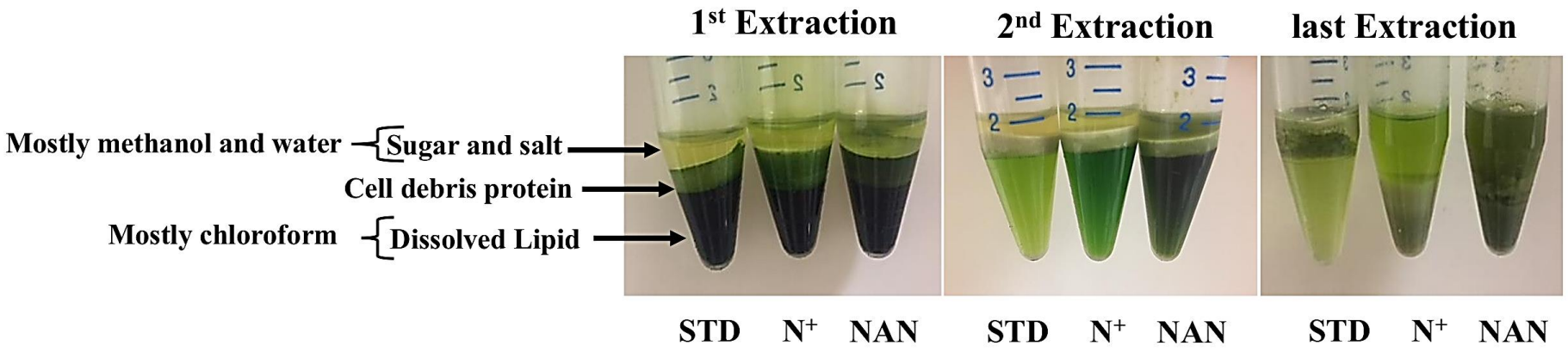


Figure 4. 13: The separation of lipid extract from freeze-dried *C. reinhardtii* biomass using in-house methods (Folch, 1985). The suspension and dissolved biomass (in chloroform/methanol/water) was separated into three layers. The top layer, mostly methanol and water, contained sugar and salts. The middle layer is the cell debris and protein. The lower layer, predominantly chloroform, was dissolved total lipids. The biomass underwent repeated extraction until only one phase existed. The pool of lipids from each chloroform layer of the extraction were collected for total lipid FA analysis of each extract 1st extraction, 2nd extraction and last extraction; NAN - *C. reinhardtii* culture in no-added nitrogen growth media; STD - *C. reinhardtii* culture with nitrogen concentration at 0.2 M growth media; and N^+ - *C. reinhardtii* culture with nitrogen concentration at 0.6 M growth media. The difference green intensities in NAN and N^+ sample presumably because more pigments content in biomass, which could delay the lipid extraction.

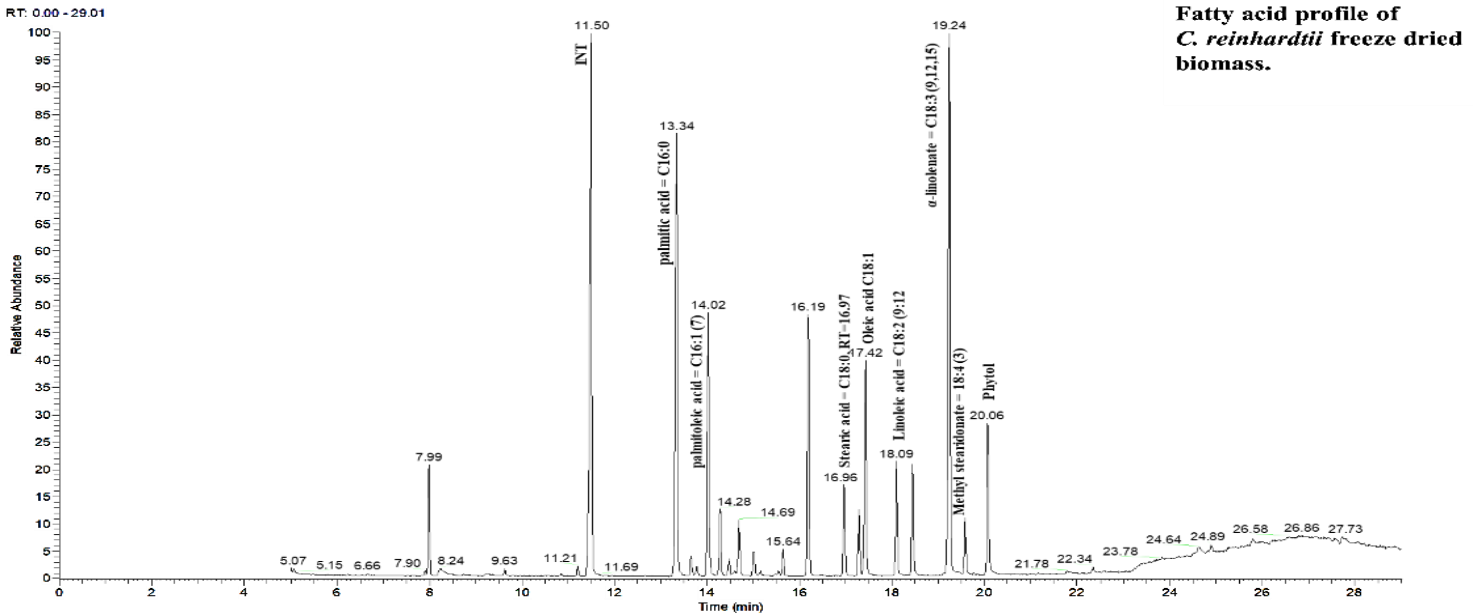


Figure 4.14: Fatty acid profile chromatogram of *C. reinhardtii* freeze-dried biomass. The *C. reinhardtii* cells were cultivated in TAP media under control conditions. The biomass was harvested during the exponential phase and freeze dried for lipid extraction and fatty acid profile analysis. INT = Internal standard = Pentadecanoic acid = C15, Retention Time (RT) = 11.50; palmitic acid = C16:0, RT=13.34; palmitoleic acid = C16:1 (7), RT=14.29; Stearic acid = C18:0, RT=16.97; trans-Vaccenic acid, methyl ester = C18:1(11), RT=17.28; Oleic acid C18:1, RT = 17.42; Linoleic acid = C18:2 (9:12), RT=18.09; Pinolenic acid = C18:3 (5,9,12), RT=18.44; α-linolenate = C18:3 (9,12,15), RT=19.23; Methyl stearidonate = 18:4 (3), RT=19.57.

Table 4.3: FA composition of *C. reinhardtii* (mg/g freeze-dried biomass) determination by FAME analysis through GC-MS. The STD biomass was cultivated in STD growth media until reach an exponential phase (seven days). The NAN and N^+ biomass were grown in standard growth media until they reach exponential phase before transfer into the nitrogen stress growth media, stress cultured were maintained for three days they were harvested. All STD, NAN and N^+ biomass were then collected for nutrition analysis.

		NAN		STD		N^+	
		mg/g	% total FA	mg/g	% total FA	mg/g	% total FA
	Fatty acids						
palmitic acid	C16:0	8.02 ^{a} ± 0.38	24.3	22.8 ^{a} ± 3.99	24.5	3.55 ^{a}± 0.24	41.6
palmitoleic acid	C16:1 (7)	6.46 ^{b} ± 0.03	19.6	3.02 ^{c} ± 0.64	3.25	0.10 ^{f}± 0.01	1.12
Stearic acid	C18:0	1.38 ^{de} ± 0.11	4.18	3.91 ^{c} ± 0.61	4.21	1.16 ^{c}± 0.03	13.6
trans-Vaccenic acid, methyl ester	C18:1(11)	2.73 ^{c} ± 0.64	8.28	12.5 ^{b} ± 2.38	13.4	1.35 ^{b}± 0.08	15.8
Oleic acid	C18:1	2.73 ^{c} ± 0.64	8.28	12.5 ^{b} ± 1.04	13.5	1.34 ^{b}± 0.04	15.7
Linoleic acid	C18:2 (9:12)	2.65 ^{c} ± 0.27	8.04	5.01 ^{c} ± 048	5.47	0.30 ^{e}± 0.05	3.47
Pinolenic acid	C18:3 (5,9,12)	1.93 ^{d} ± 0.01	5.87	4.87 ^{c} ± 1.03	5.25	0.17 ^{ef} ±0.00	1.94
α-linolenate	C18:3 (9,12,15)	6.10 ^{a} ± 0.54	18.5	25.7 ^{a} ± 4.09	27.7	0.47 ^{d} ± 0.06	5.53
Methyl stearidonate	18:4	0.94 ^{ef} ± 0.03	2.87	2.49 ^{c} ± 0.47	2.69	0.11 ^{f} ± 0.05	1.31
Total FFA		32.9		92.8		8.54	
SFA		9.39		26.7		4.71	
MUFA		5.46		25.0		2.69	
PUFA		11.6		38.2		1.05	

The peak areas were integrated using Thermo Scientific™ Xcalibur™ software. Data represent the mean± SD mg/g of each FA determined in triplicate determinations. Letters on same shaded column not sharing the common letter indicate significant differences (p<0.05). NAN - *C. reinhardtii* cultured with non-added nitrogen; STD - *C. reinhardtii* cultured with nitrogen concentration at 0.2 M and N^+ - *C. reinhardtii* cultured with nitrogen concentration at 0.6 M.

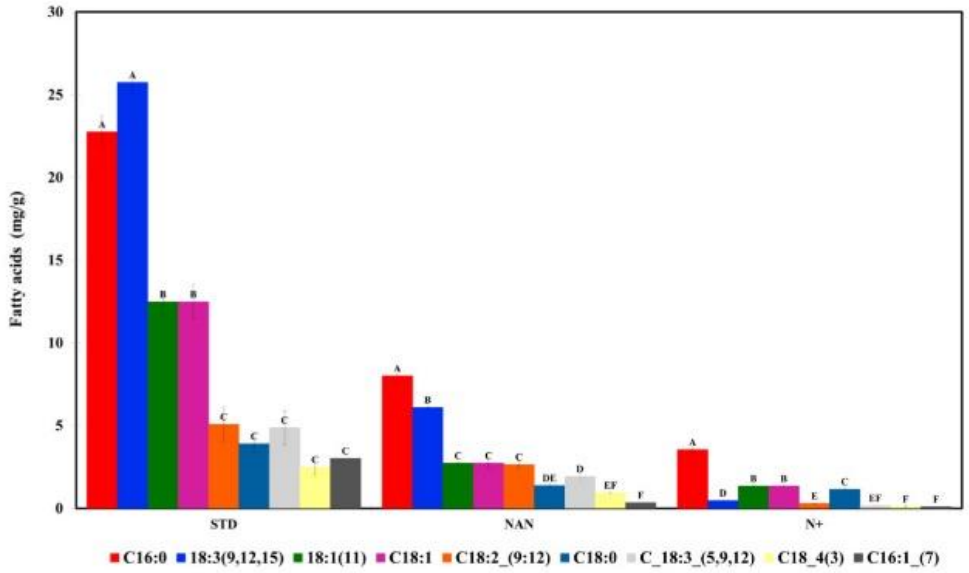


Figure 4.15: FAs composition of *C. reinhardtii* (mg/g freeze-dried biomass) determination by FAME analysis through GC-MS.

In theory, the fatty acid pathway occurs in the chloroplast, and the resulting *de novo* fatty acids (FAs), with a C16 or C18 carbon chain, then proceed to elongate or unsaturated/desaturase carbon by either adding carbon or double bonds. Following this step, FAs are transported to the cytoplasm, where they act as substrates for triglycerides (TAG) synthesis**.** The FA biosynthesis pathway can be induced by stress conditions, primarily by limiting nitrogen concentration, which leads to the arrested biosynthesis of amino acids. Therefore, the primary product of carbon fixation reactions in photosynthesis is used for lipid and starch biosynthesis. Neutral lipid accumulation (TAGs) consist of fatty acid composition dominated by palmitic acid, oleic acid, and linoleic acid, which is similar to many plants oils (Bilbao *et al.*, 2017).

Ryckebosch *et al.*, (2012) point out that analysis of fatty acids in microalgae distinguishes itself from other substrates (e.g. vegetable oil, food products, animal tissues *etc*.) because firstly, microalgae are single cells surrounded by rigid cell walls, complicating lipid extraction; secondly, microalgae contain a wide variety of lipid classes and the lipid class

distribution is highly variable (Guschina and Harwood, 2006). These different lipid classes have a wide variety in chemical structure and properties such as polarity. Also, lipid classes other than acyl lipids are produced; lastly microalgae contain a wide variety of fatty acids, ranging from 12 to 24 carbon atoms in length and containing both saturated as well as highly unsaturated fatty acids. Therefore, methods developed to analyse fatty acids in substrates other than microalgae, might not be suitable to analyse fatty acids in microalgae.

Current lipid extraction methods from microalgae show efficiency limitation and until now, extraction protocols have not been fully optimized for specific lipid compounds (Ren *et al.*, 2017). Ren *et al.*, (2017) found that lipid extraction yields efficiency of *C. protothecoides* is ranked as acetone- based method > Chl/MeOH/H_2O method > Dic/MeOH method > Chl/MeOH method. This ranking agrees with the polarity of the extraction solvents; acetone and Chl/MeOH/H_2O polarity being higher than Chl/MeOH and Dic/MeOH. They suggested that the water treatment increases solvent mixtures polarity and thus explains the resulting enhanced extraction yields. Moreover, since the cell membrane mainly contains polar lipids, the use of polar solvents could increase lipid diffusion and therefore the extraction efficiency.

The main difference between commonly used lipid extraction procedures is the solvent-systems that are used. Due to the large variety of lipid classes present in microalgae, each varying in polarity, the extracted lipid quantity will vary with solvents used (Laurens *et al.*, 2012; Iverson *et al.*, 2001). This leads to inconsistencies in the lipid content and composition published in the scientific literature (Ryckebosch *et al.*, 2012; Laurens *et al.*, 2012). Moreover, depending on the solvent system used, methods based on solvent

extraction without cell disruption through, for example, bead beating or sonication, might not extract all lipids because of the rigid structure of some microalgae species (Lee *et al.*, 2010; Ryckebosch *et al*., 2012). In the case of incomplete lipid extraction, the extraction efficiency of the different lipid classes can vary (Guckert *et al*., 1988).This can also have an effect on the measured fatty acid composition, because the fatty acid composition is variable among lipid classes (Guschina and Harwood, 2006) Nitrogen concentration variation induces storage lipid (TAG) accumulation, which mainly features SFA and MUFA rather than PUFA. Arisz *et al*. (2000) also reported overall C16:1 and C18:1 FAs were elevated in the green algae *C. moewusii* cultured under nutrient limitations whereas PUFA C16:3, C16:4, and C18:3 contents decreased. Given the discussion above on the difficulty of lipid extraction in microalgae, it should be clear that the data in this thesis may vary from published results, depending on the solvent system used and the cultivation conditions. However, within the results in this thesis, it is valid to compare the relative changes in lipid composition as the same lipid extraction method was used for all comparisons.

4.2.8 Minerals

The multi-mineral content of NAN, STD and N^+ *C. reinhardtii* freeze-dried biomass is described in **Table 4.4.** *C. reinhardtii* biomass is enriched with P (15.7 to 16.7 mg/g), followed by K (3.61 to 4.42 mg/g), Mg (2.64 to 2.79 mg/g), and Ca (2.16 to 3.52 mg/g). The average contents of other mineral elements were as follows: B (0.28 to 0.55 µg/g), Na (28.3 to 60.4 µg/g), Mn (21.2 to 43.9 µg/g), Fe (299 to 491 µg/g), Cu (66.5 to 120 µg/g), Zn (27.3 to 40.4 µg/g), and Se (4.6 to 6.7 µg/g).

The Fe contents of *C. reinhardtii* were sufficient for the recommended daily intake of an adult. The necessary amount for daily intake of is 8-18 mg/d (National Research Council, 1989). so, approximately regular consumption 32 g of STD biomass will meet that. Meanwhile, approximately 62 g/day of NAN-cultured biomass or 49 g/day of N^+-cultured biomass is necessary. The required daily amount of *C. reinhardtii* freeze-dried biomass to fulfil adult male and female demands (g) of other mineral is shown in **Table 4.4.** These indicate that the *C. reinhardtii* assessed have great potential as a multi-nutrient source for food fortification and enrichment against Fe deficiency.

C. reinhardtii biomass also contains high amounts of P, with daily consumption of roughly 3 g of freeze-dried biomass meeting the RDA for P. The P features prominently in bones and teeth: 85% of total body P is found in bone. However, P deficiency is not a fundamental problem because the average adult diet has roughly 62 mg of P per 100 kcal.

Table 4. 4: Mineral profile of major and trace minerals in freeze-dried *C. reinhardtii* biomass and DRI. The STD biomass was cultivated in STD growth media until reach an exponential phase (seven days). The NAN and N^+ biomass were grown in standard growth media until they reach exponential phase before transfer into the nitrogen stress growth media, stress cultured were maintained for three days they were harvested. All STD, NAN and N+ biomass were cultivated and collected for nutrition analysis.

Minerals		Treatments				Dietary Reference Intakes (DRIs): Recommended Dietary Allowances and Adequate Intakes						Require daily amount of *C. reinhardtii* freeze-dried biomass to fulfil the adult (male and female) demand		
		NAN	STD	N^+		Children	Male	Female	Pregnancy	Lactation		NAN	STD	N^+
K		4.42 ^{a} ± 0.50	4.53 ^{a} ± 0.07	3.61 ^{a} ± 0.22		**3000-3800***	**4500-4700***	**4500-4700***	**4700***	**5100***		1063	1037	1300
Na		0.06 ^{a} ± 16.1	0.28 ^{c} ± 0.013	46.80 ^{b} ± 0.02		**1000-1200***	**1200-1500***	**1200-1500***	**1500***	**1500***		24830	53041	32051
Ca		3.52 ^{a} ± 0.70	2.16 ^{b} ±0.29	2.57 ^{b} ± 1.32		**700-100**	**1000-3000**	**1000-3000**	**1000-3000**	**1000-3000**		852	138	117
Fe	mg/g	0.30 ^{b} ± 0.10	0.49 ^{a} ± 0.09	0.37 ^{c} ± 0.19	mg/d	**7-10**	**8-11**	**8-18**	**27**	**9-10**		62	37	49
Mg		2.79 ^{a} ± 0.08	2.74 ^{a} ± 0.07	2.64 ^{a} ± 1.81		**80-130**	**240-420**	**240-360**	**350-400**	**310-360**		150	153	159
Mn		21.2 ^{b} ±12.3	43.89 ^{a} ±2.37	40.5 ^{a} ±19.0		1.2-1.5*	1.9-2.3*	1.6-1.8*	2.0*	2.6*		109	52	87
P		16.6 ^{a} ± 0.57	15.70 ^{a} ±0.70	16.7 ^{a} ± 11.4		**460-500**	**700-1500**	**700-1250**	**700-1250**	**700-1250**	g	3	3	3
Zn		0.03 ^{a} ± 0.01	0.04 ^{a} ± 0.07	0.03 ^{a} ± 0.02		**3-5**	**8-11**	**8-9**	**11-12**	**12-13**		403	272	367
Cu		113.5 ^{a} ± 29.3	66.46 ^{b}± 37.9	120 ^{a} ± 64.3		**340-440**	**700-900**	**700-900**	**1000**	**1300**		8	14	8
Mo		3.50 ^{a} ± 1.15	1.21 ^{c} ± 0.69	2.18 ^{b} ± 0.73		**17-22**	**34-45**	**34-45**	**50**	**50**		13	38	21
Se	µg/g	6.14 ^{a} ± 1.10	4.60 ^{a} ± 1.50	6.7 ± ^{a} 3.98	µg/d	**20-30**	**40-45**	**40-45**	**60**	**70**		7	10	7
Ni		0.05 ^{a} ± 0.05	0.13 ^{b} ± 0.07	0.03 ^{a} ± 0.01		-	-	-	-	-		-	-	-
B		0.55 ^{a} ± 0.15	0.52 ^{a} ± 0.17	0.28 ^{a} ± 0.10		-	-	-	-	-		-	-	-
V		0.00 ^{a} ± 0.00	0.00 ^{a} ± 0.00	0.00 ^{a} ± 0.00		-	-	-	-	-		-	-	-

NOTE: Data represent the mean (±SD) µg/g; Different letters in the same row indicate significant differences (p<0.05). The table is taken from the National Research Council (1989).- RDAs in **bold type** and AIs in ordinary type followed by an asterisk (*****). N^- - *C. reinhardtii* cultured with non-added nitrogen; STD - *C. reinhardtii* cultured with nitrogen concentration at 0.2 M and N^+ - *C. reinhardtii* cultured with nitrogen concentration at 0.6 M. An RDA is the average daily dietary intake level sufficient to meet the nutrient requirements of nearly all (97–98 percent) healthy individuals in a group. The values for K and Na are in (g/d). The values for Ca, Fe, Mg, Mn, P, and Zn are in mg/d. The values for Cu, Mo, and Se are in µg/d.

CONCLUSION

The biochemical composition of *C. reinhardtii* at difference stages of cultivation under mixotrophic conditions in our lab scale system confirms a direct relationship between growth and nutritional composition. The end of the exponential phase is when the highest biomass and nutritional composition are achieved. The volumetric biomass production is 0.01 g/L/day. The overall biochemical composition during 30 days of cultivation shows the protein content ranging from 150 to 350 mg/g. The total lipid content ranges from 150 to 200 mg/g. The photosynthetic pigment content (chlorophyll *a*, chlorophyll *b* and carotenoids) ranges from 0.06 to 0.11 mg/g, 0.03–0.03 mg/g and 0.13–0.18 mg/g, respectively.

The nutritional composition of *C. reinhardtii* is easily manipulated by altering the composition of the cultivation medium. It has been suggested that a nitrogen stress strategy is a useful approach for *C. reinhardtii* cultivation, providing the ideal biomass value for the biofuel industry. The nutritional profile of freeze-dried *C. reinhardtii* biomass in standard and manipulated growth media (difference in the concentration of nitrogen in the TAP salt: no added nitrogen, 0.2 M and 0.6 M) reveals biomass dominant in protein content (41.4 to 43.8%), lipid (13.2 to 20.9%), carbohydrate (21.5 to 27.8%) and ash (10.1 to 12.9%). The minerals consist of a high amount of calcium magnesium phosphorus and potassium. The essential amino acids contain glutamine, leucine and alanine, with trace levels of cysteine, aspartic acid and methionine. *C. reinhardtii* protein contains a high diversity of polypeptide compositions. The large and small subunits of Rubisco were identified at the molecular masses of 50 kDa and 15 kDa. Therefore, *C. reinhardtii* has the potential to be a novel substrate for food and feed applications.

CHAPTER 5

Impact of Cavitation Disruption on *C. reinhardtii* Cell and Nutritive Compositions

5.1 Introduction

Microalgae could be used as whole biomass without extraction due to their bioactive compounds being more stable in their natural matrix than in the extracts (Gouveia and Empis, 2003; Christaki *et al*., 2015). Conventionally, valuable compounds are extracted from microalgae using solvents after breaking the cell walls through mechanical or non-mechanical disruption processes (Freitas *et al*., 2012). Therefore, an appropriate cell disruption process should be considered, as the loss of cellular integrity and cell compartments destroys the natural protection of nutrients in microalgae, exposing them to oxidative enzymes and oxygen. Furthermore, such compound decomposition could diminish biomass quality and lessen the beneficial effects of this species on human health.

Additionally, microalgae could be used as whole biomass without extraction due to their bioactive compounds being more stable in their natural matrix than in the extracts (Gouveia and Empis, 2003; Christaki *et al*., 2015). Conventionally, valuable compounds are extracted from microalgae using solvents after breaking the cell walls through mechanical or non-mechanical disruption processes (Freitas *et al*., 2012). Therefore, an appropriate cell disruption process should be considered, as the loss of cellular integrity and cell compartments destroys the natural protection of nutrients in microalgae, exposing them to oxidative enzymes and oxygen. Furthermore, such compound decomposition

could diminish biomass quality and lessen the beneficial effects of this species on human health.

This chapter assessed the efficiency of *C. reinhardtii* cell disruption using hydrodynamic cavitation (HDC) compared to that of ultrasonication. The degree of cell wall damage was established by measuring the release of metabolites (chlorophyll and protein) from *C. reinhardtii*, and by observing the physical structure of the cells after disruption. The impact of these cell disruption methods on the stability of some target nutrients (chlorophyll and carotenoids) was also studied.

5.2 Results and Discussion

5.2.1 Effect of Hydrodynamic Cavitation and Ultrasonication on Metabolite Release and Cell Structure of *C. reinhardtii*

Initial work involved a simple proof of principle experiment. Suspensions of *C. reinhardtii,* intact or exposed to mechanical forces, were placed in Eppendorf tubes and centrifuged. Clear supernatant with pelleted material indicates no cell disruption, while green colour (chlorophyll) in the supernatant indicates a degree of cell disruption. It appears from these images that ultrasonication causes notably more cell damage than HDC **(Figure 5.1).** This indication of cellular damage was confirmed via light microscopy **(Figure 5.2)**. Cells exposed to HDC seemed to retain their overall structure despite losing some colour, but the cells exposed to ultrasonication lost much of their spherical structure, leaving mostly cellular debris.

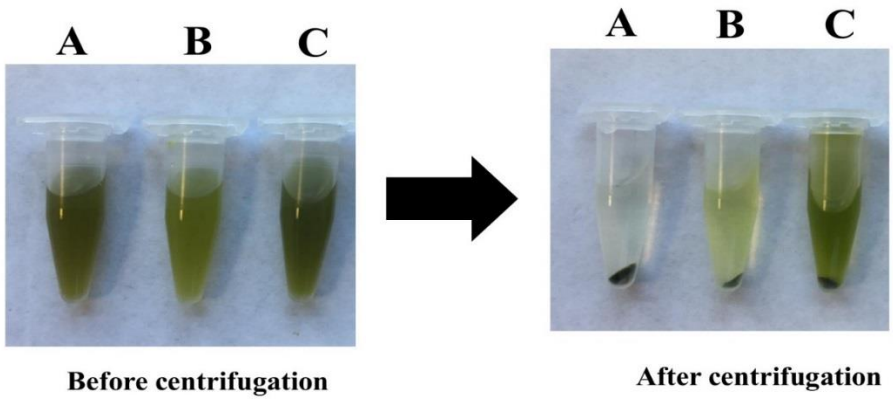


Figure 5.1: Effect of cell disruption method on *C. reinhardtii* integrity. (A): intact *C. reinhardtii*, (B): hydrodynamic cavitation-disrupted *C. reinhardtii*, (C) ultrasonication-disrupted *C. reinhardtii*

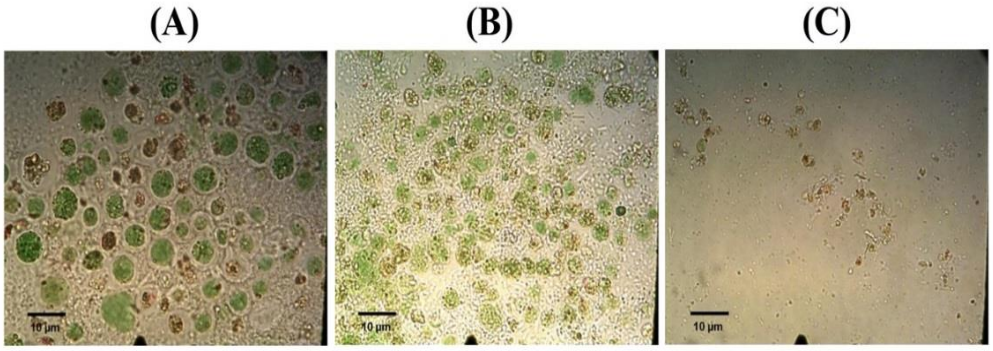


Figure 5.2: Visualising of (A) Intact, (B) Hydrodynamic cavitation-disrupted and (C) Ultrasonication-disrupted *C. reinhardtii* suspension. The biomass was harvested during the exponential phase for visualized cell structure by light microscope using 100X magnification (Scale bar 10 µm).

The degree of cell disruption (cell wall breach) was established by measuring the intracellularly released materials, such as chlorophylls and proteins, into the aqueous phase **(Table 5.1).**

The highest chlorophyll content released from *C. reinhardtii* cells was achieved using ultrasonication. This was 6 times that released from hydrodynamic cavitation, and 20 times that released from intact cells. The superior disruptive power of the ultrasonic method is also reflected in the protein release data; this was approximately 4 times higher than protein in the supernatant from intact cells and cells that had experienced hydrodynamic cavitation. Even though hydrodynamic cavitation (cavitation power 586.43 W and power density 1.17 W/cm^3) has more power than ultrasonication (cavitation power12.33 W and power density 0.02 W/cm^3), it does not cause the same level of cell damage, and seems to retain the overall cell shape. Therefore, hydrodynamic cavitation was preferred for our experiment because ultrasonication caused a significant loss of cell contents to the aqueous phase.

Mechanical disruption deforms and ruptures the cell wall in a non-specific manner. (Günerken *et al.*, 2015). Our results suggest that ultrasonication causes substantial breaches in the cell wall; whereas the forces created by hydrodynamic cavitation seem to result in numerous, smaller microperforations **(Figure 5.3** for schematic representation**).** *C. reinhardtii* cells exposed to ultrasonication in these experiments were disintegrated; whereas HDC altered their surface without complete loss of cell integrity. The objective of exposing algal cells to mechanical forces in this study is to potentially improve the nutritional value of the cells (enhanced bioaccessibility) without loss of the capsulate nature of the cells that allows

Table 5. 1: Effect of cell disruption method on the release of selected metabolites from *C. reinhardtii* into the aqueous phase (µg/mL).

	Metabolite release						% Solubility	
	µg/mL			g/g DWB				
	Intact	**HDC**	**ULT**	**Intact**	**HDC**	**ULT**	**HDC**	**ULT**
Total chlorophyll	0.16 ^{c}± 0.03	0.52 ^{b} ± 0.29	3.09 ^{a} ± 0.13	0.002 ^{c} ±0.00	0.007 ^{a} ± 0.00	0.04 ^{b} ±0.00	3.5	20
Total soluble protein	198.03 ^{b} ± 3.68	206.3 ^{b} ± 15.2	782.4 ^{a} ± 5.7	2.83 ^{c} ± 0.05	2.95 ^{b}± 0.22	11.18 ^{a} ± 0.94	1.04	3.95

Mean±SD from triplicate determinations. Letters on same row not sharing the common letter indicate significant differences (p<0.05). The fraction release was compared to the metabolite release from intact cell. HDC = Hydrodynamic cavitation, ULT = Ultrasonication.

simple concentration through e.g. centrifugation. For this reason only HDC-treated cells were used in the remaining studies. Whilst sonication was highly disruptive, it was carried out for long period of time (30 mins) as compared with the HDC that was a couple mins. Therefore, sonication might be just as effective intensity or durations. Therefore, more experiment to select the condition for example, time courses of treatment vs. solubility would help identified an optimum condition of cell wall disruption using an ultrasonication.

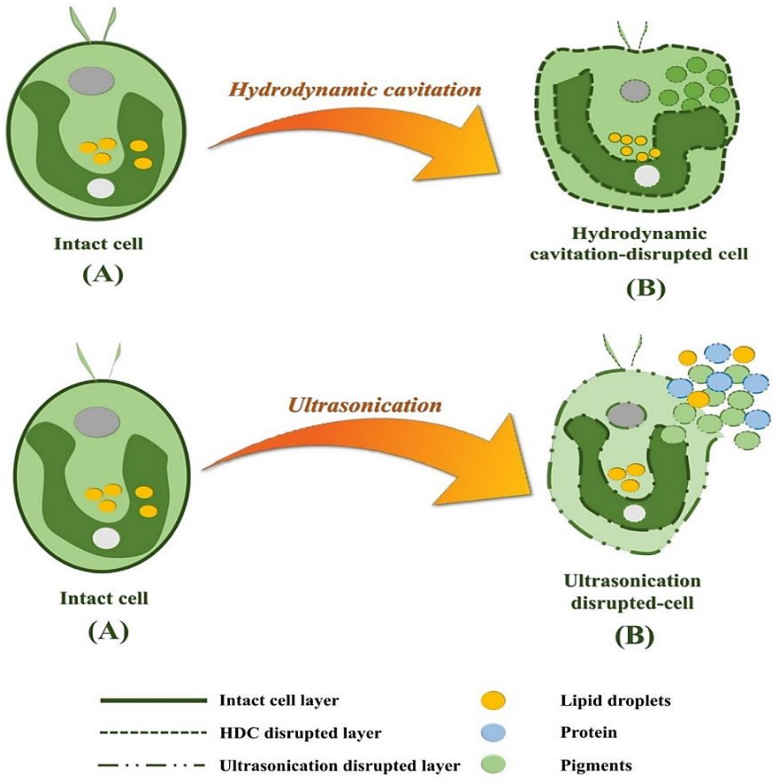


Figure 5.3: The proposed schematic effect of ultrasonication or hydrodynamic cavitation on the integrity of *C. reinhardtii* cells. The intact cell has the oval with two flagella, about half of their volume is occupied by a single cup-shaped chloroplast. HDC appears to create microperforations (dotted line); the overall structure remains intact. On the other hand, ultrasonication appears to cause substantial cell damage leading to the release of cellular contents. Intact layer: bold line, disrupted layer: dot line, chlorophyll: green circle, lipid: yellow circle, protein: blue circle.

5.2.2 Effect of Hydrodynamic Cavitation Disruption on the Retention of Selected Nutrients

Biomass produced for human consumption must be of high quality. Food quality and safety are generally assessed by analysing different factors (Serra, 2015). Careful pre-treatment of microalgae biomass to preserve valuable substances such as sensitive pigments like chlorophyll is crucial. Therefore, the chemical retention of chlorophyll and carotenoids (*β*-carotene and lutein) in *C. reinhardtii*, intact and after exposure to hydrodynamic cavitation, was measured **(Table 5.2).** The cell suspension, whole disrupted suspension and centrifuged intact cell, were freeze-dried prior to extraction and analysis. The chlorophyll *a* and *b* content were less retained at 47.6% and 45.5% respectively during HDC disruption but the carotenoids measured (*β*-carotene and lutein) were highly remained: 100% and 92.4% respectively.

Table 5. 2: Effect of exposing *C. reinhardtii* cell to HDC on the retention of selected nutrients.

Pigment content (mg/g DWB)	Intact	HDC-disrupted	Nutrient retention (%)
Chlorophyll *a*	4.83 ^{a} ± 0.31	2.30 ^{b} ± 0.01	47.6
Chlorophyll *b*	0.44 ^{a} ± 0.03	0.20 ^{b} ± 0.02	45.5
β-carotene	0.22 ^{a} ± 0.01	0.22 ^{a} ± 0.03	100
Lutein	2.77 ^{a} ± 0.10	2.56 ^{a} ± 0.01	92.4

Mean±SD from triplicate determinations. Letters on same row not sharing the common letter indicate significant differences (p<0.05).

The major degradation products of chlorophyll are pheophytins (formed when chlorophyll molecules lose their central magnesium atom), chlorophyllides (formed from the removal of the phytol group in chlorophyll) and pheophorbides (which are the result of chlorophyll molecules which lost both their phytol group and magnesium atom) (Hörtensteiner, 2012). A shift in colour from brilliant green to a less intense/olive-brown colour in the cell suspension exposed to hydrodynamic cavitation is evidence of chlorophyll degradation **(Figure 5.2).** We assume that cells exposure to disruption and heat during HDC may cause the significant loss of chlorophyll by the thylakoid-bound enzyme chlorophyllase activity, present in most diatom species and *Chlorophyceae* (Jeffrey and Hallegraeff, 1987; Chou *et al*., 2015). Chlorophyllase catalyses the hydrolytic removal of the phytol chain; this enzyme is dormant in native, unstressed green plant tissue but is activated by heat, and can still be active up to 80 °C but loses activity if it is further heated (Marangoni, 2017). The *C. reinhardtii* chlorophyllase remains active from 40 – 60 ºC. Their activity was then lower at 70 ºC (Chou *et al*., 2015). The degradation of chlorophyll can cause an undesirable swamp-green appearance in food which can lead to product rejection (Kidmose *et al*., 2005).

Numerous researchers have reported that the carotenoid molecules are prone to oxidative degradation, and loss of carotenoids occurs during the processing of food (Boon *et al*., 2010; Renukadevi *et al*., 2011).In nature, carotenoids exist primarily in the more stable all-trans(*E*) form, but a small amount of cis isomer(*Z*) is also found (Renukadevi *et al*., 2011). Non-enzymatic oxidation occurs during processing, leading to the formation of *Z*-carotenoids, which have different biological properties from *E*-carotenoids, such as decreased vitamin A activity and altered bioavailability and antioxidant capacity

(Renukadevi *et al*., 2011). Our results show that HDC, under the conditions tested, does not induce isomerisation of carotenoids.

5.2.3 Effect of Hydrodynamic Cavitation Disruption on Membrane Permeability of Lipophilic Dye

Cells were exposed to Nile Red dye to further test the idea that exposure of *C. reinhardtii* to HDC causes microporation of the cell wall system; dye ingress should be promoted by micropores and lead to intracellular lipid droplet colouration. Structured Illumination Microscopy (SIM) was chosen to visualize the intact and hydrodynamic cavitation-disrupted *C. reinhardtii* cell structure, as it allows twice the resolution of confocal microscopy. This super-resolution method revealed fine details of *C. reinhardtii* that would otherwise be undetectable with conventional microscopy. SIM has previously been used to visualize the cytoskeleton and interactions of the actin cytoskeleton with mitochondria in fixed yeast cells and compared with wide-field microscopy, which showed that SIM provides spatial resolution beyond the diffraction limit of conventional fluorescence microscopy (Higuchi-Sanabria *et al*., 2016).

We visualized the lipid droplets and cell membrane of intact and disrupted *C. reinhardtii* cells that were stained with Nile Red. The effect of cell disruption using hydrodynamic cavitation on the permeability of lipophilic dye into *C. reinhardtii* cells was also evaluated using confocal microscopy **(Figure 5.4).** The disrupted *C. reinhardtii* showed a stronger yellow colour (lipid droplets). This finding suggests that cell disruption enhances dye permeability into *C. reinhardtii* cells **(Figure 5.4B).** Due to the intact nature of the algae exposed to HDC and given that dye is able to access the organelles of the

cells, which is not possible with algae that have not been exposed to HDC, it appears that HDC is able to perforate the cell wall and membrane to allow entrance of the dye.

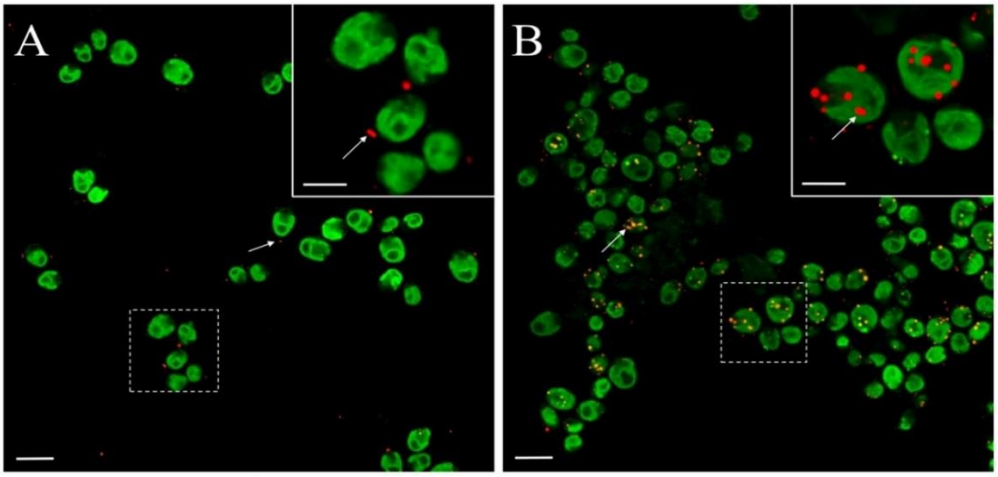


Figure 5.4: Visualization of intact (A) and HDC-disrupted (B) *C. reinhardtii* suspensions. Single optical slices are shown. Cells were stained with Nile Red fluorescent dye. The chlorophyll is shown in green. Oil droplets (arrows) are yellow in the overview and red in the inserts. Inserts are channel unmixed zoomed images of the *C. reinhardtii*. (Scale bars = 10 µm and 5 µm for inserts).

CONCLUSION

Exposure of *C. reinhardtii* to physical forces impacts the surface integrity of the cells. Ultrasonication and HDC provoke different effects on the cell surface. Ultrasonication causes complete cell rupture, whereas HDC appears to form micropores through the cell wall while retaining the overall shape and integrity of the algae. *C. reinhardtii* exposed to HDC forces loses almost 50% of its chlorophyll *a* and *b* and retains the carotenoids measured (β-carotene and lutein). Therefore, HDC has the potential to be used as a novel method for nutrient delivery and an important step in food processing using microalgae.

CHAPTER 6

In vitro Bioaccessibility of Chlorophyll (*a* and *b*) and Carotenoids (*β*-carotene and lutein) from intact and hydrodynamic disrupted *C. reinhardtii*

6.1 Introduction

Nutrient intake by consumers can be improved by food fortification, but a more sustainable approach is to enhance the delivery of nutrients to the body by, for example, enhancing the bioaccessibility of nutrients already present in biomaterials. *β*-carotene is the inactive form of vitamin A in plants that, on consumption by humans, can be converted into two molecules of vitamin A (retinol) (Guedes *et al*., 2011). Lutein is considered a non-provitamin A carotenoid, it provides the yellow-coloured pigments in the human retina macula and protects photoreceptors against light-initiated oxidation damage. It has a statistically significant inverse association with the risk of macular degeneration (EDCC: Eye Disease Case-Control) which causes irreversible blindness in the elderly (Rodriguez-Amaya and Kimura, 2004). Chlorophyll is the most abundant natural pigment in nature. Green vegetables are a rich source of both carotenoids and chlorophyll (Chen and Roca, 2018). *In vivo* and *in vitro* animal model studies have revealed that chlorophyll, or its derivatives, have various of biological properties such as antioxidant activity (Hsu *et al*., 2005) and reducing the activity of carcinogens (Carole *et al*., 2017). The chlorophyll in *C. reinhardtii* chloroplast membranes has been shown to be located in a chlorophyll a/b-protein complex (Kan and Thornber, 1976). Due to its

exclusive location, chlorophyll is a reliable marker of the presence of chloroplasts and of the biochemical changes this organelle experiences during digestion (Dawson and Hemington, 1974).

C. reinhardtii possess non-cellulosic cell wall, it is almost entirely built up from extensin-like Hydroxyproline Rech Glycoprotein (HRGPs) (Green and Lowther, 1959). The extensin (EXT) molecule also contains tyrosine residues which enable them to behave as self-assembling units and form a three-dimensional network organized by inter- and intra-molecular tyrosine linkages (Kieliszewski *et al.*, 2010; Marzol *et al.*, 2018). The cell wall layers, which act as the natural protection for their intracellular biomolecules, could notably act as a barrier for the digestive enzyme to intact cells. In the previous chapter the use of HDC to alter the diffusion properties of molecules into *C. reinhardtii* cells was noted. This chapter will test the impact of HDC on nutrient delivery by measuring micronutrients bioaccessibility from intact and HDC-disrupted *C. reinhardtii* using an *in-vitro* human model of digestion.

After foods are consumed, lipidic biomolecules which bioaccessible are combined into mixed micelles, which comprise bile acids, free fatty acids, monoglycerides and phospholipids. Solubilisation of chlorophyll and carotenoids into mixed micelles in the gastrointestinal tract is an essential step for their uptake and absorption (Hurst, 2002; Yonekura and Nagao, 2009). The amount of carotenoid incorporated into micelles depends on the polarity of the carotenoid as well as micellar fatty acid composition (Rein *et al.*, 2013). Chlorophyll's solubility and molecular properties depend on the structural changes of the native molecule of chlorophyll (Hurst, 2002). In plant food tissues, the physicochemical structure and properties of cell walls are critical factors involved in

influencing bioaccessibility (McDougall *et al.*, 1996; Waldron *et al.*, 1997). Therefore, processing of plants foods can influence the bioaccessiblity of nutrients, mainly through changes in the plant cell wall structure and properties (Berry *et al.*, 2008).

Only a few research exploring the effect of cell disruption on the bioaccessibility of nutrients from *C. reinhardtii* has been reported (Gille *et al.*, (2016). An *in vitro* model of human digestion was used to measure the bioaccesibility of chlorophyll (*a* and *b*) and carotenoids (*β*-carotene and lutein) from intact and HDC-*C. reinhardtii* biomass in this chapter.

6.2 Results and Discussion

6.2.1 The Changes on Cell Wall Morphology and Phase Behaviour of Intact *C. reinhardtii* during the *in vitro* Human Digestion

6.2.1.1 Changing of cell morphology

To understand the changing of cell wall morphology of *C. reinhardtii* during *in vitro* human digestion. The intact *C. reinhardtii* has been undergone through *in vitro* digestion condition in the present of enzyme (α-amylase, pepsin and pancreatin according to standardise methods by Minikus *et al* 2014) labelled as real sample. While, the control is the intact *C. reinhardtii* undergo the same temperature and pH change in the absence of the digestive enzyme.

The results revel in TEM imaging of the total digesta **(Figure 6.1)** confirms that all the cells in the control (no added digestive enzymes) retained the oval shape of the cells with

the cell wall (CW), cell membrane (CM) layer and the thylakoid membrane (TY) stacks overshadowing most of the other organelles after the oral and stomach phases.

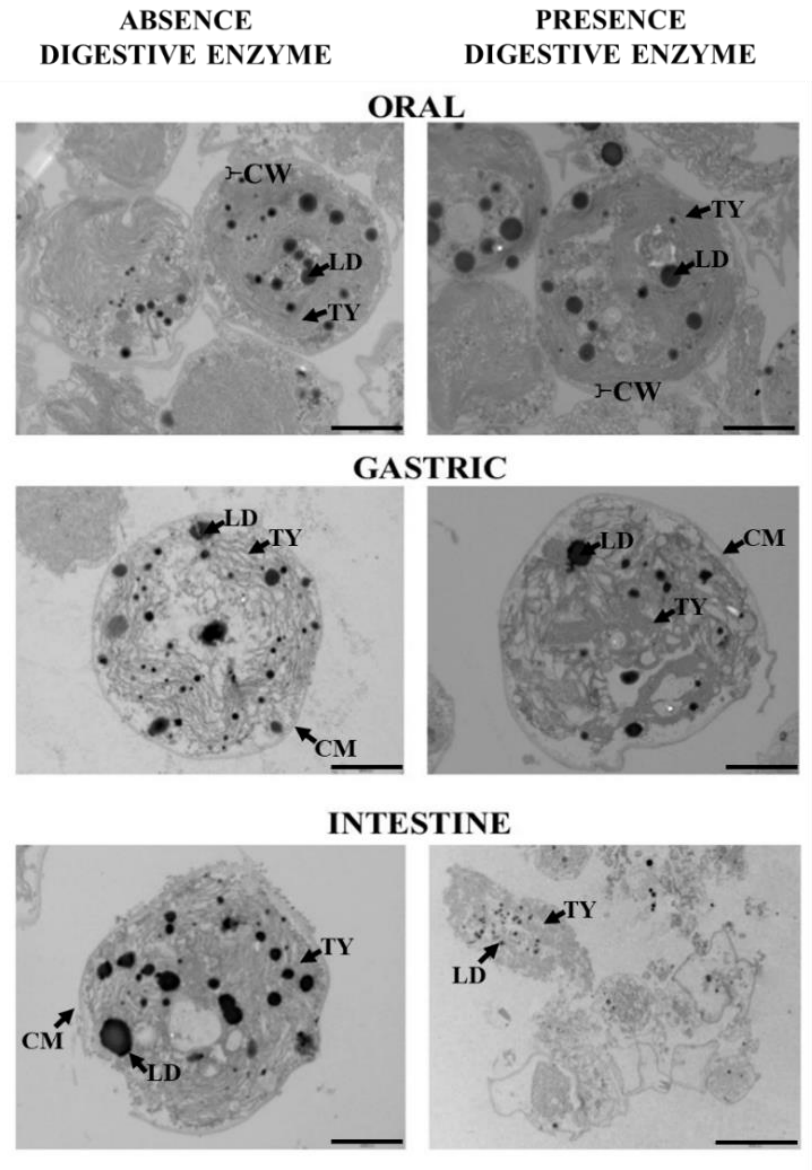


Figure 6.1: TEM images of *C. reinhardtii* throughout the digestion steps (oral, gastric, intestine) representing the intact *C. reinhardtii* freeze-dried biomass to the control sample (left) has been subject in the absence of enzymes. The real sample (right) has been subjected in the presence of enzyme with the same pH change, temperature and shaking. CW: Cell Wall, CM: Cell Membrane, TY: Thylakoid Membrane, LD: Lipid Droplet. Scale bar = 2000 nm.

In the presence of digestive enzymes *C. reinhardtii* experiences morphological changes especially during the stomach and intestinal phase of the incubation. The cell wall was digested but the cell membrane were remained through oral and stomach stage. Lipid droplets and chloroplast structure were diminished and the cell shape was lost. Particulate/membrane structures were retained to some extent, but this qualitative data suggests that a measurable proportion of the solid material has been digested, and that the ordered structure of the thylakoid membranes has been lost.

6.2.1.2 Phase behaviour

The phase behaviour of the *C. reinhardtii* in the presence and absence of digestive enzyme during *in vitro* digestion revealed in **Figure 6.2.** Phase separation are seen in the intestinal phase for only samples treated without the digestive enzymes. The samples that contain the digestive enzymes seem to promote the formation of a homogenous suspension. The digestive enzyme digest the cell membrane layer leading to the releasing of the intracellular compound into the suspension later they were emulsified with bile salt. Moreover, the addition of bile extracts in the intestinal phase in the sample also participate in colour changes as bile salts have dark green to yellowish brown colour (Agellon, 2002). The general observation of the green colour or the "greenness" appearance of the total digesta an intact *C. reinhardtii* present in **Figure 6.3.** The bright green colour is a result of the presence of chlorophyll *a* and *b*. By moving the cells to the acidic condition in the stomach (pH=3) the green colour changes to olive green. This is because at low pH, hydrogen ions can transform the chlorophylls to their corresponding pheophytins by substitution of the magnesium ion in the porphyrin ring and the color changes to the

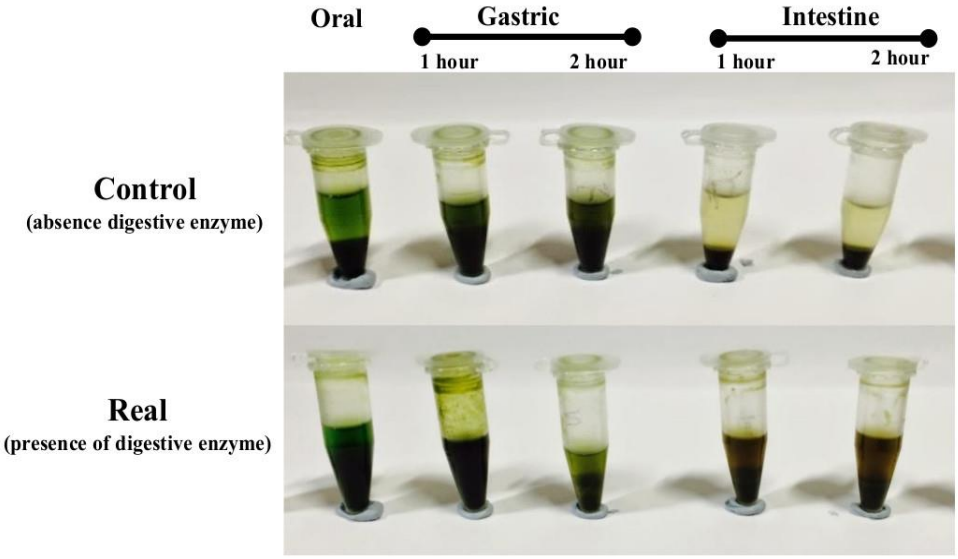


Figure 6.2: The differences between the control (absence of digestive enzyme) and the real (presence of digestive enzymes) of intact *C. reinhardtii* freeze-dried biomass throughout the digestion stages (oral, gastric and intestine).



Figure 6.3: Illustration the changing of *C. reinhardtii* digesta colour during *in vitro* digestion process.

characteristic pheophytin olive green color. Chlorophyll *a* becomes gray-green pheophytin-*a*, and chlorophyll-*b* turns into yellowish pheophytin-*b*. The chlorophyll derivatives are not reversible thus the yellow-olive green colour remains even after adjusting the pH to 7 in the intestinal phase (Hörtensteiner, 2012). The changing of the

chlorophyll structural and pheophytin formation in the acidic conditions presented in **Figure 6.4** (Arifin *et al.*, 2017).

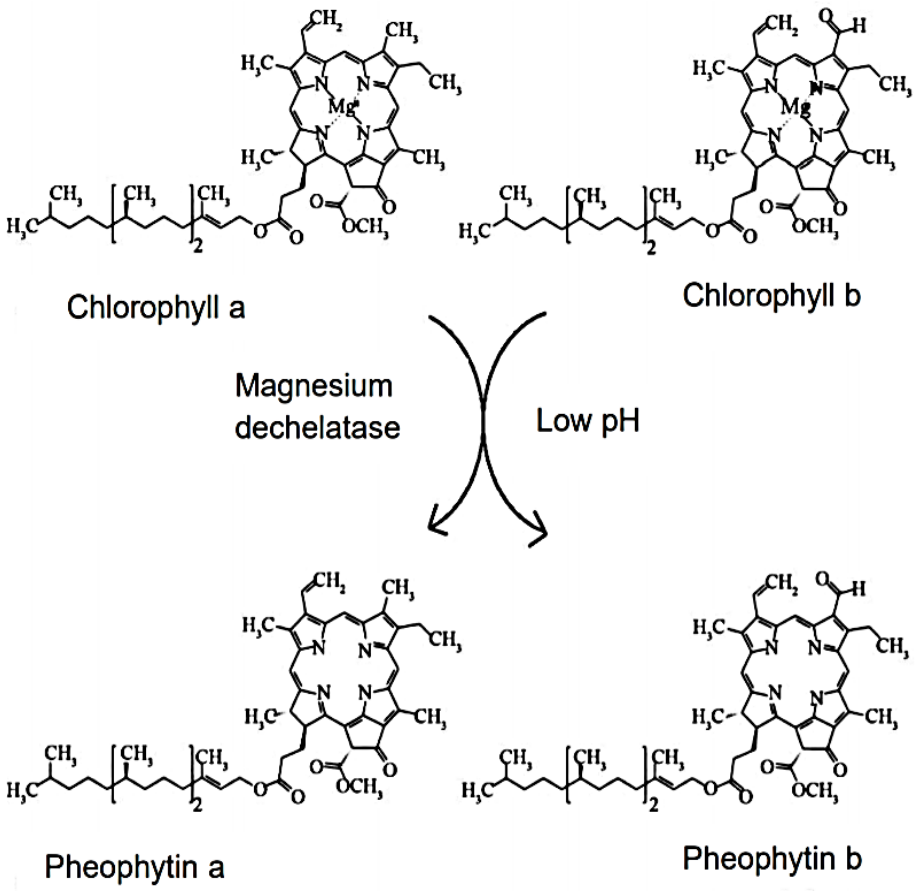


Figure 6.4: The changing of the chlorophyll structural and pheophytin formation in the acidic conditions (Arifin *et al.*, 2017).

6.2.2 Nutritive value of intact and disrupted freeze-dried *C. reinhardtii* during *in vitro* human digestion

Initially intact *C. reinhardtti* freeze-dried biomass was exposed to the *in vitro* human digestion in the presence and absence of enzymes, and the pigments of interest were measured in the total digesta phase at the incubation end point. One would expect there to be no difference in the concentration of our target pigments in the total digesta phase

of these two systems. Results **(Figure 6.5)** indicate a similar decrease in the concentration of all four pigments when cells were incubated in the presence of digestive enzymes. This suggests that there is a degree of enzyme-induced pigment degradation during digestion, or that the process of digestion (breaking down the cell wall and other cellular elements) renders the pigments more prone to degradation promoted by the temperature and pH they are exposed to during the incubation.

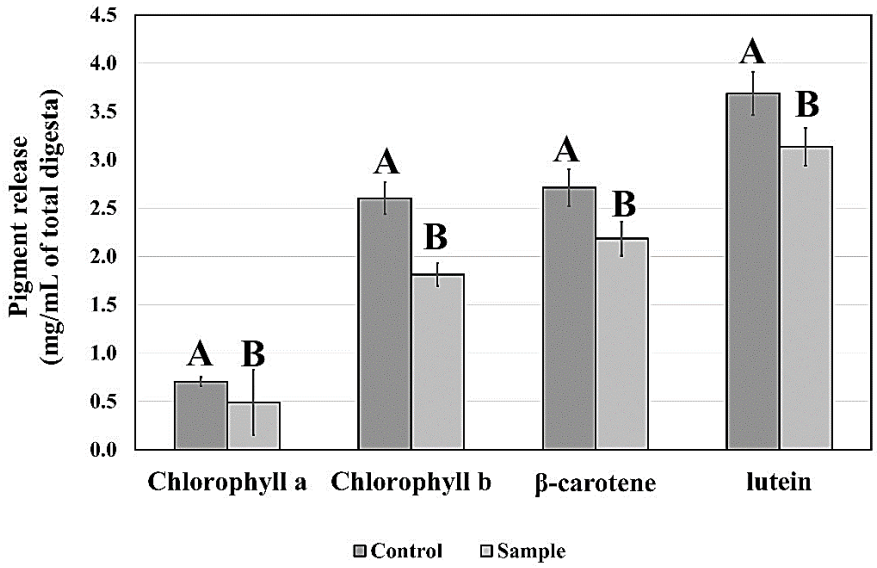


Figure 6.5: The chlorophyll (*a* and *b*) and carotenoids (*β*-carotene and lutein) content of total digesta of intact *C. reinhardtii* in the presence and absence of digestive enzyme. Values shown are from triplicate determinations. Letters on the bars not sharing the common letter indicate significant differences ($p<0.05$).

6.2.3 *In vitro* Bioaccessibility of Chlorophylls (*a* and *b*) and Carotenoids (*β*-Carotene and Lutein) from Intact and HDC-Disrupted *C. reinhardtii.*

Generally, plant cell walls are largely resistant to degradation in the upper gut, afterward, represent an important barrier for the release of bioactive compounds (Waldron, Parker

and Smith, 2003; Ellis *et al.*, 2004). The first step in making nutrient bioavailable from plant food is to liberate it from their nature structure. Therefore, an effect of HDC disruption on the release and bioaccessibility of chlorophylls (*a* and *b*) and carotenoids (*β*-carotene and lutein) from intact and HDC-disrupted *C. reinhardtii* freeze-dried biomass was studied. They were exposed to an *in vitro* human digestion model. The total digesta was collected at the end of small intestine *in vitro* human digestion **(Figure 6.6A)** then centrifuged and filtered to separate the micelle fractions (clear supernatant containing mixed micelles shown in **(Figure 6.6B).** The total digesta and micelle fractions were analysed for chlorophylls (*a* and *b*) and carotenoids (*β*-carotene and lutein) content. The bioaccessiblity index (%) were measured to evaluate the proportion of the chlorophylls (*a* and *b*) and carotenoids (*β*-carotene and lutein) in the total digesta at the end of the incubation period that is present in the micellar fractions.

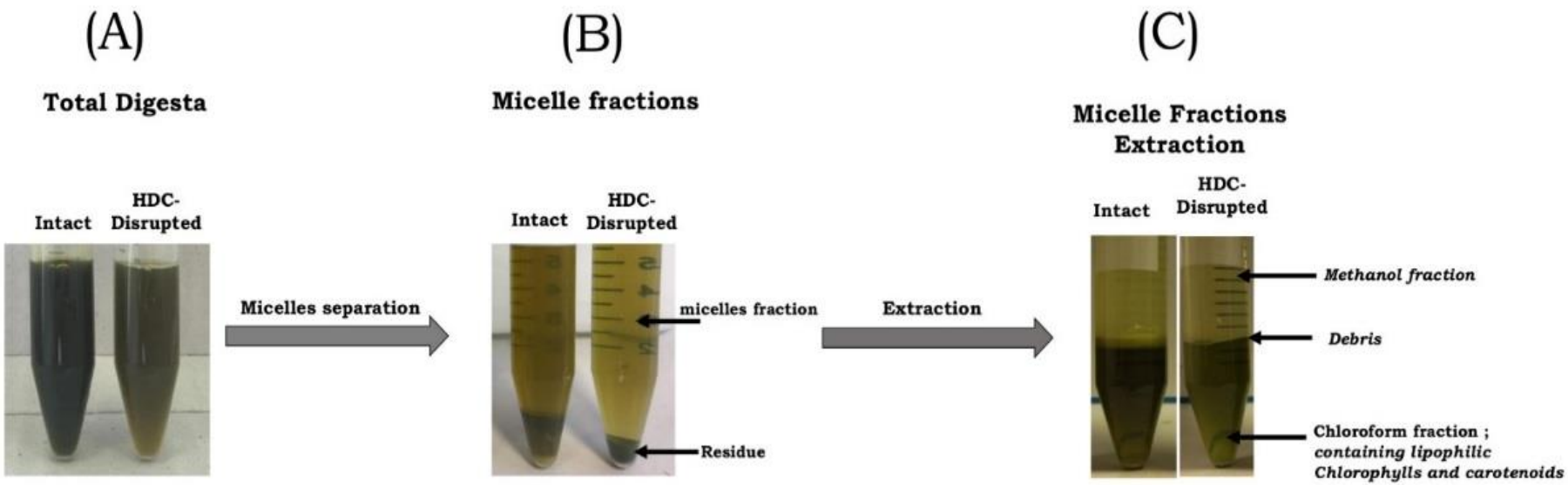


Figure 6.6: Separation of aqueous micellar fraction and extraction from intact and disrupted *C. reinhardtii*. The aqueous digesta of intact and disrupted *C. reinhardtii* at the end of simulated small intestine digestion (A). The aqueous micelle fraction was separated by centrifugation (5,000 rpm for 120 min using a Rotina 380R centrifuge) (B). The chlorophyll and carotenoids were extracted from the micelles fraction using chloroform: methanol (2:1) plus 0.1% BHT (C).

Chlorophyll is widely distributed in green fruits and vegetables as primary photosynthetic pigments, but the available information about the digestive process of chlorophyll pigments is limited (Barba *et al.*, 2017; Chen and Roca, 2018). Some studies have demonstrated the health benefits of chlorophyll and sodium copper chlorophyllin (SCC) (Ferruzzi and Blakeslee, 2007). However, information regarding the digestion, absorption, and metabolism of these phytochemicals is quite limited (Ferruzzi and Blakeslee, 2007). They are likely to be sensitive to the environmental changes and prone to chemical and enzymatic changes (Schwatrtz and Lorenzo, 1991). The most abundant chlorophyll present in all microalgae is chlorophyll *a* nonetheless chlorophyll *b* is present only in green algae (Levine and Fleurence, 2018).

After *in vitro* digestion, the chlorophyll *a* from the HDC-disrupted *C. reinhardtii* freeze-dried biomass (2.3%) appeared to be less accessible than intact *C. reinhardtii* biomass (25.3%) whereas only 11.3% of the chlorophyll *b* is accessible from the same materials **(Table 6.1).** Presumably that the loss of cell wall integrity cause by disruption process leading to an easier degradation of the total chlorophyll via the harsh condition of pH and temperature during *in-vitro* digestion.

Our proposed schematic effect of intact and HDC-disrupted on the integrity of *C. reinhardtii* cells during *in vitro* human digestion shown in **Figure 6.8.** Initially, the intact *C reinhardtii* biomass has oval in shape with multilayer in HRGPs. While, HDC-disrupted generated the microfiltration on a cell wall, but the overall structure remains intact. Once they expose to the harsh condition (pH, and temperatures changing) throughout *in vitro* human. The intact cell remains their integrity during the oral and gastric condition later they were digested at the small intestine stage. On the other hand,

Table 6.1: The nutritional composition (mg/g) of starting freeze-dried biomass, the bioaccessibility (%) and Nutrient uptake (mg/g) of intact and HDC-disrupted biomass (mg/g).

	Starting freeze-dried *C. reinhardtii* (mg/g)		Bioaccessibility (%)		Nutrient Assimilable (mg/g)	
	Intact	**Disrupted**	**Intact**	**Disrupted**	**Intact**	**Disrupted**
Chlorophyll *a*	4.83^{a}±0.31	2.30^{b}±0.01	25.3^{a}±8.79	2.29^{b}±0.29	1.22^{a}±0.42	0.05^{b}±0.01
Chlorophyll *b*	0.44^{a}±0.03	0.20^{b}±0.00	18.9^{a}±3.13	11.3^{b}±1.23	0.08^{a}±0.01	0.02^{b}±0.00
***β*-carotene**	0.22^{a}±0.01	0.22^{a}±0.00	9.12^{a}±2.77	3.25^{b}±0.21	0.02^{a}±0.01	0.01^{b}±0.00
Lutein	2.77^{a}±0.10	2.56^{b}±0.00	34.7^{a}±3.60	34.1^{a}±8.57	0.96^{a}±0.10	0.87^{a}±0.22

Mean±SD from triplicate determinations. Letters on same row not sharing the common letter indicate significant differences ($p<0.05$).

Bioaccessiblity (%) $=(C_{\text{micelle fractions}} / C_{\text{total digesta}})*100$

Nutrient Assimilated (mg/g DWB) = % Bioaccessibility * $C_{\text{Initial freeze-dried microalgae}}$

where

$C_{\text{micelle fraction}}$ = Concentration of the compound present in the micelle fraction (µg/g of an initial freeze-dried microalgae).

$C_{\text{total digesta}}$ = Concentration of the compound present in the total digesta (µg/g of an initial freeze-dried microalgae).

$C_{\text{initial freeze-dried microalgae}}$ = Concentration of the compound present in an initial freeze-dried microalgae (µg/g DWB).

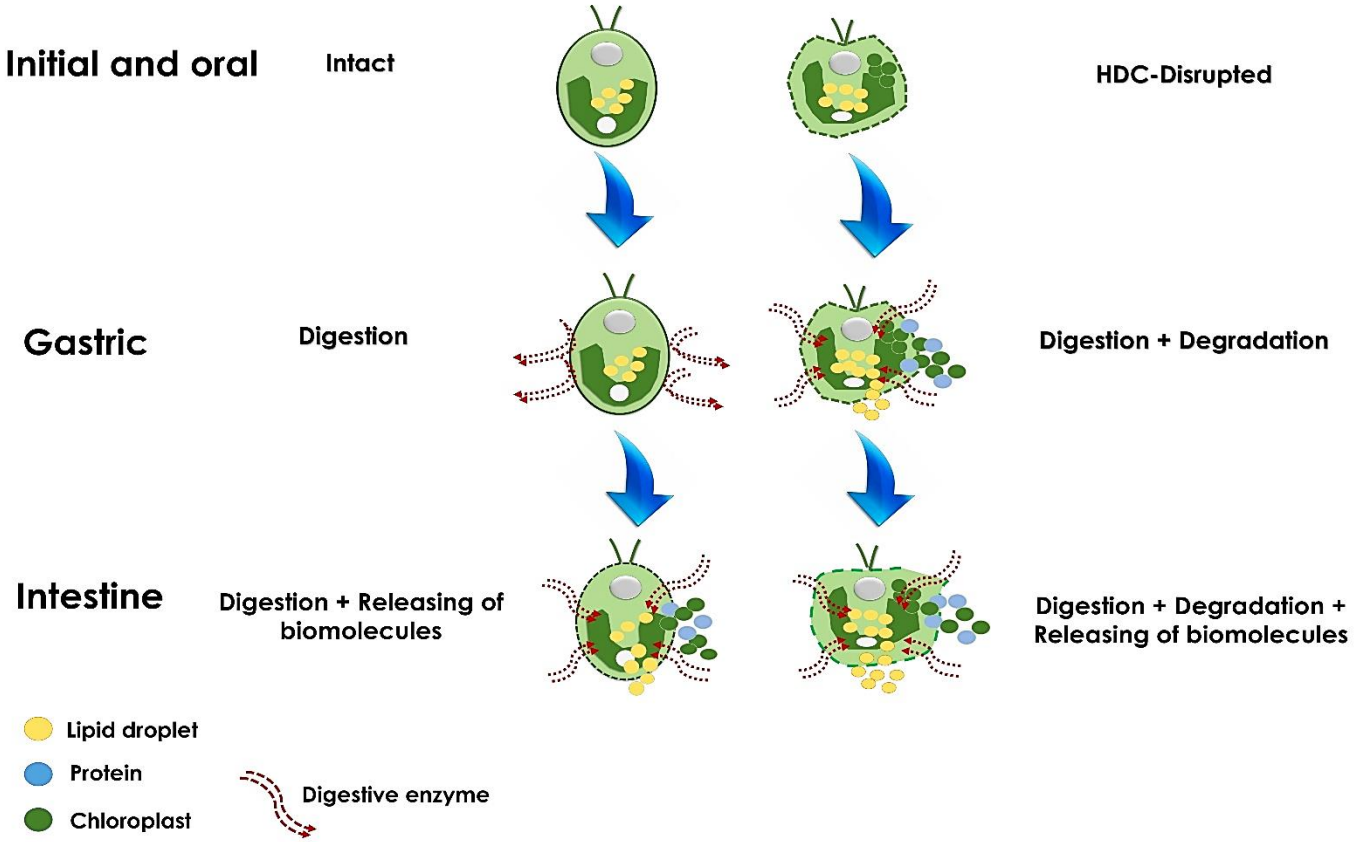


Figure 6.7: The proposed schematic effect of intact and HDC disrupted on the integrity of *C. reinhardtii* cells during *in vitro* human digestion.

HDC-disrupted cells appear to cause substantial cell damage at the earlier stage, during an exposing to the gastric condition. Presumably, the loss of the cell wall integrity cause by HDC could facilitate the digestive enzyme to penetrate the cell later release and loss of their cellular contents during digestion.

The sensitivity of natural chlorophylls to extremes in pH and temperature allows for the formation of several distinct derivatives through processing of vegetable tissue and human digestion. Ferruzzi *et al*., (2001) studied the micellization of the green vegetables including fresh spinach puree (FSP), heat- and acid-treated spinach puree (HASP), and $ZnCl_2$-treated spinach puree (ZnSP) during *in vitro* digestion. Their finding suggested that native chlorophylls were converted to Mg-free pheophytin derivatives during digestion.

Conversely, Zn-pheophytins were completely stable during the digestive process. Micellization, transfer of lipophilic chlorophyll derivatives into the aqueous micellar fraction, of total chlorophyll derivatives differed significantly for FSP (37.6%), HASP (17.2%), and ZnSP (8.7%). Micellization, of a chlorophyll *a* derivative was significantly more efficient than chlorophyll *b* derivatives in FSP and HASP, but not in ZnSP (Ferruzzi *et al*., 2001). Gandul-Rojas *et al*., (2009) measured the bioavailability of chlorophyll *a*, chlorophyll *b*, and the Mg-free chlorophyll derivatives pheophytin *a*, pheophytin *b*, pyropheophytin *a*, pheophorbide *a*, and pyropheophorbide *a*, dissolved in an oily matrix: samples were subjected to a simulated *in vitro* digestion procedure coupled with uptake by human intestinal Caco-2 cells. Their result suggested that the native chlorophylls showed greater instability to the digestive process than the Mg-free chlorophyll derivatives. After digestion, the pigment dispersion degree in the colloid system (aqueous-"micellar" phase) showed significant differences among series *a* and series *b*

derivatives. When a mixture of pheophytin *a* and pheophytin *b* was digested, there was a positive effect for pheophytin *b*; both the dispersion degree and the accumulation rate by the Caco-2 intestinal epithelial cells were significantly higher. These results showed that the structural modifications of the chlorophyll significantly increased, by an estimated 65-fold, the transfer of chlorophyll from the food matrix to the intestinal epithelial cells during digestion, making it more bioaccessible.

Carotenoids are associated with chlorophyll in the thylakoid membrane of chloroplasts, where they function as inhibitors of oxidation processes and thus protect chlorophyll molecules from degradation (Zhang *et al*., 1999). The bioaccessiblity of lutein shown a proportional level in both intact (34.7%) and HDC-disrupted cells (34.1%). In contrast, the lower level of *β*-carotene accessible from HDC-disrupted (3.25%) than intact (9.12%) **(Table 6.1).** Very low level of *β*-carotene bioaccessiblity from HDC- *C. reinhardtii* might also due to the degradation caused by heat or pH changing during mimic digestion. Carotenoids are also sensitive to temperature, enzymes and pH, these three factors are included during *in vitro* digestion (Gille *et al*., 2016). Carotenoids are highly stable within their natural plant cell environment, but once isolated, they are sensitive to situations exposing them to light, heat and acids, which promotes cis-trans isomerisation. In addition, plant tissue contains lipoxygenase, which catalyses carotenoid oxidation (Ball, 2013).

Gille *et al*., (2016) also reported that stability of carotenoids was affected by *in vitro* digestion. Our finding is in line with Gille, *et al*., (2016) whose compared an effect of sonication on the bioaccessiblity of carotenoids (lutein and *β*-carotene) from *C. reinhardtii* and *C. vulgaris*. Their results suggested that *C. reinhardtii* represents a

good source of carotenoids without further processing, at least 20% of lutein but less than 10% of initial amount of *β*–carotene was bioaccessible from *C. reinhardtii*. Their bioaccesssiblity was not improved by sonication. While application methods such as sonication are necessary for *C. vulgaris*. Only 7% of *C. vulgaris* initial amount of lutein was bioaccessible whereas *β*-carotene was shown not to be bioaccessilble.

A similar finding was also reported by Kopec *et al*., (2017) who studied the stability of carotenoids from a test meal (carotenoids in oil). They found a significant loss of carotenoids during gastric and small intestinal phases (40% and 20%, respectively). Oral dosage of carotenoids takes into account dissolution and stability in the gastrointestinal (GI) tract, including the acidic environment of the stomach (pH 1–2 in fasted state, 3–7 in fed state) and the close to neutral environment (pH 4.4–6.6) of the small intestine (Di and Kern, 2008). *β*-carotene bioaccessibility has been subject of study in many other food sources. In carrot, for example, the bioaccessibility of *β*-carotene in raw and pulped carrots estimated by Zaccari *et al*., (2015) using *in vitro* methods was very low (<0.5%). Furthermore, steaming and a smaller particle size increased the bioaccessibility of *β*-carotene by 3-16 times (Zaccari *et al*., 2015).

In 2013, the World Health Organization classified vitamin A deficiency as a public health problem affecting approximately one-third of children aged 6–59 months, with the highest rates observed in sub-Saharan Africa (48%) and South Asia (44%) (UNICEF, 2013). The bioconversion effectiveness of pro-vitamin A to vitamin A has recently been reassessed to establish the amount of carotenoids required in the diet to prevent vitamin A deficiency (VAD) which is the prominent cause of preventable blindness in children

There has been no recommended dietary allowance (RDA) established for *β*-carotene. 6 µg *β*-carotene has been shown to have 1 µg Retinol Equivalent (RE) (Bohn, 2008).

Vitamin A intakes or requirements are generally expressed in terms of RE. The RDA for vitamin A is 1,000 RE for men and 800 RE for women. An additional 500 RE per day is recommended during the first six months of lactation and a 400 RE increment for the second six months (National Research Council, 1989). Therefore, fortifying 10 g of microalgae into food would provide 0.2 mg of *β*-carotene assimilation **(Table 6.1).** RDA for lutein has been established. Some studies have reported the benefit of lutein for age-related macular degeneration (AMD) patients (Weigert *et al*., 2011; Ma *et al*., 2012). Therefore, consuming 10 g of microalgae provide 9.6 mg of lutein assimilation **(Table 6.1),** which approaches the daily recommendation (10–20 mg/day).

6.2.4 Structural Change of Intact and Disrupted Freeze-Dried *C. reinhardtii* Biomass During *in vitro* Static Human Digestion

The physicochemical structure and properties of cell walls in plant food tissues are critical factors involved in influencing bioaccessibility during digestion (Waldron *et al*., 1997; Ellis *et al*., 2004). Cell walls and chromoplasts are the two primary physical barriers to nutrients release, mainly carotenoids, from the food matrix (structure) during digestion (Jeffery *et al*., 2012). Consequently, it is crucial to an understanding of both physical and chemical changes of *C. reinhardtii* during the digestive process to clarify their nutrient bioaccessibility. To provide an indication of how *in vitro* digestion affected structure of intact and HDC-disrupted *C. reinhardtii*, microscopic observation of pellet intact and HCD-disrupted freeze-dried biomass during each stage of *in vitro* human digestion were observed **(Figure 6.7).** Overall one can see that the HDC-disrupted cells appear to be

more digested at the end of the incubation period than intact cells**(Figure 6.7H),** presumably due to some breaching of the cell wall causing the enzymes to diffuse more easily into the cell and possibly organelles. Presumably, in the same way that the stain reached the lipid droplets in disrupted microalgae. It is also possible that chloroplasts are released from fully broken cells, making it easier to digest this organelle. **Figure 6.7H** shows that disrupted cells were more digested than 'intact' *C. reinhardtii* biomass **(Figure 6.7D)** because HDC treatment made them more digestible. This is consistent with the smaller pellet in the HDC-disrupted samples after centrifugation of the total digesta phase **(Figure 6.6B).**

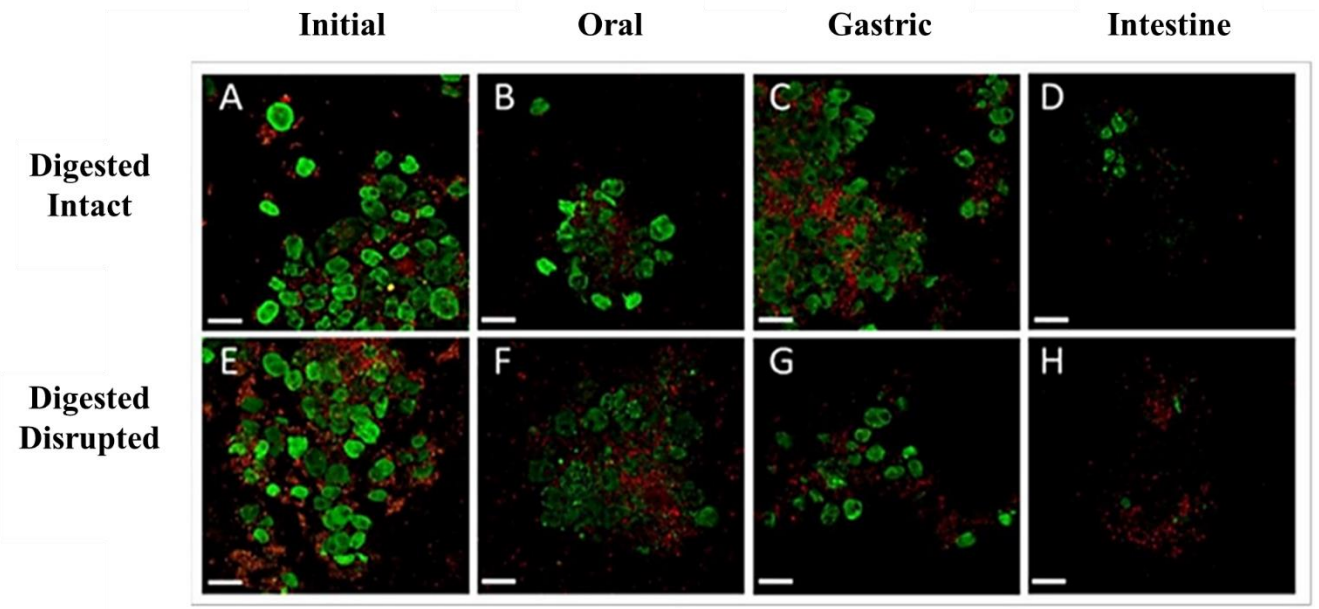


Figure 6.8: Particulate material from digested intact and disrupted freeze-dried *C. reinhardtii* at different stages during simulation of digestion. Cell membrane and lipid droplets Intact (A–D) and disrupted microalgae cells (E–H) during each stage of the *in vitro* digestion model; initial (A&E), oral (B&F), stomach (C&G) and intestine (D&H). Images were visualised by structured illumination microscopy (SIM). *C. reinhardtii* labelled for cell membrane and lipid (red; Nile Red and FM4 - 64FX) and chloroplast (green). Scale bars = 10 µm.

. CONCLUSION

The most important conclusions from this chapter can be summarised as:

- With regard to *in vitro* human digestion of intact *C. reinhardtii* freeze-dried biomass in the presence of digestive enzymes, pepsin and pancreatin significantly reduced chlorophyll and carotenoid bio-accessibility. The ultrastructure using TEM indicated that the cell wall was digested by enzymes during the gastric and intestinal stages. This supports the hypothesis that the protein-based nature of the *C. reinhardtii* cell wall makes it a unique microalgae worth investigating in light of its potential as a human and animal food source.
- The bioaccessibility of target nutrients from the intact and HDC-disrupted *C. reinhardtii* freeze-dried biomass was studied. The findings indicate that HDC treatment lowers the bio-accessibility of chlorophyll *a* and *b* (2.29% and 11.3%) carotenoids and *β*-carotene (3.25%) compared to intact cells (25.3% 18.9% 9.12% respectively). The exception was lutein bio-accessibility, the levels of which were proportionate in both intact (34.7%) and HDC-disrupted cells (34.1%). The presence of nutrients bioaccessiblity was lower, presumably due to the loss caused by HDC-disruption coupled with acid conditions during the acid phase of digestion. Thus, HDC- disruption is appropriate for more digestible structures, but is not relevant to the bio-accessibility of pigments. These findings pave the way for *in vivo* digestibility assays to establish the nutritional value of *C. reinhardtii*.

CHAPTER 7

Impact of *C. reinhardtii* Inclusion in Zebrafish Diet on Their Growth and Key Metabolites

7.1 Introduction

Microalgae and seaweeds are the basis of the aquatic food chain and is a food which many fish are adapted to consume. Thus, they have been extensively studied as a potential feed meal and/or feed ingredient of fish and aqua animals in an endeavour to move the formulation of the fish feed down to the base of the food chain (Stanley and Jones, 1976). Almost all PUFAs are synthesized by microalgae, bacteria and heterotrophic protists on which fish are fed and, therefore, fish occupy a relatively high level in the ecosystem. Fish, in turn, contribute notably to trophic upgrading, a term which originates from the marine literature and refers to the enhancement of zooplankton growth by the inclusion of micronutrient-rich heterotrophic protozoans in an otherwise herbivorous diet (Klein Breteler *et al*., 1999), as they have the capability to metabolize PUFA to produce LC-PUFA, which is consumed by humans (Monroig *et al*., 2013).

Biochemical analysis of numerous algae species proves that in spite of the large variations of their total protein content (8-50%), their amino acid profile comprises all the essential amino acids (Ortiz *et al*., 2006). Moreover, algae lipid generally shows a unique composition of fatty acids and is found to be specifically rich in the essential n-3 LC-PUFA, which makes algae a crucial candidate for further study (Wahbeh, 1997). Algae, and microalgae specifically, are distinguished not only by their high nutritional value, but

they also hold the extra advantages of possessing an appropriate cell size, antioxidant properties and high growth rate (Brown *et al*., 1997). Pigments are also a key point when feeding fish with microalgae is considered. Microalgae and seaweeds contain a wide spectra of important pigments for aquaculture, such as chlorophylls and carotenoids (Venkataraman and Becker, 1985).

Researches have tried to maintain fish by feeding microalgae or seaweeds. In this regard, several types of microalgae and seaweeds with small amounts (2.5–10% of the diet) have been associated with positive outcomes (Enyidi, 2017). These include a better performance in terms of body growth (protein production), feed utilization efficiency, physiological activity, stress response, starvation tolerance, disease resistance and flesh quality (Mustafa and Nakagawa, 1995). *Spirulina*, for example, when tested in fish diets, has been associated with an improved growth, better carcass quality and better protein digestibility as well as enhanced stress and disease resistance (Mustafa *et al*., 1994). Results from another study also showed that the inclusion of *Spirulina* in fish feed induced early maturation thereby, leading to a shorter breeding cycle and period of cultivation (Floreto *et al*., 1996).

It has also been demonstrated that certain sea plant proteins meet the tilapias requirements (Jackson *et al*., 1982). Montgomery and Gerking (1980) tried to understand the relationship between how herbivorous marine fish are fed on algae in the wild Gulf of California and which taxa are considered as high-quality food. They found that green algae are superior to the brown and red algae (Montgomery and Gerking, 1980). More positive responses beyond the growth improvement have been recorded from the use of

algae in finfish diet. These include better liver function, starvation tolerance, stress response, carcasses quality and health status (Guroy *et al*., 2010).

However, as discussed about the importance of *in-vitro* digestion studies in chapter 6, it rather depends more on the amount of nutrient release and fish can absorb and metabolize (National Research Council, 1992). Thus, careful consideration should be taken in choosing one microalga species as fish feed. The thick and cellulosic cell wall, such as it is the case in *Chlorella*, can prevent the release of cells content of nutrients. Inhibitory compounds and anti-nutritional factors, such as some phenolic compounds found in kelps and other brominated compounds produced by red algae, can render the alga biomass, which exhibits an excellent nutritional profile based on chemical analysis, unfeasible as feed materials (Soler-Vila *et al*., 2009, Oliveira *et al*., 2009). Trace elements and heavy metals can also be a detrimental factor in algae evolution as feed materials (Henry, 2012).

The aim of this chapter is to evaluate the possible inclusion of *C. reinhardtii* (whole intact) biomass, cultured under standard conditions and harvested at the stationary phase, in the feed of zebrafish diet. This was achieved by substituting the original fish meal, stated as control with three concentrations of *C. reinhardtii* 10%, 20% and 50%. Growth performance and parameters as well as some key metabolites were analyzed after 8 weeks of the feeding trials.

7.2 Results and Discussion

7.2.1 Growing and Palatability Criteria

A set of fish performance parameters were measured of the zebrafish fed with three different levels of partial replacement of fish meal by *C. reinhardtii* (10%, 20% and 50%) as compared to the zebrafish fed with the original diet set (control) Error! Reference source not found. These parameters are presented in **Figure 7.1 .**

Growth rate was measured by weighing the fish in each tank for 8 consecutive weeks, and the percentage of weight growth was depicted against time. Results revealed that for 10% and 20% inclusion, fish growth rate was similar ($p \geq 0.05$) and supported a significantly better growth rate starting from week 2, than the 50% inclusion as well as the control. Although 50% replacement gave a final higher growth rate than the control, this started only after 5 weeks.

Similarly, the specific growth rate (SGR) (the fish natural logarithm of the final fish weight subtracted by the natural logarithm of the initial fish weight over a period of time) showed that 10% and 20% inclusion levels give similar results and higher values than the 50% inclusion level and then the control **(Figure 7.1C).** The significant differences between the control diet and any experimental diet for the feed conversion ratio (FCR) was a decrease in all level of *C. reinhardtii* inclusion (10%, 20% and 50%), showing improved feed conversion. An inclusion of 20% of *C. reinhardtii* gave values closer to 1, which means it has better efficiency as a feed followed by 20%, 50% and then the control **(Figure 7.1B).**

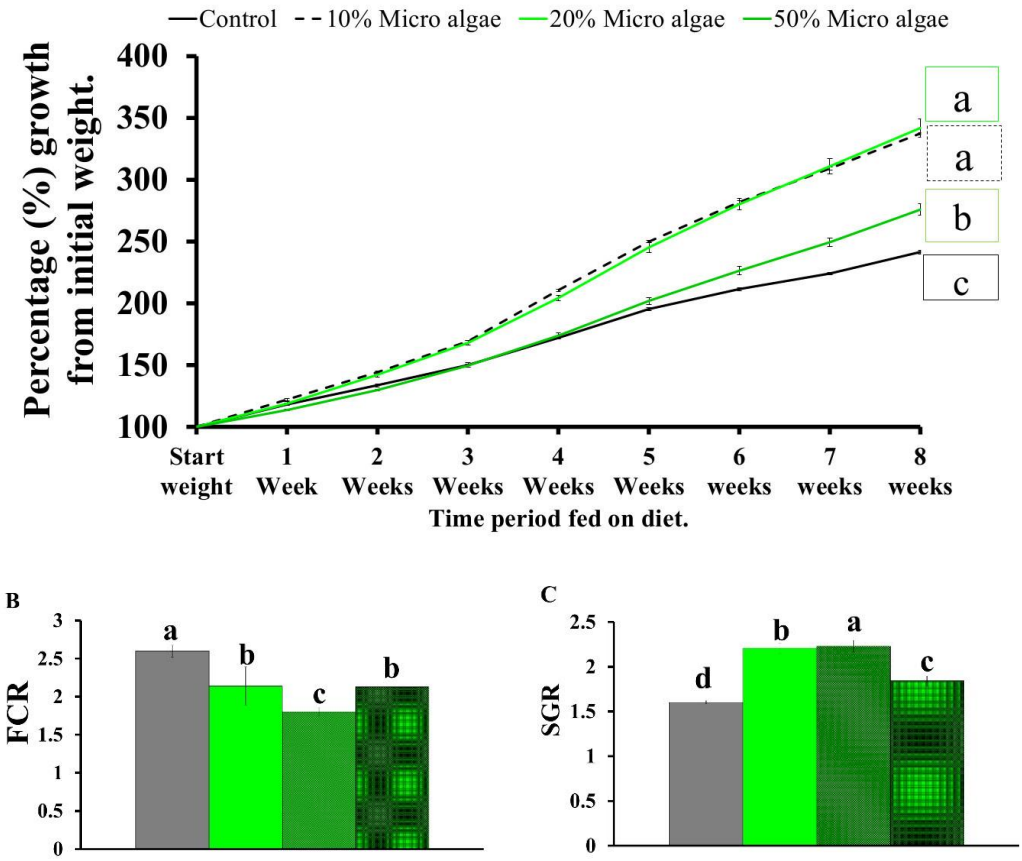


Figure 7.1: The growth and performance indicators for fish fed experimental diets. (A) Percentage growth from initial weight. (B) Feed conversion ratio (FCR). (C) Specific growth rate (SGR). (D). Difference on the bar that do not share a letter are significantly different ($p \leq 0.05$).

7.2.2 Impact of Consuming *C. reinhardtii* on Fish Body and Egg Carotenoid Levels

Generally, carotenoids accumulate in the external part of fish, in structures called chromophores in the skin, giving them the different spectra of colouration (Goodwin, 1980). These colours are present in more than 200 fish and particularly noticeable during the mating season as the colour plays an important role in the sexual selection, displayed more by the males (Czeczuga, 1972). Besides wild zebrafish, the control and *C. reinhardtii* containing diets were fed to gold zebrafish. Images of males and females as well as theirs eggs are presented in **Figure 7.2** and **Figure 7.3.**

The data shows that the eggs produced by fish fed with the *C. reinhardtii* included diet had an intense yellow to orange colour in comparison with the eggs resulted from fish fed with the control which display a white colour. Males also exhibited more colour than females with the yellow colour extended to the males' tails. The fish, male and female, fed with *C. reinhardtii* diet had more intensive colour than the control fed fish. This result comes in agreement with a study by Fox (1957), where he reported that in many fish species, the males were able to store 36% more of pigments, including carotenoids, in their skin than the females which immobilize the largest portion of their pigments to their eggs (Fox, 1957). Furthermore, it is established that the amount of the carotenoids represented by the visual quality that ultimately reach the target tissues is a convenient indicator of carotenoids bioavailability in the diet (Bjerkeng, 2008). The idea of the skin colour enhancement is particularly important in ornamental fish, hence a study by Gouveia *et al* 2003 aimed to enhance the skin colour of freshwater fish, goldfish and Koi carp (*Cyprinus carpio* and *Carassius auratus*) using three varieties of fresh water

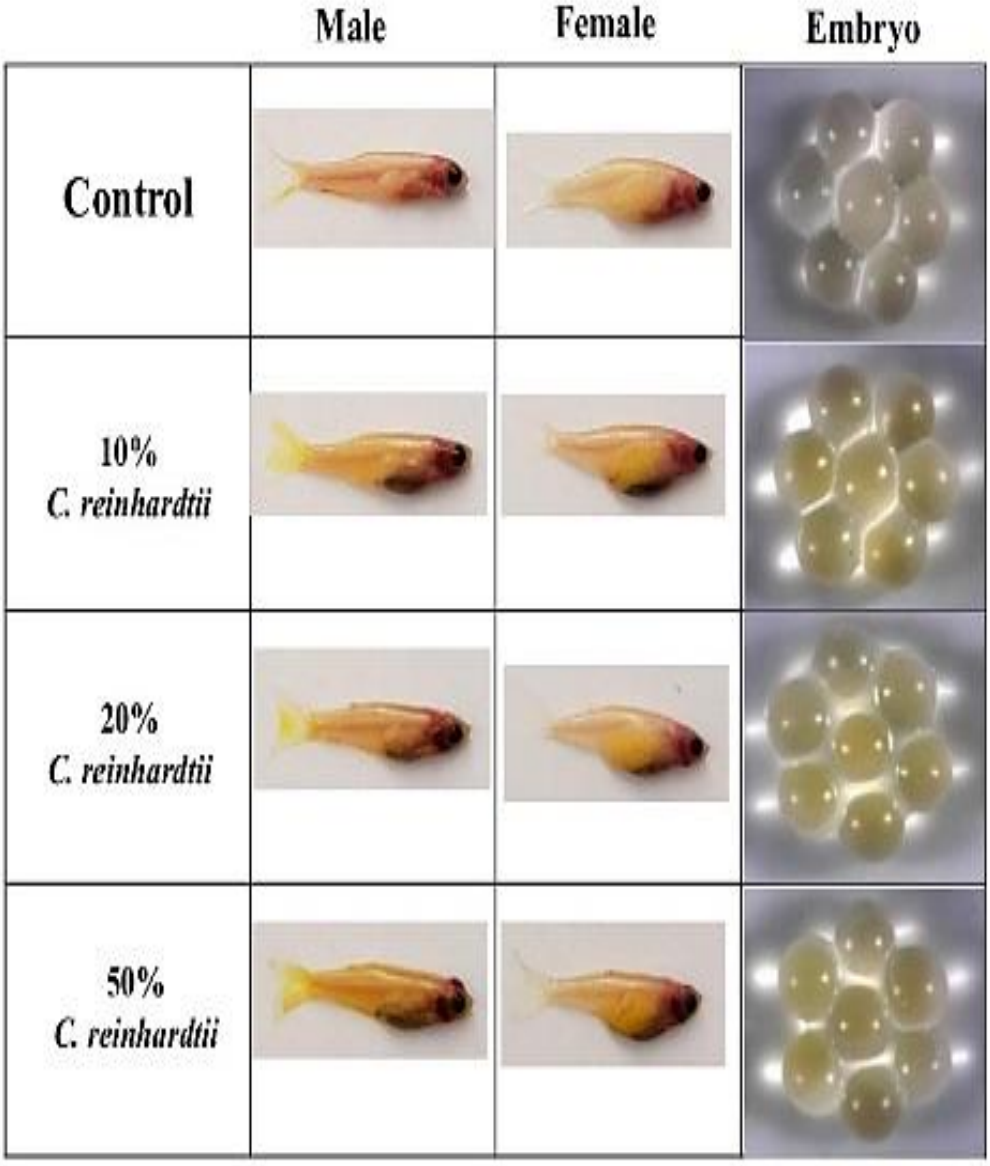


Figure 7.2: Zebrafish (*Danio rerio*) egg pigmentation and colour variation due to carotenoid accumulation in response to carotenoid- rich diets. The Zebrafish fed with three different levels of partial replacement of fish meal by *C. reinhardtii* (10%, 20% and 50%) as compared to the Zebrafish fed with the original diet set (control).

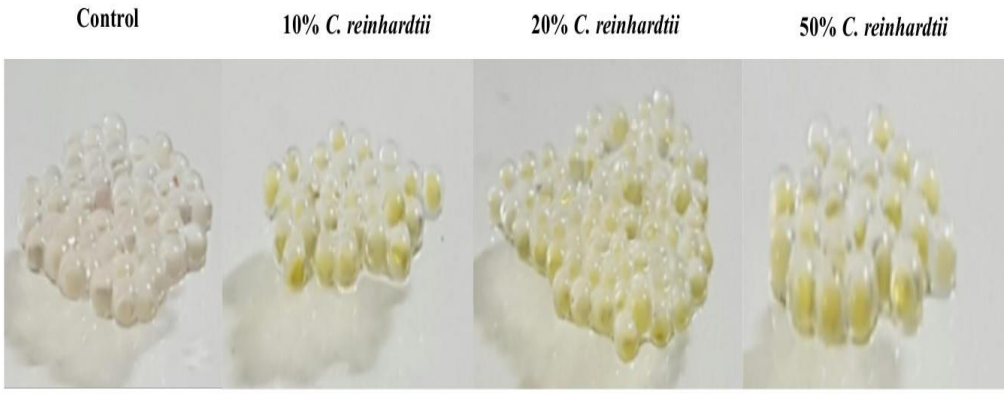


Figure 7.3: Egg colour variations depending of Zebrafish fed with three different levels of partial replacement of fish meal by *C. reinhardtii* (10%, 20% and 50%) as compared to the Zebrafish fed with the original diet set (control). These images were taken with SAMSUNG Galaxy Note 3.

microalgae namely *Chlorella vulgaris*, *Haematococcus pluvialis*, and also the cyanobacterium *Arthrospira maxima* (*Spirulina*). A diet containing synthetic astaxanthin was used and a colorless control diet was set as well. In both fish types, no significant effect was noticed on the growth and feed efficiency, and the inclusion of carotenoids enhanced the total skin colour. *C. vulgaris* inclusion achieved the highest amount of carotenoids accumulation, especially in the goldfish body. The amount and type of carotenoids retained in the fish body depends on the fish species, growth rate, size and metabolic transformation. For example, astaxanthin accumulates in salmon muscles (Robb *et al*., 2002).

7.2.3. Quantitative Analysis of Carotenoids in Fish Body and Eggs

To identify the cause of the colour differences noticed in the fish and the egg fed with different diets, pigments were extracted and analysed using HPLC. The lipid soluble pigments extract of the control and *C. reinhardtii* fed fish samples presented in **Figure 7.4**

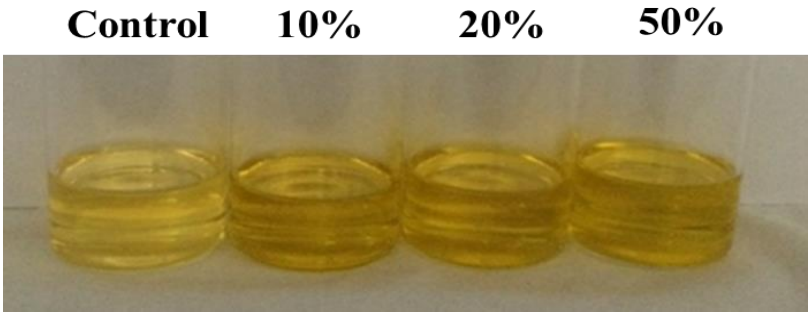


Figure 7.4: The lipid soluble pigment extract of the whole body fish of Zebrafish fed with three different levels of partial replacement of fish meal by *C. reinhardtii* (10%, 20% and 50%) as compared to the Zebrafish fed with the original diet set (control).

The carotenoids (*β*-carotene and lutein) were then analysed. The *β*-carotene and lutein are the major carotenoids in *C. reinhardtii*, whilst only lutein was detected and presented in **Figure 7.5A** for the whole body and for the eggs. The three inclusion levels of *C. reinhardtii* had significant influence on the lutein level in both the fish bodies and their eggs compared to the control. At 20% inclusion level, the lutein content of the whole body reached 4.5 µg/g DW, which is higher, although not significantly, than the 10% and 50% inclusion levels, and massively higher than the control (<0.1 µg/g DW). Likewise, the lutein content in the fish egg, **Figure7.5B** fed with the 20% replacement level of *C. reinhardtii* recorded the highest level (45.4 µg/g DW) followed by the 10% (43.3) and both were significantly higher than the 50% inclusion level (29 µg/g DW) and the control

(23 µg/g DW). There has been relatively little quantitative work previously about carotenoids metabolism in fish and this research is restricted to only a few species (Bjerkeng, 2008).

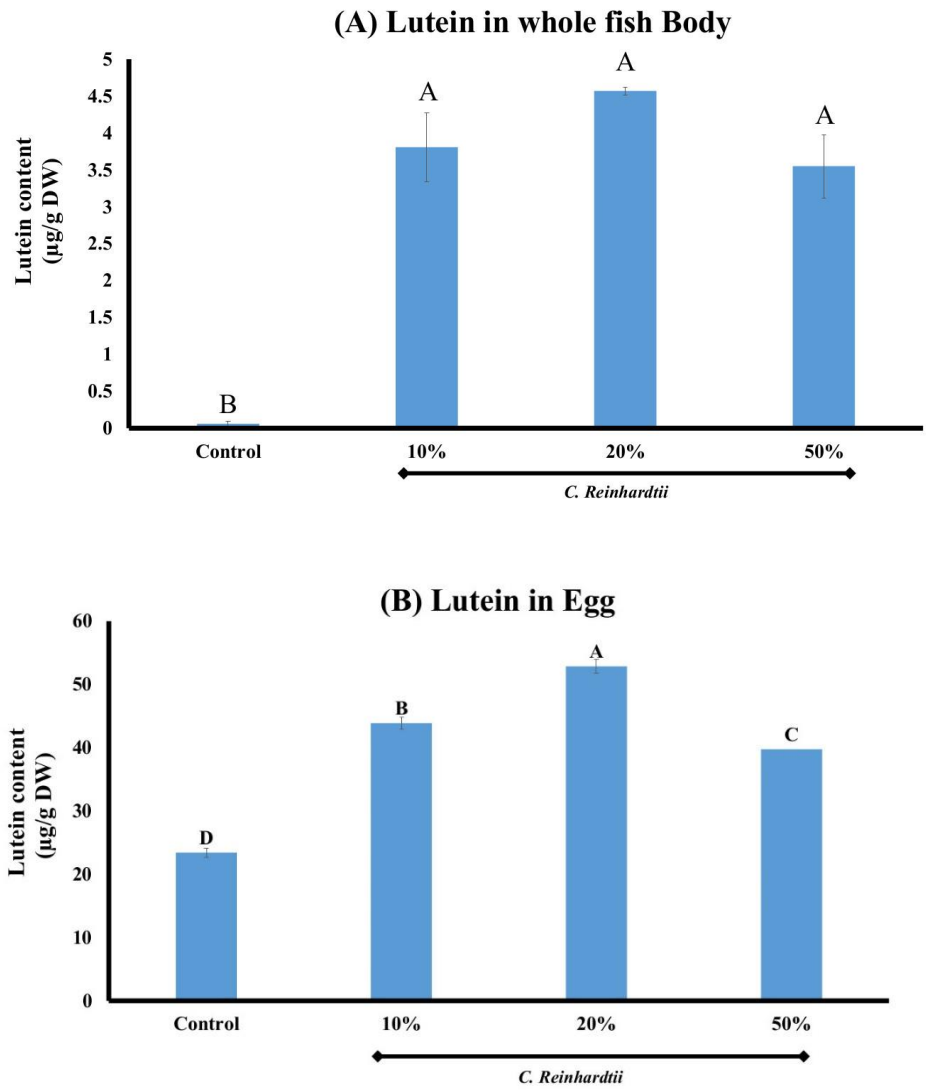


Figure 7.5: Lutein content of the lipid extracted from whole body fish (A) and egg (B) of Zebrafish fed with three different levels of partial replacement of fish meal by *C. reinhardtii* (10%, 20% and 50%) as compared to the Zebrafish fed with the original diet set (control).Values shown are from triplicate determinations. Letters on the bars not sharing the common letter indicate significant differences ($p<0.05$).

Conclusions from feeding experiments as well as the distribution of carotenoids in aquatic systems has revealed that fish differ greatly in their ability to ingest and transform different kinds of carotenoids. Lutein, for example which is normally present in wild trout and thus in farmed brook trout, when incorporated into the diet from marigold petals, was rapidly stored without any modification in the skin, fins or flesh, giving the fish a golden yellow colour (Peterson *et al*., 1966). It is agreed that astaxanthin is the main carotenoid in aquatic animals and that those animals can be divided into three groups in this regard (Stewart *et al*., 2012). The first group can convert zeaxanthin or lutein to astaxanthin, absorb and accumulate the diet astaxanthin as well; the second can convert *β*-carotene and zeaxanthin to astaxanthin; and the third cannot convert *β*-carotene, lutein or zeaxanthin to astaxanthin but can absorb it as well as lutein, zeaxanthin and tunaxanthin from the diet to the body organelles, like skin, as pigments esters (Stewart *et al*., 2012). It can be concluded from this study that zebrafish belongs to the third group based on Stewart *et al* (2012) grouping, which means it cannot convert any kind of carotenoids to astaxanthin, as astaxanthin was not detected neither in the body nor in the eggs; instead, lutein accumulated in both (Stewart *et al*., 2012).

In a study on *Acipenser ruthenus*, it was observed that the presence of *β*-carotene, astaxanthin ester, tunaxanthin, lutein and zeaxanthin in the egg collected before fertilization (Czeczuga, 1972). Evidence collected by Fox, (1957) stated that the integumentary carotenoids of teleost fish belong mainly to the lutein and taraxanthin classes without a clear differentiation between them at the time of writing the book (Fox, 1957). In trout fish, for example, its skin contains lutein rich xanthophores and astaxanthin rich erythrophores (Urich, 2013). Regarding the microalgae carotenoids in the fish feeding sector, many studies targeted the use of *Haematococcus* species as a rich source

of astaxanthin. Sommer *et al*., (1991) compared *Haematococcus* with the synthesized astaxanthinfor the purpose of flesh colour enhancement of trout and found a significantly higher amount of total carotenoids of the trout skin fed with the synthetic xanthophyll compared to the *Haematococcus* biomass. Like other similar studies they refer to the high level of esterified astaxanthin and the poor digestibility of its cell wall (Sommer *et al*., 1991). More importantly, recent studies have confirmed that carotenoids are crucial for zebrafish development from egg to adult fish. Egg yolk is found to contain significant amounts of carotenoids which undergoes mobilization and redistribution during embryogenesis. Moreover, zebrafish genes encode the vitamin A-cleaving enzyme from *β*-carotene, a *β*, β-carotene-15, 15'-oxygenase (Kiefer *et al*., 2001;Lampert *et al*, 2003)

CONCLUSION

*Z*ebrafish was employed as an animal model to investigate intact *C. reinhardtii* biomass *in vivo* digestibility. Clearly, the growth parameters showed a significant improvement over the control ($p \leq 0.05$). A 20% inclusion level supported the best growth and feed utilisation of *C. reinhardtii* by zebrafish. Carotenoid accumulation in the body of the zebrafish was represented by lutein accumulation in the whole body and egg. This finding proved that these carotenoids had been released from the *C. reinhardtii* cells and that at least part of them were absorbed and assimilated by the fish.

CHAPTER 8

Summary

C. reinhardtii can be a new source of food and animal feed. The microalgae were successfully grown under the lab scale system using standard media in mixotrophic conditions. *C. reinhardtii* growth in the lab scale system provided 0.07 g/L or 70 mg/L at the end of the exponential phase. The biochemical composition of the freeze-dried biomass is correlated with the age of cultivation. The protein level (140–170 mg/g) and photosynthetic pigment content – chlorophyll *a*, chlorophyll *b* and carotenoids – were 0.06–0.08 mg/g, 0.01–0.02 mg/g and 0.11–0.13 mg/g, respectively, reaching their lowest point during the decline or death phase. In contrast, total lipid content rose and then remained high (196 mg/g) during the stationary phase.

C. reinhardtii can be manipulated under nitrogen stress conditions, providing nourishing biomass. Stressing the cell growth of *C. reinhardtii* by reducing the levels of nitrogen in the media leads to an increase in protein content ranging from 41.4 to 43.8% in this species. Their protein contains the large (50 kDa) and small (15 kDa) subunits of Rubisco. The biomass accumulated amino acid, glutamine, leucine and alanine, with trace levels of cysteine, aspartic acid and methionine. The total lipid content was 13.17–20.90%. The most significant FA found, in both the standard and stress freeze-dried biomass, is PUFA, which comprised 27.73% of total fatty acids with a mean of α-linolenic acid (C18:3ω3). The level of accumulation increased with nitrogen stress on the medium, and the degree of accumulation was nitrogen dependent. *C. reinhardtii* also proved to be a rich source of

major minerals, such as Mg, P, K and Ca, as well as trace minerals, such as Fe, Mn, Zn and Cu.

The efficiency of *C. reinhardtii* cell wall disruption using the cavitation techniques provided by hydrodynamic cavitation and ultrasonication were compared. The use of HDC disruption is less damaging to cell walls, although ultrasonication quenches the cell structure, in addition to providing a higher percentage of pigment and protein solubility. The chlorophyll and protein solubility of HDC and ULT-disrupted cells is 3.5% and 20%, and 1.04% and 3.95%, respectively. The breach of the cell wall by HDC was confirmed by evidence of the higher permeability of HDC-disrupted as compared to intact cells, as shown by lipophilic staining dye. HDC-disrupted biomass retains its carotenoid content but contains less chlorophyll than intact biomass. As a consequence, HDC could be an innovative cell disruption method to improve the nutrient bio-accessibility of *C. reinhardtii*.

An *in vitro* digestion study using the latest INFOGEST model was applied to determine whether cell wall disruption is required to enhance the bio-accessibility of nutrients. The HDC-disrupted biomass resulted in a lower degree of lipophilic pigmentation (chlorophyll *a*, chlorophyll *b*, *β*-carotene and lutein), indicating that it is more accessible and assimilable than intact cell walls. Presumably, this is due to the losses caused by the HDC process together with the acid-liability of the pigment during the gastric phase of mimic digestion. The morphology observation using TEM reveals that the digestive enzymes completely digest the cell wall of intact *C. reinhardtii.* This observation could explain the very successful nutritional contribution made by *C. reinhardtii* in the fish diet, as described in the following section.

The digestibility of intact *C. reinhardtii* was further tested *in vivo* by incorporating it into feed for zebrafish; the fish digestive system is not too dissimilar to that of humans as regards the enzymes involved. Partial replacement of fishmeal with *C. reinhardtii* at 10% and 20% yielded promising growth rate results, further supporting the hypothesis that the *C. reinhardtii* cell wall was entirely broken down in the presence of the digestive system tested in this research. The visible yellow pigmentation of zebrafish (egg in the female and skin in the male) fed with *C. reinhardtii* (at three inclusion levels), which resulted from lutein, was distinct from the control. Retinol in the body of zebrafish increased from 0.5 in control to 1.85 and 3.5 μg/g at *C. reinhardtii* inclusion levels in the feed of 10% and 20%, respectively. Thus, it is deduced that zebrafish is able to assimilate β-carotene from *C. reinhardtii* and convert it to vitamin A.

In conclusion, the potential commercial applications of microalgae are numerous, but so are the challenges of exploiting different species of microalgae for food, fuel and profit. This study lays the groundwork by providing fundamental information regarding *C. reinhardtii* for introducing novel applications.

CHAPTER 9

Suggested Future Research

I. Cultivation Conditions

C. reinhardtii cultivation within the laboratory can be scaled up from flask-scale to a designed photobioreactor which gives more control over all the growing parameters and the use of CO_2 inlet. There is also a possibility to study the growth performance and the compositional response of *C. reinhardtii* under different light wavelength and intensities. This will give us better opportunity to manipulate the growing conditions/modes and hence allow the cells to accumulate the target components without compromising the yield.

II. Cell wall disruption

Hydrodynamic cavitation disruption applied in this study, proved to be successful downstream processing method for *C. reinhardtii* biomass. This paves the way for further investigation with different microalgae species with more rigid cell wall like diatoms with silica-base cell wall. The biomass concentration in combination with the runs frequency still need optimization to achieve the required degree of cell wall disruption while controlling the release/loss of nutrients to the aqueous phase. This can further be finalised to achieve direct separation and biorefinery of the high values compounds from *C. reinhardtii*.

III. Bioaccessibility Studies

The bioaccessiblity of other micronutrients such as fatty acids, amino acids and minerals should be performed to assess the efficiency of HDC - disruption on the micronutrients bioaccessiblity from *C. reinhardtii* as a model and for other economically important microalgae species. *In-vivo* digestion studies could support the *in-vitro* ones and the fish feeding trials already established within our group could be further tested using the HDC – disrupted *C. reinhardtii* cells.

IV. Potential of Commercial Development and Impact

Towards commercialisation as a food ingredient, the growing media of the *C. reinhardtii* should be considered to be food grade. Also, pasteurization step along with its impact on the cell composition should be investigated. For other non-food application, a nitrogen rich waste stream from food industry could be studied to achieve more sustainable biomass production.

Within this study and under current laboratory growing conditions, approximately 1L media is required to obtain 1g of freeze-dried *C. reinhardtii*. 1L media as prepared in the lab costs between £ 2-3, while to buy the premix media the cost increases 10-fold. Added to the media cost is the energy consumption to run and maintain the temperature, lightening and drying. Dewatering/drying is the most energy intense step and getting the greatest attention in production scaling up to the industrial level.

Similar products in the supplement market sold as dried powder like *Spirulina* and *Chlorella* costs between £0.05-0.5 per gram. However, most of them are collected from

natural lakes with high risk of pollution (should we mention like for example *Spirulina* from Naturya analysed, in our lab, contained high level of Lead (2.97 ± 0.20)).

REFERENCES

Adair, W. (1987). Nucleated assembly of *Chlamydomonas* and *Volvox* cell walls. *The Journal of Cell Biology*, 105(5), pp.2373-2382.

Adl, S., Simpson, A., Farmer, M., Andersen, R., Anderson, O., Barta, J., Bowser, S., Brugerolle, G., Fensome, R., Fredericq, S., James, T., Karpov, S., Kugrens, P., Krug, J., Lane, C., Lewis, L., Lodge, J., Lynn, D., Mann, D., Mccourt, R., Mendoza, L., Moestrup, O., Mozley-Standridge, S., Nerad, T., Shearer, C., Smirnov, A., Spiegel, F. and Taylor, M. (2005). The new higher level classification of eukaryotes with emphasis on the taxonomy of protists. *The Journal of Eukaryotic Microbiology*, 52(5), pp.399-451.

Agellon, L.B. (2002). Metabolism and function of bile acids. New Comprehensive Biochemistry. Elsevier.

Ahmed, T., Hossain, M. and Sanin, K.I. (2012). Global burden of maternal and child undernutrition and micronutrient deficiencies, *Annals of Nutrition and Metabolism*, 61(1), pp. 8–17.

Akhtar, S. (2016). Malnutrition in South Asia—A Critical Reappraisal, *Critical Reviews in Food Science and Nutrition*, 56(14), pp. 2320–2330.

Annamalai, J. and Nallamuthu, T. (2014). Antioxidant potential phytochemicals from methanol extract of *Chlorella vulgaris* and *Chlamydomonas reinhardtii*, *Journal of Algae biomass Utilization*, 5(4), pp. 60–67.

Araya, B., Gouveia, L., Nobre, B., Reis, A., Chamy, R. and Poirrier, P. (2014). Evaluation of the simultaneous production of lutein and lipids using a vertical alveolar panel bioreactor for three *Chlorella* species. *Algal Research*. pp. 218–222.

Arifin, Z., Soeparman, S., Widhiyanuriyawan, D., Suyitno, S. and Setyaji, A. (2017). Improve stability of chlorophyll as natural dye for dye-sensitized solar Cells. *Jurnal Teknologi*, 80(1), pp. 27-33.

Arisz, S., van Himbergen, J., Musgrave, A., van den Ende, H. and Munnik, T. (2000). Polar glycerolipids of *Chlamydomonas moewusii*. *Phytochemistry*, 53(2). pp.265-270.

Ball, G.F.M. (1995). Vitamins In Foods Analysis, Bioavailability, and Stability. *Lancet*. Chapman and Hall. 345, pp.104–107.

Barba, F.J., Mariutti, L.R.B., Bragagnolog, N., Mercadanta, A.Z. Barbosa-Canova, G.V. and Orlien, V. (2017). Bioaccessibility of bioactive compounds from fruits and vegetables after thermal and nonthermal processing. *Trends in Food Science and Technology*, 67, pp.195–206.

Baroukh, C., Muñoz-Tamayo, R., Steyer, J. and Bernard, O. (2013). A new framework for metabolic modeling under non-balanced growth. Application to carbon metabolism of unicellular microalgae. *IFAC Proceedings Volumes*, 46(31), pp.107-112.

Barsanti, L. and Gualtieri, P. (2014). *Algae: anatomy, biochemistry, and biotechnology*. Boca Raton, Fla.: CRC Press.

Benavente-Valdés, J., Aguilar, C., Contreras-Esquivel, J., Méndez-Zavala, A. and Montañez, J. (2016). Strategies to enhance the production of photosynthetic

pigments and lipids in *chlorophycae* species. *Biotechnology Reports*, 10, pp.117-125.

Berry, S., Tydeman, E., Lewis, H., Phalora, R., Rosborough, J., Picout, D. and Ellis, P. (2008). Manipulation of lipid bioaccessibility of almond seeds influences postprandial lipemia in healthy human subjects. *The American Journal of Clinical Nutrition*, 88(4), pp.922-929.

Bilbao, P.S., Salvador, G.A. and Leonardi, P.I. (2017). Fatty Acids from Microalgae: Targeting the Accumulation of Triacylglycerides, *In* Catala, A. (ed.) *Fatty acid*. London: IntechOpen Limited, pp. 119–141.

Bjerkeng, B. (2008). Carotenoids in Aquaculture: Fish and Crustaceans. *In:* Britton, G., Liaaen-Jensen, S. and Pfander, H. (eds.) *Carotenoids: Volume 4: Natural Functions*. Basel: Birkhäuser Basel.

Bohn, T. (2008). Bioavailability of Non-Provitamin A Carotenoids. *Current Nutrition & Food Science*, 4(4), pp.240–258.

Bollig, K. Lamshöft, M., Schweimer, K., Marner, F.J., Budzikiewiczc, H., Waffenschmidt, S. (2007). Structural analysis of linear hydroxyproline-bound O-glycans of *Chlamydomonas reinhardtii*-conservation of the inner core in *Chlamydomonas* and land plants. *Carbohydrate Research*, 342(17), pp. 2557–2566.

Boon, C.S., Mcclements, D.J., Weiss, J. and Decker, E.A. (2010). Factors Influencing the chemical stability of carotenoids in foods. Critical Reviews in Food Science and Nutrition, 50, pp. 515–532.

Boyd, C.E., Tucker, C., Mcnevin, A., Bostick, K. and Clay, J. (2007). Indicators of resource use efficiency and environmental performance in fish and crustacean aquaculture. *Reviews in Fisheries Science*, 15(4)**,** pp.327–360.

Brady, J., Sadler, I. and Fry, S. (1996). Di-isodityrosine, a novel tetrametric derivative of tyrosine in plant cell wall proteins: a new potential cross-link. *Biochemical Journal*, 315(1), pp.323-327.

Brady, J., Sadler, I. and Fry, S. (1998). Pulcherosine, an oxidatively coupled trimer of tyrosine in plant cell walls: Its role in cross-link formation. *Phytochemistry*, 47(3), pp.349-353.

Brady, J.D. and Fry, S.C. (1997). Formation of Di-lsodityrosine and loss of lsodityrosine in the cell walls of tomato cell-suspension cultures treated with funga1 *Elicitors* or H_2O_2. *Plant Physiol*, 115, pp.87–92.

Breton, G. and Kay, S.A. (2006). Circadian rhythms lit up in *Chlamydomonas*, *Genome Biology*, 7(4), p.215.

Brett, C.T, Waldron, K.W. (1996). Physiology and biochemistry of plant cell walls. *In*: Black M. and Charlwood, B., (eds), *Topics in plant functional biology*. London, U.K.: Chapman and Hall.

Briars, R. (2013). Examining the Extraction of Artemisini from *Artemisia Annau* using Ultrasound. Doctor of Philosophy. Coventry University.

Brown, M.R., Jeffrey, S.W., Volkman, J.K. and Dunstan, G.A. (1997). Nutritional properties of microalgae for mariculture. *Aquaculture*, 151(1-4), pp.315-331.

Brugman, S. (2016). The zebrafish as a model to study intestinal inflammation. *Developmental & Comparative Immunology*, 64, pp.82-92.

Bzducha-Wróbel, A., Błażejak, S., Kawarska, A., Stasiak-Różańska, L., Gientka, I. and Majewska, E. (2014). Evaluation of the efficiency of different disruption methods on yeast cell wall preparation for *β*-Glucan isolation. *Molecules*, 19(12), pp.20941-20961.

Canselier, J., Delmas, H., Wilhelm, A. and Abismaïl, B. (2002). Ultrasound emulsification—An Overview. *Journal of Dispersion Science and Technology*, 23(1-3), pp.333-349.

Carissimi, M., Flôres, S. and Rech, R. (2018). Effect of microalgae addition on active biodegradable starch film. *Algal Research*, 32, pp.201-209.

Cavalier-Smith, T. (2007). Evolution and relationships. *In:* Brodie, J., (ed); *Unravelling the Algae: The Past, Present, and Future of Algal Systematics*, CRC Press: Boca Raton, FL, USA, 2007; p. 21.

Cavonius, L. (2016). *Fractionation of lipids and proteins from the microalga Nannochloropsis oculata pH-shift process characterization and in vitro accessibility*. PhD Thesis. Chalmers University of Technology, Sweden.

Chacon-Lee, T.L. and Gonzalez-Marino, G.E. (2010). Microalgae for Healthy Foods-Posibility and Challenge. *Comprehensive Reviews in Food Science and Food Safety*, 9(6), pp. 655–675.

Chamila, J. and Gray, D.A. (2014). Lipid Bodies Isolated Microalgae Resudues as a Source of Bioethanol Production. *In:* Kim S.K. (ed), *Seafood Processin by-product trends and applications*. New York: Springer, pp. 407–421.

Chen, K. and Roca, M. (2018). *In vitro* bioavailability of chlorophyll pigments from edible seaweeds. *Journal of Functional Foods*, 41(October 2017),

Cheng, D., Shami, G., Morsch, M., Chung, R. and Braet, F. (2016). Ultrastructural Mapping of the Zebrafish Gastrointestinal System as a Basis for Experimental Drug Studies. *BioMed Research International*, pp.1-13.

Chisti, Y. (2007) Biodiesel from Microalgae. Biotechnology Advances, 25, 294-306.

Chou, Y., Ko, C., Yen, C., Chen, L. and Shaw, J. (2015). A Novel recombinant *Chlorophyllase1* from *Chlamydomonas reinhardtii* for the production of chlorophyllide derivatives. *Journal of Agricultural and Food Chemistry*, 63(43), pp. 9496-9503.

Christaki, E., Bonos, E., Florou-Paneri, P. (2015). Innovative Microalgae Pigments as Functional Ingredients in Nutrition. *In*: Kim S.K. (ed.) *Handbook of Marine Microalgae*: Biotechnology Advances. Elsevier Academic Press, London, UK, pp.233-243

Chronakis L.S. and Madsen, M. (2011). Algae Protein. *In*: Philips, G.O. and Williams, P.A. (eds), *Handbook of food protein*. Woodhead Publishing Series in Food Sciences, Technology and Nutritional. pp. 355-394.

Ciccarelli, F.D., Doerks, T., Mering, C.V., Crevey, C.I., Snel, B. and Bork, P. (2006). Toward automatic reconstruction of a highly resolved tree of life. *Science*, 311(5765), pp.1283-1287.

Ciccone, M., Cortese, F., Gesualdo, M., Carbonara, S., Zito, A., Ricci, G., De Pascalis, F., Scicchitano, P. and Riccioni, G. (2013). Dietary intake of carotenoids and

their antioxidant and anti-Inflammatory effects in aardiovascular care. *Mediators of Inflammation,* 2013, pp.1-11.

Conradie, T., Pieterse, E. and Jacobs, K. (2017). Application of *Paracoccus marcusii* as a potential feed additive for laying hens. *Poultry Science*, 97(3), pp.986-994.

Cubas, C., Gloria Lobo, M. and González, M. (2008). Optimization of the extraction of chlorophylls in green beans (*Phaseolus vulgaris L.*) by N,N-dimethylformamide using response surface methodology. *Journal of Food Composition and Analysis,* 21(2), pp. 125–133.

Czeczuga, B. (1972). Carotenoids in fish I. Carotenoids in the eggs of *Acipenser ruthenus* ruthenus L. (*Acipenseridae*) from the Danube. *Hydrobiologia*, 39(1), pp.9-16.

Darwish, R. (2017). *Investigating Chlamydomonas reinhardtii as a Functional Food and Feed Ingredient*. Degree of Doctor of Philosophy. University of Nottingham.

Dawson, R. and Hemington, N. (1974). Digestion of grass lipids and pigments in the sheep rumen. *British Journal of Nutrition*, 32(02), p.327.

Di L. and Kern, E. (2008). *Drug-like properties: concepts, Structure Design and Methods, Drug Metabolism and Disposition*. London: Academic Press.

Di Lena, G., Casini, I., Lucarini, M. and Lombardi-Boccia, G. (2018). Carotenoid profiling of five microalgae species from large-scale production. *Food Research International*.

Dixon, C. and Wilken, L. (2018). Green microalgae biomolecule separations and recovery. *Bioresources and Bioprocessing*, 5(14).

Domozych, D., Ciancia, M., Fangel, J., Mikkelsen, M., Ulvskov, P. and Willats, W. (2012). The Cell Walls of Green Algae: A Journey through Evolution and Diversity. *Frontiers in Plant Science*, 3(82).

Dron, J., Linke, R., Rosenberg, E. and Schreiner, M. (2004). Trimethylsulfonium hydroxide as derivatization reagent for the chemical investigation of drying oils in works of art by gas chromatography. *Journal of Chromatography A*, 1047(1), pp. 111–116.

Dufosse, L., Galaupa, P., Yaronb, A., Aradb, S.M, Blancc, P., Murthyd, K.N.C and Ravishankar, G.A. (2005). Microorganisms and microalgae as sources of pigments for food use: A scientific oddity or an industrial reality?. *Trends in Food Science and Technology*, 16(9), pp. 389–406.

Dvoretsky, D.S. and Akulinin, E. (2016). Defining Optimal Conditions for *Chlorella* Vulgaris Micoralgae Biomass Cell Walls Disruption in the Process of Biofuel. (August).

Ellis, P., Kendall, C., Ren, Y., Parker, C., Pacy, J., Waldron, K. and Jenkins, D. (2004). Role of cell walls in the bioaccessibility of lipids in almond seeds. *The American Journal of Clinical Nutrition*, 80(3), pp. 604-613.

Engel, B., Schaffer, M., Kuhn Cuellar, L., Villa, E., Plitzko, J. and Baumeister, W. (2015). Native architecture of the *Chlamydomonas* chloroplast revealed by *in situ* cryo-electron tomography. *eLife*, 4(e04889).

Enyidi, U.D. (2017). *Chlorella vulgaris* as Protein Source in the Diets of African Catfish *Clarias gariepinus*. *Fishes*, 2(17), pp. 1–12.

Epstein, L. and Lamport, D.T.A., (1984). An intramolecular linkage involving isodityrosine in extensin. *Phytochemistry* , 23(6), pp.1241-1246.

Evans, D.H., Claiborne, J.B. and Currie S. (1998). *The physiology of fishes*. 4th Edition CRC Press. Bosa Roca, United States.

FAO. (2012). *Sustainable nutrition security Restoring the bridge between agriculture and health*. Rome.

FAO/WHO/UN. (2007). Protein and amino acid requirements in human nutrition. *World Health Organization technical report series*. World Health Organization, pp.1–265.

FAO/WHO/UNU. (1985). Energy and Protein Requirements. Report of a Joint FAO/WHO/UNU Expert Consultation, WHO Technical Report, No. 724.

Feliu, J.X., Cubarsi, R. and Villaverde, A. (1998). Optimized release of recombinant proteins by ultrasonication of *E. coli* cells. *Biotechnology and Bioengineering*.

Feng, H., Barbosa-Cánovas, G. and Weiss, J. (2011). *Ultrasound technologies for food and bioprocessing*. New York: Springer.

Fernández-García, E., Carvajal-Lérida, I. and Pérez-Gálvez, A. (2009). *In vitro* bioaccessibility assessment as a prediction tool of nutritional efficiency. *Nutrition Research*, 29(11), pp.751–760.

Ferris, P.J., Woessner, J.P., Waffenschmidt, S., Kilz, S., Drees, J. and Goodenough, U.W. (2001). Glycosylated polyproline II rods with kinks as a structural motif in

plant hydroxyproline-rich glycoproteins. *Biochemistry*, 40(9), pp. 2978–2987.

Ferruzzi, M. G. and Blakeslee, J. (2007). Digestion, absorption, and cancer preventative activity of dietary chlorophyll derivatives. *Nutrition Research*. 27(1), pp.1–12.

Ferruzzi, M. G., Failla, M. L. and Schwartz, S. J. (2001). Assessment of degradation and intestinal cell uptake of carotenoids and chlorophyll derivatives from spinach puree using an *in vitro* digestion and Caco-2 human cell model, *Journal of Agricultural and Food Chemistry*, 49(4), pp. 2082–2089.

Flickinger M.C. (2013). *Downstram Industrial Biotechnology: Recovery and Purification.* A John Wiley & Sons, Inc., Publication. USA.

Floreto, E.A.T., Teshima, S.-I. and Koshio, S. (1996). The effects of seaweed diets on the lipid and fatty acids of the Japanese disc abalone Haliotis discus hannai. *Fisheries science*, 62**,** pp.582-588.

Folch, J., Lees, M. and Stanley, G.H.S. (1957). A simple method for the isolation and purification of total lipides from animal tissues. *The Journal of biological chemistry*. 226, pp.497-509.

Fox, D. (1957). The Pigments of Fishes. In: M. Brown, ed., *The Physiology of Fishes*. Academic Press.

Fredriksson, Å. and Nyström, T. (2006). Conditional and replicative senescence in *Escherichia coli*. *Current Opinion in Microbiology*, 9(6), pp.612-618.

Freitas, A., Rodrigues, D., Rocha-Santos, T., Gomes, A. and Duarte, A. (2012). Marine biotechnology advances towards applications in new functional foods. *Biotechnology Advances*, 30(6), pp.1506-1515.

Fry, S. (1982). Isodityrosine, a new cross-linking amino acid from plant cell-wall glycoprotein. *Biochemical Journal*, 204(2), pp.449-455.

Fry, S.C. (1986). Cross-linking of matrix polymers in the growing cell walls of angiosperms, *Annual Review of Plant Physiology*, 37(1), pp.165–186.

Gandul-Rojas, B., Gallardo-Guerrero, L. and Mínguez-Mosquera, M.I. (2009). Influence of the chlorophyll pigment structure on its transfer from an oily food matrix to intestinal epithelium cells', *Journal of Agricultural and Food Chemistry*, 57(12), pp.5306–5314.

Gayer, J. and Smith, G. (2015). Micronutrient fortification of food in Southeast Asia: recommendations from an expert workshop, *Nutrients*, 7(1), pp.646–658.

Gemberling, M., Bailey, T., Hyde, D. and Poss, K. (2013). The zebrafish as a model for complex tissue regeneration. *Trends in Genetics*, 29(11), pp.611-620.

Gerken, H., Donohoe, B. and Knoshaug, E. (2012). Enzymatic cell wall degradation of *Chlorella vulgaris* and other microalgae for biofuels production. *Planta*, 237(1), pp.239-253.

Gille, A., Trautmann, A., Posten, C., and Briviba, K. (2016). Bioaccessibility of carotenoids from *Chlorella vulgaris* and *Chlamydomonas reinhardtii'*, *International Journal of Food Sciences and Nutrition*, 67(5), pp.507–513.

Gogate, P. (2002). Cavitation: an auxiliary technique in wastewater treatment schemes. *Advances in Environmental Research*, 6(3), pp.335-358.

Gogate, P. and Pandit, A. (2005). A review and assessment of hydrodynamic cavitation as a technology for the future. *Ultrasonics Sonochemistry*, 12(1-2), pp.21-27.

Gogate, P. and Pandit, A. (2008). Application of cavitational reactors for cell disruption for recovery of intracellular enzymes. *Journal of Chemical Technology & Biotechnology*, 83(8), pp.1083-1093.

Gogate, P. and Pandit, A. (2008). Application of cavitational reactors for cell disruption for recovery of intracellular enzymes. *Journal of Chemical Technology & Biotechnology*, 83(8), pp.1083-1093.

Goodenough, U. (1985). The *Chlamydomonas cell* wall and its constituent glycoproteins analyzed by the quick-freeze, deep-etch technique. *The Journal of Cell Biology*, 101(4), pp.1550-1568.

Goodwin, T. (1980). *The biochemistry of the carotenoids.* London: Chapman and Hall.

Gould, S.B., Waller, R.F. and McFadden, G.I. (2008). Plastid Evolution, *Annual Review of Plant Biology*, 59, pp. 491-517

Gouveia, L. and Empis, J. (2003). Relative stabilities of microalgal carotenoids in microalgal extracts, biomass and fish feed: effect of storage conditions', *Innovative Food Science & Emerging Technologies*, 4(2), pp. 227–233.

Gouveia, L., Batista, A., Sousa, I., Raymundo, A. and Bandarra, N. (2008). Microalgae in Novel Food Products. *In:* K. Papadopoulos, (ed.), *Food Chemistry Research Developments*. Nova Science Publishers, Inc.

Gray, D., Payne, G., McClements, D., Decker, E. and Lad, M. (2010). Oxidative stability of *Echium plantagineum* seed oil bodies. *European Journal of Lipid Science and Technology*, 112(7), pp.741-749.

Green, N.M. and Lowther, D.A. (1959). Formation of collagen hydroxyproline *in vitro*, *The Biochemistry journal*, 71(1), pp.55-66.

Greenspan, P. (1985). Nile red: a selective fluorescent stain for intracellular lipid droplets. *The Journal of Cell Biology*, 100(3), pp.965-973.

Grief, C. and Shaw, P. (1987). Assembly of cell-wall glycoproteins of *Chlamydomonas reinhardii:* Oligosaccharides are added in medial and trans Golgi compartments. *Planta*, 171(3), pp.302-312.

Griesbeck, C., Kobl, I. and Heitzer, M. (2006). *Chlamydomonas reinhardtii*: A Protein expression system for pharmaceutical and biotechnological proteins. *Molecular Biotechnology*, 34(2), pp.213-224.

Guckert, J., Cooksey, K. and Jackson, L. (1988). Lipid sovent systems are not equivalent for analysis of lipid classes in the microeukaryotic green alga, Chlorella. *Journal of Microbiological Methods*, 8(3), pp.139-149.

Guedes, A., Amaro, H. and Malcata, F. (2011). Microalgae as sources of high added-value compounds-a brief review of recent work. *Biotechnology Progress*, 27(3), pp.597-613.

Günerken, E., D'Hondt, E., Eppink, M., Garcia-Gonzalez, L., Elst, K. and Wijffels, R. (2015). Cell disruption for microalgae biorefineries. *Biotechnology Advances*, 33(2), pp.243-260.

Guo, Q., Ye, A., Bellissimo, N., Singh, H. and Rousseau, D. (2017). Modulating fat digestion through food structure design. *Progress in Lipid Research*, 68, pp.109-118.

Gupta, R., Gangoliya, S. and Singh, N. (2013). Reduction of phytic acid and enhancement of bioavailable micronutrients in food grains. *Journal of Food Science and Technology*, 52(2), pp.676-684.

Güroy, D., Güroy, B., Merrifield, D., Ergün, S., Tekinay, A. and Yiğit, M. (2010). Effect of dietary *Ulva* and *Spirulina* on weight loss and body composition of rainbow trout, *Oncorhynchus mykiss* (*Walbaum*), during a starvation period. *Journal of Animal Physiology and Animal Nutrition*, 95(3), pp.320-327.

Guschina, I. and Harwood, J. (2006). Lipids and lipid metabolism in eukaryotic algae. *Progress in Lipid Research*, 45(2), pp.160-186.

Hallmann, A. (2010). Evolution of reproductive development in the *volvocine* algae. *Sexual Plant Reproduction*, 24(2), pp.97-112.

Harper, C. and Lawrence, C. (2011). *The laboratory zebrafish*. Boca Raton: CRC Press.

Harris, E. (2009). *Introduction to Chlamydomonas and its laboratory use*. Amsterdam: Academic Press.

Harris, E.H. (2001). *Chlamydomonas* as a model Organism, *Annual Review of Plant Physiology and Plant Molecular Biology*. 52, pp.363-406

Hart, D. and Scott, K. (1995). Development and evaluation of an HPLC method for the analysis of carotenoids in foods, and the measurement of the carotenoid content of vegetables and fruits commonly consumed in the UK. *Food Chemistry*, 54(1), pp.101-111.

Harwood, J.L. and Jones, A.L. (1989). Lipid Metabolism in Algae, *Advances in Botanical Research*, 16, pp. 1–53.

Henry, E. (2012). The use of algae in fish feeds as alternatives to fishmeal. *International AquaFeed,* pp.10 - 13.

Hidalgo, M., Urea, E. and Sanz, A. (1999). Comparative study of digestive enzymes in fish with different nutritional habits. Proteolytic and amylase activities. *Aquaculture*, 170(3-4), pp.267-283.

Higuchi-Sanabria, R., Swayne, T. and Boldogh, I. (2019). Live-Cell Imaging of Mitochondria and the Actin Cytoskeleton in Budding Yeast. *In:* R. Gavin, (ed.), *Cytoskeleton: Methods and Protocols, Methods in Molecular Biology*. Springer Science and Business Media, pp.25-62.

Ho, S.Y., Thorpe, J.L., Deng, Y., Santana, E., Derose, R.A. and Farber, S. A. (2004). Lipid metabolism in zebrafish. *Methods in cell biology*, 76, pp.87-108

Hoham, R., Bonome, T., Martin, C. and Leebens-Mack, J. (2002). A comnined 18S rDNA and rbcL phylogenetic of *Chloromonas* and *Chlamydomonas* (*Chlorophyceae, Volvovales*) emphasizing snow and other cold temperature habitatis. *Journal of Phycology*, 38(5), pp.1051-1064.

Hörtensteiner, S. (2012). Update on the biochemistry of chlorophyll breakdown. *Plant Molecular Biology*, 82(6), pp.505-517.

Howe, K., Clark, M.D., Torroja, C.F., Torrance, J. Berthelot, C., Muffato, M., Collins, J.E., Humphray, S., McLaren, K., Matthews, L., McLaren, S., Sealy,I., Caccamo, M., Churcher, C., Scott, C., Barrett, J.C. Koch, R., Rauch, G.J., White, S., Chow, W., Kilian, K., Quintais, L.T., Guerra-Assunção, J.A., Zhou, Y., Gu, Y., Yen, J., Vogel, J.H., Eyre, T., Redmond, S., Banerjee, R., Chi,J., Fu, B., Langley, E., Maguire, S.F., Laird, G.K., Lloyd, D., Kenyon, E., Donaldson, S., Sehra, H., Almeida-King, J., Loveland, J., Trevanion,S., Jones, M., Quail, M., Willey, D., Hunt, A., Burton, J., Sims, S., McLay, K., Plumb,B., Davis, J., Clee, C., Oliver, K., Clark, R., Riddle, C., Eliott, E., Threadgold, G., Harden, G., Ware, D., Mortimer, B., Kerry, G., Heath,P., Phillimore, B., Tracey, A., Corby, N., Dunn, M., Johnson, C., Wood, J., Clark, S., Pelan, S., Griffiths, G., Smith, M., Glithero, R., Howden, P., Barker, N., Stevens,C., Harley, J., Holt, K., Panagiotidis,G., Lovell, J., Beasley, H., Henderson, C., Gordon, D., Auger, K., Wright, D., Collins, J., Raisen, C., Dyer, L., Leung, K., Robertson, L., Ambridge, K., Leongamornlert, D., McGuire, M., Gilderthorp, R., Griffiths, C., Manthravadi, D., Nichol, S., Barker, G., Whitehead, S., Kay, M., Brown, J., Murnane, C., Gray, E., Humphries, M., Sycamore, N., Barker, D., Saunders, S., Wallis, J., Babbage, A., Hammond, S., Mohammadi, M.M., Barr, L., Martin, S., Wray, P., Ellington, A., Matthews, N., Ellwood, M., Woodmansey, R., Clark, G., Cooper, J., Tromans, A., Grafham, A., Skuce, C., Pandian, R., Andrews, R., Harrison, E., Kimberley, A., Garnett, J., Fosker, N., Hall, R., Garner, P., Kelly, D., Bird, C., Palmer, S., Gehring, I., Berger, A., Dooley, C.M., Ürün, Z.E., Eser, C., Geiger, H., Geisler,M.,

Karotki,L., Kirn, A., Konantz, J., Konantz, M., Oberländer, M., Rudolph-Geiger, S., Teucke, M., Osoegawa, K., Zhu, B., Rapp, A., Widaa, S., Langford, C., Yang, F., Carter, N.P, Harrow, J., Ning, Z., Herrero, J., Searle, J.M.J., Enright, A., Geisler, R., Plasterk, R.H.A., Lee, C., Westerfield, M., de Jong, P.J. Zon, L.I., Postlethwait, J.H., Nüsslein-Volhard, C., Hubbard, J.P.T, Crollius, H.R, Rogers., J. and Stemple., D.L. (2013). The zebrafish reference genome sequence and its relationship to the human genome. *Nature*, 496(7446)**,** pp.498-503.

Hsu, C., Yang, C., Chen, C., Chao, P. and Hu, S. (2005). Effects of chlorophyll-related compounds on hydrogen peroxide induced DNA damage within human lymphocytes. *Journal of Agricultural and Food Chemistry*, 53(7), pp. 2746-2750.

Humby, P., Snyder, E. and Durnford, D. (2013). Conditional senescence in *Chlamydomonas reinhardtii* (*Chlorophyceae*). *Journal of Phycology*, 49(2), pp.389-400.

Humphrey, B.B. (1980). Chlorophyll', *Food Chemistry*, 5(1), pp. 57–67.

Hurst, W. (2002). *Methods of analysis for functional foods and nutraceuticals*. Boca Raton, CRC Press.

International Life Science Institute (ILSI) Europe Novel Food Task Force (2000). *Safety Considerations of DNA in Foods*. ILSI Press, Belgium.

Iverson, S., Lang, S. and Cooper, M. (2001). Comparison of the bligh and Dyer and Folch methods for total lipid determination in a broad range of marine tissue. *Lipids*, 36(11), pp.1283-1287.

Jackson, A.J., Capper, B.S. and Matty, A.J. (1982). Evaluation of some plant proteins in complete diets for the tilapia *Sarotherodon mossambicus*. *Aquaculture*, 27**,** pp. 97-109.

Jeffery, J., Holzenburg, A. and King, S. (2012). Physical barriers to carotenoid bioaccessibility. Ultrastructure survey of chromoplast and cell wall morphology in nine carotenoid-containing fruits and vegetables. *Journal of the Science of Food and Agriculture*, 92(13), pp.2594-2602.

Jeffrey, S. and Hallegraeff, G. (1987). Chlorophyllase distribution in ten classes of phytoplankton: a problem for chlorophyll analysis. *Marine Ecology Progress Series*, 35, pp.293-304.

Johnson, I. and Williamson, G. (2003). *Phytochemical functional foods*. Boca Raton, FL: CRC Press.

Jonas, D.A., Elmadfa, I., Engel, K.H., Heller, K.J., Kozianowski, G., König, A., Müller D., Narbonne, J.F., Wackernagel, W., Kleiner, J. (2001). Safety Considerations of DNA in Food. *Annual of Nutrition & Metabolism.* 45, pp. 235–254

Jubert, C. Mata, J. Bench, G. Dashwood, R.,Pereira, G., Tracewell, W.,Turteltaub, K. (2017) HHS Public Access', *Cancer Prev Res (Phila)*, 4(11), pp.1015–1022.

Kan, K.S. and Thornber, J.P. (1976). The light-harvesting chlorophyll a/b-protein complex of *Chlamydomonas reinhardii*', *Plant Physiology*, 57(1), pp. 47–52.

Keeling, P.J., Burger, G., Durnford, D.G., Lang, B..F., Bec, R.W., Pearlman, R.E. (2005). The tree of eukaryotes', *TRENDS in Ecology and Evolution*, 20(12). pp. 670-676.

Kent, M., Harper, C. and Wolf, J. (2012). Documented and potential research impacts of subclinical diseases in zebrafish. *ILAR Journal*, 53(2), pp.126-134.

Khanra, S., Mondal, M., Halder, G., Tiwari, O., Gayen, K. and Bhowmick, T. (2018). Downstream processing of microalgae for pigments, protein and carbohydrate in industrial application: A review. *Food and Bioproducts Processing*, 110, pp.60-84.

Kidmose, U., Edelenbos, M., Christensen, L. and Hegelund, E. (2005). Chromatographic determination of changes in pigments in spinach (*Spinacia oleracea L.*) during processing. *Journal of Chromatographic Science*, 43(9), pp.466-472.

Kiefer, C., Hessel, S., Lampert, J. M., Vogt, K., Lederer, M. O., Breithaupt, D. E. and Von Lintig, J. (2001). Identification and characterization of a mammalian enzyme catalyzing the asymmetric oxidative cleavage of provitamin A. *Journal of Biological Chemistry,* 276**,** pp.14110-14116.

Kieliszewski, M. and Shpak, E. (2001). Synthetic genes for the elucidation of glycosylation codes for arabinogalactan-proteins and other hydroxyproline-rich glycoproteins. *Cellular and Molecular Life Sciences*, 58(10), pp.1386-1398.

Kieliszewski, M. J. and Lamport, D. T. A. (1994). Extensin: repetitive motifs, functional sites, post translational codes, and phylogeny, *The Plant Journal*, (5)2, pp. 157–172.

Kieliszewski, M.J., Derek, T.A, Lamport, Tan, LI., and Cannon, C.M. (2010). Hydroxyproline-Rich Glycoproteins: Form and Function, *Annual Plant Reviews*, 41, pp. 321–342.

Kitamoto, D, Morita, T., Fukuoka, T., Konishi, M., Imura, T., (2009). Self-assembling properties of glycolipid biosurfactants and their potential applications. Current Opinion in Colloid & Interface Science, 14, pp. 315-328.

Klein Breteler W.C.M., Schogt, N., Baas, M., Schouten S., Kraay G.W. (1999). Dynamics of bacterial community composition during degradation of copepod fecal pellets. *Marine Biology*. 135(1), pp.191–198.

Kopec, R., Gleize, B., Borel, P., Desmarchelier, C. and Caris-Veyrat, C. (2017). Are lutein, lycopene, and *β*-carotene lost through the digestive process?. *Food & Function*, 8(4), pp.1494-1503.

Korkmaz, A. and Cakirogull, G. (2011). Effects of partial replacement of fish meal by dried baker's Yeast (*Saccharomyces cerevisiae*) on growth performance, feed utilization and digestibility in Koi Carp (*Cyprinus Carpio L., 1758*) fingerlings. *Journal of Animal and Veterinary Advances*, 10(3), pp.346-351.

Kose, A., Ozen, M., Elibol, M. and Oncel, S. (2017). Investigation of in vitro digestibility of dietary microalga *Chlorella vulgaris* and cyanobacterium Spirulina platensis as a nutritional supplement. *3 Biotech*, 7(3).

Kuiken, K.A., Lyman, C.M., Dieterich, S., Bradford, M. and Trant, M. (1948). Availability of amino acids in some foods. *Journal of Nutrition*, 36 (3). pp 359–368.

Kwek, J., De Iongh, R., Nicholas, K. and Familari, M. (2009). Molecular insights into evolution of the vertebrate gut: focus on stomach and parietal cells in the marsupial,*Macropus eugenii*. *Journal of Experimental Zoology Part B: Molecular and Developmental Evolution*, 312B(6), pp.613-624.

Laemmli, U. (1970). Cleavage of structural proteins during the assembly of the head of bacteriophage T4. *Nature*, 227(5259), pp.680-685.

Lee, A., Lewis, D. and Ashman, P. (2012). Disruption of microalgal cells for the extraction of lipids for biofuels: Processes and specific energy requirements. *Biomass and Bioenergy*, 46, pp.89-101.

Lee, E., Jalalizadeh, M. and Zhang, Q. (2015). Growth kinetic models for microalgae cultivation: A review. *Algal Research*, 12, pp.497-512.

Leliaert, F.,Smith, D.R.., Moreau, H., Herron, M.D. Verbruggen, H., Delwiche, C.F. and Clerck, O.D. (2012). Phylogeny and molecular evolution of the green algae, *Critical Reviews in Plant Sciences*, 31, pp. 1–46.

Levine, I. and Fleurence, J. (2018). *Microalgae in health and disease prevention*. Academic Press.

Limón, P., Malheiro, R., Casal, S., Acién-Fernández, F., Fernández-Sevilla, J., Rodrigues, N., Cruz, R., Bermejo, R. and Pereira, J. (2015). Improvement of stability and carotenoids fraction of virgin olive oils by addition of microalgae *Scenedesmus almeriensis* extracts. *Food Chemistry*, 175, pp.203-211.

Loos, E. and Meindl, D. (1982). Composition of the cell wall of *Chlorella fusca*, *Planta*, 156(3), pp. 270–273.

Lopez-Sanchez, P., Nijsse, J., Blonk, H., Bialek, L., Schumm, S. and Langton, M. (2010). Effect of mechanical and thermal treatments on the microstructure and rheological properties of carrot, broccoli and tomato dispersions. *Journal of the Science of Food and Agriculture*, 91(2), pp.207-217.

Losh, J.L., Young, J.N. and Morel, F.M.M. (2013). Rubisco is a small fraction of total protein in marine phytoplankton', *New Phytologist*, 198(1), pp.52–58.

Louda, J., Li, J., Liu, L., Winfree, M. and Baker, E. (1998). Chlorophyll-a degradation during cellular senescence and death. *Organic Geochemistry*, 29(5-7), pp.1233-1251.

Lowry, O.H., Rosebrough, N.J., Farr, A.L, Randall, R.J. (1951), Protein measurement with the Folin phenol reagent.', *The Journal of biological chemistry*. 193(1), pp.265-275.

Lundquist, P. and Artursson, P. (2016). Oral absorption of peptides and nanoparticles across the human intestine: Opportunities, limitations and studies in human tissues. *Advanced Drug Delivery Reviews*, 106, pp.256-276.

Lunn, J. (2006), Superfoods. *Nutritional Bullet*. 31 (3), pp.171–172.

Ma, L., Dou, H., Huang, Y., Lu, X., Xu, X., Qian, F., Zou, Z., Pang, H., Dong, P., Xiao, X., Wang, X., Sun, T. and Lin, X. (2012). Improvement of retinal function in early age-related macular degeneration after lutein and zeaxanthin supplementation: A randomized, double-masked, placebo-controlled trial. *American Journal of Ophthalmology*, 154(4), pp.625-634.

Marangoni, A.G. (2019). *Kinetic Analysis of Food Systems*. Springer.

Martins, N., Petropoulos, S. and Ferreira, I. (2016). Chemical composition and bioactive compounds of garlic (*Allium sativum L.*) as affected by pre- and post-harvest conditions: A review. *Food Chemistry*, 211, pp.41-50.

Marzol E., Borassi C., Bringas M., Seda A., Rosa D., Garcia R., Capece L., Estevez J.M. (2018). Filling the gaps to solve the extensin puzzle, *Molecular Plant*, 11(5), pp. 645–658.

Mayfield, L.E., Bennett, R.M., Tranter, R.B., and Wooldridge, M.J. (2007). Consumption of welfare-friendly food products in Great Britain, Italy and Sweden, and how it may be influenced by consumer attitudes to, and behaviour towards, animal welfare attributes', *International Journal of Food and Agriculture*. International. 15(3).

McClements, D.J. and Decker, E. (2009). *Designing functional foods : measuring and controlling food structure breakdown and nutrient absorption*. CRC Press.

McCusker, S. Buff, P.R., Yu, Z. and Fascetti, A.J. (2014). Amino acid content of selected plant, algae and insect species: a search for alternative protein sources for use in pet foods, *Journal of nutritional science*, 3(39), pp. 1-5.

McDougal,G.D., Morrison, I.M., Stewart, D., Hillman, J.R. (1996). Plant cell walls as dietary fibre: range, structure, processing and function, *Journal of the Science of Food and Agriculture*, 70(2), pp.133–150.

MerchantSS, Prochnik, S.E., Vallon O, Harris, E.H., Karpowicz, S.J., Witman, G.B., Terry, A., Salamov, A., Fritz-Laylin, L.K., Maréchal-Drouard, L., Marshall W.F., Qu, L.H., Nelson, D.R., Sanderfoot, A.A., Spalding, M.H., Kapitonov, V.V., Ren, Q., Ferris, P., Lindquist, E., Shapiro, H., Lucas, S.M.,

Grimwood, J., Schmutz, J., Cardol, P., Cerutti, H., Chanfreau, G., Chen, C.L., Cognat, V., Croft, M.T., Dent, R., Dutcher, S., Fernández, E., Fukuzawa, H., González-Ballester, D., González-Halphen, D., Hallmann, A., Hanikenne, M., Hippler, M., Inwood, W., Jabbari, K., Kalanon, M., Kuras, R., Lefebvre, P.A., Lemaire, S.D., Lobanov, A.V., Lohr, M., Manuell, A., Meier, I., Mets, L., Mittag, M., Mittelmeier, T., Moroney, J.V., Moseley, J., Napoli, C., Nedelcu, A.M., Niyogi, K., Novoselov, S.V., Paulsen, I.T., Pazour, G., Purton, S., Ral, J.P., Riaño-Pachón, D.M.,Riekhof, W., Rymarquis, L., Schroda, M., Stern, D., Umen, J., Willows, R., Wilson, N., Zimmer, S.L., Allmer, J., Balk, J., Bisova, K., Chen, C.J., Elias, M., Gendler, K., Hauser, C., Lamb, M.R., Ledford, H., Long, J.C., Minagawa, J., Page, M.D., Pan, J., Pootakham, W., Roje, S., Rose, A., Stahlberg, E., Terauchi, A.M., Yang, P., Ball, S., Bowler, C., Dieckmann, C.L., Gladyshev, V.N., Green, P., Jorgensen, R., Mayfield, S., Mueller-Roeber, B., Rajamani, S., Sayre, R.T., Brokstein, P., Dubchak, I., Goodstein, D., Hornick, L., Huang, Y.W., Jhaveri, J., Luo, Y., Martínez D., Ngau W.C., Otillar, B., Poliakov, A., Porter, A., Szajkowski, L., Werner, G., Zhou, K., Grigoriev, I.V., Rokhsar, D.S., Grossman, A.R. (2010). The *Chlamydomonas* Genome Reveals the Evolution of Key Animal and Plant Functions, *Science*, 318(5848), pp. 245–250.

Metting, F. (1996). Biodiversity and application of microalgae. *Journal of Industrial Microbiology & Biotechnology*, 17(5-6), pp.477-489.

Middelberg, A. (1995). Process-scale disruption of microorganisms. *Biotechnology Advances*, 13(3), pp.491-551.

Miller, D.H., Mellman, I.S., Lampart, D.T.A. and Miller, M. (1974). The chemical composition of the cell wall of *Chlamydomonas gymnogama* and the concept of a plant cell wall protein, *Journal of Cell Biology*, 63(2), pp. 420–429.

Minekus, M., Alminger, M., Alvito, P., Ballance, S., Bohn, T., Bourlieu, C., Carrière, F., Boutrou, R., Corredig, M., Dupont, D., Dufour, C., Egger, L., Golding, M., Karakaya, S., Kirkhus, B., Le Feunteun, S., Lesmes, U., Macierzanka, A., Mackie, A., Marze, S., McClements, D., Ménard, O., Recio, I., Santos, C., Singh, R., Vegarud, G., Wickham, M., Weitschies, W. and Brodkorb, A. (2014). A standardised static in vitro digestion method suitable for food – an international consensus. *Food Funct.*, 5(6), pp.1113-1124.

Monks, L., Rigo, A., Mazutti, M., Vladimir Oliveira, J. and Valduga, E. (2013). Use of chemical, enzymatic and ultrasound-assisted methods for cell disruption to obtain carotenoids. *Biocatalysis and Agricultural Biotechnology*, 2(2), pp.165-169.

Monroig, Ó., Tocher, D.R. and Navarro, J.C. (2013). Biosynthesis of polyunsaturated fatty acids in marine invertebrates: Recent advances in molecular mechanisms. *Marine Drugs*,11(10)**,** pp. 3998-4018.

Montgomery, W.L. and Gerking, S.D. (1980). Marine macroalgae as foods for fishes: an evaluation of potential food quality. *Environmental Biology of Fishes*, 5(2)**,** pp.143-153.

Mudumana, S., Wan, H., Singh, M., Korzh, V. and Gong, Z. (2004). Expression analyses of zebrafish transferrin,ifabp, andelastaseB mRNAs as differentiation

markers for the three major endodermal organs: Liver, intestine, and exocrine pancreas. *Developmental Dynamics*, 230(1), pp.165-173.

Murbach, T., Glávits, R., Endres, J., Hirka, G., Vértesi, A., Béres, E. and Szakonyiné, I. (2018). A Toxicological vvaluation of *Chlamydomonas reinhardtii*, a green algae. *International Journal of Toxicology*, 37(1), pp.53-62.

Mussgnug, J.H., Klassen, V., Schluter, A. and Kruse, O. (2010). Microalgae as substrates for fermentative biogas production in a combined biorefinery concept. *Journal of Biotechnology*, 150(1)**,** 51-56.

Mustafa, M. G. and Nakagawa, H. (1995). A review: dietary benefits of algae as an additive in fish feed. *Israeli Journal of Aquaculture-Bamidgeh*, 47**,** pp.155-162.

Mustafa, M.G., Umino, T. and Nakagawa, H. (1994). The effect of Spirulina feeding on muscle protein deposition in red sea bream, *Pagrus major*. *Journal of applied ichthyology*, 10**,** pp.141-145.

Nakamura, Y., and Li-Beisson, Y. (2016). *Lipids in Plant and Algae Development*. Cham: Springer.

Nalbant, P., Boehmer, C., Dehmelt, L., Wehner, F. and Werner, A. (1999). Functional characterization of a Na(+)–phosphate cotransporter (NaP(i)-II) from zebrafish and identification of related transcripts. *The Journal of Physiology*, 520**,** pp.79-89.

National Research Council, S. (1992). *Nutrient Requirements of Fish*, Washington, United State, National Academies Press.

National Research Council. (1989). Recommended Dietary Allowances. 10th Edition, National Academy Press, Washington DC.

Natrah, F.M.I.. Yusoff, F.M. Shariff, M., Abas, F. and Mariana, N.S. (2007), Screening of Malaysian indigenous microalgae for antioxidant properties and nutritional value', *Journal of Applied Phycology*, 19(6), pp.711–718.

Oliveira, M.N.D., Freitas, A.L.P., Carvalho, A.F.U., Sampaio, T.M.T., Farias, D.F., Alves Teixeira, D.I., Gouveia, S.T., Pereira, J.G. and Sena, M.M.D.C.C.D. (2009). Nutritive and non-nutritive attributes of washed-up seaweeds from the coast of Ceará, Brazil. *Food Chemistry*, 115(1)**,** pp.254-259.

Ortiz, J., Romero, N., Robert, P., Araya, J., Lopez Hernandez, J., Bozzo, C., Navarrete, E., Osorio, A. and Rios, A. (2006). Dietary fiber, amino acid, fatty acid and tocopherol contents of the edible seaweeds *Ulva lactuca* and *Durvillaea antarctica*. *Food chemistry*, 99(1)**,** pp. 98-104.

Palinska, K. A. and Krumbein, W. E. (2000). Perforation patterns in the peptidoglycan wall of filamentous cyanobacteria', *Journal of Phycology*, 36(1), pp.139–145.

Park, J., Wang, H., Gargouri, M., Deshpande, R., Skepper, J., Holguin, F., Juergens, M., Shachar-Hill, Y., Hicks, L. and Gang, D. (2015). The response of *Chlamydomonas reinhardtii* to nitrogen deprivation: a systems biology analysis. *The Plant Journal*, 81(4), pp.611-624.

Pereira, L and Neto, J.M. (2015). *Marine Algae : Biodiversity, Taxonomy, Environmental Asessment, and Biotechnology*. Edited by CRC Press.

Perez-Garcia, O. and Bashan, Y. (2015) *Algal biorefineries: Volume 2: Products and refinery design*, Springer International Publishing.

Peterson, D. H., Jager, H. K., Savage, G. M., Washburn, G. N. and Westers, H. (1966). Natural coloration of Trout Using xanthophylls. *Transactions of the American Fisheries Society,* 95(4)**,** pp.408-414.

Polívka, T. and Frank, H. (2010). Molecular factors controlling photosynthetic light harvesting by carotenoids. *Accounts of Chemical Research*, 43(8), pp.1125-1134.

Prokop, A., Bajpai, R. and Zappi, M. (2015). *Algal Biorefineries*. Cham: Springer International Publishing.

Pulz, O. and Gross, W. (2004). Valuable products from biotechnology of microalgae', *Applied Microbiology and Biotechnology*, 65(6), pp. 635–648.

Qaim, M. (2017). Conference on "Sustainable food consumption" Globalisation of agrifood systems and sustainable nutrition', *Proceedings of the Nutrition Society*, 76(1), pp.12–21.

Ratha, S., Rao, P., Govindaswamy, K., Jaswin, R., Lakshmidevi, R., Bhaskar, S. and Chinnasamy, S. (2015). A rapid and reliable method for estimating microalgal biomass using a moisture analyser. *Journal of Applied Phycology*, 28(3), pp.1725-1734.

Rebolloso Fuentes, M. (2000). Biomass nutrient profiles of the microalga *Porphyridium cruentum*. *Food Chemistry*, 70(3), pp.345-353.

Rein, M., Renouf, M., Cruz-Hernandez, C., Actis-Goretta, L., Thakkar, S. and da Silva Pinto, M. (2013). Bioavailability of bioactive food compounds: a

challenging journey to bioefficacy. *British Journal of Clinical Pharmacology*, 75(3), pp.588-602.

Ren, X., Zhao, X., Turcotte, F., Deschênes, J., Tremblay, R. and Jolicoeur, M. (2017). Current lipid extraction methods are significantly enhanced adding a water treatment step in *Chlorella protothecoides*. *Microbial Cell Factories*, 16(1).

Renukadevi, K.P., Saravana, P.S., (2011). Antimicrobial and Antioxidant Activity of *Chlamydomonas Reinhardtii Sp*. *International Journal of Pharmaceutical Sciences and Research*, 4(2), pp. 1467–1472.

Richmond, A. and Hu, Q. (2013). *Handbook of Microalgal Culture : Applied Phycology and Biotechnology*. Second Edi. West Sussex: Wiley-Blackwell.

Ritchie, R. (2006). Consistent sets of spectrophotometric Chlorophyll equations for acetone, methanol and ethanol solvents. *Photosynthesis Research*, 89(1), pp.27-41.

Robb, D.H.F., Kestin, S.C., Warriss, P.D. and Nute, G.R. (2002). Muscle lipid content determines the eating quality of smoked and cooked Atlantic salmon (*Salmo salar*). *Aquaculture*, 205(3-4)**,** pp.345-358.

Roberts, K. (1974). Crystalline glycoprotein cell walls of algae: their stucture, composition and assembly.', *Philosophical transactions of the Royal Society of London. Series B, Biological sciences*, 268(891), pp.129–146.

Roberts, K., Grief, C., Hills, G. and Shaw, P. (1985). Cell wall glycoproteins: structure and function. *Journal of Cell Science*, 1985(Supplement 2), pp.105-127.

Rochaix, J. (2001). Assembly, function, and dynamics of the photosynthetic machinery in *Chlamydomonas reinhardtii*. *Plant Physiology,* 127(4), pp.1394-1398.

Rodriguez-Amaya, D. and Kimura, M. (2004). *HarvestPlus handbook for carotenoid analysis*. Washington, D.C.: International Food Policy Research Institute (IFPRI).

Ruxton, C., Reed, S., Simpson, M. and Millington, K. (2004). The health benefits of omega-3 polyunsaturated fatty acids: a review of the evidence. *Journal of Human Nutrition and Dietetics,* 17(5), pp.449-459.

Ryckebosch, E., Muylaert, K. and Foubert, I. (2012). Optimization of an analytical procedure for extraction of lipids from microalgae, *JAOCS, Journal of the American Oil Chemists' Society*, 89(2), pp.189–198.

Safi, C., Frances, C., Ursu, A., Laroche, C., Pouzet, C., Vaca-Garcia, C. and Pontalier, P. (2015). Understanding the effect of cell disruption methods on the diffusion of *Chlorella vulgaris* proteins and pigments in the aqueous phase. *Algal Research,* 8, pp.61-68.

Sager, R. and Palade, G.E. (1957). Structure and development of the chloroplast in *Chlamydomonas.* I. The normal green cell, *The Journal of biophysical and biochemical cytology*. Rockefeller University Press, 3(3), pp.463–88.

Sarker, P. K.., Gamble M.M, Kelson, S, and Kapuscinski A.R (2016). Nile tilapia (*Oreochromis niloticus*) show high digestibility of lipid and fatty acids from marine *Schizochytrium sp*. and of protein and essential amino acids from freshwater *Spirulina sp*. feed ingredients, *Aquaculture Nutrition,* 22(1), pp. 109–119.

Schoepp, N., Stewart, R., Sun, V., Quigley, A., Mendola, D., Mayfield, S. and Burkart, M. (2014). System and method for research-scale outdoor production of microalgae and cyanobacteria. *Bioresource Technology*, 166, pp.273-281.

Scholz, M., Weiss, T., Jinkerson, R., Jing, J., Roth, R., Goodenough, U., Posewitz, M. and Gerken, H. (2014). Ultrastructure and composition of the *Nannochloropsis gaditana* cell wall. *Eukaryotic Cell*, 13(11), pp.1450-1464.

Schwartz, S. and Lorenzo, T. (1991). Chlorophyll stability during continuous aseptic processing and storage. *Journal of Food Science*, 56(4), pp.1059-1062.

Schwendinger-Schreck, J. (2013). The zebrafish: atlas of macroscopic and microscopic anatomy. *The Yale journal of biology and medicine,* 86(3)**,** p.435.

Schwenzfeier, A., Wierenga, P. and Gruppen, H. (2011). Isolation and characterization of soluble protein from the green microalgae *Tetraselmis sp*. *Bioresource Technology*, 102(19), pp.9121-9127.

Scoma, A., Giannelli, L., Faraloni, C., and Torzillo, G. (2012). Outdoor H2production in a 50-L tubular photobioreactor by means of a sulfur-deprived culture of the microalga *Chlamydomonas reinhardtii*, *Journal of Biotechnology*. 157(4), pp. 620–627.

Serra, A. (2015). *Process and product control in an industrial scale microalgae production plant*. Master of Science Degree. Techico Lisbo.

Sharma, K., Schuhmann, H. and Schenk, P. (2012). High lipid induction in microalgae for biodiesel production. *Energies*, 5(5), pp.1532-1553.

Showalter, A. M. (1993). Structure and function of plant cell wall proteins, *the Plant Cell Online*, 5(1), pp.9–23.

Simionato, D., Block, M. A., LA Rocca, N., Jouhet, J., Marechal, E., Finazzi, G. and Morosinotto, T. (2013). The response of *Nannochloropsis gaditana* to nitrogen starvation includes *de novo* biosynthesis of triacylglycerols, a decrease of chloroplast galactolipids, and reorganization of the photosynthetic apparatus. *Eukaryotic Cell*, 12**,** pp.665-676.

Singh, A., Nigam, P. S. and Murphy, J. D. (2011) Mechanism and challenges in commercialisation of algal biofuels, *Bioresource Technology*, 102(1), pp. 26–34.

Sluiter, A., Hames, B., Hyman,, D., Payne, C., Ruiz, R., Scarlata, C., Sluiter, J., Templeton, D. and Wolfe, J. (2008). *Determination of total solids in biomass and total dissolved solids in liquid process samples*. Golden, Colo.: National Renewable Energy Laboratory.

Soler-Vila, A., Coughlan, S., Guiry, M. D. and Kraan, S. (2009). The red alga *Porphyra dioica* as a fish-feed ingredient for rainbow trout (*Oncorhynchus mykiss*): effects on growth, feed efficiency, and carcass composition. *Journal of Applied Phycology*, 21**,** pp.617-624.

Soletto, D. Lodi, L.B. Carvalho, J.C.M and Converti, A. (2005) Batch and fed-batch cultivations of *Spirulina platensis* using ammonium sulphate and urea as nitrogen sources. *Aquaculture*, 243(1–4), pp. 217–224.

Sommer, T.R., Potts, W.T. and Morrissy, N.M. 1991. Utilization of microalgal astaxanthin by rainbow trout (*Oncorhynchus mykiss*). *Aquaculture,* 94(1)**,** pp.79-88.

Spence, R., Gerlach, G., Lawrence, C. and Smith, C. (2007). The behaviour and ecology of the zebrafish, *Danio rerio*. *Biological Reviews*, 83(1), pp.13-34.

Spolaore, P., Joannis-Cassan, C., Duran, E. and Isambert, A. (2006). Commercial applications of microalgae. *Journal of Bioscience and Bioengineering*, 101(2), pp.87-96.

Stanley, J. and Jones, J. (1976). Feeding algae to fish. *Aquaculture*, 7(3), pp.219-223.

Stephen, B. and Maria, H. (2017). Algal proteins: Extraction, application, and challenges concerning production. *Foods*, 6(33), pp. 1–34.

Stewart, G., Schweigert, B., Hawthorn, J. and Bauernfeind, J. (2014). *Carotenoids as Colorants and Vitamin A Precursors*. Saint Louis: Elsevier Science.

Suarez Ruiz, C., van den Berg, C., Wijffels, R. and Eppink, M. (2018). Rubisco separation using biocompatible aqueous two-phase systems. *Separation and Purification Technology*, 196, pp.254-261.

Suganya, T., Varman, M., Masjuki, H. and Renganathan, S. (2016). Macroalgae and microalgae as a potential source for commercial applications along with biofuels production: A biorefinery approach. *Renewable and Sustainable Energy Reviews*, 55, pp.909-941.

Sun, Z., Li, T., Zhou, Z., and Jiang, Y. (2015). Microalgae as a source of lutein: chemistry, biosynthesis, and carotenogenesis. *Advances in Biochemical Engineering Biotechnology*. 153, pp.37-58.

Takeda, H. and Hirokawa, T. (1978). Studies on the cell wall of *Chlorella* I. Quantitative changes in cell wall polysaccharides during the cell cycle of *Chlorella ellipsoidea*, *Plant and Cell Physiology*, 19(4), pp.591–598.

Tamagnini, P., Axelsson, R., Lindberg, P., Oxelfelt, F., Wunschiers, R. and Lindblad, P. (2002). Hydrogenases and hydrogen metabolism of cyanobacteria. *Microbiology and Molecular Biology Reviews*, 66(1), pp.1-20.

Teuling, E., Schrama, W.W., Groppen H., Wierenga. P.A (2017). Effect of cell wall characteristics on algae nutrient digestibility in Nile tilapia (*Oreochromis niloticus*) and African catfish (*Clarus gariepinus*), *Aquaculture*, 479(4), pp. 490–500.

Tokuşoglu, O. and uunal, M. (2003). Biomass nutrient profiles of three Microalgae: *Spirulina platensis*, *Chlorella vulgaris*, and *Isochrisis galbana*. *Journal of Food Science*, 68(4), pp.1144-1148.

Tornabene, T., Bourne, T., Raziuddin, S. and Ben-Amotz, A. (1985). Lipid and lipopolysaccharide constituents of cyanobacterium *Spirulina platensis* (*Cyanophyceae, Nostocales*). *Marine Ecology Progress Series*, 22, pp.121-125.

Ugwu, C. U., Aoyagi, H. and Uchiyama, H. (2008). Photobioreactors for mass cultivation of algae, *Bioresource Technology*, 99(10), pp.4021–4028.

UNICEF (2013) *Improving child nutrition: The achievable imperative for global progress.*, *Division of Communication, UNICEF*.

Urich, K. 2013. *Comparative animal biochemistry,* Springer Science & Business Media. Academic Press.

van de Velde, F., Alting, A. and Pouvreau, L. (2011). From waste product to food ingredient : The extraction of the abondant plant protein Rubisco, *New food*, 14(2), pp. 10–13.

Vaughn, K. (2013). *Immunocytochemistry of plant cells*. Dordrecht, Netherlands: Springer.

Velasquez, S., Marzol, E., Borassi, C., Pol-Fachin, L., Ricardi, M., Mangano, S., Juarez, S., Salter, J., Dorosz, J., Marcus, S., Knox, J., Dinneny, J., Iusem, N., Verli, H. and Estevez, J. (2015). Low Sugar Is Not Always Good: Impact of SpecificO-Glycan Defects on Tip Growth in *Arabidopsis*. *Plant Physiology*, 168(3), pp. 808-813.

Venkataraman, L.V. and Becker, E.W. (1985). *Biotechnology and utilization of algae: The Indian experience*, Department of Science & Technology and Central Food Technological Research Institute, Mysore, India.

Verhoeckx, K., Cotter, P., López-Expósito, I., Kleiveland, C., Lea, T., Mackie, A., Requena, T., Swiatecka, D. and Wichers, H. (2015). *The Impact of Food Bioactives on Health*. Cham: Springer International Publishing.

Vizcaíno A.J., López G, Sáez M.I, Jiménez J.A. Barros A., Hidalgo L., Camacho-Rodríguez J., Martínez T.F. Cerón-García M.C. and Alarcón F.J. (2014). Effects of the microalga *Scenedesmus almeriensis* as fishmeal alternative in diets for gilthead sea bream, *Sparus aurata*, juveniles, *Aquaculture*, 431, pp.34–43.

Vogel, A. and Lauterborn, W. (1988). Acoustic transient generation by laser-produced cavitation bubbles near solid boundaries. *The Journal of the Acoustical Society of America*, 84(2), pp.719-731.

Wahbeh, M. (1997). Amino acid and fatty acid profiles of four species of macroalgae from Aqaba and their suitability for use in fish diets. *Aquaculture*, 159(1-2), pp.101-109.

Waldron, K., Smith, A., Parr, A., Ng, A. and Parker, M. (1997). New approaches to understanding and controlling cell separation in relation to fruit and vegetable texture. *Trends in Food Science & Technology*, 8(7), pp.213-221.

Wallace, K., Akhter, S., Smith, E., Lorent, K. and Pack, M. (2005). Intestinal growth and differentiation in zebrafish. *Mechanisms of Development*, 122(2), pp.157-173.

Wang, H., Chen, C., Huynh, P. and Chang, J. (2015). Exploring the potential of using algae in cosmetics. *Bioresource Technology*, 184, pp.355-362.

Wang, Z., Du, J., Lam, S., Mathavan, S., Matsudaira, P. and Gong, Z. (2010). Morphological and molecular evidence for functional organization along the rostrocaudal axis of the adult zebrafish intestine. *BMC Genomics*, 11(1), p.392.

Wase, N., Black, P., Stanley, B. and DiRusso, C. (2014). Integrated Quantitative Analysis of Nitrogen Stress Response in *Chlamydomonas reinhardtii* Using Metabolite and Protein Profiling. *Journal of Proteome Research*, 13(3), pp.1373-1396.

Weber, K. and Osborn, P.M. (1972). Measurement of molecular weights by electrophoresis on SDS-acrylamide gel. *Methods in Enzymology*. 26, pp.3-27.

Weigert, G., Kaya, S., Pemp, B., Sacu, S., Lasta, M., Werkmeister, R., Dragostinoff, N., Simader, C., Garhöfer, G., Schmidt-Erfurth, U. and Schmetterer, L. (2011). Effects of lutein supplementation on macular pigment optical density and visual acuity in patients with age-related macular degeneration. *Investigative Opthalmology & Visual Science*, 52(11), p. 8174.

Wells, M., Potin, P., Craigie, J., Raven, J., Merchant, S., Helliwell, K., Smith, A., Camire, M. and Brawley, S. (2016). Algae as nutritional and functional food sources: revisiting our understanding. *Journal of Applied Phycology*, 29(2), pp.949-982.

Woo, P.T., Leatherland, J.F. and Bruno, D.W. (2011). *Fish diseases and disorders*, CABI.

Yang, D. Song, D., Kind, T., Ma, Y., Hoefkens, J. and Fiehn, O. (2015). Lipidomic analysis of *chlamydomonas reinhardtii* under nitrogen and sulfur deprivation, *PLoS ONE*, 10(9), pp. 1–16.

Yonekura, L. and Nagao, A. (2009). Soluble Fibers Inhibit Carotenoid Micellization in Vitro and Uptake by Caco-2 Cells, *Bioscience, Biotechnology, and Biochemistry*, 73(1), pp.196–199.

Zaccari, F., Cabrera, M. C., Ramos, A. and Saadoun, A. (2015). *In vitro* bioaccessibility of beta- carotene, Ca, Mg and Zn in landrace carrots (*Daucus carota, L.*). *Food Chemistry*, 166(1), pp.365-371.

Zhang, H., Huang, D. and Cramer, W. (1999). Stoichiometrically Bound β-Carotene in the Cytochromeb6fComplex of Oxygenic Photosynthesis Protects against Oxygen Damage. *Journal of Biological Chemistry*, 274(3), pp.1581-1587.

Zhang, H., Wang W., Li Y., Yang W., Shen G.. (2011). Mixotrophic cultivation of Botryococcus braunii, *Biomass and Bioenergy*, 35(5), pp.1710–1715.

APPENDIX A

Table 1: the spectrum scan of *C. reinhardtii* suspension by spectrophotometer(LKB Biochro Model 4050 Ultraspect II Spectrophotometer, Dickenson, TX, USA).

wavelength	Abs
564	0.822
568	0.823
570	0.821
572	0.824
578	0.817
584	0.82
594	0.822
600	0.817
602	0.819
608	0.815
612	0.819
618	0.814
624	0.822
636	0.813
680	0.942
720	0.757
722	0.761
728	0.745
732	0.75
754	0.727
758	0.729
760	0.726
762	0.715
778	0.717
780	0.712
782	0.718

Table 2: Rate of change temperature over time from hydrodynamic cavitation using cavitator version 1.4. The pump device create pressure via motor (1.5 kW pump, Pedro, Italy) with flow rate 30 ~ 140 L/min.

time	Temperature (ºC)			
	rep 1	rep 2	rep 3	AVG
0	18.6	18.9	19.2	18.90
5	19.5	28.8	24.5	24.27
10	21.3	30.4	27.6	26.43
15	24.6	33	30.2	29.27
20	25.4	35.8	35.6	32.27
30	30.5	38.4	38.8	35.90
40	33	40.3	40.9	38.07
50	36.7	42.8	42.3	40.60
60	39	43.8	44.3	42.37
90	44.5	53.5	50.3	49.43
120	56	61.9	58.9	58.93
180	69.9	74	72	71.97

Table 3: Rate of change temperature over time from ultrasonication using 20 kHz (probe 13 mm).

time	Temperature (°C)			AVG
	rep 1	rep 2	rep 3	
0	21.20	21	20.2	20.80
5	21.20	21	20.2	20.80
10	21.20	21	20.2	20.80
15	21.30	21.1	20.3	20.90
20	21.30	21.1	20.3	20.90
30	21.30	21.1	20.4	20.93
40	21.40	21.2	20.4	21.00
50	21.40	21.3	20.5	21.07
60	21.50	21.3	20.5	21.10
90	21.6	21.5	20.6	21.23
120	21.9	21.8	21	21.57
180	22.2	22	21.3	21.83

APPENDIX B

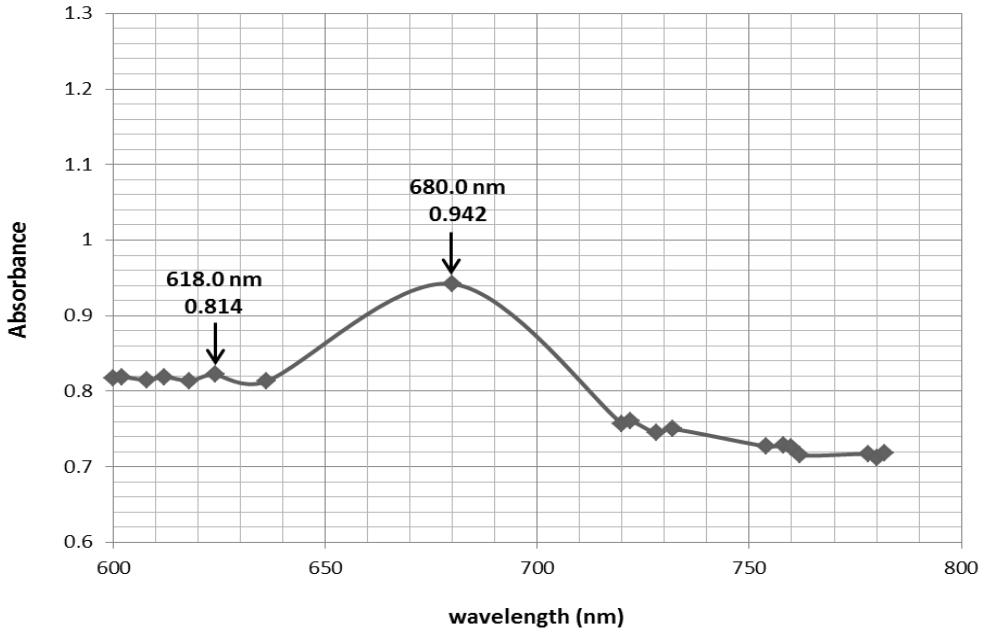


Figure 1: Pattern of light absorbance for *C. reinhardtii* screening between 600 - 800 nm using spectrophotometer (LKB Biochro Model 4050 Ultraspect II Spectrophotometer, Dickenson, TX, USA).

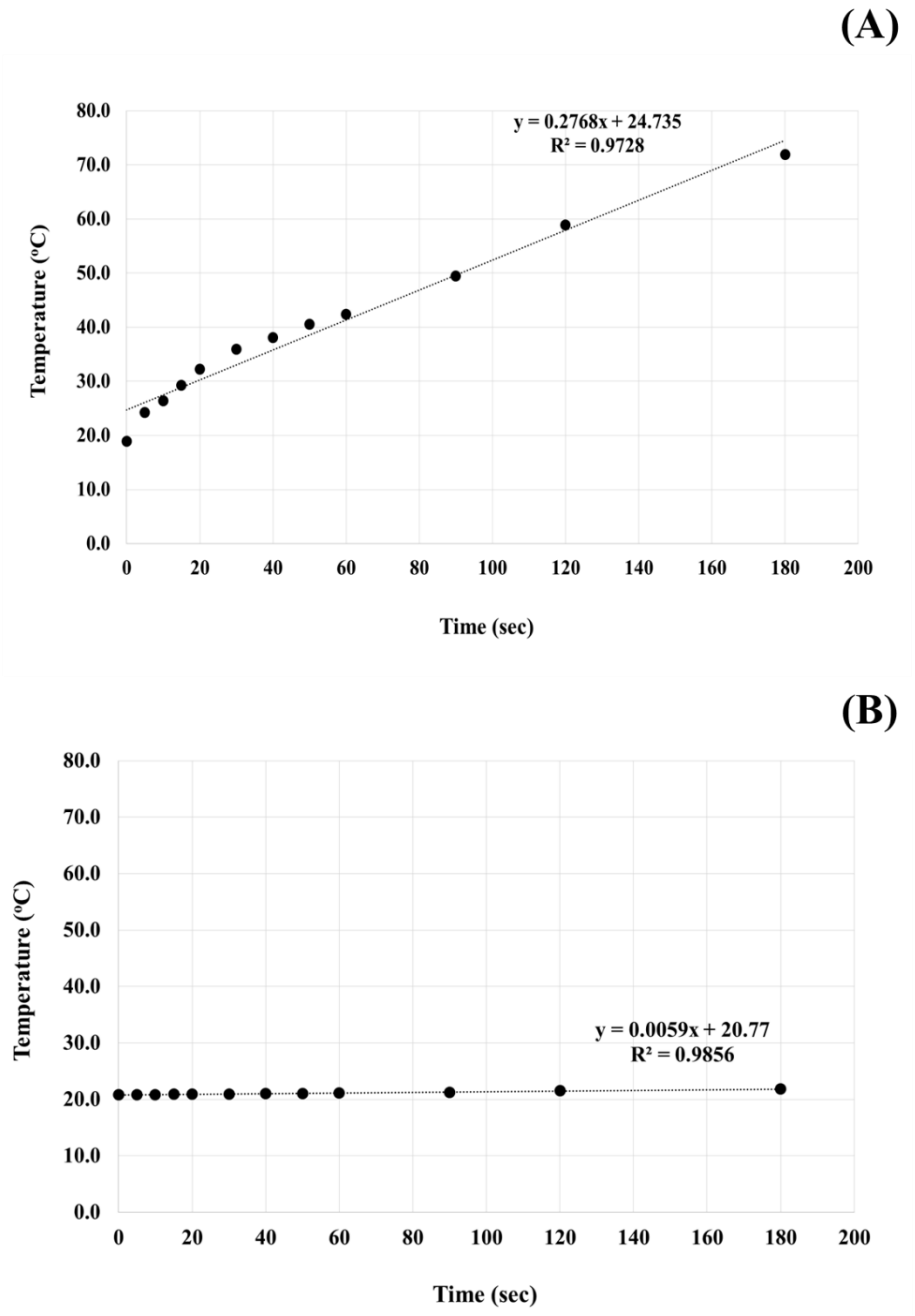


Figure 2: The graph produced through charting experiment data of Appendix A Table 1 and Table 2 The charts provide an equation with the rate of change value (change in temperature over time) from hydrodynamic cavitation (A) and ultrasonication (B) that was used to calculate power of each device.